# THE MASS TRANSPORT PROPERTIES OF SELECTED MEMBRANES IN POTASSIUM HYDROXIDE SOLUTIONS OF VARIOUS CONCENTRATIONS

A thesis submitted to the Council for National Academic Awards in partial fulfilment of the requirements for the degree of Master of Philosophy

David George Malpas

Energy Technology Centre
School of Mechanical and Production Engineering
Middlesex University

August 1992

# ABSTRACT

Aspects of the mass transport processes occurring in the ion-exchange membranes, PUDO 193, a Cellophane membrane derived from regenerated cellulose and Permion 2291 40/30, a grafted co-polymer of polyethylene and methacrylic acid, were studied while the membranes were swollen in solutions of KOH of a wide range of concentrations.

Measurement of the dimensional changes (length, width and thickness) of as received Cellophane films, after immersion in solutions of KOH, revealed a complex swelling behaviour with the majority of swelling resulting in changes in thickness. Unlike Cellophane, and as a consequence of their different structure, the swelling behaviour of Permion films were found to be less complex. The swelling behaviour was used to determine the porosity of the swollen membranes.

The ion-exchange capacity of the mono-functional Permion was obtained by pH titration, a method unsuitable for use with Cellophane since it is not fully exchanged at low external electrolyte concentrations. The ion-exchange properties of Cellophane were determined using atomic absorption techniques and a $Cl^-$ ion tracer method which was deemed suitable since similar results were obtained for Permion by this method and by pH titration.

Transport numbers of potassium ions and transference numbers of water through Cellophane and Permion as single membrane types were obtained using a meticulous technique, which minimised the unwanted effects of diffusion and osmosis. The method obtained transport numbers relevant to a specific concentration by holding solution composition constant and equal on either side of the membrane. The confidence gained in the technique, enhanced by careful cell testing and the application of correction factors, provided a sound basis for the measurement and subsequent understanding of transport behaviour in the less obvious situation, namely in assemblies of membranes.

Measurements of the resistance of Cellophane and Permion films equilibrated in solutions of KOH were made. Membrane resistance vs. membrane thickness plots were curved due to current refraction into the region where the membrane was clamped between the two halves of the conductivity cell. The data was linearised using a non-empirical correction factor and hence the accuracy of the measured membrane conductivity was improved.

From the primary resistance data, electrolyte conductivity and the mobilities of the potassium and hydroxyl ions in free solution were calculated. The ratio of potassium to hydroxyl ion mobility in free solution formed a basis for a comparison with a similar mobility ratio in the membrane phase. This method allowed a comparison of mobilities in free solution and the membrane phase without the necessity of estimating a suitable tortuosity factor. Models of tortuosity were then introduced to assess the blocking characteristics of the two membranes.

The transport properties of assemblies of Cellophane and Permion were investigated. Transport numbers entering and leaving the assembly were found to be different and depended on the orientation of the assembly. For the situation where transport numbers were greater leaving the assembly and at low current densities a steady state was reached and the depletion of electrolyte at the interface was replaced by diffusion, osmosis and hydraulic flow. At high current densities depletion of electrolyte at the interface was rapid causing the decomposition of the Cellophane. For the situation where transport numbers were greater entering the assembly, the assembly separated at the Permion/Cellophane interface due to the accumulation of electrolyte, the difference between measured and predicted transport numbers was accounted for by the effects of diffusion and osmosis which occurred mainly in the Cellophane.

# ACKNOWLEDGEMENTS

I wish to express my sincere gratitude to my director of studies, Professor Frank L. Tye for his continued interest and valuable discussions during this work. My thesis has evolved into an endurance test for me which could not have been completed without his patience and guidance, thank-you.

Thanks are also due to Dr. William C. Maskell for inspiring discussions and comments on sections of the written text. I wish to thank my second supervisor, Dr. Margaret A. Carter for her advice and support during the experimental work and for her comments on the draft copy of the thesis.

Thanks are due to Duracell Batteries for their partial sponsorship of this work, Andrew Ashton and Paul Collman for their help in transferring the handwritten text to the word processor and Eileen, Alice, Adele and Maggie in the print room at Bounds Green for their help with the presentation and printing of this thesis.

Finally I would like to thank my parents for their encouragement and support throughout my education so far.

# CONTENTS

Page number

# CHAPTER 5
# MASS TRANSPORT THROUGH ASSEMBLIES OF CELLOPHANE AND PERMION

# CHAPTER 1

# INTRODUCTION

## 1.1 Preliminary remarks

A membrane phase is a permeable film of ion-exchange material having a thickness which is small compared to its length and width. In general a membrane has a polymeric structure containing fixed ionic sites capable of ion exchange. Electrical neutrality is maintained throughout the structure with exchangeable ions balancing the fixed charge groups. Additional ions may be absorbed into the membrane. Ions having the same charge as the fixed ion framework are termed co-ions and those of opposite charge are termed counter-ions. Membranes are described as cation or anion exchangers. A cation-exchange membrane has a fixed anion framework and selectively transports cations through the membrane whereas an anion-exchange membrane has a fixed cation framework and selectively transports anions through the membrane.

Figure (1.1) shows the processes occurring in an electrochemical system with the passage of one faraday of electrical charge.

Figure 1.1 Processes occurring in the system on the passage of current

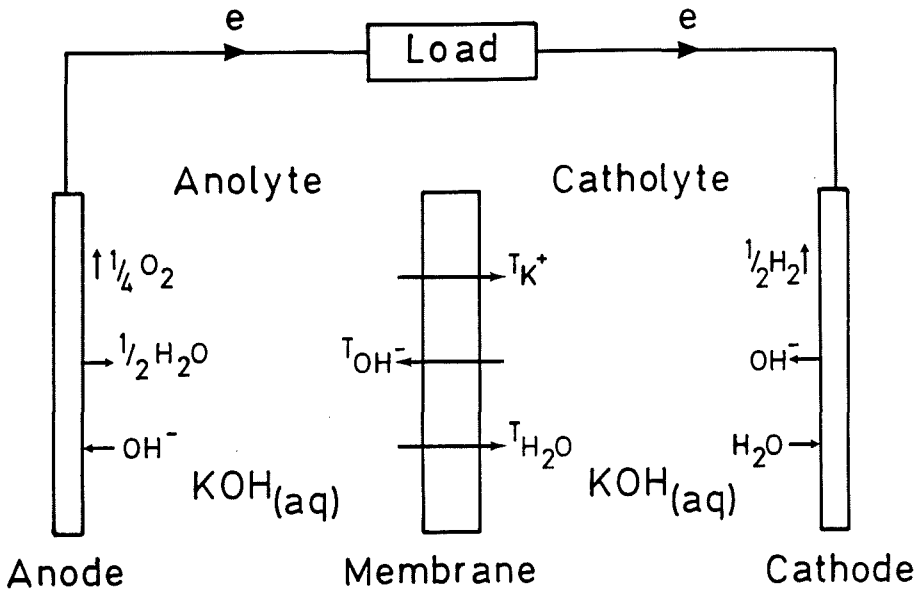

Potassium ions are selectively transported ($T_K+$) from the anolyte through the membrane to the catholyte. For a cation-exchange membrane the catholyte is on the side of the membrane receiving the counter-ions and is therefore termed the receiving side electrolyte, likewise the side donating the counter-ions, i.e. that containing the anolyte, is termed the donating side of the membrane. Water is transferred ($T_{H2O}$) through the membrane in the same direction as counter-ion transport; hydroxyl ions, the co-ions, are transported ($T_{OH}-$) in the opposite direction. The electrode reactions are a consequence of the electrolysis of water as follows :-

$$\text{Anode} \quad : \quad OH^- \rightarrow \tfrac{1}{4} O_2 + \tfrac{1}{2} H_2O + e^- \qquad (1.1)$$

$$\text{Cathode} \quad : \quad H_2O + e^- \rightarrow \tfrac{1}{2} H_2 + OH^- \qquad (1.2)$$

In its simplest form the electrochemical system of interest in this study comprised three phases, an ion-exchange membrane separating two electrolyte solutions. The membranes were PUDO 193, a Cellophane membrane derived from regenerated cellulose and Permion 2291 40/30, a grafted co-polymer of polyethylene and methacrylic acid. Both membranes were cation exchangers which necessitated a fixed anion framework. The electrolyte was KOH and hence the $K^+$ ions were counter-ions and the $OH^-$ ions were co-ions. The system was part of an electrolytic cell used in the investigation of the mass transport processes occurring through an ion-exchange membrane during the passage of current.

## 1.2 Electrochemical power sources

The membranes in this study are used as components in electrochemical power sources (or batteries), devices which enable the energy liberated in a chemical reaction to be converted directly into electricity. The essential features of a battery are, positive and negative active materials, electronic conduction between each active material and a terminal of the battery and ionic conduction between the active materials via the

electrolyte and the membrane or separator. The batteries of interest are primarily "miniature" or "button" cells whose market has grown over recent years due to the development of electric watches and the advancement of other small electronic devices. It has been suggested [1] that a working definition of the term miniature, would be, "... too small to allow the printing of information such as maker's name, voltage, etc., on the cell case". Practically the maximum dimensions for round button cell batteries are, 11.6mm for overall diameter and 5.4mm for overall height (including the pip, if present), down to a minimum height of 1.1mm and a minimum diameter of 6.8mm [2].

$Ag_2O$/Zn and HgO/Zn batteries are representative of two electrochemical systems, encased in a button cell form, and using a separator relevant to this work. An example of their construction is shown in figure (1.2 (a)), [3] and cutaway views in figures (1.2 (b) and (c)), [4].

The 0.2-0.3mm thick top cap is manufactured from mild or sometimes stainless steel and is plated with Ni or Au, (or occasionally Cu or Sn), to minimise corrosion arising from the hydrogen evolution / zinc dissolution couple. The case is usually nickel plated mild steel. Design of the cell may incorporate provision for automatic venting of any pressure caused by hydrogen evolution, with displaced electrolyte being absorbed in the safety sleeve between the inner and outer case.

The cathode consists of HgO or $Ag_2O$ together with 5-10% of finely divided graphite, consolidated in pellet form against the inner surface of the case to ensure good electronic contact and to provide a firm base for the mechanical seal. Graphite increases the electronic conductivity and, in the case of the mercury cell, minimises the coalescence of mercury formed during discharge.

The anode is a porous compressed cylindrical pellet of amalgamated zinc powder and electrolyte (possibly gelled). The anode must have sufficient porosity to accommodate the discharge product, ZnO, which occupies 2.7ml more space per faraday than zinc [5]. The anode capacity is designed to be less than the cathode capacity so that the cell is "zinc limited" i.e. in an exhausted cell there is no zinc left which might corrode and lead to hydrogen pressure developing in the cell [6].

The electrolyte is usually a 7-10M solution of KOH saturated with zinc oxide to which corrosion inhibitors have been added. This concentration is just above that of maximum conductivity. NaOH, of concentration two-thirds that of KOH, is used in

Figure 1.2(a) Constructions of $Ag_2O$/Zn and HgO/Zn button batteries [3].

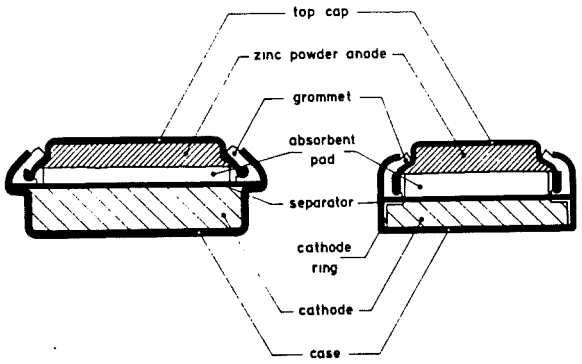


Figure 1.2(b) Cutaway view of a zinc-silver oxide button cell [4].

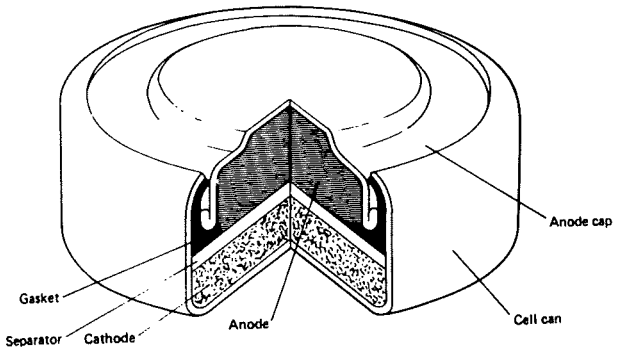


Figure 1.2(c) Cutaway view of a zinc-mercuric oxide button cell [4].

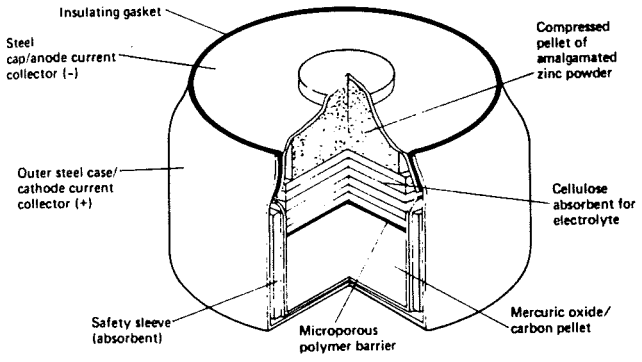

batteries intended for low current drain applications eg. button batteries for LCD watches. Caustic soda solutions have a lower tendency to creep [7] which makes the cell easier to seal but have a higher electrical resistance.

$Ag_2O$/Zn and HgO/Zn button cells usually contain two separator materials, an absorbent pad and an ion-exchange membrane or separator, both fulfilling different functions. A necessary function of the membrane or separator when situated in the region between the electrodes of an electrochemical power source is ionic conduction. The distinction between separators and membranes may be defined as follows. The separator framework takes no part in ionic conduction, but is penetrated by a conducting phase, the electrolyte, whereas membranes contain ion-exchange groups which together with absorbed electrolyte contribute to ionic conduction. The separator/membrane also separates the electrodes, and prevents the premature and spontaneous reaction of the active materials which would reduce the amount of energy available from the cell on discharge. Premature discharge would also occur if electronic conduction existed through the separator/membrane, hence the separator/membrane must be an electronic insulator.

The absorbent pad provides a reservoir of electrolyte which is required for mass transfer and to ensure that the cathode surface is sufficiently wetted. Equation (1.6) shows the cathodic reaction consumes 0.5 mol of water per Faraday and although this is replaced by an equal quantity generated at the anode as shown in equation (1.5), the absorbent pad provides a more readily available supply of water. The separator/membrane must therefore allow the transference of water. Non-woven cotton is the preferred absorbent separator in button cells for a number of reasons [8]. It rapidly absorbs the electrolyte; an important consideration during production line assembly. The resilient nature of the swollen cotton ensures that the absorbent pad puts pressure upon the zinc electrode to maintain good contact with the top cap, its external terminal. The porosity of the absorbent separator should be as a high as possible while fulfilling pressure transmission requirement. The absorbent pad also increases the distance a mercury globule or silver dendrite would need to span in order to cause an internal short circuit between the anode and cathode.

The membrane must allow electrical transport and diffusion of species participating in the electrode reactions but inhibit the transference of ionic species which if deposited at an electrode give rise to undesirable side reactions. Layers of membrane,

one or two for HgO/Zn cells and two to four for $Ag_2O$ cells, are placed between the absorbent pad and the cathode pellet. Cellophane, first introduced by André in 1941 [9], inhibits the diffusion of dissolved $Ag_2O$ (which is slightly soluble in alkali) to the zinc anode on which silver would deposit and promote corrosion [10]. Suitable commercially available membranes are Acropor W A (Gelman Hawksley), which has a crosslinked carboxylic ion-exchange resin held in a polymer film, and Permion (RAI Research Corporation), which has carboxylic acid groups grafted onto polyethylene. For HgO/Zn batteries the primary function of the membrane is to resist penetration by mercury globules formed on discharge while allowing adequate mass transport. The membrane/separator should also be chemically and physically stable in the battery environment, which will be strongly alkaline and at high or low temperature, and unaffected by direct contact with the oxidant forming the positive electrode.

The button cell is sealed by crimping a grommet between the top cap and the case.

The overall cell reactions for the $Ag_2O$/Zn and HgO/Zn systems are shown in equations (1.3 and 1.4) respectively.

$$Ag_2O + Zn \rightarrow 2Ag + ZnO \qquad (1.3)$$

$$HgO + Zn \rightarrow Hg + ZnO \qquad (1.4)$$

The anodic reaction is shown in equation (1.5).

$$Zn(s) + 2OH^-(aq) \rightarrow ZnO(s) + H_2O(l) + 2e \qquad (1.5)$$

It has been proposed [11,12], that the cathodic reduction of the mercuric oxide, equation (1.6).

$$HgO + H_2O + 2e \rightarrow Hg + 2OH^- \qquad (1.6)$$

occurs by dissolution of the mercuric oxide,

$$HgO + H_2O \rightleftharpoons Hg(OH)_2 \qquad (1.7)$$

followed by migration of the dissolved species to an electronic conductor. Charge transfer then occurs at the surface of the conductor.

$$Hg(OH)_2 + 2e \rightarrow Hg + 2(OH)^- \qquad (1.8)$$

Evidence to support this mechanism is the appearance of small mercury particles at positions remote from the HgO. A dissolution-precipitation mechanism has also been proposed for $Ag_2O$ cathodes [13]. The first stage in the reaction is dissolution of $Ag_2O$,

$$Ag_2O + 2OH^- + H_2O \rightleftharpoons 2Ag(OH)_2^- \qquad (1.9)$$

followed by migration of the dissolved silver species to an electronic conductor, (joined electrically with the positive terminal), and charge transfer producing the precipitation of silver.

$$Ag(OH)_2^- + e \rightarrow Ag + 2OH^- \qquad (1.10)$$

## 1.3 The structure of cellulose

The chemical and physical properties of cellulose are derived from the chemical nature of the cellulose molecules and their structural and morphological arrangement in the solid state. The cellulose molecule is a chain like structure of 1,4-β-D-linked polyanhydro glucopyranose, as shown in figure (1.3). This conclusion is the result of many investigations.

The elemental composition of cellulose, ie the proportions of Carbon, Hydrogen and Oxygen was determined in 1842 by Payen [14], and its macromolecular nature was established by Straudinger in 1932 [15]. Cellulose is a polysaccharide and hence the constituent sugars must be identified and their proportions determined in order to describe fully the structure. Acetolysis of cellulose with $Cl_2$ and $SO_2$ catalysts produced highly degraded acetates which upon subsequent methanolysis formed D-glucose [16]. The nature of the C-O-C bond between the glucose units was first recognised by Haworth [17 and 18]. Later the polarimetric and kinetic evidence of Freudenberg et al [19 and 20] demonstrated that 99% of the glycoside bonds are a 1,4-β-D-link.

X-ray and NMR studies reviewed by Krassig [21] have shown that the β-D-glucose exists in the pyranose form and the latter in the $^4C_1$ chair formation - the lowest energy conformation of β-D-glucopyranose. Figure (1.4) shows D-glucose and the formation of β-D-glucopyranose. Cellulose is a natural high polymer, the pyranose rings are linked together in thread like chains with a molecular length of 1,000 to 15,000 glucoside units. The chains are joined together by H-bonds in one plane and Van der Waals forces in the other as shown in figure (1.5). These lateral forces can be so regular that a crystalline structure is obtained.

Perfectly dry cellulose may be classified into four different crystal structures [22]. Natural cellulose, designated cellulose I, is found to varying extents as a constituent part of many plants and microorganisms. Its purest form, cotton-seed hairs, contains only 2% non-cellulosic material whereas wood is only 40-50% cellulose [16]. Isolation and purification of cellulose depends on its source and the purpose for which it is required. The basic principle of recovery is to subject native cellulose to reagents which dissolve or destroy non-cellulosic impurities and have no or little effect on the cellulose itself.

Figure 1.3 1,4-β-D-linked polyanhydro glucopyranose

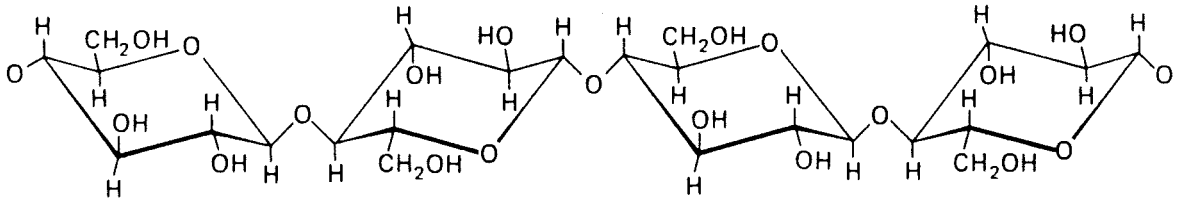

Figure 1.4(a) D-glucose

* Chiral carbon atom

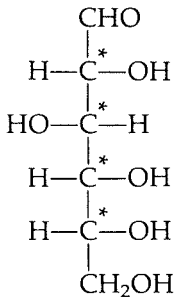

D-glucose

Figure 1.4(b) Formation of the pyranose ring.

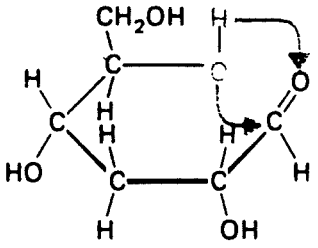

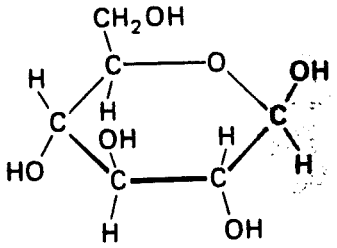

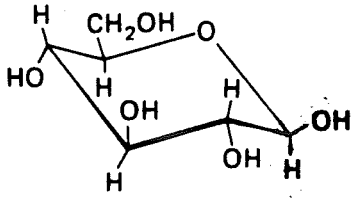

$^4C_1$ Chair conformation

Figure 1.5 Crystal lattice of native cellulose showing the relationship between Hydrogen bonds and Van der Waals forces [23].

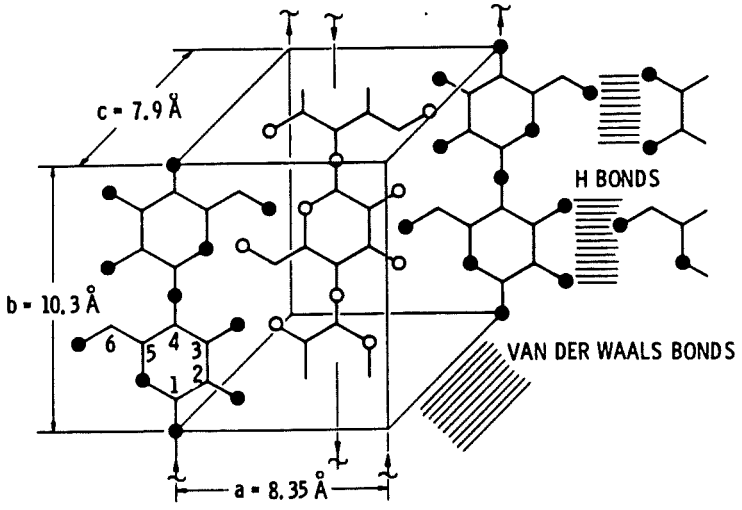

Cellulose II is obtained from cellulose I by regeneration [24], by precipitation [24] or mercerisation [25]. PUDO 193, Cellophane, the cellulose type of interest in this study has cellulose II structure, which has been regenerated from cellulose I. Besides the cellulose I and cellulose II modifications, two other polymorphic lattice structures are known, namely the cellulose III and cellulose IV. Cellulose III is formed by treating native or regenerated cellulose in liquid ammonia or dry ethylamine and has a lattice structure closely related to cellulose II. Cellulose IV is obtained by the treatment of regenerated cellulose fibres in hot baths under stretch, yielding a structure similar to cellulose I.

A crystal structure is characterised by its unit cell and the positions of the atoms or molecules within it. The differences in the crystalline structures of cellulose I and cellulose II can be seen in figure (1.6). Cellulose I is defined by the crystal structures of Meyer and Misch [26 and 27] and Meyer and Mark [28], their monoclinic lattice is based on a unit cell with dimensions a = 8.35Å, b = 10.3Å (fibre axis), c = 7.9Å and $\beta$ = 84°. Figure (1.6) shows the arrangement of chains in the cross-section of the unit cell perpendicular to the fibre axis. For cellulose I, a cellulose chain is located in the corner of each cell and another in the centre. Overall cellulose I has a parallel chain structure.

Cellulose II is described by the crystal structure of Andress' [29] which is based on a unit cell with dimensions a = 8.1Å, b = 10.3Å (fibre axis), c = 9.1Å and $\beta$ = 62°. This unit cell has almost the same volume as cellulose I and the same density, 1.59gcm$^{-3}$ (based on two residues per unit cell), but the pyranose rings of the cellulose chains are rotated until nearly parallel to the $(10\bar{1})$ planes. The chains at corners and centres form two families with reverse chain directions, producing an anti-parallel structure. The centre chain is displaced longitudinally from the cellulose I position to allow hydrogen bonding to occur in the diagonal direction.

Figure (1.7) shows an X-ray diffraction spectra of PUDO 193 cellulose [30] viewed from three perpendicular directions. The principal peaks are due to the 002, 101, and $10\bar{1}$ planes (figure (1.6)). As previously reported [22] the film is highly orientated, with the 101 and $10\bar{1}$ planes lying approximately parallel and perpendicular to the film surface respectively. A single cellulose polymer chain may start in a crystalline region, pass through an amorphous region and finish in a crystalline region. In amorphous

Figure 1.6 Unit cell structures of native cellulose I [26, 27 and 28] and of mercerised cellulose II [29].

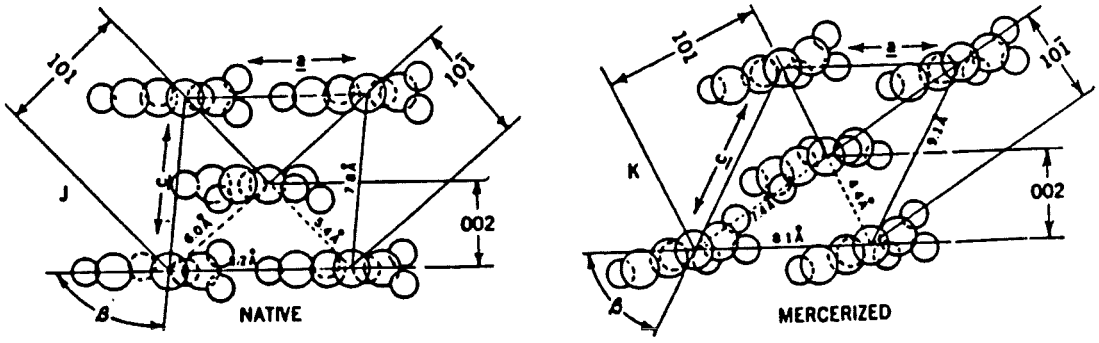


Cellulose I
ac projection

Cellulose II
ac projection

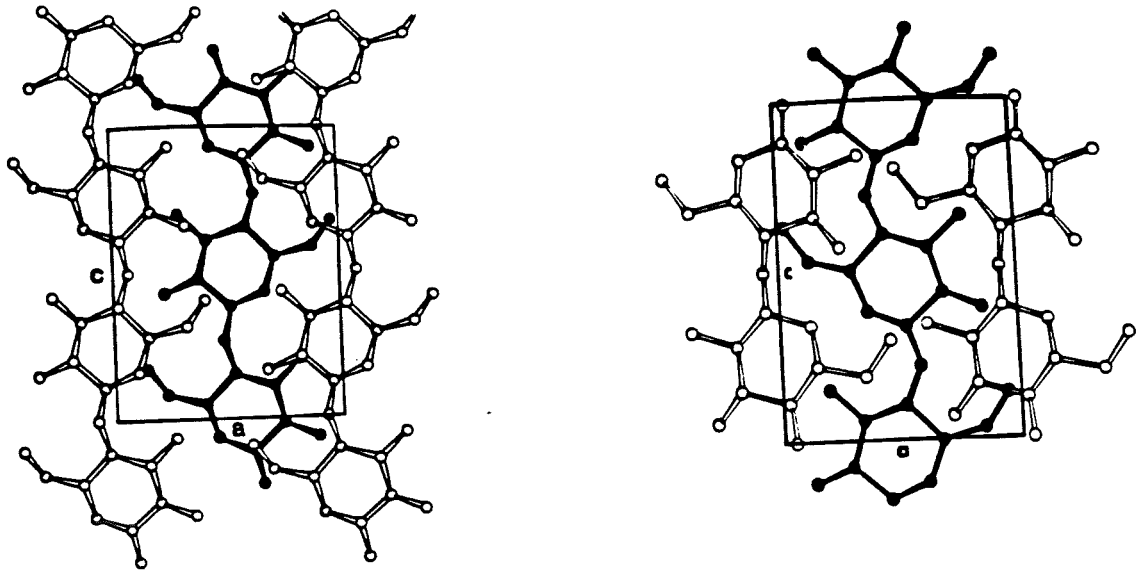

Figure 1.7 X-ray diffraction spectra of PUDO 193 cellulose aligned in three perpendicular directions. Beam impinging upon (A) edge cut along length, (B) edge cut across width, and (C) flat surface of film [30].

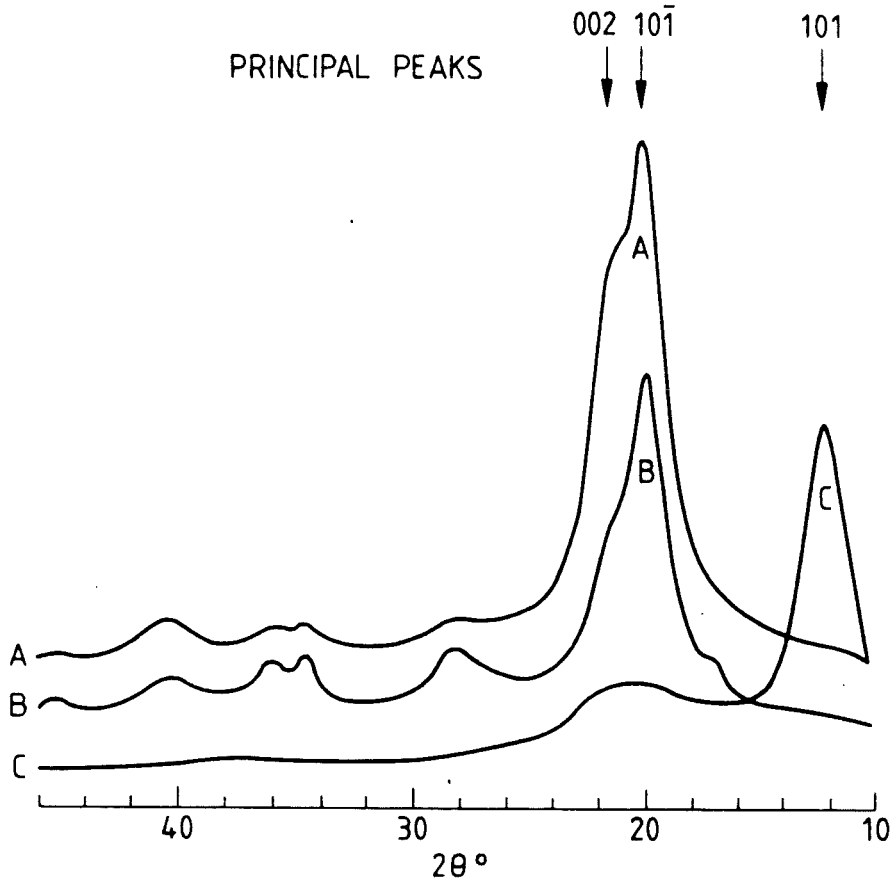

regions the chains though approximately parallel to the fibre axis are less highly orientated and possess a lower degree of hydrogen bonding.

A general representation of a cellulose fibre, figure (1.8), has a number of roughly parallel chains which come together forming discrete regions of a crystalline nature. The high strength of cellulose fibres may be due to the chain ends held in lattices by strong hydrogen bonding forces [16]. Spectroscopic methods may be used to shed light on the intra- and intermolecular hydrogen bond schemes within the cellulose fibres.

A recent review of the structure of cellulose [31] discusses a new method of structure determination namely, X-ray diffraction analysis combined with computer based stereochemical modelling and cross polarisation-magic angle spinning $^{13}C$ NMR (CP-MAS) spectroscopy. Using CP-MAS, Kamide et al [32] have shown that cellulose I has cellobiose units with $O_3H$---O-5′ and $O_2H$---O-6′ intramolecular hydrogen bonds and units without hydrogen bonds and cellulose II contains cellobiose units with $O_3H$---O-5′, $O_2H$---O-6′, $O_6H$---O-2′ intramolecular hydrogen bonds and units without intramolecular hydrogen bonds.

Earlier, polarised infrared spectroscopy [33] was used to select possible arrangements of interchain hydrogen bonding with crystalline polysaccharides. Hermans [34 and 35] proposed two different intramolecular hydrogen bonds in cellulose I, $O_3H$---O5′ and $O_6H$---O-1 the latter undetected by Kamide. Intermolecular hydrogen bonding is in the 002 plane between the $O_2H$ group and the O-6 oxygen [33]. Figure (1.9) compares the hydrogen bond schemes proposed for cellulose II. The scheme proposed by Marrinam and Mann [36 and 37] is in agreement with the CP-MAS data though Blackwell and Marchessault [33] suggest the more likely solution is the one proposed by Marchessault and Liang [38] where the two parallel bands in the observed IR spectra are both assigned to $O_3H$---O-5′ bonding.

The chemical character of cellulose is governed by the 3 reactive hydroxyls, one primary and two secondary in each repeating glucose unit. The acidic nature of the hydroxyl group is shown by their reaction with metallic sodium in liquid ammonia [25].

$$2ROH + 2Na \rightarrow 2RONa + H_2 \qquad (1.11)$$

Sodium alcholates are formed with the liberation of an atom of hydrogen for each atom of sodium consumed.

Figure 1.8 General representation of a cellulose fibre [16].

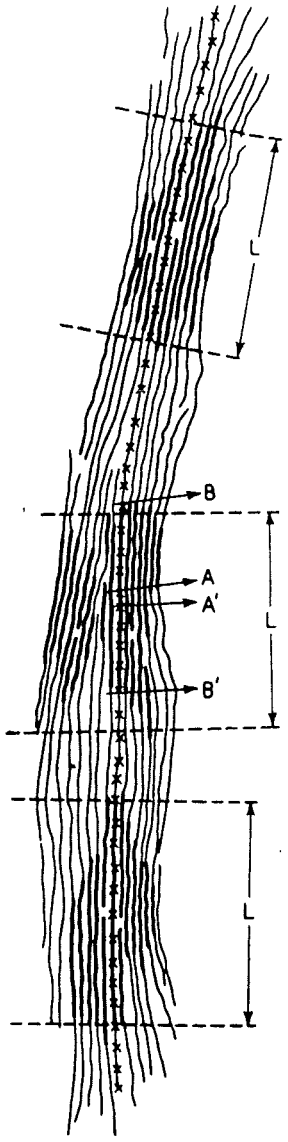


(Mark,[80] by courtesy of the *Journal of Physical Chemistry*)

A, A', B' are chain-ends within the crystallized region;
B is a chain-end outside the crystallized region;
L is the length of the crystallized region

*Main-valence chains going through more than one micella*

Figure 1.9 Comparison of the hydrogen bond schemes proposed for cellulose II [33].

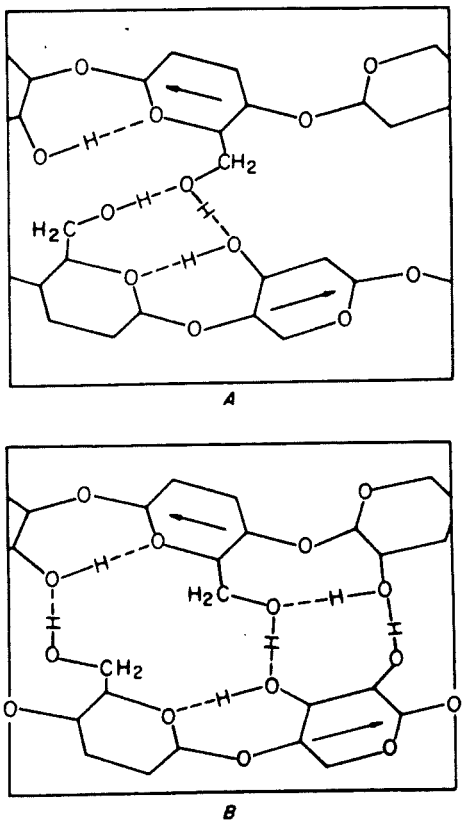

## 1.4 The structure and preparation of Permion.

The term Permion describes a series of ion-exchange membranes prepared by the RAI corporation by the modification of inert polyethylene, polypropylene and Teflon base films. In this thesis, the term Permion describes one of these membranes, namely Permion 2291 40/30, a co-polymer of methacrylic acid and cross-linked low density polyethylene.

Permion membranes are prepared by grafting - a chemical or radiation initiated process whereby the base polymer is modified by adding onto the long polymer chains, side chains which have a chemical characteristic different from that of the polymer. Hence polyethylene which is resistant to oxidation, (a desirable membrane property) but ionically resistive, (an undesirable membrane property), is modified by grafting to yield a material capable of ionic conduction. When polyethylene is exposed to gamma rays a free radical is formed by the cleavage of a C-H bond. This free radical can undergo three processes, cross-linking, degradation and grafting, as shown in figure (1.10). If no other reactant is present then cross-linking and degradation occur simultaneously. Fortunately, with polyethylene the desirable reaction, ie. cross-linking, is predominant. Cross-linking modifies the polyethylene chains giving a tight three-dimensional structure, whereas degradation decreases the chain length or the molecular weight (MW) of the polyethylene. Grafting is the process whereby a monomer reacts with the free radical producing a grafted side chain on the polymer. The monomer may be a strong or weak acid such as sulphonic or acrylic, a strong or weak base such as quaternary amines or amides, or a non-ionic graft for example vinylpyrrolidone. A schematic diagram of the membrane structure is shown in figure (1.11). In the formulation of membranes the following parameters are important, (i) The molecular properties of the base resin, including crystallinity, MW distribution and the absence of low MW fractions. (ii) The extent to which the base resin in film form is cross-linked. (iii) The type of monomer grafted to the cross-linked film.

The preparation of Permion is a stepwise process [39]. The polyethylene resin, Bakelite DFD-0602 is selected on the basis of it's narrow MW distribution and because it contains few low MW fractions. The molecular weight distribution is gauged from the ratio, weight average molecular weight to the no. average molecular weight (MW/MN)

Figure 1.10 Possible reactions of the free radical showing the desirable end product, Permion [40].

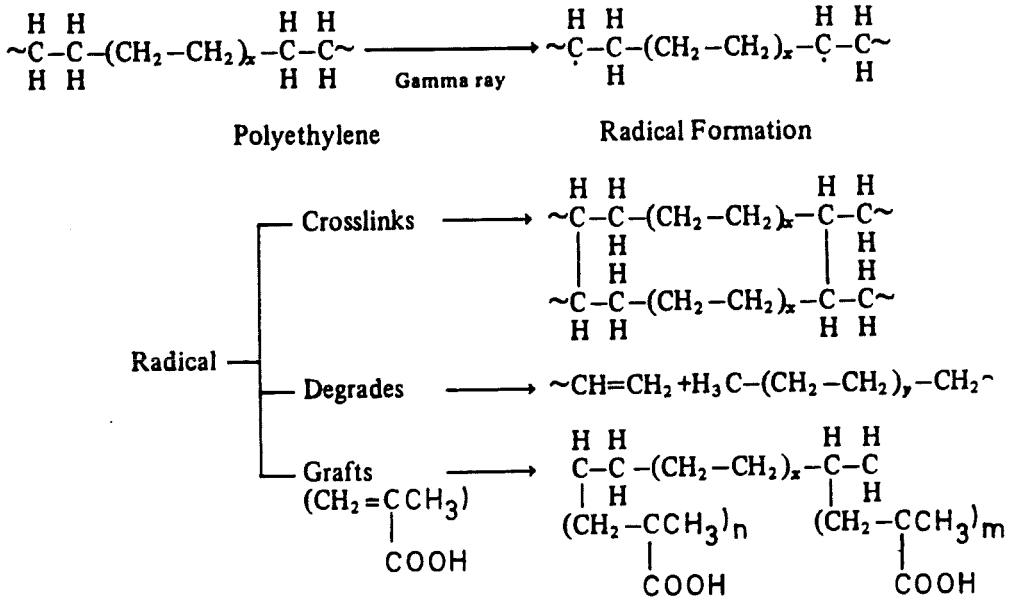


Figure 1.11 Schematic diagram of Permion [41]

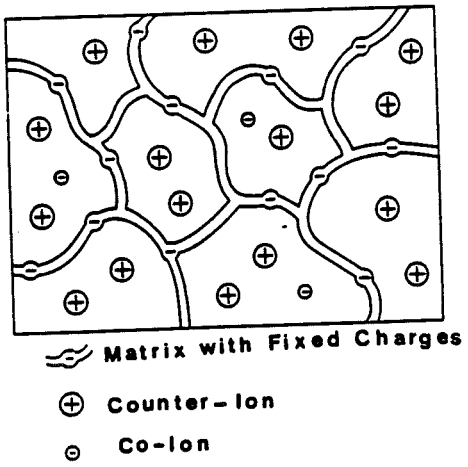

of the resin. A resin with a small MW/MN ratio is more efficient at cross-linking [40]. The base film is then extruded as a lay-flat film to 1 ± 0.1mm.

In production terms it is easier firstly to graft a monomer to the polymeric chain and then perform the cross-linking, but a membrane of superior quality is obtained by cross-linking then grafting. The base film is cross-linked using a high energy electron accelerator. The dose of electrons received by the film varies with the thickness of the film. Hence to minimise the variation in amount of cross-linking through the film, one side of the film is irradiated for half of the required dose, the film is then turned over for the remainder of the 90Mrads dose.

The linear polymer has now been converted to a three-dimensional structure. The extent of cross-linking is indicated by gel fractions and Mc values, the molecular weight between cross-links. The gel fraction (% Gel) of a cross-linked polymer film is given in equation (1.12)

$$\% \text{ Gel} = \frac{W_G}{W_O} \times 100 \qquad (1.12)$$

where $W_O$ (g) is the weight of the as received film and $W_G$ (g) is the dry weight of the film after extraction with hot xylene to remove any soluble polymer leaving an insoluble three-dimensional fraction. Mc can be determined by extraction with a solvent or by a hot modulus measurement. In the former method, Mc is related to $q_o$ as shown in equation (1.13),

$$Mc = \frac{w}{q_o r} \qquad (1.13)$$

where $q_o$ is the cross-link density per unit dose ($rads^{-1}$) and can be obtained from a solvent-dose plot, r is the dose (rads) and w ($gmol^{-1}$) is the molecular weight of the repeating unit in the polymer. In the latter, Mc is related to the modulus $E_P$ ($Nm^{-2}$) of the polymer as follows

$$E_P = \frac{3\rho RT}{Mc} \qquad (1.14)$$

where $\rho$ ($gcm^{-3}$) is the density of the polymer at temperature T (K), and R is the gas constant, ($8.314JK^{-1}mol^{-1}$). Quality control demands that the membrane is acceptable if the gel content is greater than or equal to 70% and the Mc value is less than or equal to 5,000. A small Mc value means a tight structure.

The cross-linked film is interwound on a three inch core with a paper mesh spacer (Lenonet), placed in the grafting solution and swelled to equilibrium for a period of at least 24 hours. Typically the composition of the grafting solution, expressed as % by weight, is glacial Methacrylic Acid 17.5%, Benzene 80.2% and Carbon Tetrachloride 2.3%. The reaction vessel with the polyethylene film and solution is then placed in a radiation vault, exposed to Cobalt 60 gamma radiation at a dose rate of 10,100rads/hr to a total dose of 1.51Mrads, and is thereby grafted. Upon completion of the grafting process the roll is removed from the reaction vessel and the membrane film is separated from the Lenonet spacer. The grafted film is subsequently washed in water (90-95°C) to remove homopolymer formed during the radiation and converted from the acid to the salt form by reaction in 5% KOH solution at 90-95°C. The converted membrane is washed in water to remove residual homopolymer and alkali and is finally dried.

## 1.5 The aims and objectives of the work

Button cells constructed by the partial sponsor of this work, Duracell Batteries Ltd., incorporated a tri-laminate separator of Cellophane and Permion. The initial purpose of this work was to characterise each membrane as follows.

(i) Investigation of the swelling behaviour and the ion-exchange properties, including ion-exchange capacity.

(ii) Measurement of ionic ($K^+$) and solvent ($H_2O$) transport numbers.

(iii) Measurement of ionic conductivity and the derivation of ionic mobilities.

The above parameters were measured whilst the membranes were swollen in solutions of KOH, the electrolyte used in the construction of the button cells. Although in batteries the concentration of the electrolyte is between 7 and 10M, the experimental work was conducted over a much wider concentration range of KOH solutions.

If a Cellophane and a Permion membrane, swollen in a solution of KOH are placed juxtaposition an interface between the two membranes is established. Since the individual membranes are likely to have dissimilar transport properties the interface will have an effect on the transport of potassium and water through an assembly. This was investigated by the determination of potassium ion and water transport numbers through assemblies of the two membranes. Two orientations were investigated, firstly where Cellophane was positioned on the side receiving the cation, then where Permion was adjacent to the electrolyte receiving the cation, i.e. both the Cellophane/Permion and the Permion/Cellophane interface occurring in a tri-laminate. From this primary data, behaviour of the membranes in the battery environment should be evident.

# CHAPTER 2

# THE SWELLING AND ION-EXCHANGE PROPERTIES OF PERMION AND CELLOPHANE

## 2.1 Introduction

### 2.1.1 Swelling behaviour and osmotic pressure

When a dry membrane is placed in water or aqueous electrolyte (in this study potassium hydroxide solutions) it has the ability to sorb these solvents with the effect that the membrane usually expands or "swells". By this process firstly the ionisation groups close to the membrane surface attract and hold water of hydration. The strength of binding depends on the charge and the size of the ions formed. The swelling process continues to be driven by osmotic forces and the $H_2O$ activity differences between the external solution and the membrane phase. The coiled and packed chains of the matrix unfold and make room for the water molecules, but due to the crosslinking the chains cannot separate completely and as a result the membrane swells but does not dissolve. Insertion of water into the network, enables some of the counter-ions to diffuse away from the fixed charge groups. The need to maintain electroneutrality prevents them from leaving the membrane and they create an osmotic pressure which draws more water into the membrane and swells it further.

An osmotic pressure arises when two solutions of different concentrations (or a pure solvent and a solution) are separated by a semipermeable membrane. The osmotic pressure across the membrane/solution interface is determined by the condition that, for equilibrium the chemical potential of the solvent in the solution on one side of the membrane must be equal to the chemical potential of the solvent in the solution in the membrane where it is subjected to a hydrostatic pressure equal to the osmotic pressure. Initially the chemical potential of the water in the electrolyte solution in the membrane is less than the chemical potential of the water in the more dilute external electrolyte solution and so the solvent has a tendency to flow into the membrane. However the chemical potential increases with pressure and so a balance is reached when

$$\mu_w = \bar{\mu}_w \qquad (2.1)$$

where $\mu_w$ ($Jmol^{-1}$) is the chemical potential of water and the barred symbol refers to the membrane phase. There are two factors tending to cause the value of $\bar{\mu}_w$ to depart from

$\mu_w$ and these have equal and opposite effects on $\bar{\mu}_w$. The dilution process occurring in the membrane causes a change in the chemical potential equal to,

$$\Delta \mu_w = RT \ln \frac{\bar{P}_w}{P_w} \qquad (2.2)$$

where P (atm) is the partial vapour pressure and R and T take their usual meanings of gas constant (8.314 $JK^{-1}mol^{-1}$) and temperature (K) respectively. Exactly counteracting this is the increase in $\bar{\mu}_w$ in the membrane due to the imposed osmotic pressure, $\Pi$ (atm) generated by the expanded polymer framework.

It is known that ;

$$d\mu_w = V_w dP \qquad (2.3)$$

where V ($mol^{-1}m^3$) is the partial molar volume of the solvent in the solution, so that

$$\Delta \mu_w = \int_0^{\pi} V_w dP \qquad (2.4)$$

At equilibrium, therefore, in order that $\bar{\mu}_w$ in the membrane should equal $\mu_w$ in the external electrolyte solution,

$$\int_0^{\pi} V_w \, dP = -RT \ln \frac{\bar{P}_w}{P_w} \qquad (2.5)$$

If it is assumed that the partial molar volume $V_w$ is independent of pressure, i.e., the solution is incompressible,

$$V_w \Pi = RT \ln \frac{P_w}{P_w} \qquad (2.6)$$

The significance of this equation can be stated as follows, the osmotic pressure is the internal pressure that must be exerted by the membrane framework to the internal solution to raise the vapour pressure of the solution in the membrane to that of the external solution.

Swelling equilibrium is a balance of opposing forces. The tendency of the polar and ionic constituents to surround themselves with solvent and thus to stretch the membrane meets with an increasing resistance by the latter. Equilibrium is attained when the elastic forces of the membrane balance the dissolution tendency.

### 2.1.2 Donnan equilibrium

Comprehension of the electrolyte absorption properties of a membrane needs consideration of Donnan equilibrium. Consider placing a cation exchange membrane (containing no sorbed electrolyte) in a dilute solution of strong electrolyte. There are concentration differences between the membrane and the electrolyte phases. The cation concentration is larger in the membrane and the (mobile) anion concentration is larger in the solution. If the ions carried no charge then this concentration difference would be levelled out by diffusion. This process would disturb the electroneutrality since actually the ions are charged. Migration both of cations into the solution and of anions into the membrane would result in the accumulation of positive charge in the solution and of negative charge in the membrane. Therefore the first few ions which diffuse build up an electric potential difference between the two phases. This is the Donnan potential and pulls back cations into the negatively charged membrane and anions back into the positively charged solution.

A sketch of a membrane and an electrolyte phase with the interface between them is shown in Figure (2.1).

Figure 2.1 The interface between membrane and electrolyte phases.

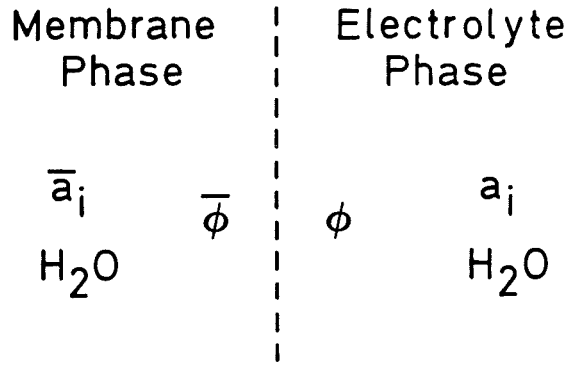


where $\phi$ (V) is the electrical potential and a the activity which is dimensionless.

An equilibrium is established, in which the tendency of ions to level out the existing concentration difference is balanced by the action of the electric field. At equilibrium the electrochemical potential, $\mu_i^*$, of a species, i, must be the same in both phases [42] i.e.,

$$\bar{\mu}_i^* = \mu_i^* \tag{2.7}$$

The electrochemical potential is comprised of a chemical potential and an electrical potential, according to

$$\bar{\mu}_i^* = \bar{\mu}_i + z_i F\bar{\phi} \tag{2.8}$$

$$\mu_i^* = \mu_i + z_i F\phi \tag{2.9}$$

where, z is the magnitude of the charge of species, i and F the Faraday constant (96485 $Cmol^{-1}$). The activity a is introduced with the help of the following relations

$$\bar{\mu}_i = \bar{\mu}_i^0 + RT\ln\bar{a}_i \tag{2.10}$$

$$\mu_i = \mu_i^0 + RT\ln a_i \tag{2.11}$$

where $\mu_i^0$, the standard chemical potential, is considered to be equal in both phases.

Combination of equations (2.7, 2.8, and 2.9) leads to

$$\bar{\phi} - \phi = \frac{(\mu_i - \bar{\mu}_i)}{z_i F} \tag{2.12}$$

The term on the left symbolises the Donnan potential, the force that arises, at the boundary of a charged membrane, to balance the tendency of ions to level out any difference in concentration. Equation (2.12) can be further simplified by substitution of equations (2.10 and 2.11). The resulting relation becomes

$$\bar{\phi} - \phi = \frac{RT}{z_i F} \ln\frac{a_i}{\bar{a}_i} \tag{2.13}$$

After rearranging equation (2.13), we obtain the following Donnan Equilibrium expression

$$\left(\frac{a_i}{\bar{a}_i}\right)^{\frac{1}{z_i}} = \exp\left(\frac{F}{RT}(\bar{\phi} - \phi)\right) = \text{const} \qquad (2.14)$$

where the exponential term is a constant, particular to a given system. In this study with the ions $K^+$ and $OH^-$ the activities may be expressed

$$\left(\frac{a_1}{\bar{a}_1}\right)^{+1} = \left(\frac{a_2}{\bar{a}_2}\right)^{-1} \qquad (2.15)$$

The $^+1$ and $^-1$ are the charges of the $K^+$ and $OH^-$ ions respectively. Further more, the activity of a species i, is related to the concentration by

$$a_i = \gamma_i c_i \qquad (2.16)$$

and

$$\bar{a}_i = \bar{\gamma}_i \bar{c}_i \qquad (2.17)$$

where $\gamma_i$ denotes the activity coefficient of an ion and c ($moledm^{-3}$) is the concentration. With the following ratio equal to one [43 & 44]

$$\frac{\bar{\gamma}_{K^+}\bar{\gamma}_{OH^-}}{\gamma^2_{KOH}} = 1 \qquad (2.18)$$

equation (2.16) reduces to

$$\bar{c}_{K^+}\bar{c}_{OH^-} = c^2_{KOH} \qquad (2.19)$$

The electroneutrality in the membrane phase is given by

$$\bar{c}_{K^+} = X + \bar{c}_{OH^-} \qquad (2.20)$$

where X is the concentration of the fixed charge groups. Combination of equations (2.19 and 2.20) yields the following expressions;

$$\bar{C}_{K^+} = \left(C^2_{KOH} + \frac{X^2}{4}\right)^{\frac{1}{2}} + \frac{X}{2} \qquad (2.21)$$

$$\bar{C}_{OH^-} = \left(C^2_{KOH} + \frac{X^2}{4}\right)^{\frac{1}{2}} - \frac{X}{2} \qquad (2.22)$$

where the internal concentrations of $K^+$ and $OH^-$ are written in terms of the external concentrations. Therefore in the ion-exchanger the counter-ion concentration remains much higher and the co-ion concentration much lower than in the external solution. The situation is analogous for an anion exchange membrane except that the Donnan potential is of opposite polarity.

The electrical potential difference between the membrane and the external

solutions can attain very high values. But chemical analysis of membrane or solution cannot detect deviation from electroneutrality. Migration of a few ions is sufficient to build up so strong an electric field counteracting any further migration that deviations from electroneutrality remains far below limit of accuracy of measurement. (Except by measuring the electric field itself).

Donnan potential has the consequence, for electrolyte sorption that it repels co-ions from the membrane and thus prevents the internal co-ion concentration from rising beyond an equilibrium value, which is usually much smaller than the concentration in the external solution. Co-ion uptake and electrolyte sorption are equivalent because of the electroneutrality requirement.

Therefore electrolyte is partially excluded by the ion-exchange membrane. This Donnan exclusion is a unique feature of electrolyte sorption by ionic sorbents.

The aim of the chapter is to report the swelling behaviour and the ion-exchange properties of Cellophane and Permion membranes when equilibrated in KOH solutions.

## 2.2 Experimental

### 2.2.1 Materials and reagents

The Cellophane ion-exchange membrane studied was PUDO 193, manufactured by DuPont from regenerated cellulose. The grafted co-polymer was Permion 2291 40/30 prepared by the RAI research corporation of Hauppauge, New York. For these experiments both membranes were cut from dry rolls of width 30cm.

The electrolyte solutions were freshly prepared from BDH Analar potassium hydroxide pellets and singly distilled water. For volumetric analysis of the electrolyte solutions, solutions of hydrochloric acid were prepared by direct dilution of a BDH analytical volumetric solution of molar HCl. In later experiments a BDH A.V.S. of 0.1M HCl was used directly.

Where KOH/KCl solutions were required, the KCl (Aristar or Analar grade from BDH) concentration was determined by weight and the KOH concentration was determined by titration with HCl. Determination of ion-exchange capacities required the following AVS solutions, 1M $HNO_3$, 0.05M $H_2SO_4$, 2M HCl and 0.1M NaOH, from BDH.

The pH indicator solutions were methyl orange solution, pH = 2.9-4.6, with a colour change of orange-red to orange-yellow and BDH 4460 indicator, pH = 4.4-6.0, with a colour change of red to green.

Standard solutions for atomic absorption spectrophotometric analysis were prepared by direct dilution of 1,000ppm. $KNO_3$ and $AgNO_3$ Spectrosol solutions. Dilution was made using deionised water. It was found that aspirating a deionised water blank produced a similar absorbance to a distilled water blank with potassium and silver lamps.

### 2.2.2 Measurement of dimensional changes

Rectangles of membrane, 5cm. by 8cm, were cut from each roll and their dimensions noted, before and after equilibration in electrolyte, with a steel rule (length and width) and a Alfred Herbert Ltd. sigameasure (thickness).

A corner of each rectangle was cut off to distinguish between the two lengths

and the two widths. Soaked films were stored in a stoppered flask at room temperature in air for one week. Since films were soaked for a shorter period prior to transport number determinations, films were removed after one day in a few experiments.

The sigameasure could be fitted with flat anvils of diameter 9.53mm, 3.19mm, 1.26mm, 0.076mm and 0.010mm. In early Cellophane work thickness was determined by one reading with the 3.19mm anvil. In later work and for Permion, the 3.19mm anvil was used, but the thickness was taken as the average of 25 readings.

After immersion the excess electrolyte was removed using tissue paper, a technique which tended to slightly shrink the Permion membrane. To obtain an accurate swollen length and width for Permion the wet membrane was placed on a glass slide with a few drops of electrolyte on top and then measured. An alternative method for removing excess electrolyte was to wipe each face of the membrane three times with a glass slide.

Dimensional changes were determined in a wide range of KOH concentrations.

### 2.2.3 Determination of ion-exchange capacity by pH titration

The apparent ion-exchange capacity of a weak acid membrane such as Permion may be determined by the classical method of Topp and Pepper [45]. In this method the capacity is determined as a function of pH by titration. The membrane, in the acid form, is equilibrated with a known quantity of alkali and an aliquot of the final solution is analyzed to determine the loss of base from the solution.

Strips of Permion, 15cm x 2cm in dimension, were cut from the roll and soaked together overnight in a solution of 2M HCl to regenerate the acid form of the membrane. The carboxylic acid group of the membrane is in the potassium form when received from the manufacturer.

Three series of KOH/KCl solutions were prepared. Each series of five solutions contained KOH of the following concentrations 0.1M, 0.05M, 0.025M, 0.01M and 0.001M. KCl was added to each solution in the first and second series to a concentration of 0.1M and 1.0M respectively. No KCl was added to the third series. Concentrations of 0.1M, 0.05M and 0.025M KOH were determined by titration with 0.1M HCl, and concentrations of 0.01M and 0.001M KOH were determined by titration with 0.005M

HCl prepared by the direct dilution of a 0.1M HCl AVS. The concentration of the added KCl was known because it was accurately prepared by weight.

The strips of Permion were removed from the acid, washed three times in distilled water with 10 minutes soaking between washing, mopped dry with tissue paper and a single piece of membrane was soaked in 25ml of each solution. After two days 10ml of this solution was extracted and its concentration determined by titration. The pH of the remaining solution was recorded.

The acid form of the membrane was regenerated by soaking in a 25ml solution of 2M HCl for 3-4 hours. Membranes were washed three times in water, with 10 minutes soaking in between, and the weights obtained after drying overnight in an oven at 110°C.

Plots were obtained of the loss of base from the solution in mmol/g of dry membrane versus the pH of the remaining solution.

### 2.2.4 Determination of ion-exchange capacity using a $Cl^-$ ion tracer

Cellophane, a very weak-acid membrane ionises only in strongly alkaline solutions [46]. The ion-exchange capacity of Cellophane can therefore not be determined by the method described in the previous section and an alternative approach is required. The alternative technique was tested with Permion. If similar ion-exchange capacities were obtained by the two methods then the alternative technique could be adopted for Cellophane.

After equilibration in KOH solutions the potassium ion content of the membrane and the weight of the solution sorbed by the membrane could be determined by direct analysis. The mobile anion ($OH^-$) content and consequently the ion-exchange capacity could not be measured directly. To obtain this data a technique was employed which assumed that the membrane showed no preferential Donnan exclusion for anions [46]. A small quantity of KCl was added to the electrolyte, sufficient such that the resultant electrolyte was typically 0.1M with respect to $Cl^-$, and the $Cl^-$ content in the membrane could then be determined. Since the ratio of $OH^-$:$Cl^-$ was known in the external solution this was used to deduce the $OH^-$ content in the membrane from the $Cl^-$ content in the membrane.

At each external electrolyte concentration studied ten samples of membrane, each approximately $16cm^2$, were stored for one week in a stoppered flask containing approximately 60ml of electrolyte (KOH/KCl). The KOH concentration of the electrolyte prior to use was determined by titrating a solution, diluted to about 0.1M, with 0.1M HCl. The KCl, of approximate concentration 0.1M, was accurately known because it had been prepared by weight. After one week the films were removed and blotted dry on tissue paper.

The ten pieces of membrane were analysed as follows. Five pieces were analysed together for $Cl^-$. The membrane films were placed in a dish and the chlorine ions leached out by soaking overnight in 10ml of 1.0M $HNO_3$. The acid was decanted off and the membrane washed three times with 3ml portions of distilled water, each time leaving the membrane in the water for at least 10 minutes. During this time to aid the washing process the pieces were turned and separated by tweezers. The combined acid and water washings were made up to 25ml with distilled water in a volumetric flask. A 20ml aliquot was removed for analysis.

To this aliquot, 10ml of 1000ppm $AgNO_3$ spectrosol solution was added to precipitate $Cl^-$ as AgCl(s). This was filtered through a No.4 sintered glass crucible by gentle suction, and the precipitate washed with 1M $HNO_3$ (2x3ml). The filtrate containing excess silver was made up to 1 litre in a volumetric flask. The solution was diluted by an amount appropriate to give a concentration of silver in the range 0-5$\mu gml^{-1}$ and analysed by atomic absorption spectrophotometry. Its concentration was determined relative to the standard silver solutions. The instrument was auto-zeroed against a blank (de-ionised water), and the absorption of the aspirated solution taken to be the average of 10 readings.

From the amount of silver determined, the concentration of silver precipitated as AgCl could be calculated and hence the quantity of $Cl^-$ ions in the membrane. The membrane was dried overnight at 110°C and weighed, hence the $Cl^-$ content could be quoted, milligram per gram of dry material. From the $Cl^-$ content the $OH^-$ content was determined by application of the $OH^-$:$Cl^-$ ratio in the external solution.

The potassium content of the film was determined by two methods:- (i) direct titration and (ii) analysis using AAS. The total $K^+$ value in the membrane was taken to be the average of these determinations. Two samples of membrane were placed in two

flasks together with a small volume of water. The KOH content of each was determined by titration with 0.05M $H_2SO_4$. The titration detects the $K^+$ associated with the $OH^-$ and the $K^+$ associated with fixed charges but obviously not the $K^+$ associated with the $Cl^-$, hence the $K^+$ content of the film is the sum of the amount determined by titration together with the $Cl^-$ content of the film as determined by precipitation of AgCl.

A further two membrane films were placed in separate dishes and the $K^+$ leached out by soaking overnight in 10ml of 1M $HNO_3$. The solution was decanted off and the membrane was washed three times with 3ml portions of distilled water. The acid solution and washings were combined and the final solution made up to 1 litre in a volumetric flask.

The solution was diluted by an appropriate amount to give a concentration of potassium in the range 0-2$\mu gml^{-1}$. The amount of $K^+$ in the membrane determined by titration was used to estimate the dilution factor required to achieve this. The filtrate from the silver determination was also diluted and analysed for potassium. The three solutions were analysed by atomic absorption spectrophotometry and their concentration determined relative to the standard Potassium solutions.

The final piece of membrane was weighed immediately after blotting to determine the weight of the solution sorbed. Each sample, after use, was dried overnight in an oven at 110°C, then weighed. Hence all the results were related to the final dry weight.

Analysis for ppm. of potassium and silver ions was achieved using a Phillips SP9 atomic absorption spectrophotometer. Standard solutions were prepared within the linear working range at concentration 0.5, 1.0 and 2.0$\mu gml^{-1}$ potassium and 1.0, 2.0, 3.0 and 5.0$\mu gml^{-1}$ silver. Instrumental conditions for silver required a lamp current of 3mA, an Ag absorption line at 328.1nm and a stoichiometric air/acetylene flame. Potassium required a current of 6mA a K absorption line at 766.5nm and a stoichiometric air/acetylene flame. All atomic absorption solutions were prepared with de-ionised water. There was found to be negligible difference in the absorbance of de-ionised water compared with distilled water.

## 2.3 Results and discussion

### 2.3.1 Swelling behaviour

The observed swelling behaviour must be a consequence of the structures of Cellophane and Permion previously described. The dimensional changes of Cellophane and Permion films when equilibrated in solutions of KOH are shown in figures (2.2) and (2.3) respectively. Cellophane swelling is primarily seen as changes in thickness with a percentage increase of 114% in water. Urquhart [47] found that when water penetrated dry Cellophane hydrogen bonds in amorphous regions were broken and new intermolecular hydrogen bonds were formed with the water molecules. During swelling Van der Waals bonds maintained their spacings [23]. Swelling was limited by the non-disrupted hydrogen bonds in the crystalline regions. The accessability of the amorphous regions over the crystalline regions has been shown by Mann [48] by following the exchange of $D_2O$ using infra-red spectroscopy.

Neale [49] treated cellulose as a monobasic acid in alkaline solutions and correctly proposed that swelling was due to the osmotic pressure generated as the result of a Donnan equilibrium. His theory did not take into account the differing accessibilities of crystalline and amorphous regions and the anionic content of the membrane was not measured.

A fuller interpretation of Cellophane swelling by Jenkins et al [30] is discussed in section (2.3.4) together with its ion-exchange properties. The swelling characteristic follows the results reported by Jenkins et al. [30]. Both sets of data have a maximum percentage increase in thickness at an external electrolyte concentration of 5.7M; 293% in this work compared with 315% reported by Jenkins.

Compared with Cellophane, swelling in Permion is significantly less : figure (2.4) illustrates this. With Permion, for each of the measured dimensions, the percentage increase compared with the as received membrane is at a maximum in dilute solutions. The apparent variability of thickness swelling of Permion is a consequence of the non-uniformity of thickness in the as received membrane. The sales literature of the manufacturer [50], reports a maximum expansion by the film of 8% in length and 9% in width after equilibration i.e. 40% KOH for 24 hours. Figure (2.3) shows an expansion of less than 3% in length and confirms 9% in width at this concentration.

Figure 2.2 Percentage change in thickness, length and width of Cellophane relative to the dry membrane vs. KOH concentration.

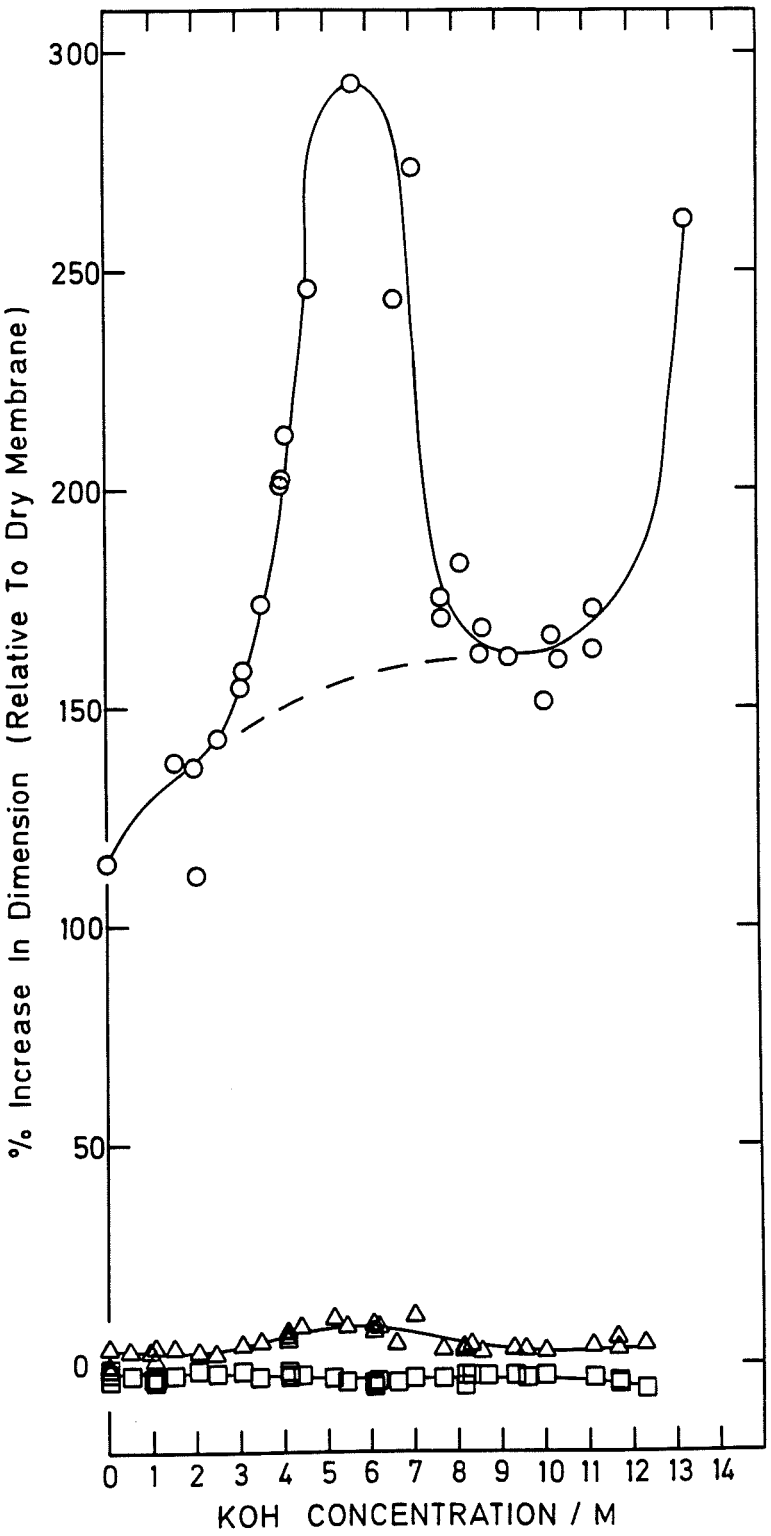

Figure 2.3 Percentage increase in thickness, length and width of Permion relative to the dry membrane vs. KOH concentration.

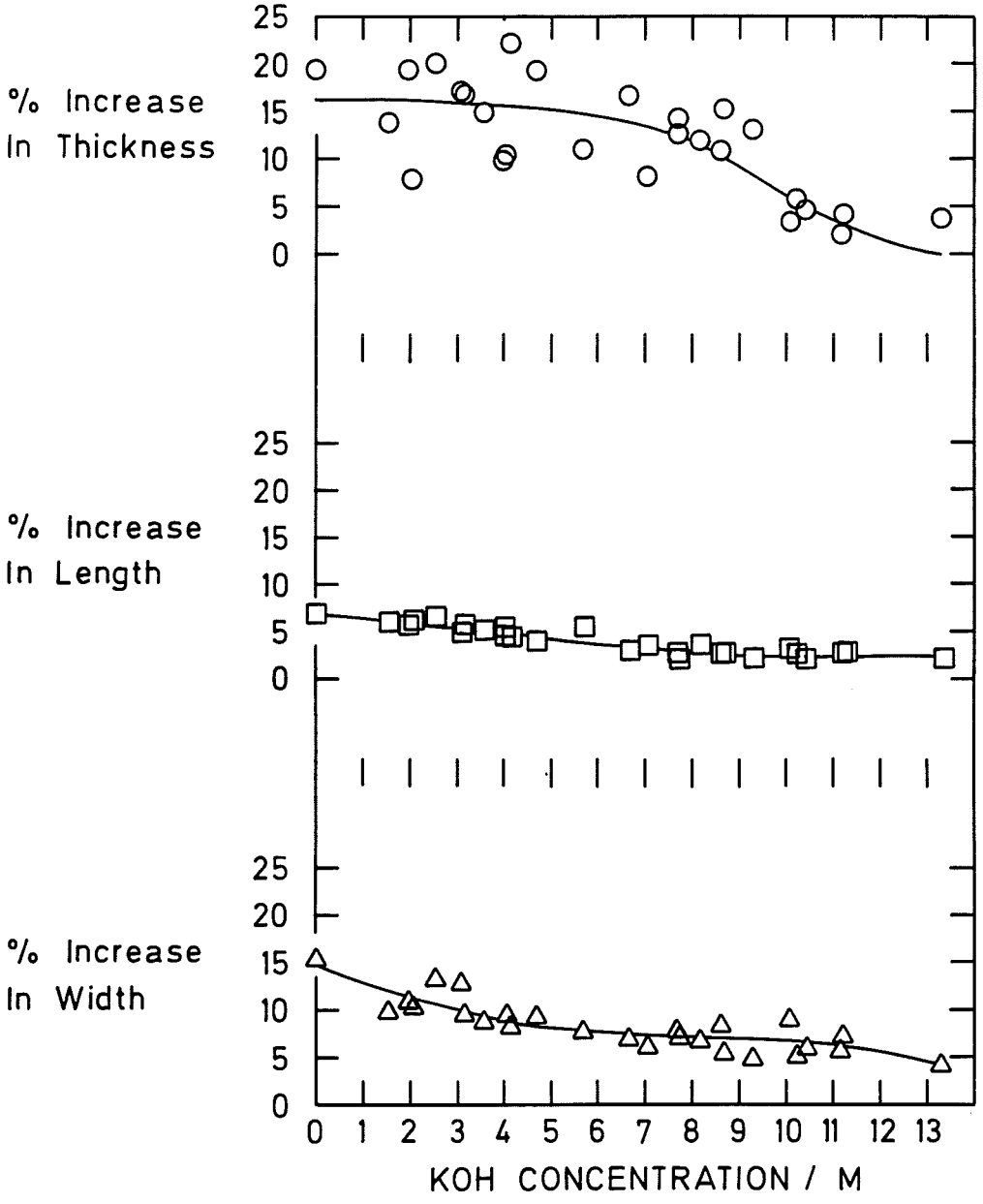

Figure 2.4 A comparison of the increase in thickness of Cellophane and Permion vs. KOH concentration.

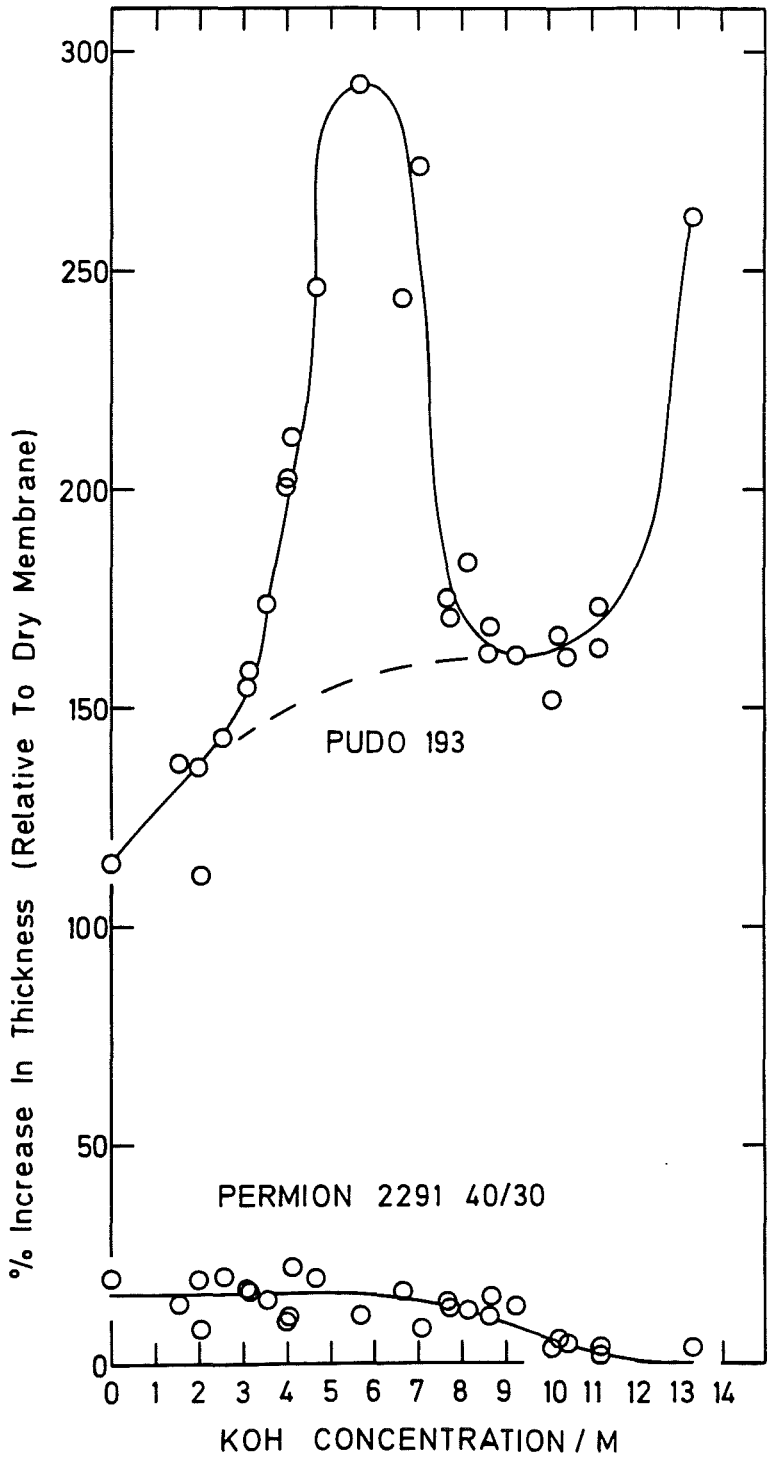

It is proposed that the dotted line in figures (2.2 and 2.4) represents the extent of swelling in the amorphous regions and the perturbation above the dotted line is due to penetration of the crystalline region.

Helfferich [51] reports that the extent of swelling of a membrane experiences depends on a number of factors. The first point is the nature of the solvent, polar solvents are better swelling agents due to stronger interactions with the ions and polar groups of the membrane. The structure of Permion is such that the polymer chains are cross-linked giving a tighter, more compact membrane than Cellophane. A high degree of cross-linking reduces the membranes ability to swell since a greater number of cross links makes the anion framework less flexible and less able to expand. Figure (2.4) illustrates how the differences in joining the polymer chains, i.e. hydrogen-bonds in Cellophane and cross-links in Permion, affects the swelling properties. The nature of the fixed ionic groups, the greater the affinity for the (polar) solvents the more strongly does the membrane swell. High-capacity ion-exchange membranes contain ions in higher concentrations. Therefore, the tendency of the pore liquid to dilute itself due to the difference in osmotic pressure and the resulting swelling are more pronounced than with a low-capacity membrane.

The nature of the counter-ion is also important. Jenkins et al [30] agreed with an earlier report by Warwicker [52] that the volume changes of Cellophane, PUDO 193 the effect of electrolyte type is to decrease swelling in the order LiOH > NaOH > KOH, the same sequence as that of the hydrated cationic volume. Swelling is reduced when fixed-charge groups and counter ions form complexes thus reducing the osmotic activity. This was proposed by Jenkins et al [30] to be the reason why swelling decreases when the external electrolyte is greater than 5.7M. The final factor affecting swelling is the concentration of the electrolyte solution. Swelling is strong when the concentration of external electrolyte is low. Increase in solution concentration reduces osmotic pressure, therefore the driving force for solvent uptake is smaller. This effect was observed with Permion, figure (2.3).

### 2.3.2 Calculation of Porosities

The porosity of a swollen membrane, $(1-V_p)$ is defined by equation (2.23).

$$(1-V_p) = 1 - \frac{c}{V_2} \qquad (2.23)$$

where $V_2$ is the volume of the swollen membrane, per g of dry membrane and c is the volume of membrane polymer per g of dry membrane. $V_p$ is the gel fraction of the membrane or the volume fraction occupied by the solid in the swollen membrane.

Figures (2.5 and 2.6) show the swollen volume of Cellophane and Permion respectively in solutions of KOH, per g of dry membrane and were calculated from swelling data, (figures 2.2 and 2.3), and the volume of as received membrane per g of dry membrane. The later value was obtained for each membrane by measuring the volume of a piece of as received membrane and then drying the membrane sample overnight in an oven at 110°C. Hence the volume of as received membrane was expressed per g of dry membrane. A value of $0.7226 cm^3 g^{-1}$ was measured for Cellophane and $1.086 cm^3 g^{-1}$ was measured for Permion, both results were the mean of five determinations. The volume of membrane polymer per g of dry membrane, c, was determined from the volume of each piece of dried membrane and was found to be $0.6708 cm^3 g^{-1}$ for Cellophane and $1.049 cm^3 g^{-1}$ for Permion. A value of $0.66 cm^3 g^{-1}$ is quoted for Cellophane [53].

Figure (2.7) shows the porosity of Cellophane vs. KOH concentration. Porosities may easily be obtained from the curve at a specific concentration. The dotted line in figures (2.5 and 2.7) show the limit of electrolyte penetration of the amorphous regions. Figure (2.8) shows the variation of the porosity of Permion with respect to external electrolyte concentration. To determine the porosity of the swollen Permion at a given concentration a reasonable approach, given the data shown in figure (2.8), was to draw a straight line through the points. The line was obtained by linear regression and is given in equation (2.24)

$$(1-V_p) = -0.01567C + 0.332121 \qquad (2.24)$$

and has been used to determine the porosity of the swollen Permion relative to a given external KOH concentration. The rogue value at 4M KOH was omitted from the regression analysis.

Figure 2.5 Swollen volume of Cellophane per g of dry Cellophane as a function of KOH concentration

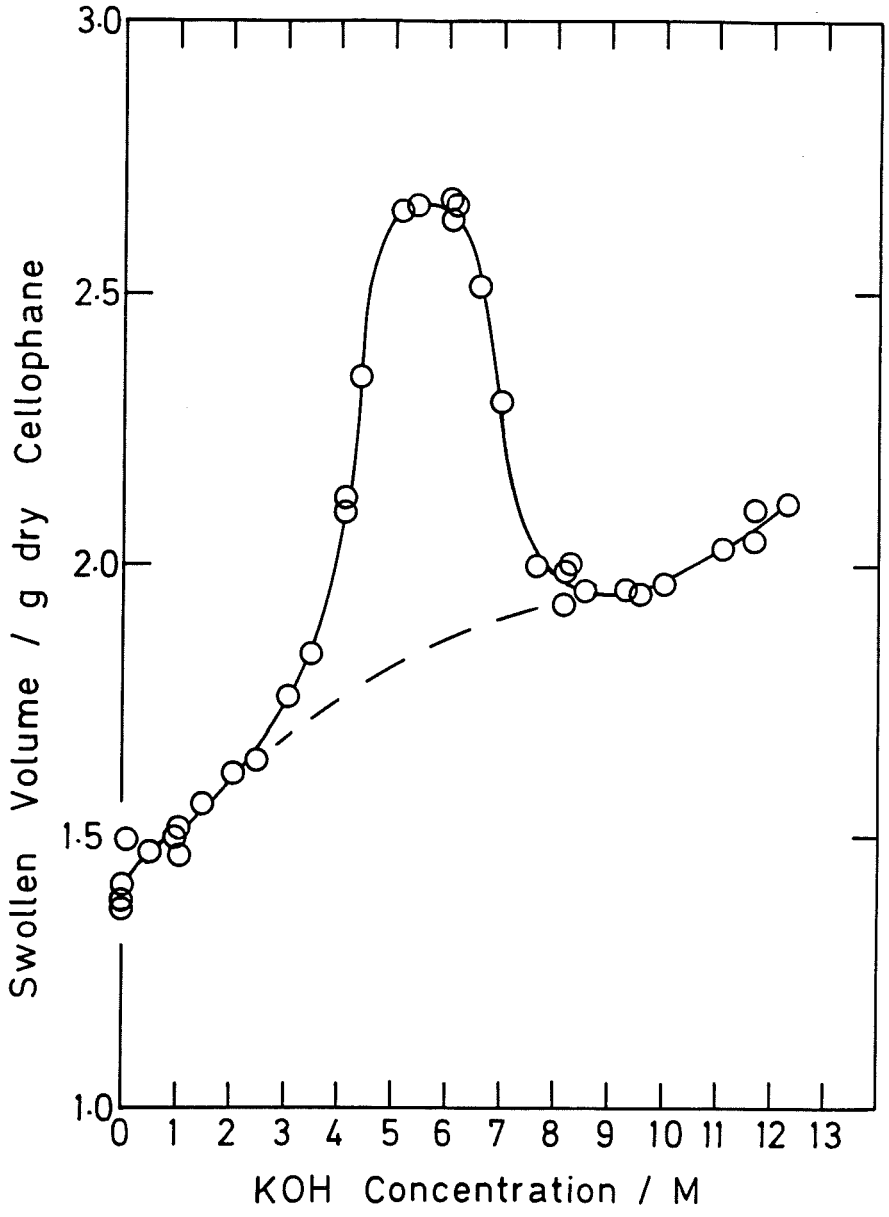

Figure 2.6 Swollen volume of Permion per g of dry Permion as a function of KOH concentration

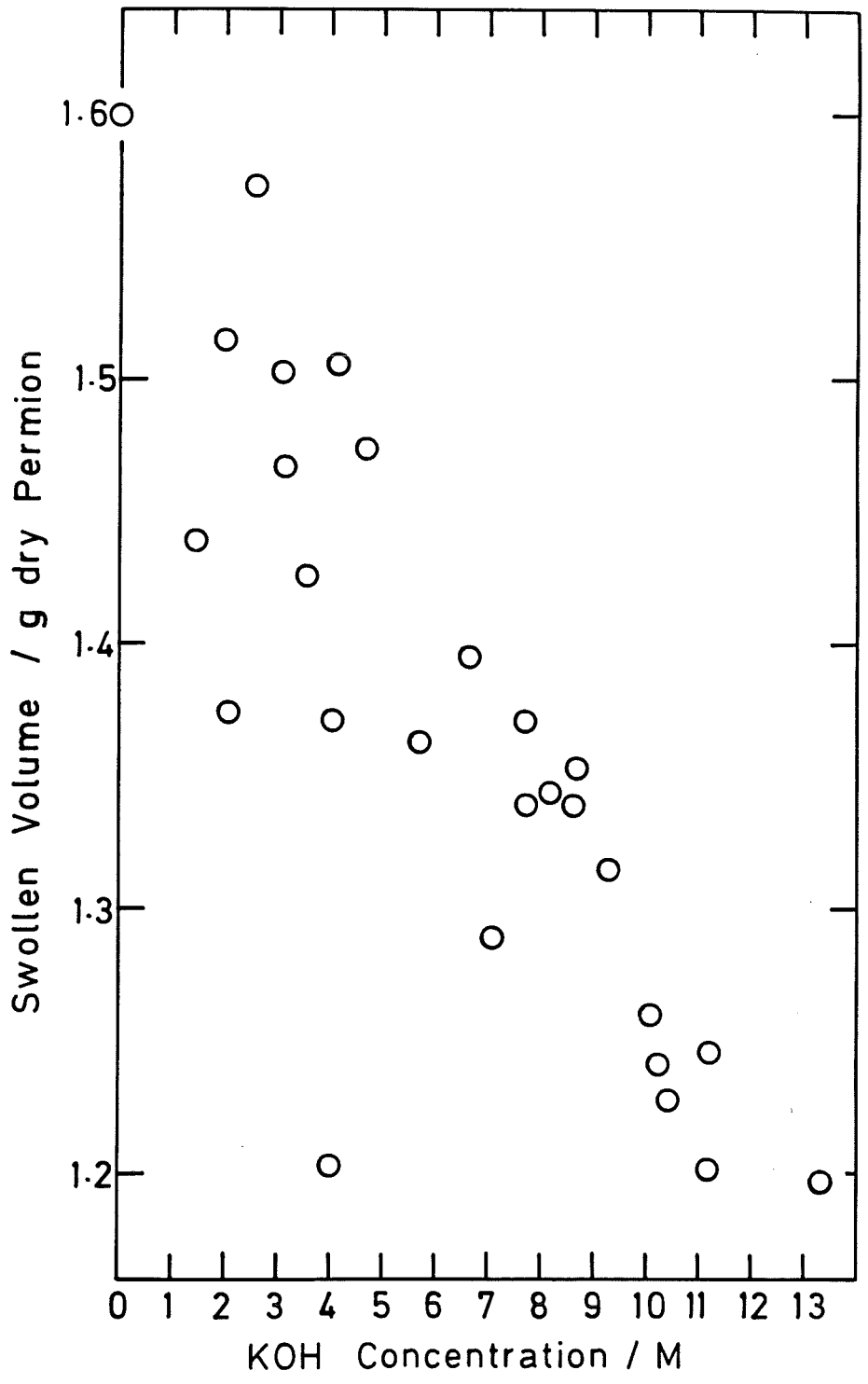

Figure 2.7 Porosity of Cellophane vs. KOH concentration

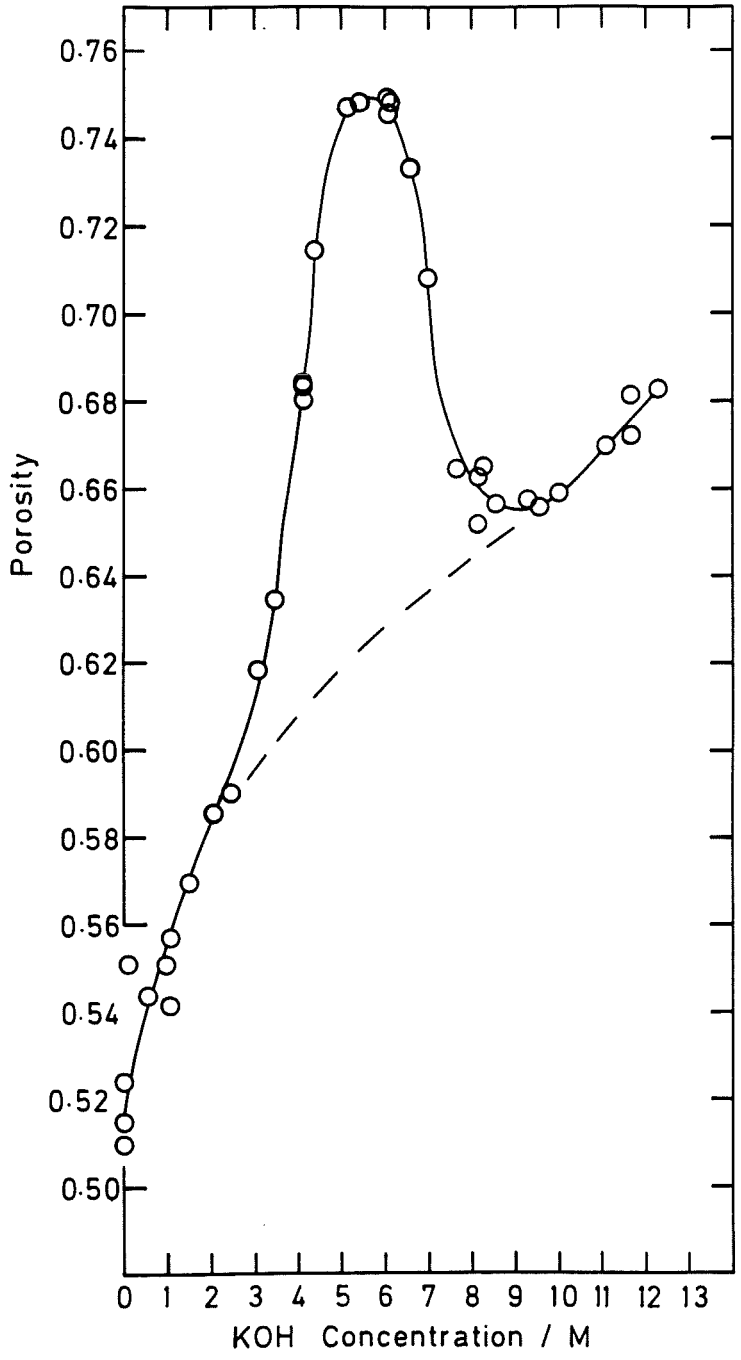

Figure 2.8 Porosity of Permion vs. KOH concentration

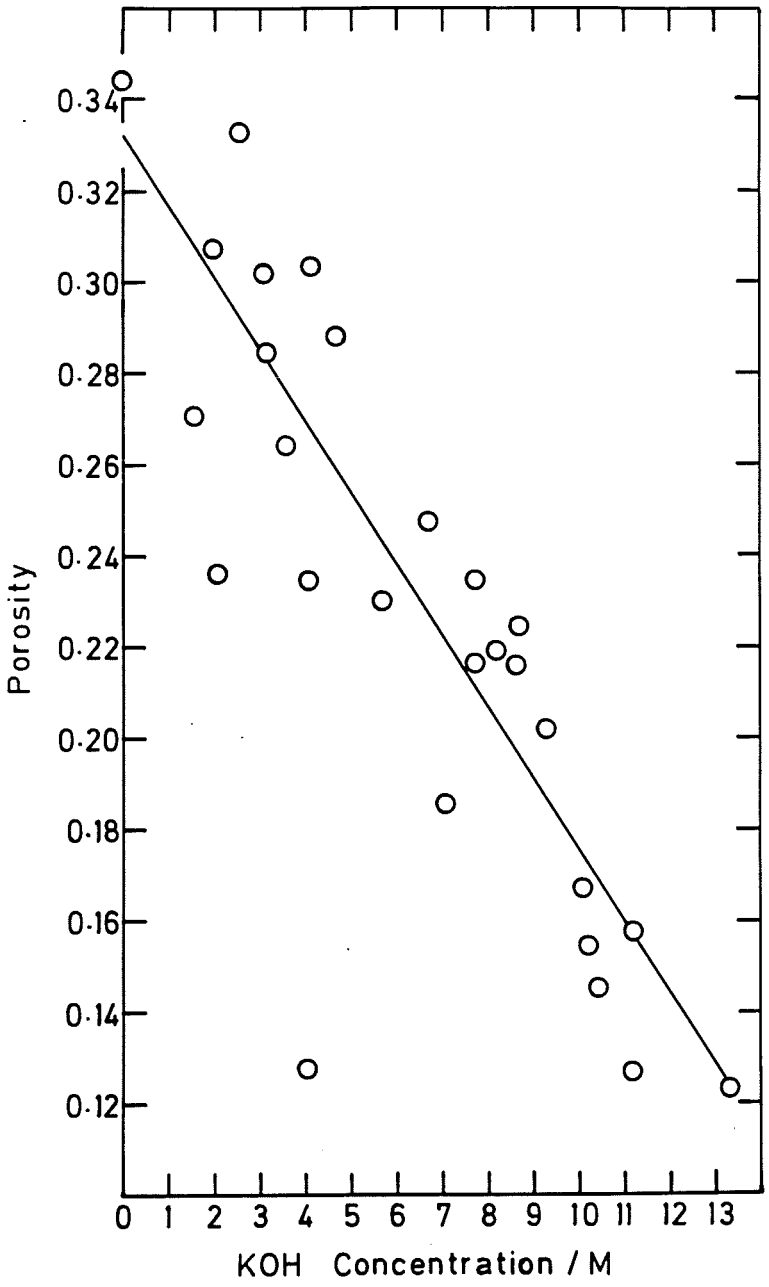

### 2.3.3 Ion-exchange : Permion 2291 40/30

Permion is a weak acid membrane which exchanges protons for potassium in alkaline solutions by the following reaction.

$$\overline{RCOOH} + K^+ + OH^- \rightarrow \overline{RCOO^-} + K^+ + H_2O \qquad (2.25)$$

The barred species are in the membrane phase, and the unbarred in the external electrolyte. $RCOO^-$ is a fixed charge group. The membrane is fully exchanged in KOH solutions of very low concentration and since the membrane is monofunctional, the ion exchange capacity (ie. number of exchangeable sites) is not expected to change over the concentration range of interest in this study, and indeed up to the solubility limit of the alkali.

The ion-exchange capacity of Permion was obtained from figure (2.9), the loss of base from the electrolyte solution vs the pH of the solution using the method described in section (2.2.3). The three parallel curves are for KOH solutions containing varying quantities of KCl. The plateau at 2.91mmoleg$^{-1}$ was determined from the mean of the points at pH>10. This is the ion-exchange capacity of Permion 2291 40/30. Jenkins et al. [46] reported an ion-exchange capacity of 2.85mmoleg$^{-1}$ for the same membrane.

Experimental section (2.2.4) introduced the problems concerning the measurement of the ion-exchange capacity of Cellophane using the Topp and Pepper method [45]. An alternative method involving a $Cl^-$ ion tracer was discussed. It was envisaged that if similar ion-exchange capacities for Permion were obtained using both methods then the $Cl^-$ ion tracer method would be suitable for determining the ion-exchange capacity of Cellophane. The $K^+$, $Cl^-$ and electrolyte contents of films of Permion were obtained over a range of KOH solutions. These results are shown in figure (2.10). The water content of the membrane was calculated from these primary data. At each external electrolyte concentration one determination of ionic species was obtained using atomic absorption spectroscopy.

Figure (2.11) shows how the $K^+$, $Cl^-$ and $OH^-$ content of the Permion changes

Figure 2.9 Loss of base from solution vs. pH of solution at equilibrium.

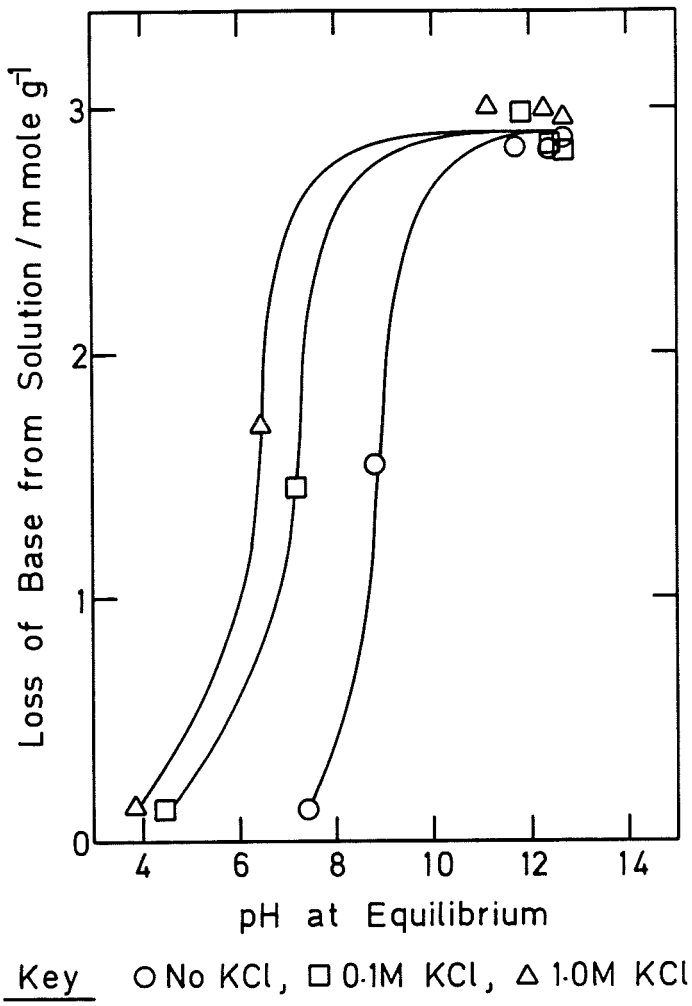

Figure 2.10 Electrolyte content of Permion vs. KOH concentration.

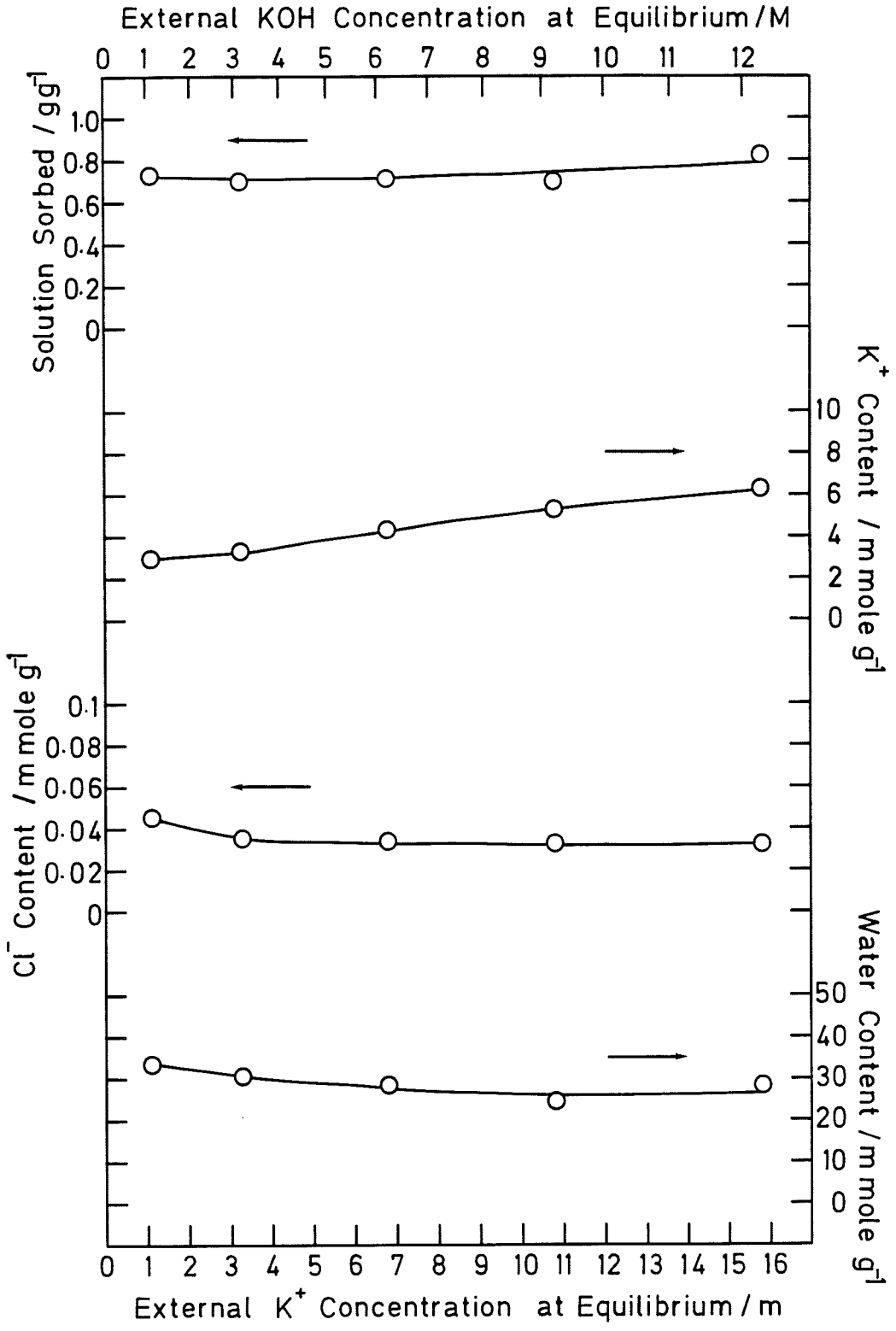

Figure 2.11 Ionic content of Permion vs. external KOH concentration.

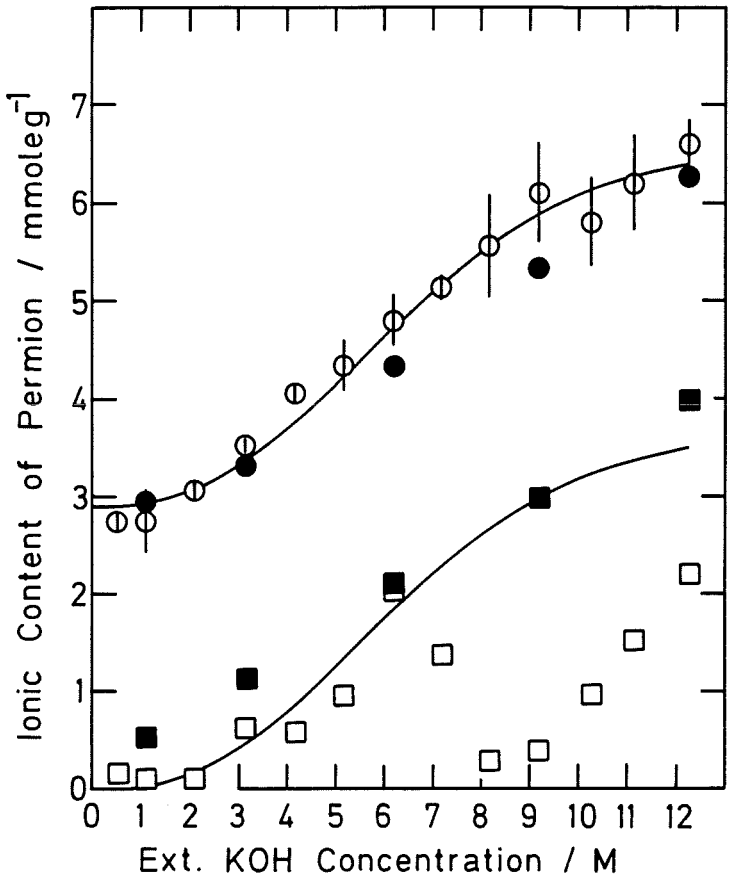


KEY
- ● $K^+$, one determination
- ○ $K^+$, average showing Std. Devn.
- ■ $OH^- + Cl^-$ associated with ●
- □ $OH^- + Cl^-$ associated with ○

with increase in external electrolyte concentration. The graph illustrates two sets of data obtained using slightly different experimental conditions. To optimise the measurement of anionic content a greater amount of $Cl^-$ had to be precipitated as AgCl(s). This was achieved by increasing the amount of membrane to be analysed to 1g and by adding $AgNO_3$ of a volume 1.5 times the expected amount of $Cl^-$. The filled in symbols represent the data from figure (2.10) where approximately 1g of Permion was used, and the $K^+$ and $Cl^-$ contents were obtained from one determination. The unfilled circles are the mean of 4 or 5 potassium content determinations, using a smaller mass of Permion, the error bar represents the standard deviation ($\sigma_n \pm 1\sigma$). Two experimental methods were employed to obtain this value, atomic absorption spectroscopy and by direct titration with correction for the $Cl^-$ content. The results from atomic absorption spectroscopy have been corrected for an error in the calibration of the standard solutions. The good fit between the two sets of data gives confidence to this correction. With respect to the cation content, the unfilled symbols are more likely to be representative of the true value since they represent the mean of 4 or 5 determinations. Since the anion content of the membrane is small, if a greater mass of Permion is used in its determination then this is more likely to yield the true content hence the filled symbols show the realistic situation.

The cations and anions have been separated by two lines 2.91mmoleg$^{-1}$ apart, this is the equivalent to the ion-exchange capacity of the membrane as determined by the Topp and Pepper method. The square symbols are the sum of the $OH^-$ and $Cl^-$ contents of the membrane. Whatever the KOH concentration, the same trace concentration of KCl is added. The drift in unfilled squares from the line in figure (2.11) shows that imprecise measurement of $Cl^-$ content introduces a large error in estimation of $OH^-$ content especially at high external electrolyte concentrations. There is a greater margin for error at this end of the KOH concentration range since with 10M KOH the $OH^-$:$Cl^-$ ratio is typically 100:1 compared with 10:1 for 1M KOH. The filled squares are from a modified technique which had greater precision in the determination of the $Cl^-$ content.

With Permion either the direct method of determining the ion-exchange capacity for the loss of base from solution as a function of pH or the indirect method using a $Cl^-$ tracer may be used. Therefore providing care is taken with the determination of the $Cl^-$ content of the membrane, the indirect method is suitable for determining the mobile anion content and the ion exchange capacity of Cellophane.

### 2.3.4 Ion-exchange : PUDO 193 cellulose

The $K^+$, $Cl^-$ and electrolyte content of Cellophane films as a function of external electrolyte concentration are shown in figures (2.12) and (2.13). Equation (2.26) shows the ion-exchange between the alcohol groups on Cellophane and KOH.

$$\overline{ROH} + K^+ + OH^- \rightarrow \overline{RO^-} + K^+ + H_2O \qquad (2.26)$$

The unbarred and barred symbols represent the membrane and the electrolyte phases respectively.

The indirect method of measuring the anion content of a cation exchange membrane, as discussed in the previous section, allows calculation of the apparent internal ionic concentrations. Figure (2.14), shows these concentrations as determined for Cellophane. In equation (2.26), $RO^-$ represents the fixed anion framework of the membrane. It can be seen from figure (2.14) how the Donnan exclusion of the anion by the fixed anion framework lowers its internal concentration compared to that of the cation.

The quantities of protons exchanged as shown by reaction (2.26) can be calculated from the difference between the $K^+$ and the ($OH^-$ + $Cl^-$) content of the membrane, figure (2.15). As the external KOH concentration increased the membrane ionised (figure (2.15)) and the swelling increased (figure (2.2)). A theory to explain the complex swelling and ion-exchange behaviour has been proposed [30]. Figures (2.2 and 2.4) in section (2.3.1) showed a distinction between electrolyte penetration of amorphous and crystalline regions, this effect is also observed in figures (2.12, 2.13 and 2.15)

Nicholl et al [25] while investigating the swelling of cellulose in NaOH solutions, proposed a critical concentration below which ion-exchange occurs only in amorphous regions. Evidence for this is from X-ray diffraction measurement of the d-spacing in the crystalline regions. No change is observed below the critical concentration. From figure (2.2) and the work by Jenkins et al [30] this critical concentration is around 3M, ie. below an external electrolyte solution of 3M KOH exchange occurs only in the amorphous regions. Since the protons on primary alcohol

Figure 2.12 Quantity of solution and $K^+$ sorbed by Cellophane in KOH / 0.1M KCl at 25°C vs. electrolyte concentration.

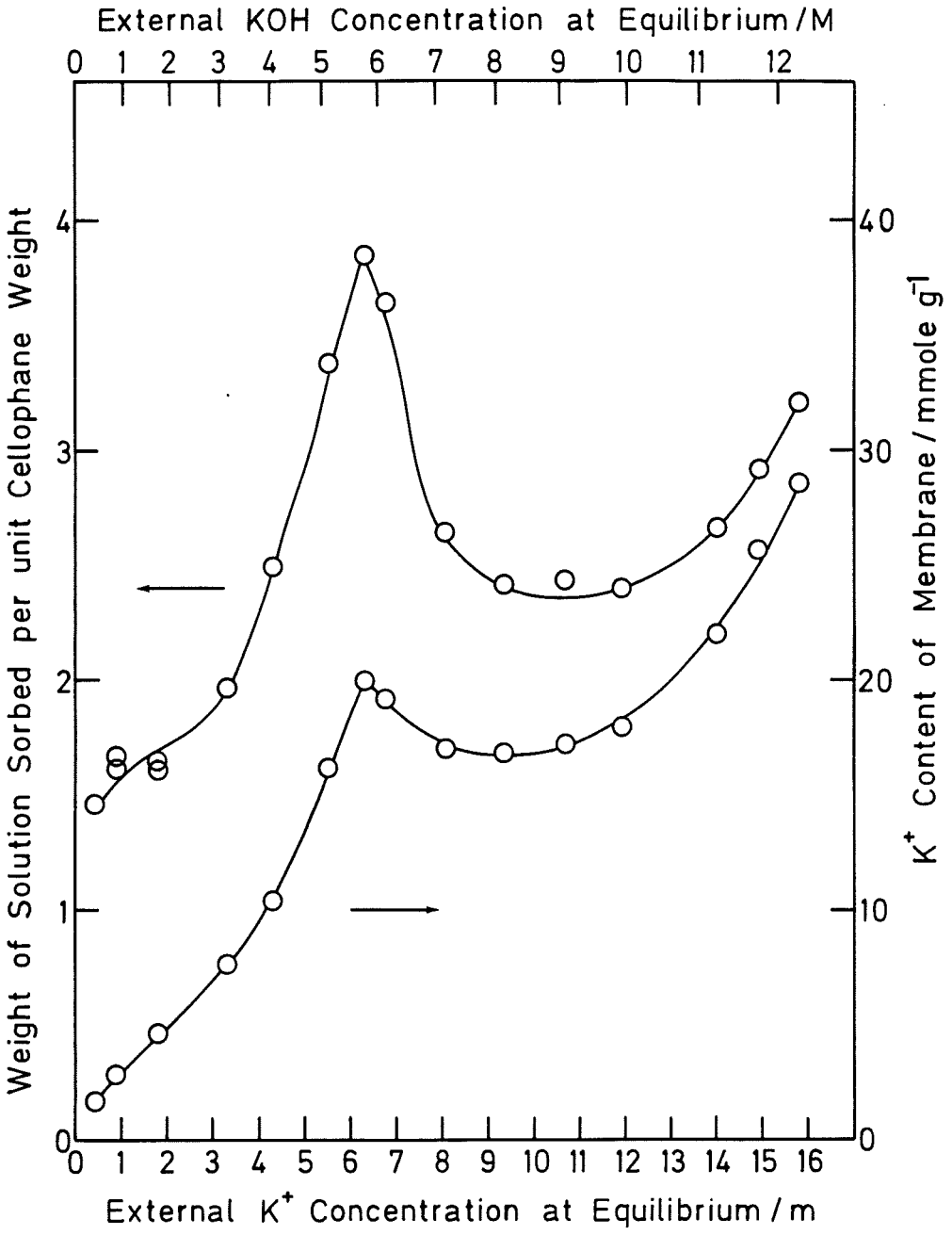

Figure 2.13 Quantity of $Cl^-$ and water sorbed by Cellophane in KOH / 0.1M KCl at 25°C vs. electrolyte concentration.

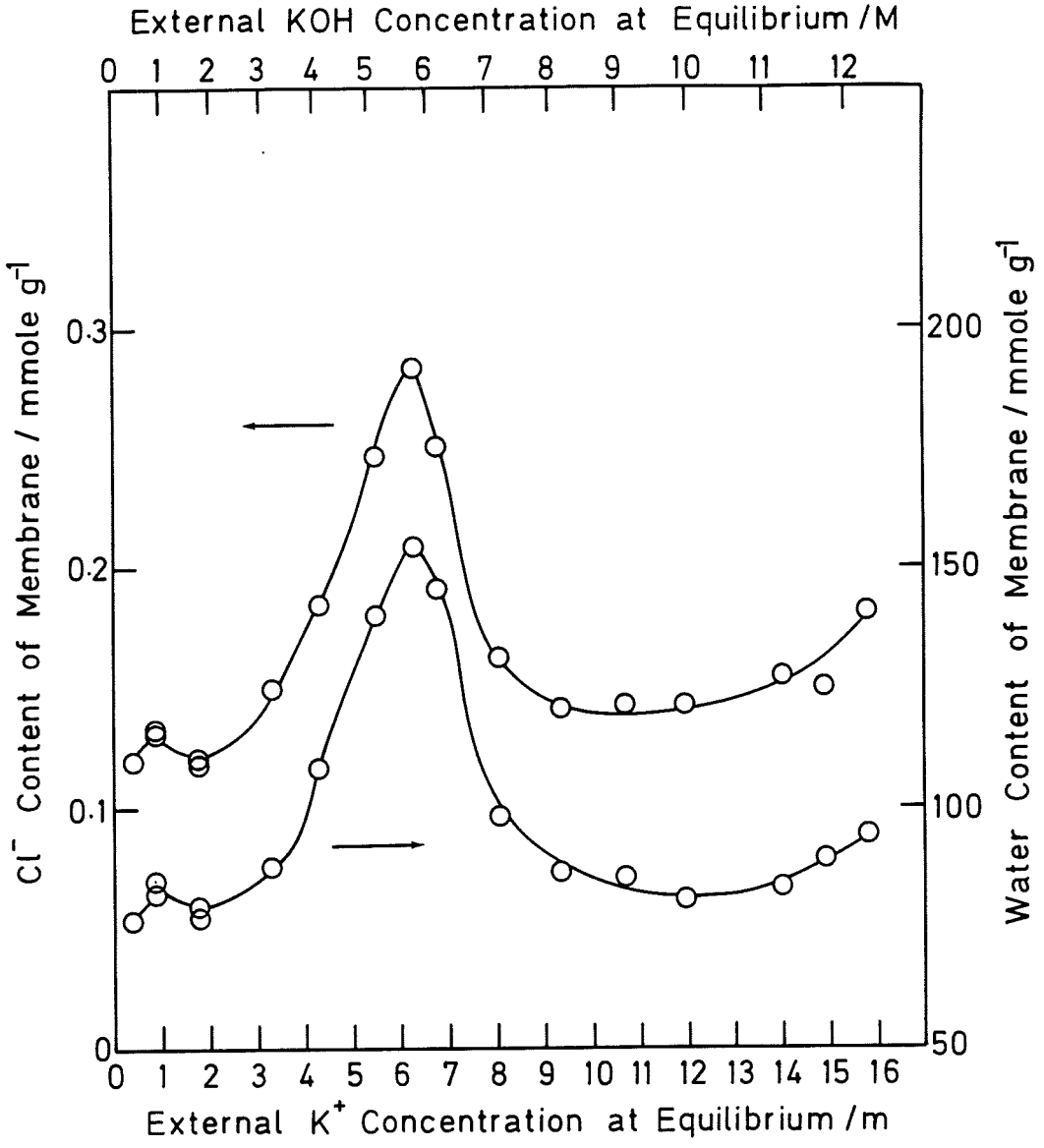

Figure 2.14 The apparent internal cation and anion concentrations within Cellophane equilibrated in KOH / 0.1M KCl at 25°C vs. electrolyte concentration.

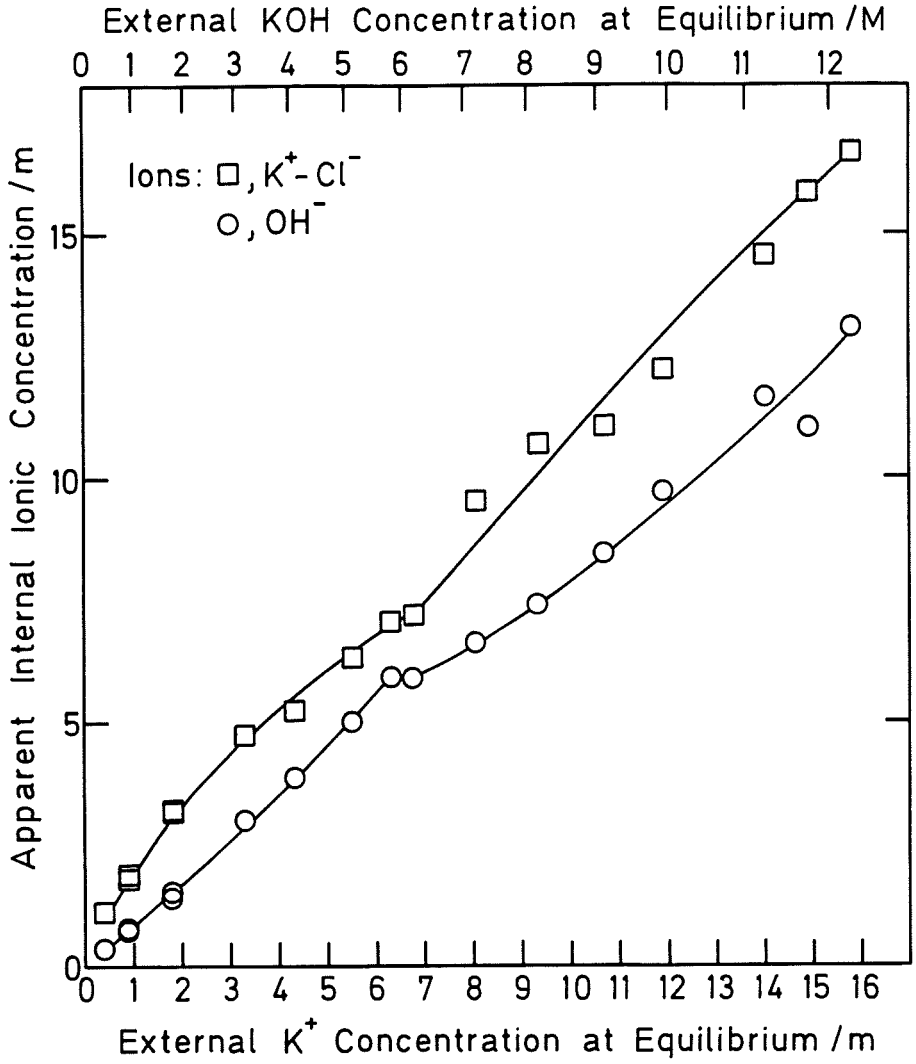

Figure 2.15 The quantity of protons exchanged per unit membrane weight by Cellophane in KOH / 0.1M KCl at 25°C vs. electrolyte concentration.

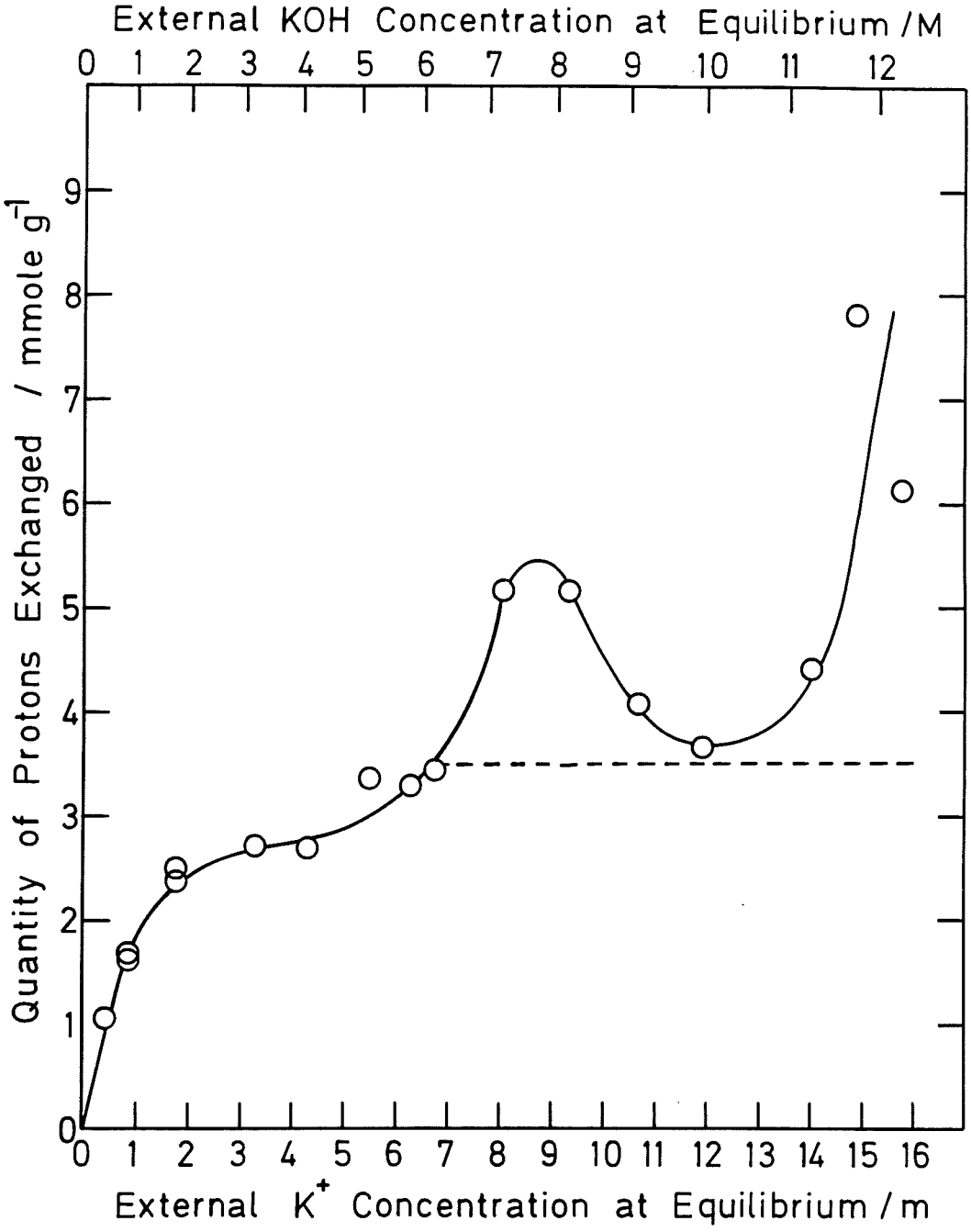

groups are more acidic than protons on secondary alcohols then this exchange will be of protons on primary alcohol groups.

For a 1,1-valent electrolyte, such as KOH, the Donnan equation for equilibrium sorption of an electrolyte by a membrane may be expressed as follows [54]

$$\bar{m}_\gamma ( \bar{m}_\gamma + \bar{m}_R ) = m_\gamma^2 \left( \frac{\gamma}{\bar{\gamma}} \right)^2 \qquad (2.27)$$

where $m_\gamma$ (molekg$^{-1}$) is the molality of the anions, $m_R$ is the molality of the fixed charge groups and $\gamma$ the activity coefficient. As before, the barred and unbarred species refer to the membrane and electrolyte phase respectively. Figure (2.16), shows a plot of ($\gamma/\bar{\gamma}$) vs $K^+$ concentration for both Cellophane and Permion. High values of $\gamma/\bar{\gamma}$ at low external concentrations are typical of ion-exchange materials [55]. The ratio does not tend to unity as concentration decreases as the Debye-Hückel theory predicts for free electrolyte but to a value significantly greater than unity due to low values of $\bar{\gamma}$ in dilute solutions. At low electrolyte concentrations the fixed charges cause potential gradients in the pores of the ion-exchange material, as a result $\bar{\gamma}$ is less than the Debye-Hückel activity coefficient which is independent of potential terms arising from the presence of fixed charges. Jenkins [30] suggested that low values of $\gamma/\bar{\gamma}$ at high external electrolyte concentrations were indicative of immobilised water in the membrane which was not available to solvate internal mobile ions.

The quantities of protons exchanged in amorphous regions may be estimated as follows [30]. Ionisation within the membrane may be expressed as equation (2.28).

$$\overline{ROH} + OH^- \rightleftharpoons \overline{RO^-} + H_2O \qquad (2.28)$$

The basicity constant, $K_b$ for the above ionisation is given by

$$K_b = \frac{\bar{a}_{ROH}\, \bar{a}_{OH^-}}{\bar{a}_{RO^-}} \qquad (2.29)$$

Figure 2.16 The apparent ratio of the mean molal ionic activity coefficients outside and inside Cellophane and Permion in KOH / 0.1M KCl at 25°C vs. electrolyte concentration.

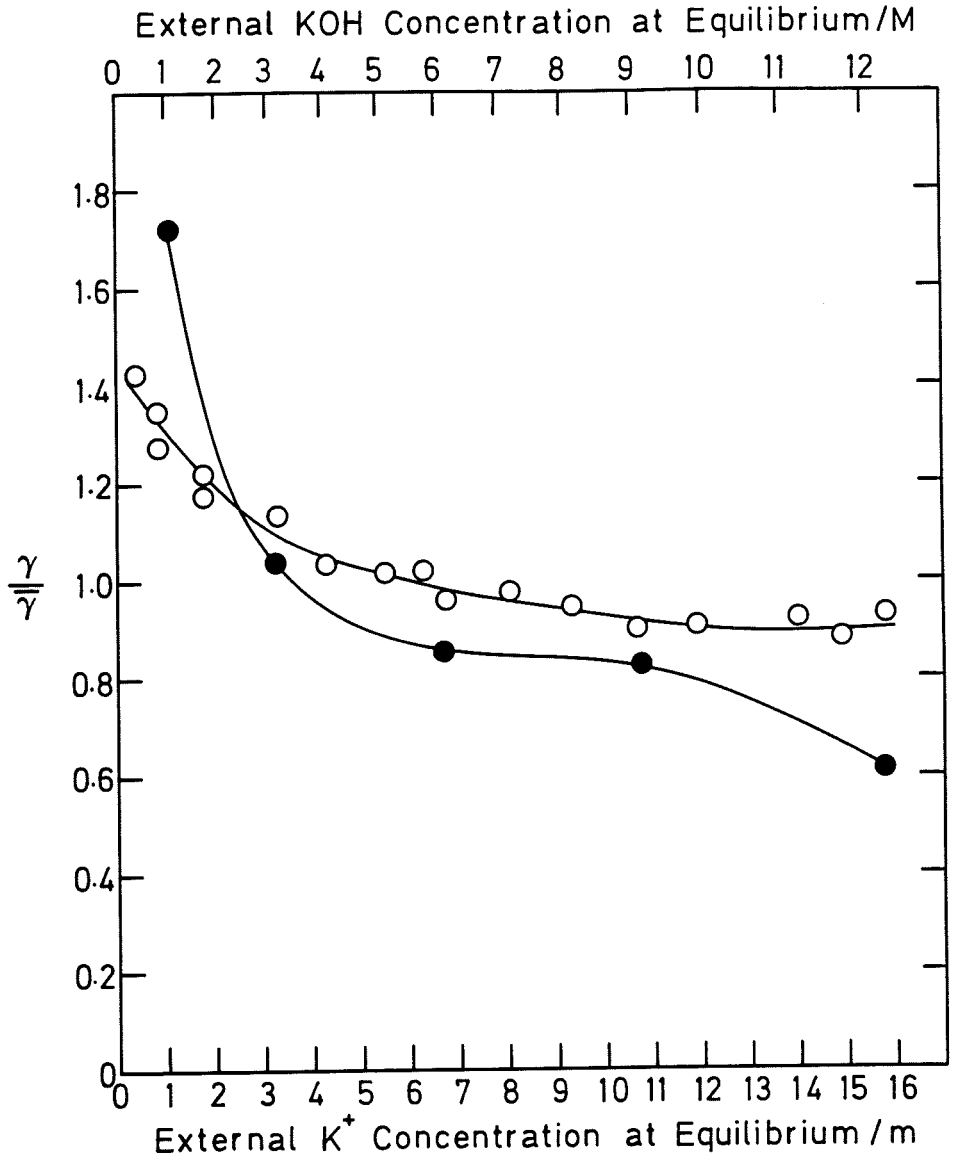

where a represents the activity of the subscript species. Equating the activities of the cellulosic species with their concentrations and writing the degree of ionisation as $\alpha$ equation (2.29) becomes

$$K_b = \frac{(1 - \alpha)\,\bar{a}_{OH^-}}{\alpha} \tag{2.30}$$

The degree of ionisation is a function of Z ($mmoleg^{-1}$), the total available, and Q ($mmoleg^{-1}$), the actual exchanged, quantities of protons per unit membrane weight.

$$\alpha = \frac{Q}{Z} \tag{2.31}$$

From equation (2.30) and (2.31) it follows that

$$Q^{-1} = \left(\frac{Z\,\bar{a}_{OH^-}}{K_b}\right)^{-1} + Z^{-1} \tag{2.32}$$

Although the activity of $OH^-$ in the membrane is not known it can be approximated assuming $\bar{\gamma}_- = \bar{\gamma}$. Then,

$$\bar{a}_{OH^-} = \bar{m}_{OH^-}\,\bar{\gamma} = \left(\frac{\bar{m}_{OH}\,\gamma}{\left(\frac{\gamma}{\bar{\gamma}}\right)}\right) \tag{2.33}$$

For an external electrolyte concentration less than 3.2M Jenkin's data [30] and data obtained by this author have been combined and a plot $Q^{-1}$ vs $(\bar{m}_{OH}\bar{\gamma})^{-1}$ obtained, figure (2.17). $\bar{\gamma}$ was obtained from $\gamma/\bar{\gamma}$, figure (2.16) and tabulated values of $\gamma$ [56].

Figure 2.17 The reciprocal of the quantity of protons exchanged, $Q^{-1}$, vs. the reciprocal of the estimated internal activity of $OH^-$ in Cellophane for concentrations of KOH not exceeding 3.2M.

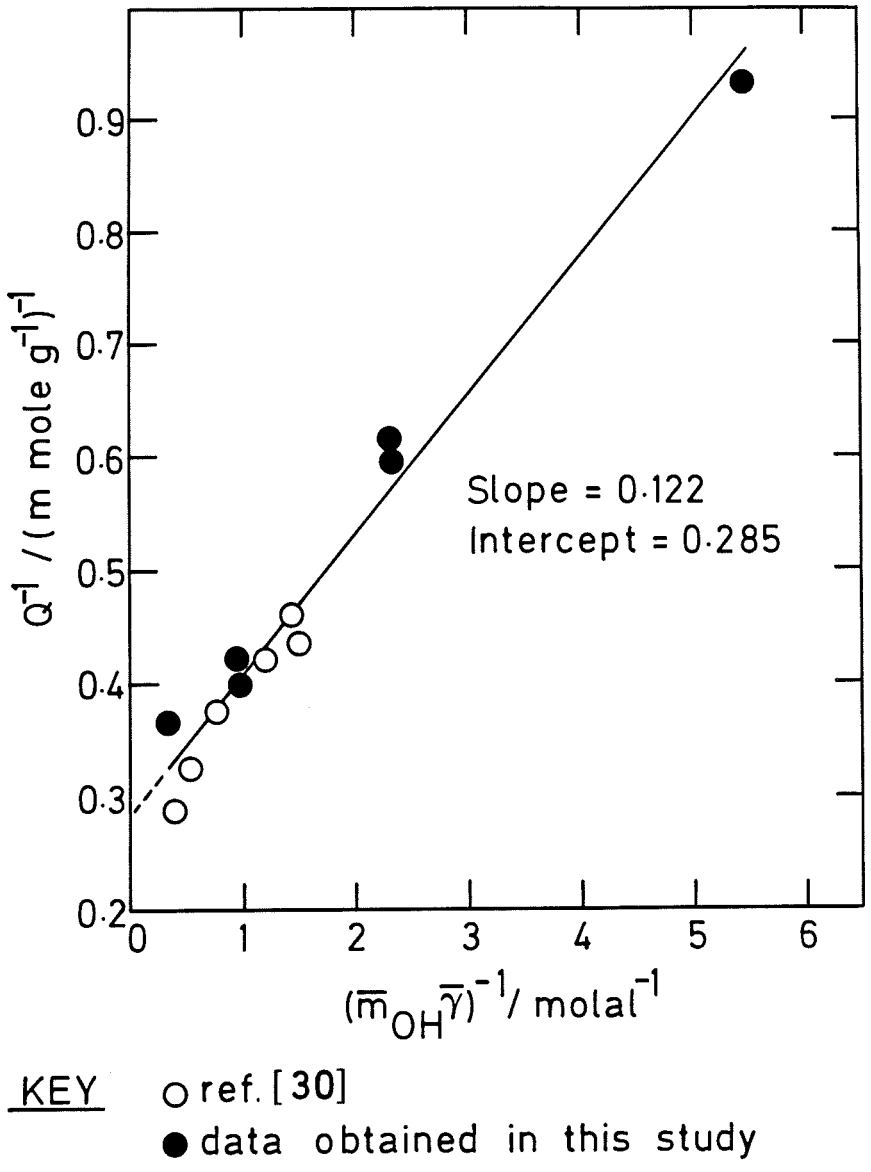

Regression analysis by the least mean square method gives a straight line plot of slope $K_b/Z$ and intercept $Z^{-1}$. Hence a basicity constant $K_b = 0.428$ was obtained and the total available protons in amorphous regions were found to be $Z = 3.50 mmoleg^{-1}$. The value Z is represented as a dotted line in figure (2.15). The theoretical quantity of protons available for exchange on primary alcohol groups on cellulose is $6.22 mmoleg^{-1}$. Hence the proportion of amorphous and crystalline regions is 56% and 44% respectively. Table (2.1) shows a comparison between these values and other estimates.

Table 2.1 A comparison between the percentage amorphous regions in Cellophane found in this study with other types of cellulose.

| Cellulose type | % Amorphous region | Reference |
|---|---|---|
| PUDO 193 | 56 | This study |
| PUDO 193 | 64 | [30] |
| Mercerised cotton | 54 | [48] |
| Regenerated Vicose | 75 | [48] |
| Cotton | 35 | [48] |
| Cotton | 17 | [21] |
| Rayon | 33 | [21] |

The $pK_a$ of the hydroxyl group may be calculated from equation (2.34)

$$K_W = K_a K_b \qquad (2.34)$$

where $K_w$ is the autoprotolysis constant of water ($=10^{-14}$). $K_b$ was obtained experimentally from figure (2.17) and hence $pK_a = 13.6$. Literature values of $pK_a$ are presented in table (2.2) [57].

Table 2.2 $pK_a$ values of some alcohols and water.

| Compound | $pK_a$ |
|---|---|
| $CH{\equiv}CCH_2OH$ | 13.55 |
| $C(CH_2OH)_4$ | 14.10 |
| $CH_2OHCHOHCH_2OH$ | 14.40 |
| $CH_2OHCH_2OH$ | 14.77 |
| $CH_3OCH_2OH$ | 14.82 |
| $CH_3OH$ | 15.54 |
| $CH_2{=}CHCH_2OH$ | 15.50 |
| $H_2O$ | 15.57 |
| $CH_3CH_2OH$ | 16.00 |

Above an external electrolyte concentration of 3M KOH swelling increases sharply to a maximum at 5.7M (figure (2.2)). This indicates ionization of the crystalline region is commencing. Hydrogen bonds between the molecular chains (as discussed in section (1.3)) are breaking and this decreases the degree of cross-linking allowing the crystal lattice to expand.

Further increase in concentration sees a dramatic reduction in swelling. Jenkins et al [30] proposed that this phenomenon was due to association between the fixed charge group and the cation to form the complex shown in equation (2.35).

$$\overline{RO^-} + \overline{K^+} \rightleftharpoons \overline{ROK} \qquad (2.35)$$

This decreases swelling by reducing the effective quantity of fixed charge groups within the membrane, one of Helfferich's criteria as mentioned in section (2.3.1).

It is interesting to note, from figure (2.15) that in this region the quantity of protons exchanged also decreases. Hence a reduction in swelling due to less available fixed charge groups means that the crystalline regions are not accessible and therefore cannot be ionised. Swelling is decreased to a degree insufficient to rupture the hydrogen bonds in the crystalline regions.

It must be remembered that the dry membrane is equilibrated in an external electrolyte of fixed concentration. Figures (2.2) and (2.15) showing the swelling and ion-exchange behaviour were not obtained by measuring equilibration in one concentration, the concentration then changed and the behaviour reassessed in the new equilibrium situation. Hence any effects at one concentration do not influence effects at a different concentration. Further work might be to equilibrate the membrane in one concentration then change the concentration and investigate the subsequent effect this has on the ionisation and swelling of the membrane. Jenkins et al [30] reported a disintegration of Cellophane in NaOH solutions between 1.5 and 6M. For this situation it is important to determine behaviour at a fixed concentration since once the membrane has disintegrated at 1.5M KOH it is improbable that the cellulose chains would recombine in solutions in excess of 6M KOH.

Ionisation above the value of the theoretical quantity of protons available for exchange on primary alcohol groups, i.e. 6.22mmoleg$^{-1}$ as shown in figure (2.15), is a result of ionisation of protons on secondary alcohol groups. This increase in fixed charges increases the degree of swelling as seen in figure (2.2) at the highest KOH concentrations.

## 2.4 Conclusion

The difference in the structure of Cellophane compared to Permion largely explains the difference in the swelling behaviour. The three dimensional cross-linked structure of Permion allows similar degrees of swelling in each direction with restriction by the swelling equilibrium attained when the elastic forces of the membrane balance the dissolution tendency. Cellophane thickness swelling is not as restrictive since the three dimensional structure incorporates hydrogen bonds between the cellulose chains which can rupture forming new intermolecular hydrogen bonds with the intruding water. The Cellophane membrane is therefore more able to swell in thickness than Permion. The complex swelling behaviour of Cellophane is attributed to the differing accessibilities of the crystalline and amorphous region, the formation of a potassium ion complex with the fixed charge groups and the differing ion-exchange capabilities of the primary and secondary alcohol groups.

The ion-exchange capacity of Permion is uncomplicated since the membrane is fully exchanged to the degree of 2.91 $mmoleg^{-1}$ at very low concentrations, this is not the case for Cellophane. Two methods were used to measurement the ion-exchange capacity of Permion, pH titration and by use of a $Cl^-$ tracer. Similar results were obtained and the later method was then successfully applied to Cellophane. The ion-exchange behaviour of Cellophane showed a direct correlation with the swelling behaviour. Hence the swelling and the ion-exchange behaviour should be interpreted simultaneously.

# CHAPTER 3

# MASS TRANSPORT THROUGH PUDO 193 CELLOPHANE AND PERMION 2291 40/30 WHEN USED SEPARATELY

## 3.1 Introduction

### 3.1.1 Transport of ions

The terms transport number and transference number are often used interchangeably. This author subscribes to the view that transport should be applied to current carrying species i.e. ions and that transference should be used for non-current carrying species i.e. solvent.

Current physical chemistry text books [58] define the transport number of an ion as the fraction of the total ionic current carried by that ion ; it is dimensionless. Transport number is directly related to the mobility of an ion, u, defined as its speed in an electric field of unit strength, with units $m^2s^{-1}V^{-1}$.

For a 1:1 electrolyte the relationship between transport numbers, t and mobility, u may be expressed,

$$t_+ = \frac{u_+}{u_+ + u_-} \quad , \quad t_- = \frac{u_-}{u_+ + u_-} \tag{3.1}$$

where the subscripts + and - refer to cations and anions respectively.

Moore [59] , uses the same definition as Atkins but makes no distinction between transport number and transference number of an ion. Kohlrausch [60] , defines the law of independent migration of ions,

$$\Lambda_0 = \nu_+\Lambda_0^+ + \nu_-\Lambda_0^- \tag{3.2}$$

where $\Lambda_o^+$ and $\Lambda_o^-$ , ($\Omega^{-1}m^2mol^{-1}$), are the molar ionic conductivities at infinite dilution and $\nu_+$ and $\nu_-$ are the numbers of cations and anions needed to form one molecule of the salt (e.g., $\nu_+ = \nu_- = 1$ for KOH, but $\nu_+ = 1$, and $\nu_- = 2$ in the case of $MgCl_2$). From equation (3.2) the transport numbers, $t_o^+$ and $t_o^-$ of the cation and the anion at infinite dilution may be written,

$$t_0^+ = \nu_+ \frac{\Lambda_0^+}{\Lambda_0} \quad , \quad t_0^- = \nu_- \frac{\Lambda_0^-}{\Lambda_0} \tag{3.3}$$

Hence transport numbers may be expressed equally well in terms of either mobilities or molar ionic conductivities since,

$$\Lambda_\pm = \nu_\pm u_\pm F \tag{3.4}$$

where F is the Faraday constant.

Helfferich [61] states the transport number $t_i$ of a species i is defined as the number of moles of the species transferred by 1 Faraday of electricity through a stationary cross-section in the direction of positive current. The significance of this definition is that the transport number of the anion must be negative relative to the direction of the current. Although transport number is dimensionless, a physical mass is transferred and is measured in $moleF^{-1}$. It seems reasonable that when referring to this quantity the term transference number is appropriate. Helfferich relates transport number to transference number by defining transport number as the product of the transference number and the valence of the species.

An important consideration to complete the definitions is the frame of reference. In this study the membrane is the frame of reference and transport numbers are measured relative to this. Lengyel et al [62] measured transport numbers through ion-exchange membranes using concentrated alkaline solutions by a method where the solvent, water was the fixed frame of reference.

In this work transport numbers are considered to be positive for all ions, and zero for the electrically neutral solvent. By definition the sum over all transport numbers is equal to unity ;

$$\sum_i |z_i| t_i = 1 \tag{3.5}$$

In ion-exchange membranes the counter-ion concentration is much greater than

the co-ion concentration, particularly if the solution in equilibrium with the membrane is dilute, due to Donnan exclusion. If an electric field is applied to the membrane the transport of electric current is nearly exclusively carried by counter-ions, and the transport number of the counter-ion therefore approaches unity.

When the concentration of electrolyte in the external solution increases the Donnan exclusion of the co-ion becomes less efficient, and the increase in concentration of the co-ion in the ion-exchanger causes a decrease in the transport number of the counter-ion.

### 3.1.2 Transference of solvent

Transference of solvent or electro-osmotic flow is defined as the number of moles of solvent transferred per faraday of electricity passed, with units $moleF^{-1}$. In this work water is the solvent and is transferred as a non-current carrying species through the membrane as water of hydration and by electro-convection.

Water of hydration is self-explanatory and refers to the solvation shells of counter- and co-ions. Hence if the majority of the current in the membrane is carried by the counter-ion which is the case at low external concentrations, then more water is transferred in the same direction as counter-ion transport than is transferred by the smaller number of co-ions in the reverse direction.

Electroconvection contributes to the transference of solvent as a result of the electric field moving ions which convey momentum to the solvent. In solution electroconvection is difficult to detect. In an ion-exchange membrane counter-ions are in the majority and therefore impart more momentum to the solvent than do the co-ions. Solvent is carried along by the counter-ions, i.e. there is convection in the direction of counter-ion transport. The amount of convection is dependent on counter-ion concentration, the electric field and the flow resistance of the membrane.

Water may also be transferred by osmosis and by hydraulic flow but this has been eliminated by careful choice of experimental technique (see section (3.2.6)). In this work therefore water is considered to be transferred by electroconvection and in solvation shells only although it is not possible to quantify the contribution of each to the overall electro-osmotic flow. The transference number of water decreases with

increasing external electrolyte concentration and this is almost entirely due to the decrease in counter-ion transference number.

The review of Lee et al [63] states that, "a full treatment of electro-osmosis should take into consideration water transported in ionic solvation shells, water immobilised by association with fixed charge groups, movement of the remaining water as a result of interaction with counter-ions, co-ions, fixed charge groups and polymer, and changes in these factors with increasing external concentration as a result of membrane shrinkage and increasing co-/counter-ion concentration ratio". Fortunately, a simple treatment accounts for much of the data.

### 3.1.3 Measurement of transport numbers in solution

Transport numbers of ions in solution may be measured by the moving boundary method, the Hittorf method or from emf measurements.

The moving boundary method is based on observation of the motion of an interface separating two solutions having a common ion, under the influence of an electric field. Figure (3.1) shows how, experimentally transport numbers may be obtained by this method. In this example $M^+$, is the ion whose transport number is to be determined. In the experiment the denser indicator solution, NX, occupies the lower part of a vertical tube, and the leading solution, MX, occupies the upper part with a sharp boundary between them. Moreover, the cation of the indicator solution ($N^+$) must have a mobility lower than the cation of the leading solution ($M^+$).

When a current, I (A) is passed for time, t (s) the boundary is observed to move from AB to CD therefore all the $M^+$ ions in the volume between AB and CD must have passed through CD. The transport number, t of the $M^+$ ions is given by equation (3.6)

$$t_{M^+} = \frac{zc_M.VF}{It} \qquad (3.6)$$

where, z is the valency, c ($moldm^{-3}$) is the concentration of the $M^+$ ions, F is the Faraday constant and V ($dm^{-3}$) is the volume of solution between AB and CD. Hence, knowing

Figure 3.1 The moving boundary method for the measurement of transport numbers in solution.

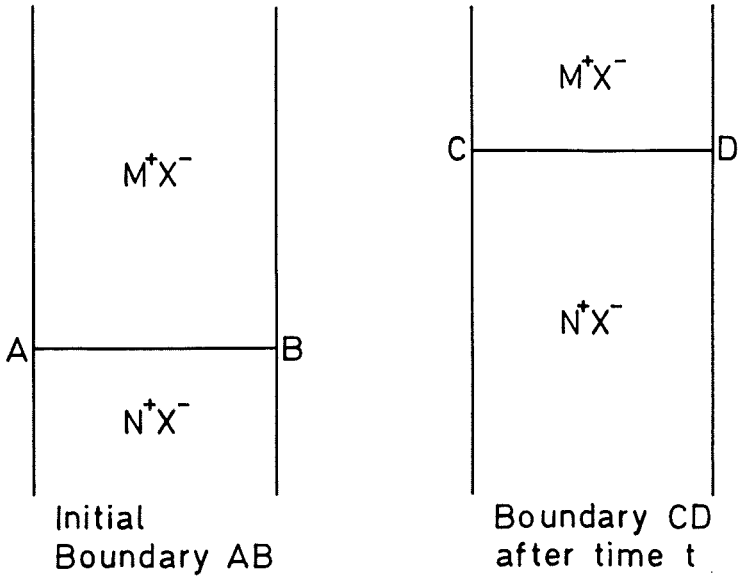


Figure 3.2 The Hittorf method for the measurement of transport numbers in solution.

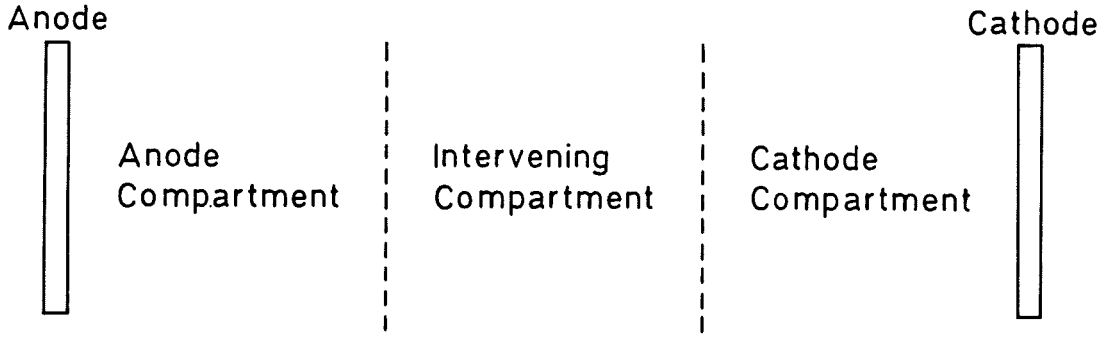

the diameter of the tube and the distance travelled by the boundary in time, t, the transport number of the $M^+$ ion may be determined.

The Hittorf method, devised in 1853 [64], is based upon concentration changes in the solution in the neighbourhood of the electrodes caused by the passage of current through the electrolyte. Essentially the apparatus used to measure transport numbers by the Hittorf method consists of an anode compartment, a cathode compartment and a third intervening compartment as shown schematically in figure (3.2).

The amount of charge passed, Q (C), is measured using a coulometer and the change in composition of each section is determined analytically. Assuming that the current is not passed for so long that the composition of the intervening compartment changes then the transport numbers are determined by the change in composition of the anolyte and catholyte as follows:

A quantity, Q/F (moles) of cations are present in the cathode compartment and an amount, $t_+(Q/F)$ of cations move into the cathode compartment. The change in composition of the cathode compartment is $\delta n_C$ and gives $t_-$, the anion transport number as shown in equation (3.7).

$$\delta n_c = \frac{Q}{F} - t_+\frac{Q}{F} = \frac{Q}{F}(1 - t_+) = \frac{Q}{F}t_- \qquad (3.7)$$

Likewise the change in composition of anions at the anode, $\delta n_A$, gives the transport number of the cation. Thus,

$$t_+ = \frac{\delta n_A F}{Q} \quad , \quad t_- = \frac{\delta n_C F}{Q} \qquad (3.8)$$

One point to note which will become important in the following section on the measurement of transport numbers in membranes was that the motion of the ions and hence the measurement of the transport numbers in solution was relative to the solvent.

The final method for measuring transport numbers in solution compares the emf of a cell with transference to the emf of a cell without transference, given the condition

that both cells have the same overall cell reaction.

For example, the potential, E (V), of the cell without transference:

$$\text{Ag, AgCl} \mid \text{MCl}(m') \mid \text{M} \mid \text{MCl}(m) \mid \text{Ag, AgCl} \qquad (3.9)$$

can be combined with the potential, $E_t$, of the cell with transference:

$$\text{Ag, AgCl} \mid \text{MCl}(m') \mid \text{MCl}(m) \mid \text{Ag, AgCl} \qquad (3.10)$$

to give the transport number of the cation, $t_{M^+}$, as:

$$t_{M^+} = \frac{E_t}{E} \qquad (3.11)$$

The problem with this method is the concentration to which $t_{M^+}$ referred since the experiment requires that $m' \neq m$.

### 3.1.4 Measurement of transport numbers through membranes

Determination of the transport numbers through membranes may be made in a number of ways. This section discusses the methods and ideas of previous workers in order to show how the techniques used in this work have been developed.

To measure a transport number, a flux of ions has to be measured and this is most easily done by allowing a change in concentration on either side of the membrane to occur. The problem with this is that, transport numbers are dependent on concentration and also that a difference in concentration on either side of the membrane allows diffusion to influence the results. The relationship between transport number and external concentration is unambiguous where concentrations on either side of the membrane are equal. Kressman and Tye [65] considered the less simple situation where

concentrations on either side of the membrane were different. Dependence or independence of the transport number on the donating- or receiving-side concentration were established by considering the stationary concentration profiles that were set up within the membrane during the passage of current. A "true" transport number due solely to the passage of electric current, and an "observed" transport number, obtained experimentally from concentration changes and possible diffusion effects were defined. These became equal if the concentration profile within the membrane was horizontal at one of the surfaces, i.e. there was no diffusion.

It was shown that where transport number was a function of concentration and decreased with increasing concentration, as was the case with the two membranes used in this study, then the transport number was dependent on the receiving-side concentration and independent of the donating-side concentration. Results were independent of current density, thus indicating that a true transport number had been measured and not a quantity complicated by diffusion [65].

Several workers [66,67,68 & 69] have measured transport numbers in conditions where from identical anolyte and catholyte concentrations, a concentration difference was allowed to build up with flow of current. This method was clearly unsatisfactory since transport number is not independent of both concentrations, such a concentration difference will encourage diffusion and osmosis to influence the results and it is impossible to state the concentration to which the transport number relates. The conclusion of Kressman and Tye [65] , " ..... it follows from this study that the preferred procedure must be to establish by preliminary experiments whether the transport number is dependent on the donating- or receiving-side concentration, and then to keep the concentration constant on the concentration-dependent side, the transport number being determined from the change in electrolyte content on the other side", should be noted. In their experiments the concentration of the concentration dependent side was allowed to change but the effects were minimised by working with a large volume of solution. Recently, Atieh and Cheh [70] obtained transport numbers for a Permion/KOH system similar to the one investigated in this study, using the experimental techniques of Kressman and Tye [71].

Oda and Yawataya [66] compared transport numbers measured whilst allowing concentrations to change using a mass transport technique with those measured from

membrane potentials. The transport number through a membrane was computed from the measurement of membrane potentials which arose across a membrane separating two solutions of different concentrations. The Nernst equation was used to correlate the membrane potential with the transport number as follows :-

$$t_+ = \frac{1}{2}\left(1 + \frac{E_{obs}}{E_{th}}\right) \qquad (3.12)$$

$$E_{th} = \frac{RT}{nF} \ln\frac{a_2}{a_1} \qquad (3.13)$$

where $t_+$ was the cation transport number, $E_{obs}$ (V) was the observed value of the membrane potential, $E_{th}$ was the calculated value of the membrane potential, $a_1$ and $a_2$ were the activities of the solutions separated by the membrane and R, T, n, and F took their usual significance. The method was simple but indirect since the potential was recorded when there was no current flowing through the membrane. The Nernst method also required the concentration on either side of the membrane to be different. The problem was then to decide on the concentration to which the observed transport number applied. In the mass transport technique a two compartment cell was used with an ion-exchange membrane separating the two electrolyte compartments. The cell contained reversible electrodes and transport numbers were determined from the contents of the electrolyte compartments before and after the passage of current. The transport number measured using this technique was found to be greater than values obtained from membrane potentials.

Rosenberg, George and Potter [69], using a sulphonated cation exchange membrane did a similar comparison to Oda and Yawataya, but obtained converse results. The membrane potential transport number was greater.

These authors highlighted an inconsistency in the literature, in that the term "Hittorf" transport number had been applied both to "mass transport" and "membrane potential" transport numbers. In solution the Hittorf transport number was calculated from the changes in concentration of solution after the passage of current without taking

account of transport of solvent molecules since it was usually measured relative to them. Oda and Yawataya [66], stated that since the Nernst method held where only ion transport was considered it was identical with the Hittorf transport number, and there after this term was used. They went further to define a "true" transport as being determined from the changes in concentration of solution on either of a membrane after the passage of current. For membranes, this author considers this to be a Hittorf type experiment with the membrane acting as the frame of reference.

The differences in transport numbers obtained from the mass transport (Hittorf) method which took into account the transference of solvent and the membrane potential method which did not, were first highlighted by Staverman [72] and Scatchard [73].

A modification in techniques which allowed a concentration difference to develop with flow of current was to start the experiment with an initial concentration difference across the membrane. The requisite quantity of charge was then passed to reverse the concentration gradient. The advantage of this technique was that errors caused by diffusion and osmosis were reduced [74 & 75].

In general the transport number of a species is different through the membrane than in solution and the resultant effects of concentration polarisation in the solution adjacent to the membrane must be avoided. On the imposition of a constant current density normal to the interface ions will either accumulate or deplete at the interface and as soon as the concentration at the interface becomes different from that elsewhere in the system, diffusion will commence, both in the free solution and within the membrane, in such a direction as would correct the change [76]. Kressman and Tye [77] investigated the effect changing the current density had on the transport of ions through ion-exchange membranes. The anolyte and catholyte were either stirred or unstirred. Working at low current densities transport numbers were found to be independent of stirring but affected by diffusion. At high current densities and in an unstirred system ions were transported through the membrane at a faster rate than they could diffuse and be transported through the solution and up to the membrane face. This resulted in the concentration of ions in solution adjacent to the membrane falling and hence lowered transport numbers. Normal transport numbers were obtained once the solution was stirred. The transport numbers obtained were therefore solely due to the passage of electric current and not enhanced or depleted by other fluxes. Even if the electrolyte is

stirred, there is still a thin layer of solution adjacent to the membrane, the Nernst film which remains unstirred. The chosen current density is therefore a compromise. It must be high enough so that diffusion is minimised but not too high so as to deplete the Nernst film of ions.

In ideal circumstances measurements should be made while maintaining concentrations constant and equal on either side of the membrane . Zelman, Kwak, Leibovitz and Spiegler [78] and Brun, Berg and Spiegler [79] describe a method in which this condition was satisfied by a "concentration-clamp". Transport was not measured by determination of solution concentration before and after the passage of current but by the amount of electrolyte added to the solutions so as to keep their concentration constant. The constant concentration was achieved by feedback mechanisms based on electrical conductivity sensors which detected small changes and actuated a microburette or a demineralising loop (containing a mixed bed of ion-exchange resins) for introduction or removal of salt from the respective half cell. The technique had the following disadvantages :

(i) The equipment was complex, expensive and time-consuming to construct and commission.

(ii) Precise temperature control was necessary due to the use of conductivity probes.

(iii) Reversible or rechargeable electrodes were required since the evolution of gas bubbles made concentration sensing by conductivity probes inaccurate.

Water transference is often measured simultaneously with ionic transport by determining weight [71,80 & 81] and volume [68,69,74 & 75] changes. In the latter method water transference may be underestimated due to bowing of the membrane in the opposite direction to solvent flow.

A review of recent literature [82,83,84 & 85] reveals that Hittorf and Emf measurement remain popular methods for determining transport numbers through ion-exchange membranes. However a concentration difference is still tolerated [82]. Both methods give good agreement when the water contribution to the potentiometric

transport numbers is taken into account.

A new method by Kontturi et al [86] measured individual transport numbers in a mixed counter-ion electrolyte by the analysis of individual membrane layers after a run. Their two compartment cell was separated by a membrane stack. Experimental conditions were chosen to create a diffusion free zone in the membrane stack when a constant current was passed. The ionic content throughout the stack was determined by flame photometry and the transport of ions through the homogeneous region was calculated from the change in ionic content of the individual membrane layers before and after the passage of current. A problem with the method was determination of the ionic content by flame photometry. This led to errors in transport numbers of 5%. The authors suggest the technique is analogous to the Hittorf method for determination of transport numbers in electrolyte solution.

The Hittorf method was adapted by Forland [87] to measure single transport numbers from a mixed counter-ion electrolyte. A four chamber cell was described. A middle chamber was connected to two anode chambers and one cathode chamber by membranes, the one of interest being adjacent to the cathode. The anode compartment contained single counter-ion electrolyte and correct currents were chosen so as to keep the mixed electrolyte concentration of the dependent middle chamber constant. The problem of diffusion from the anolyte compartments to the middle chamber is still present. Transport number ratios were determined from the cation current ratios.

The importance of maintaining concentrations constant and equal on either side of the membrane and working at a high current density has been shown. A final point for consideration is the thin layer of electrolyte in between the membrane layers occurring when a stack of membranes is used for transport number determinations. Forssell et al [88] have shown both theoretically and experimentally that this inhomogeneity adapts itself to the transport in the ion-exchange membrane provided the layer is thin enough and the electric current does not exceed the limiting current since the diffusion coefficients in the electrolyte layers between the membrane films were found to be of the same order of magnitude as in the membrane itself.

## 3.2 Experimental

### 3.2.1 Apparatus

The main body sections of the cylindrical transport cell (figures (3.3 and 3.4)) used in the transport experiments consisted of four polytetrafluoroethylene (P.T.F.E) compartments. The function of the inner two compartments was to house the electrolyte solution during a run. These compartments were fitted with stirrers of the same material to maintain uniform concentration and had orifices for introducing and removing electrolyte. The stirrers were connected to 12V d.c. motors. A pre-soaked membrane assembly was placed between the two electrolyte compartments.

Water was circulated through the outer two P.T.F.E compartments at a rate of 50ml/min. by means of a peristaltic pump from a reservoir maintained at 25°C.

A platinum anode and a nickel cathode, both in the form of metallic sheets separated the inner electrolyte compartments from the outer water jacket. The pressure required to seal the cell caused slight indentations in the surface of the metal electrodes. After regular use these became more pronounced and it became important to position the electrodes in the same manner each time the cell was assembled in order to minimise leakage from the cell. Circular electrodes of the same diameter as the cell were therefore used to facilitate positioning. A triangular tag protruded from each electrode, as shown in figure (3.5), for the attachment of the power lines. The shape was economical as regards the cost of the platinum.

The cell was supported by a steel base (figure (3.6)) with steel pegs from each compartment slotting into a groove thus preventing rotation of the cell.

The cell was sealed by means of a screw arrangement with the applied force acting on steel plates which snugly fitted the water jacket. Sufficient force was required to ensure no leakage from the cell during the run (see section (3.2.3) on electrolyte recovery).

The transport cell was incorporated into an electrical circuit (figures (3.7 & 3.8)) in series with a Coutant LA 200-2 power supply and a Tindsley 1Ohm, 3Amp standard resistor. For transport runs at a high current (up to 10Amps) ten, 10ohm 17W ceramic resistors connected in parallel were used in conjunction with a Coutant LB 1000 power supply.

Figure 3.3 Photograph of the transport cell

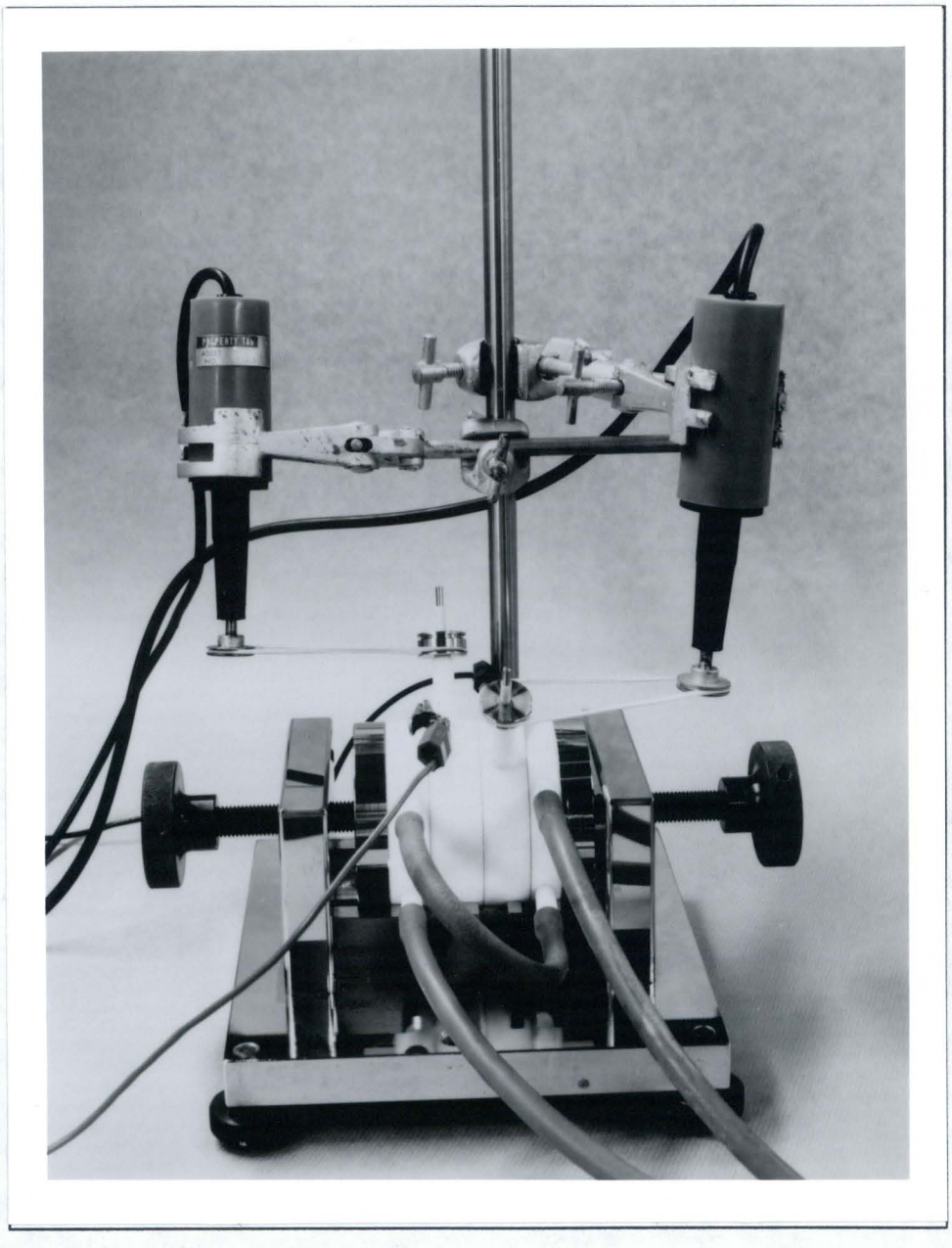

Figure 3.4 Cross-sectional drawing of the transport cell

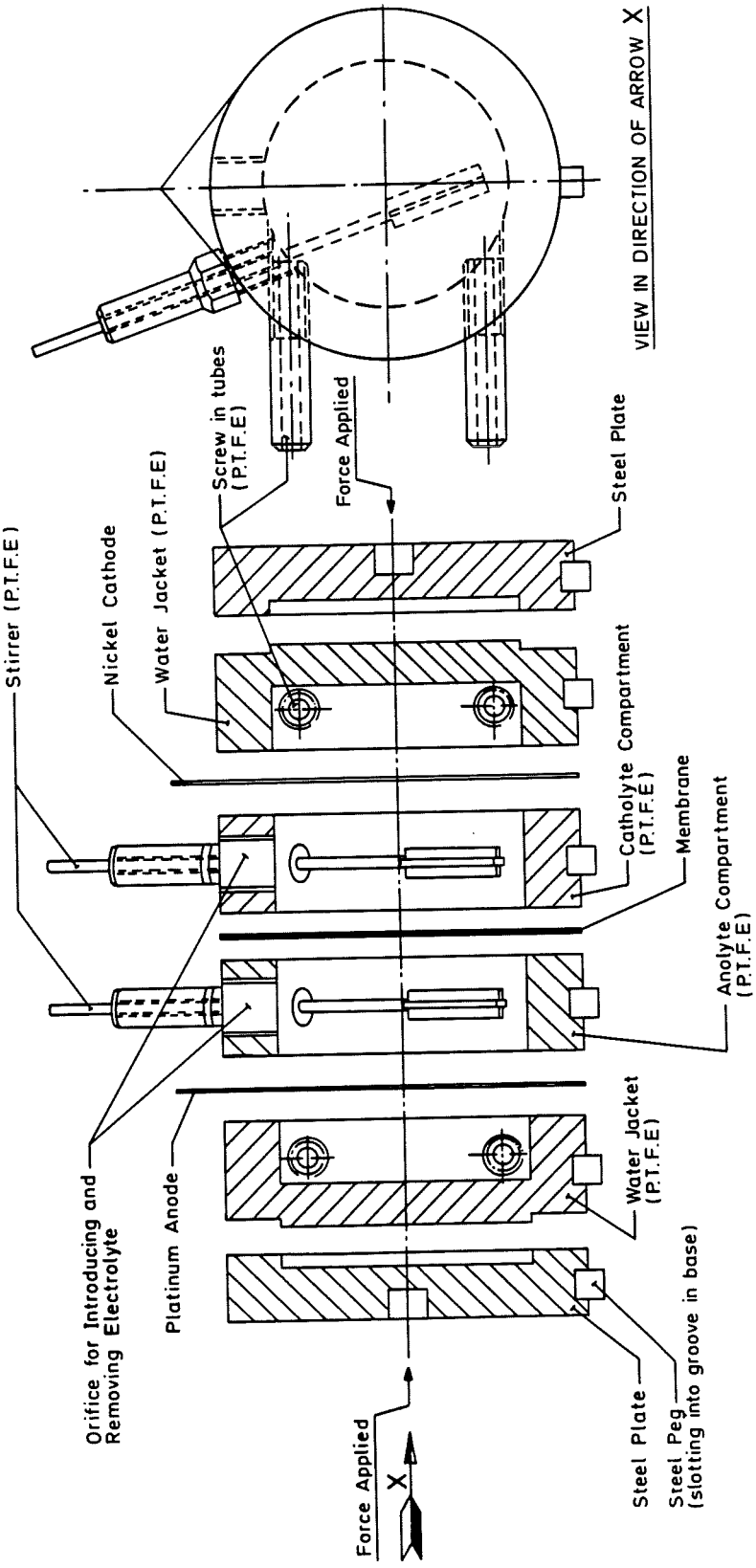

Figure 3.5 Electrode design

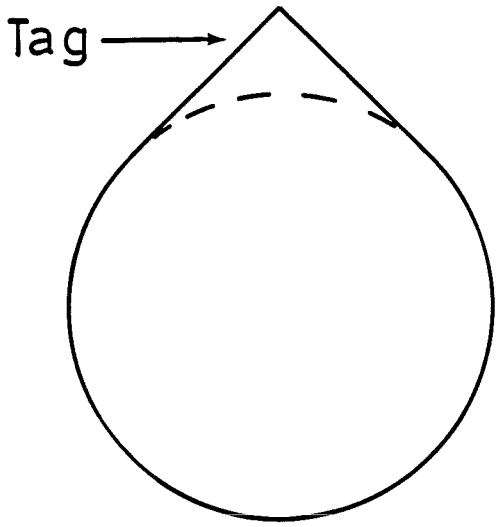


Figure 3.6 Drawing of transport cell base

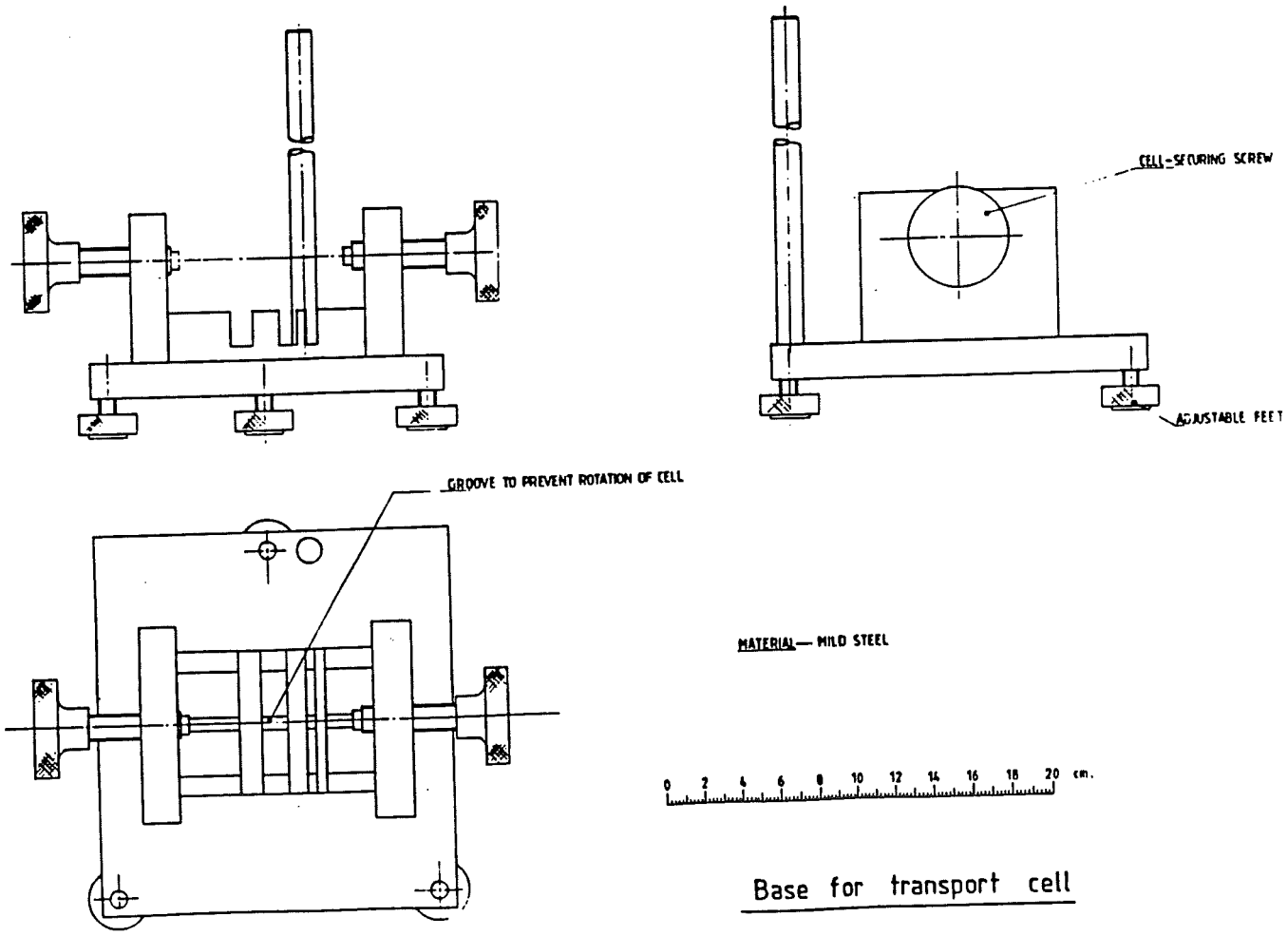

Figure 3.7 Photograph of transport cell and associated apparatus

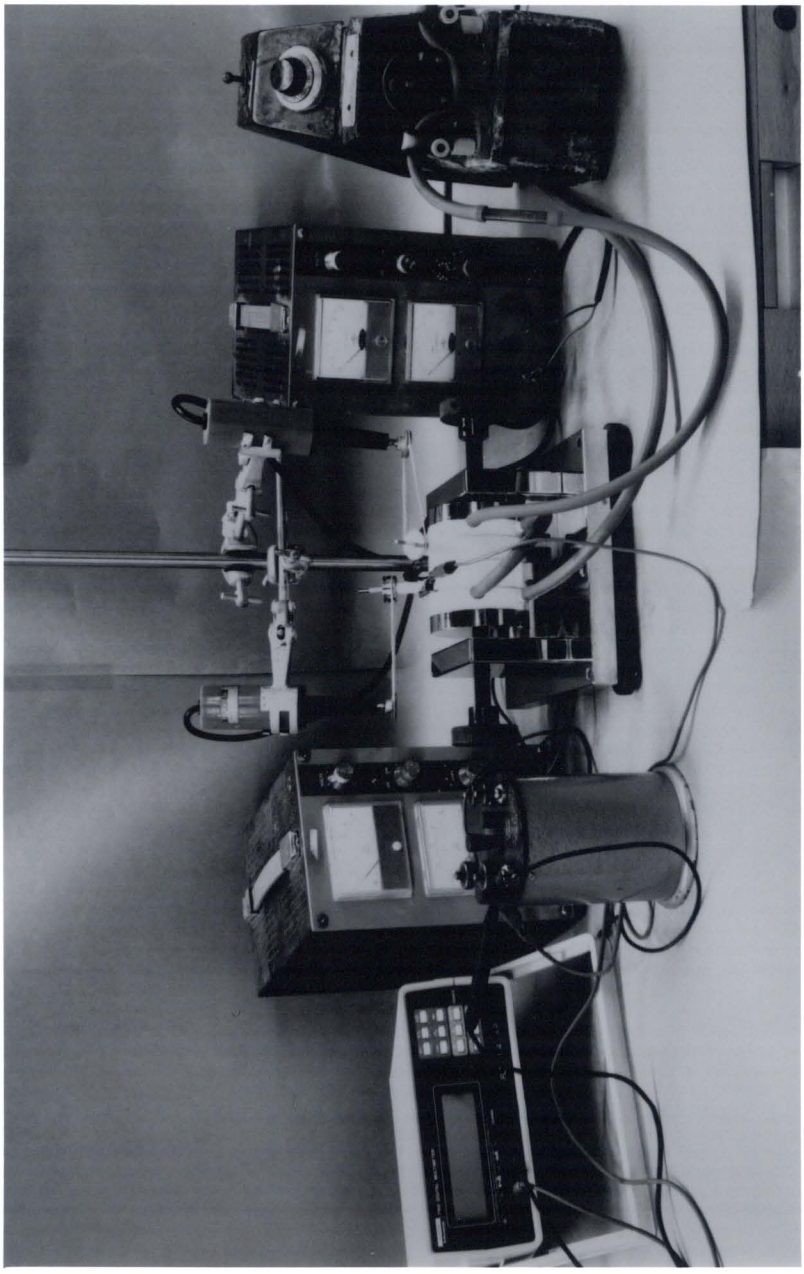

Figure 3.8 Transport cell and electrical circuit

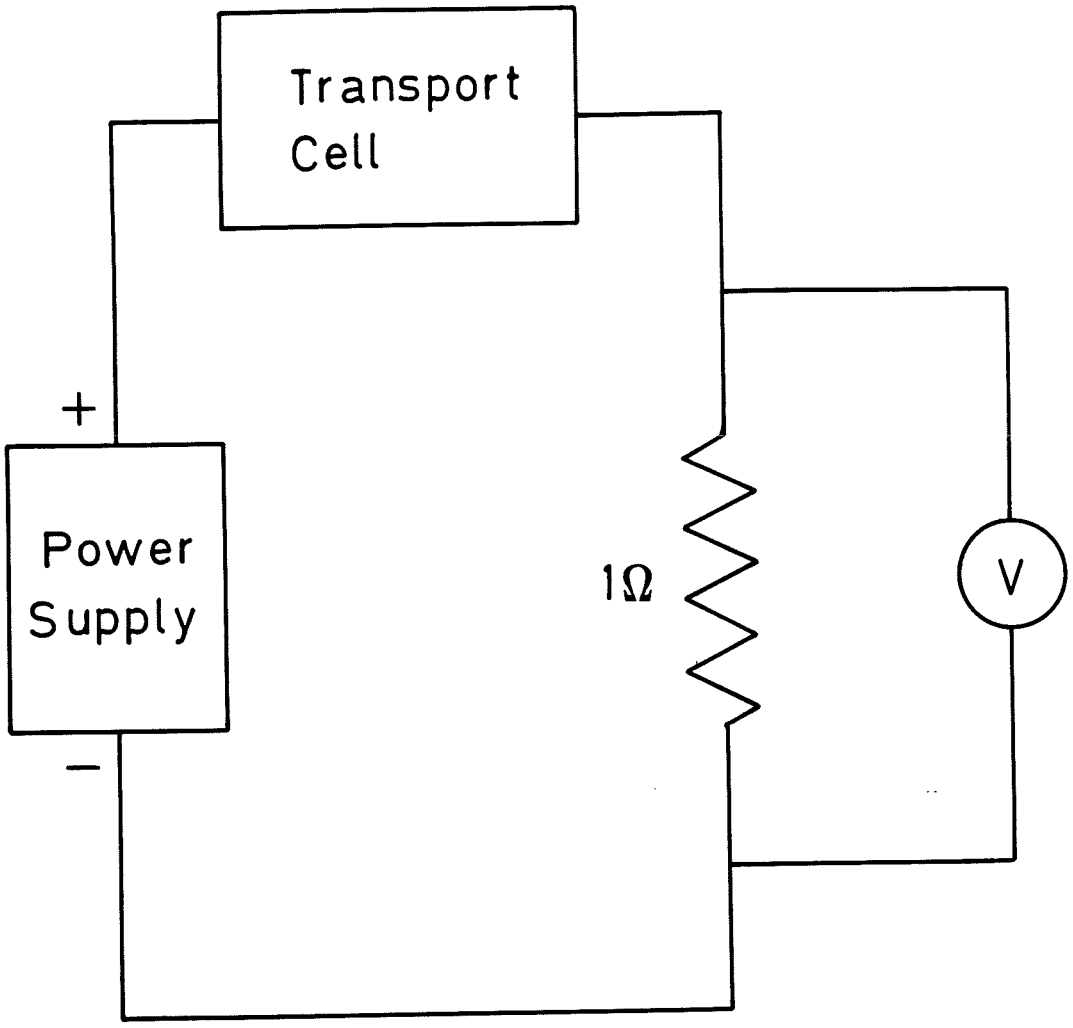

The required current was achieved and maintained throughout the experiment by monitoring the voltage across the resistor with a Solatron 7150 digital multimeter, and varying the power supply accordingly.

The experiment was timed using a quartz Casio stopwatch reading to 1/100 of a second.

In some experiments the resistance across the cell was monitored with a Linseis chart recorder.

### 3.2.2 Procedure used for the measurement of transport numbers through Cellophane.

The molarity of the solution to be studied together with the amount of KOH by weight in this solution were determined by titration with 0.1M HCl using Methyl Orange solution as indicator.

Both of these parameters were determined in one titration by weighing the volume of solution delivered from a pipette, and then diluting this to approximately 0.1M, in a suitable volumetric flask.

At the start of a series of experiments a stock solution of about 12-14M KOH was prepared and analyzed in the same manner. This was stored in an inert airtight container.

Squares of membrane, of side 10cm, were cut from the roll and soaked overnight in a solution of the KOH of the concentration to be studied. This was done in a sealed container to prevent the adsorption of $CO_2$ from the air.

The soaked membrane films were removed individually from the electrolyte solution and stacked. Each layer adhered to the previous layer by the action of a small hand held roller. The rolling served to remove excess electrolyte and air bubbles from between the layers. The excess electrolyte on either face of the resultant membrane stack was then removed by careful mopping with pieces of filter paper.

At the start of the run the cell was clean and dry. The membrane stack was placed on the inner side of the catholyte compartment, having previously been cut to slightly overhang the circular shape. The rest of the cell was assembled around this as follows. The cell-securing screws were released sufficiently so that the steel plates backed onto the vertical, supporting walls of the transport cell base. The water jacket

was then slotted into position touching the steel plates. The catholyte compartment was positioned vertically with the membrane stack adhering to the P.T.F.E. The anolyte compartment was then located and all compartments joined by adjustment of the screws arrangement. The force was relaxed slightly so that the sheet metal electrodes could be slid between the water jacket and the electrolyte compartments. Enough force was then applied to seal the cell, but care was taken, not to squeeze any electrolyte from the membrane stack by over-tightening.

The KOH solution, approximately 10ml, was introduced into each compartment from a syringe stirred and then removed with another syringe fitted with a hypodermic needle. Care was taken not to pierce the membrane during this process. The cell was then opened and all internal surfaces were mopped visibly dry with a piece of filter paper. This pre-run filling and emptying exercise was necessary so as to have the cell in the same condition at the start of the experiment as it would be, when emptied at the end of the run.

The cell was re-assembled and a weighed 10ml, of KOH solution was introduced to each compartment via a syringe. The compartment was then plugged and a water reservoir and power lines connected. Throughout the run the solutions were stirred vigorously to discourage the formation of stagnant layers in the solution immediately adjacent to the separator and to ensure uniform concentration throughout the compartment. Each determination of transport number experiment was carried out at current densities given by equation (3.14) with a maximum of $200mAcm^{-2}$ [71].

$$\text{Current Density } (mAcm^{-2}) = 30 \times N \qquad (3.14)$$

where N ($moledm^{-3}$) is the external normality of the initial solution.

The area of the membrane in contact with the electrolyte solution was $5cm^2$, ie. the initial volume of electrolyte solution, $10cm^3$, divided by the thickness of the electrolyte compartment, 2cm. Hence the current maintained through the resistor was set at five times the value of the current density given in equation (3.14), with a maximum of 1Amp.

During the run the anolyte and catholyte concentrations decreased and increased

respectively due to the passage of the current. To compensate for this, small additions of 12-14M KOH were made to the anolyte and additions of water to the catholyte at regular intervals. These additional solutions were delivered from syringes which were weighed before and after the run, and thus the total amount of solution or water added was determined as a weight.

The quantities to be added were calculated from the following equations [80],

$$x = Q\left[M_A\left(\frac{100}{X}-1\right)t_M^{/} - M_W(t_W^{/} - 1)\right] \qquad (3.15)$$

$$y = Q\left[M_A t_M^{/}\left(\frac{100 - X}{X-Y}\right) - M_W(t_W^{/} - 0.5)X\right] \qquad (3.16)$$

where x is the total weight of water to be added to the catholyte (g), y is the total weight of Y% KOH to be added to the anolyte (g). Concentrations as % by weight are tabulated [89]. The initial concentration of KOH in the cell is X% ; $M_A$ and $M_W$ are the molecular weights of KOH and water respectively : $t_M^{/}$ and $t_W^{/}$ are the approximate assumed transference numbers of $K^+$ and water, taken from true transference numbers [80] and Q is the charge passed (F).

A BASIC computer program was written to calculate these additions, as a weight (g) and a volume (ml) together with the current required through the resistor (mA) given the concentration of the electrolyte solution (M), the concentration of the addition solution (M) and the approximate assumed transference numbers for the potassium ion and water.

Equations (3.15) and (3.16) allow for the electrolysis of water which removes 1 $moleF^{-1}$ at the cathode and generates 0.5 $moleF^{-1}$ at the anode :-

$$\text{Cathode} \quad 2H_2O + 2e \rightarrow H_2 + 2OH^- \qquad (3.17)$$

$$\text{Anode} \quad 4OH^- \rightarrow O_2 + 2H_2O + 4e \qquad (3.18)$$

The duration of each run for Cellophane experiments was two hours, with 12 additions each of approximately the same volume. The first after 5 minutes and then further additions after every subsequent 10 minutes. The length of time of a run was chosen as a compromise since longer runs lead to greater concentration differences between the compartments and shorter runs mean a smaller change in concentration, both of which will increase the experimental error.

The current was passed for a measured time by simultaneously switching on the power supply and starting the stop watch. After two hours had passed the watch was stopped and the power switched off.

Before the electrolyte was removed, the cell was unclipped from the circuit and the stirring motor removed. The water jacket was emptied by blowing water out of the system with compressed air, thus drying the outer faces of the electrode.

The cell was emptied of electrolyte, anolyte compartment first, using 1ml syringes of known weight fitted with hypodermic needles into flasks of known weight. The syringes and flasks were reweighed after emptying the compartment and hence the amount of bulk solution by weight in each compartment at the end of the experiment was determined. Whilst one compartment was being emptied the other was kept plugged.

The concentration of the bulk solution was established by transferring the solution from the flasks and syringes to volumetric flasks of a capacity to make the solutions approximately 0.1M. Determination of KOH content was by titration with 0.1M HCl using a Methyl Orange solution as pH indicator.

The crucial part of the procedure was now to remove the residual electrolyte from the electrode compartment without losing a significant amount. The method adopted was to turn the cell and base on it's side before releasing the screw arrangement. In this way the cell could be removed from the base with the membrane and electrode still in place. Each electrode, compartment and membrane surface was then mopped individually and the used filter paper dropped into a conical flask containing 200ml. of distilled water. The amount (no. of moles) of KOH in the moppings was determined by titrating with 0.01M HCl, using BDH 4406 pH indicator to detect the end point.

### 3.2.3 Recovery procedure

If there is a small leakage of electrolyte from the cell during the run, then large discrepancies occur when calculating the true transference number. An investigation into the amount of leakage from the cell was conducted to quantify this error. From this calibration a possible correction factor was obtained and applied to the actual transference number experiments.

The calibration was carried out by assembling the cell as if a run was to be performed. The electrolyte compartments were primed with KOH solution, emptied as previously described and then refilled with weighed quantities of KOH solution. The weight of solution recovered was recorded as a percentage of the initial amount of the solution.

The amounts of moppings left in the cell were calculated in the earlier experiments as a weight by difference from the filter paper before and after mopping out the cell. In the later experiments the weights of moppings were estimated by titration using the known concentration of the solution.

As a check on the latter procedure an experiment was performed to test whether or not all the potassium hydroxide could be retrieved from the filter paper. This was achieved by soaking the filter paper in a known amount of KOH and then analyzing with 0.1M HCl. Complete retrieval of the KOH was confirmed.

In order to minimise leakage and establish adequate recovery procedure a significant amount of time was spent trying different methods. Percentage recoveries together with variations in the experimental conditions of the cell including the removal of electrolyte have been tabulated (Appendix (A)). Although good recoveries were achieved the average was never 100% recovery. The most significant development that improved yield was to turn the cell (and stand) on its side for the mopping procedure. This crucial technique was described in section (3.2.2). In this way the cell could be opened without losing any electrolyte. When the cell was opened upright and the force holding the cell together was removed, some electrolyte adhering to the electrode faces was lost due to the electrodes slipping. The eventual recovery procedure was consistent and therefore a correction factor was derived.

### 3.2.4 Statistical analysis of the recovery data in order to obtain a correction factor

The average percentage recovery was below 100, and since the calculation of the true transference number assumes 100% recovery an adjustment factor was sought. To find a suitable value by which the amount of solution recovered could be multiplied the results from cell test run numbers 15-55 (excluding those with obvious experimental error) were analyzed on a DEC-10 mainframe computer using the Minitab statistical package.

Minitab is a statistical computing system for use with small to medium data sets. Its analysis procedures can be applied to graph plotting, regression and other statistical tests.

The following statistical conclusions were drawn :-

(i) Percentage recoveries were independent of the length of time the solution was left in the cell.

(ii) Recoveries were independent of whether the anolyte or catholyte compartment was emptied first.

(iii) Recovery from the anolyte compartment was constantly higher than that from the catholyte compartment and the spread of recoveries from each compartment was small.

In light of the above conclusions it was decided that a suitable correction factor for recovery from each electrode compartment should be based upon the mean percentage recovery from that compartment over the data set used in the statistical analysis. The mean percentage recoveries were found to be 99.926% and 99.671% for the anolyte and catholyte respectively. Hence recoveries from the anolyte compartment were multiplied by 100/99.926 and recoveries from the catholyte compartment by 100/99.671.

### 3.2.5 Procedure used for the measurement of transport numbers through Permion

The same basic method was adopted for Permion as for Cellophane, as described in section (3.2.2). In order to estimate the required additions, values of the transference numbers for Cellophane at similar concentrations were used as approximate transference numbers. This proved to be a bad approximation since $t_K+$ and $t_{H2O}$ for Permion were too dissimilar to those found for Cellophane at a particular concentration.

Better approximations could be obtained by the following iterative process :-

(i) Use Cellophane transport numbers as a first approximation giving a result for Permion to be used as a second approximation at that concentration.

(ii) Having obtained one reasonable Permion result, use this as the approximate transference number for runs at concentrations 1M either side of this concentration and hence obtain values over a wide range of KOH concentrations.

To complete the experimental method for Permion it is necessary to introduce some discussion of the previous approximations. Although the results for Permion produced the kinds of trends expected, the desired precision of the data was not present.

In some experiments there was twice as much electrolyte in one compartment as in the other at the end of a run. It was thought that this might influence the transport numbers and therefore needed to be taken into account. Transport numbers were obtained in the following way :-

(i) A run was performed using additions calculated from an approximate transference value from the Permion curve. This produced a better approximate transference number at that concentration and a difference in weight of electrolyte retrieved from the compartments.

(ii) A second run was then performed with additions calculated using the transport number obtained from the first run. The difference in volume, established from the first run was then compensated by making extra additions to the low volume

side of the electrolyte at the concentration being studied. These were made at the same times as the additions to maintain constant concentration.

Hence the volume as well as the concentration of the electrolyte were maintained constant on either side of the membrane throughout the run.

### 3.2.6 The advantages of the mass transport technique used in this work

The meticulous technique described in section (3.2), for the measurement of transport numbers, was developed from the work pioneered by Jenkins et al [80]. To minimise the adverse effects of diffusion and osmosis, and to obtain a transport number related to a specific electrolyte concentration, the technique holds solution composition constant and equal on either side of the membrane. The equipment unlike that used by other authors [78] is relatively simple and the use of reversible electrodes is not required.

The design of the cell allows rapid assembly which is important since it is desirable that the pre-soaked membrane does not dry out. Assembly gives an excellent membrane/cell seal, which as shown in section (3.2.3) eliminates solution leakage.

The passage of an electric current across a membrane separating two finite volumes of electrolyte results in concentration changes in the anolyte and catholyte which must be minimised. Knowledge of the initial and final contents of the compartments, the additions required to maintain concentration constant and equal on either side of the membrane and the total charge passed allows calculation of the true ionic and solvent transference numbers within the membrane. The technique determines these values simultaneously.

The initial contents of the compartments and the additions made to keep the concentration constant are accurately determined by weight. The investigation into recovery shows an efficient and consistent removal of electrolyte and hence an accurate determination of final contents. A small error in this determination would introduce large errors in transport numbers. The significant part of the procedure to ensure good recovery was turning the cell on its side for mopping (see section (3.2.2)).

## 3.3 Results and discussion

### 3.3.1 Determination of precise transference numbers

With each run the percentage recovery of the final amounts of the anolyte and catholyte combined was slightly less than 100%. This loss was greater than the losses discovered when testing the cell (as described in section (3.2.3)).

It has been previously reported [80] that in the absence of leakage a loss of electrolyte from the cell could arise due to spray. The spray would be expected to contain KOH and water in the same proportions as the solution, the water lost as spray was determined from the loss of KOH. It was surmised that the spray was caused by the evolution of gas at the electrodes. The same authors found a loss of water over and above that which could be accounted for by spray and it was presumed that this was due to evaporation into the gas evolved from the electrodes. An average loss of solution by spray of $0.5mlF^{-1}$ and of water by evaporation of $0.07moleF^{-1}$ was reported.

A similar treatment for this investigation, described in Appendix (B), gave an average loss of solution by spray of $1.54mlF^{-1}$ and loss of water by evaporation of $-0.067moleF^{-1}$. The negative value indicates that no water was lost due to evaporation. These results were obtained using data from transport runs where the final concentration in either compartment differed by no more than 3% from the starting value, the difference between the final anolyte and catholyte concentrations did not exceed 3% of the starting concentration and the current was passed for 2 hours. Due to the electrolysis of water the volume of gas evolved from the anode is one half of that evolved from the cathode, therefore it is presumed that the loss of spray from the anolyte is one third of $1.54mlF^{-1}$ and the loss of spray from the catholyte is two thirds of $1.54mlF^{-1}$.

The primary transport data obtained from each compartment may be corrected as follows.

Corrections to the anolyte,

$$\Delta t_{K^+}^{/} = -\frac{1}{3}\left(\frac{1.54\ C_s}{1000\ M_{KOH}}\right) \qquad (3.19)$$

$$\Delta t'_{H_2O} = -\frac{1}{3}\left(\frac{1.54\ C_w}{1000\ M_{H_2O}}\right) \qquad (3.20)$$

Corrections to the catholyte,

$$\Delta t'_{K^+} = +\frac{2}{3}\left(\frac{1.54\ C_s}{1000\ M_{KOH}}\right) \qquad (3.21)$$

$$\Delta t'_{H_2O} = +\frac{2}{3}\left(\frac{1.54\ C_w}{1000\ M_{H_2O}}\right) \qquad (3.22)$$

$\Delta t'm$ and $\Delta t'w$ are the corrections to the measured values, the negative and positive signs indicate they must be subtracted from or added to the measured values respectively. $C_s$ and $C_w$ are the contents of KOH and water ($gl^{-1}$) in the solution and $M_K$+ and $M_{H2O}$ their respective molecular weights ($gmole^{-1}$).

The correction is deduced from averaged data and as there is considerable variation between experiments it would be preferable to eliminate the need for it. This is possible with the treatment explained in the following section.

### 3.3.2 Elimination of the need for a correction factor

Let x, ($mlF^{-1}$) equal the solution lost from the cell during a run as spray, caused by the evolution of gas at the electrodes. During the electrolysis of water twice the amount of gas is evolved from the cathode compared to the anode. Assuming a similar size of hydrogen and oxygen gas bubble, loss of solution from the anolyte equals 1/3x and loss of solution from the catholyte equals 2/3x. A loss of solution from the anolyte would increase apparent transport numbers whilst a loss of solution from the catholyte decreases apparent transport numbers.

For corrected transport numbers from each compartment;

$$t_A = t_A' - \frac{1}{3}x \tag{3.23}$$

$$t_C = t_C' + \frac{2}{3}x \tag{3.24}$$

where $t_A'$ and $t_C'$ are the measured transport numbers and $t_A$ and $t_C$ the corrected transport numbers of the same type of ion. Subscripts A and C refer to the anolyte and catholyte compartments respectively.

In ideal circumstances,

$$t = t_A = t_C \tag{3.25}$$

where t is the precise transport number across the membrane at a specific concentration. By the nature of the experiment the transport number determined from the anolyte compartment should be the same as the transport number from the catholyte compartment since the mass transported from the anolyte is gained by the catholyte.

Rearrangement of equations (3.23) and (3.24), and substitution of t for $t_A$ and $t_C$ from equation (3.25) gives;

$$t_A' = t + \frac{1}{3}x \tag{3.26}$$

$$t_C' = t - \frac{2}{3}x \tag{3.27}$$

To remove x ;

$$t = \frac{1}{3}\left(t - \frac{2}{3}x\right) + \frac{2}{3}\left(t + \frac{1}{3}x\right) \qquad (3.28)$$

Hence a precise determination of the ionic transport number and the transference of solvent taking into account the loss of solution by spray may be achieved without the need for individual corrections by use of the following equations.

$$t_{K^+} = \frac{1}{3}\left(t'_{K_C^+}\right) + \frac{2}{3}\left(t'_{K_A^+}\right) \qquad (3.29)$$

and

$$t_{H_2O} = \frac{1}{3}\left(t'_{H_2O_C}\right) + \frac{2}{3}\left(t'_{H_2O_A}\right) \qquad (3.30)$$

The subscripts $K^+$ and $H_2O$ refer to potassium and water respectively. The method of calculating $t'_{K^+A}$, $t'_{K^+C}$, $t'_{H2O\ A}$ and $t'_{H2O\ C}$ from the experimental data is shown in Appendix (C).

### 3.3.3 PUDO 193, Cellophane

Transport numbers of potassium and transference numbers of water through PUDO 193 Cellophane as obtained by analysis of the anolyte and catholyte compartments and with correction for recovery are shown in table (3.1). There is good agreement between each pair of potassium ion transport numbers and each pair of water transference numbers. The sixth column in table (3.1) is of transport numbers corrected for spray, using the method described in section (3.3.2). A tick in the seventh column is for a run where both the final anolyte and the final catholyte concentrations were within 3% of the starting value and the difference between the final anolyte and catholyte concentration was less than 3% of the starting concentration.

The reasons for these limits are as follows. If the concentrations on either side of the membrane at the end of a run are similar then the approximate transport numbers used to determine the additions during the run must have been correct. Hence diffusion and the effects of osmosis have been minimised and the transport numbers are representative of a specific KOH concentration.

Transport numbers of potassium and transference numbers of water through Cellophane, corrected for recovery and spray, versus external electrolyte concentration are shown in figures (3.9) and (3.10). Both the transport number of the potassium ion and the transference number of the water decrease progressively with increase in the external KOH concentration. This behaviour is typical of an ion-exchange membrane and is due to decreasing effectiveness of co-ion exclusion with increasing bulk solution concentration. At higher external electrolyte concentrations the membrane contains more co-ions (see section (2.3.4)) and hence the proportion of current carried by this species will be greater.

Similar values were obtained when 10, 5 and 2 sheets of membrane were used, confirming that diffusion of potassium and osmosis of water in the reverse direction were eliminated and the flux was solely due to the current.

A comparison of the results reported here and those reported by Jenkins et al [80] are shown in figures (3.11) and (3.12). To avoid any confusion the points from figures (3.9) and (3.10) have been omitted from figures (3.11) and (3.12). The following conclusions may be drawn :-

Table 3.1(a) Potassium ion transport numbers through Cellophane.

| Run | Conc. [M] | No. of Layers | $T_K+$ Anolyte | $T_K+$ Catholyte | $T_K+$ | 3% |
|---|---|---|---|---|---|---|
| 3.1 | 3.108 | 10 | 0.376 | 0.336 | 0.362 | |
| 3.2 | 2.060 | 10 | 0.377 | 0.370 | 0.375 | ✓ |
| 3.3 | 6.175 | 10 | 0.320 | 0.308 | 0.316 | |
| 3.4 | 4.113 | 10 | 0.347 | 0.352 | 0.349 | ✓ |
| 3.5 | 5.100 | 10 | 0.339 | 0.343 | 0.340 | ✓ |
| 3.6 | 2.945 | 10 | 0.354 | 0.357 | 0.355 | ✓ |
| 3.7 | 1.045 | 10 | 0.397 | 0.381 | 0.391 | ✓ |
| 3.8 | 7.490 | 10 | 0.331 | 0.320 | 0.327 | ✓ |
| 3.9 | 2.580 | 10 | 0.364 | 0.360 | 0.363 | ✓ |
| 3.10 | 8.875 | 10 | 0.317 | 0.300 | 0.311 | ✓ |
| 3.11 | 1.575 | 10 | 0.390 | 0.371 | 0.384 | ✓ |
| 3.12 | 3.648 | 10 | 0.351 | 0.345 | 0.349 | ✓ |
| 3.13 | 0.506 | 10 | 0.427 | 0.435 | 0.430 | |
| 3.14 | 6.200 | 10 | 0.328 | 0.321 | 0.326 | ✓ |
| 3.15 | 6.210 | 10 | 0.334 | 0.329 | 0.332 | ✓ |
| 3.16 | 6.210 | 5 | 0.336 | 0.319 | 0.331 | ✓ |
| 3.17 | 10.26 | 10 | 0.297 | 0.306 | 0.300 | ✓ |
| 3.18 | 3.550 | 5 | 0.358 | 0.330 | 0.349 | ✓ |
| 3.19 | 3.268 | 5 | 0.360 | 0.351 | 0.357 | ✓ |
| 3.20 | 11.28 | 10 | 0.309 | 0.276 | 0.298 | ✓ |
| 3.21 | 1.493 | 5 | 0.360 | 0.391 | 0.370 | ✓ |
| 3.22 | 9.392 | 5 | 0.315 | 0.298 | 0.310 | ✓ |
| 3.23 | 3.280 | 10 | 0.354 | 0.350 | 0.353 | ✓ |
| 3.24 | 3.280 | 5 | 0.353 | 0.347 | 0.351 | ✓ |
| 3.25 | 3.280 | 2 | 0.353 | 0.344 | 0.350 | ✓ |

Table 3.1(b) Water transport numbers through Cellophane

| Run | Conc. [M] | No. of Layers | $T_{H2O}$ Anolyte | $T_{H2O}$ Catholyte | $T_{H2O}$ | 3% |
|---|---|---|---|---|---|---|
| 3.1 | 3.108 | 10 | 1.57 | 1.41 | 1.52 | |
| 3.2 | 2.060 | 10 | 1.95 | 1.89 | 1.93 | ✓ |
| 3.3 | 6.175 | 10 | 0.866 | 0.678 | 0.803 | |
| 3.4 | 4.113 | 10 | 1.17 | 1.13 | 1.16 | ✓ |
| 3.5 | 5.100 | 10 | 0.977 | 0.909 | 0.955 | ✓ |
| 3.6 | 2.945 | 10 | 1.58 | 1.45 | 1.54 | ✓ |
| 3.7 | 1.045 | 10 | 3.02 | 2.87 | 2.97 | ✓ |
| 3.8 | 7.490 | 10 | 0.650 | 0.657 | 0.653 | ✓ |
| 3.9 | 2.580 | 10 | 1.69 | 1.67 | 1.69 | ✓ |
| 3.10 | 8.875 | 10 | 0.551 | 0.577 | 0.559 | ✓ |
| 3.11 | 1.575 | 10 | 2.37 | 2.27 | 2.34 | ✓ |
| 3.12 | 3.648 | 10 | 1.32 | 1.24 | 1.30 | ✓ |
| 3.13 | 0.506 | 10 | 3.86 | 4.06 | 3.92 | |
| 3.14 | 6.200 | 10 | 0.794 | 0.744 | 0.777 | ✓ |
| 3.15 | 6.210 | 10 | 0.771 | 0.751 | 0.764 | ✓ |
| 3.16 | 6.210 | 5 | 0.736 | 0.663 | 0.712 | ✓ |
| 3.17 | 10.26 | 10 | 0.432 | 0.483 | 0.449 | ✓ |
| 3.18 | 3.550 | 5 | 1.32 | 1.34 | 1.33 | ✓ |
| 3.19 | 3.268 | 5 | 1.42 | 1.37 | 1.40 | ✓ |
| 3.20 | 11.28 | 10 | 0.318 | 0.466 | 0.367 | ✓ |
| 3.21 | 1.493 | 5 | 2.49 | 2.30 | 2.43 | ✓ |
| 3.22 | 9.392 | 5 | 0.530 | 0.515 | 0.525 | ✓ |
| 3.23 | 3.280 | 10 | 1.41 | 1.42 | 1.41 | ✓ |
| 3.24 | 3.280 | 5 | 1.43 | 1.41 | 1.42 | ✓ |
| 3.25 | 3.280 | 2 | 1.41 | 1.43 | 1.42 | ✓ |

Figure 3.9 Transport numbers of potassium through Cellophane vs. external KOH concentration.

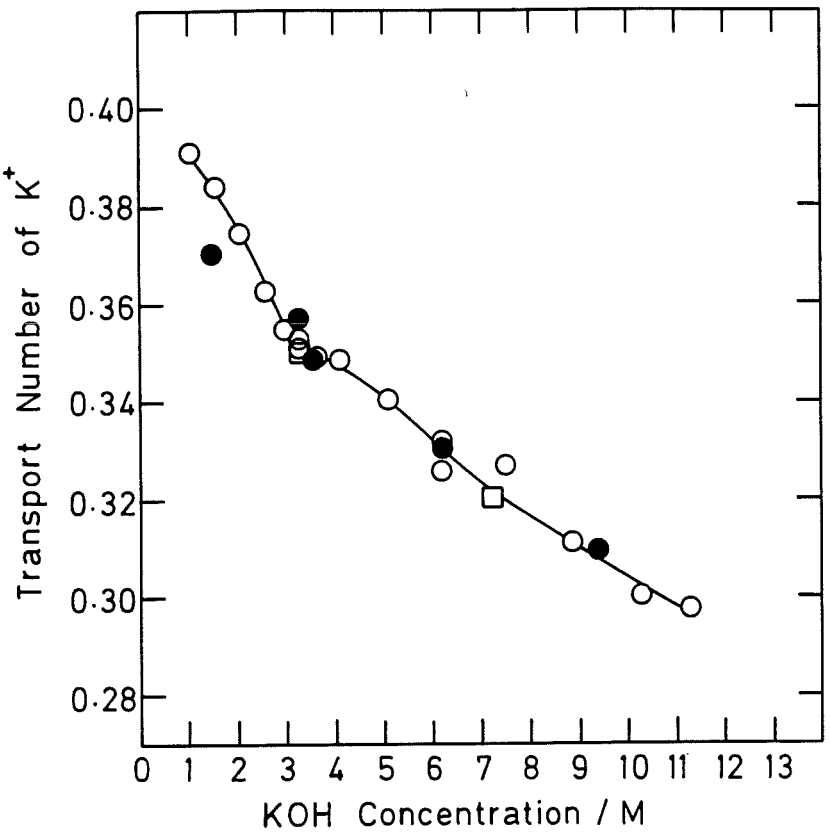


KEY
○ 10 sheets of Cellophane
● 5 sheets of Cellophane
□ 2 sheets of Cellophane

Figure 3.10 Transference numbers of water through Cellophane vs. KOH concentration.

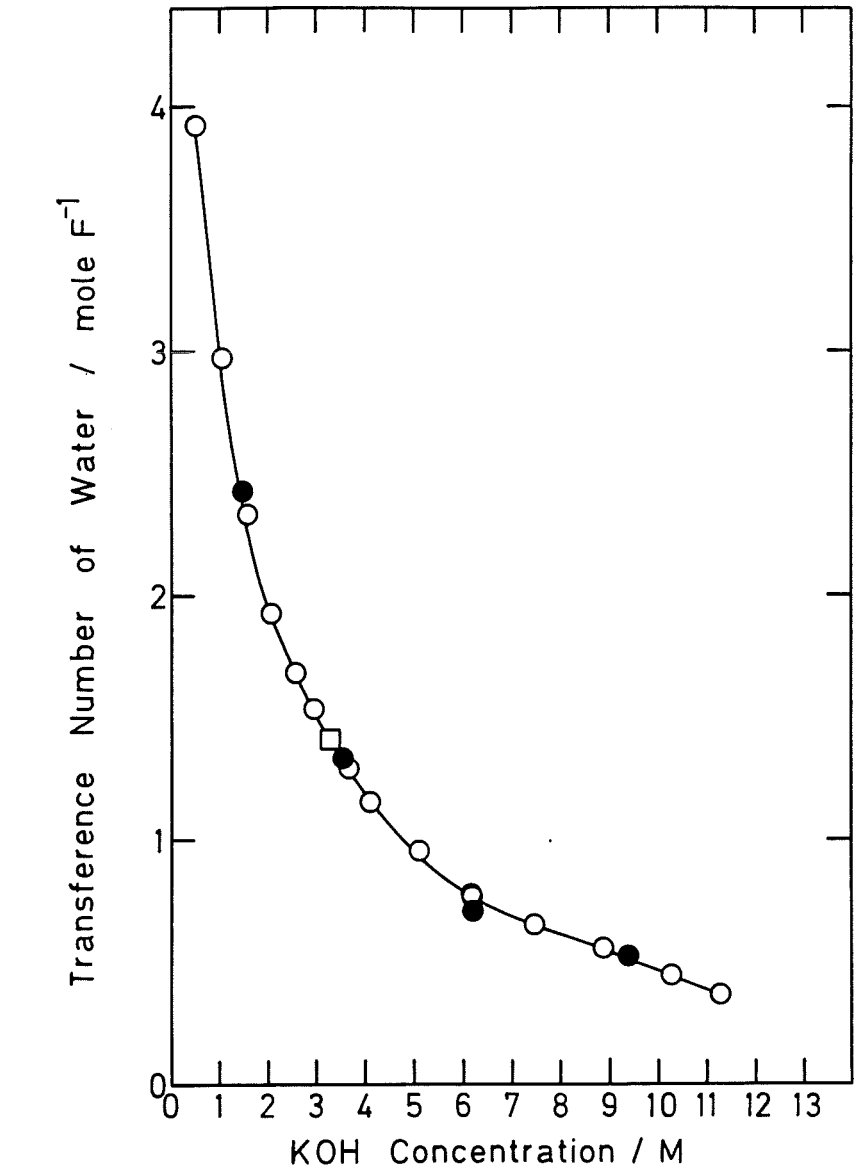

Figure 3.11 Comparison of potassium ion transport numbers through PUDO 193 Cellophane.

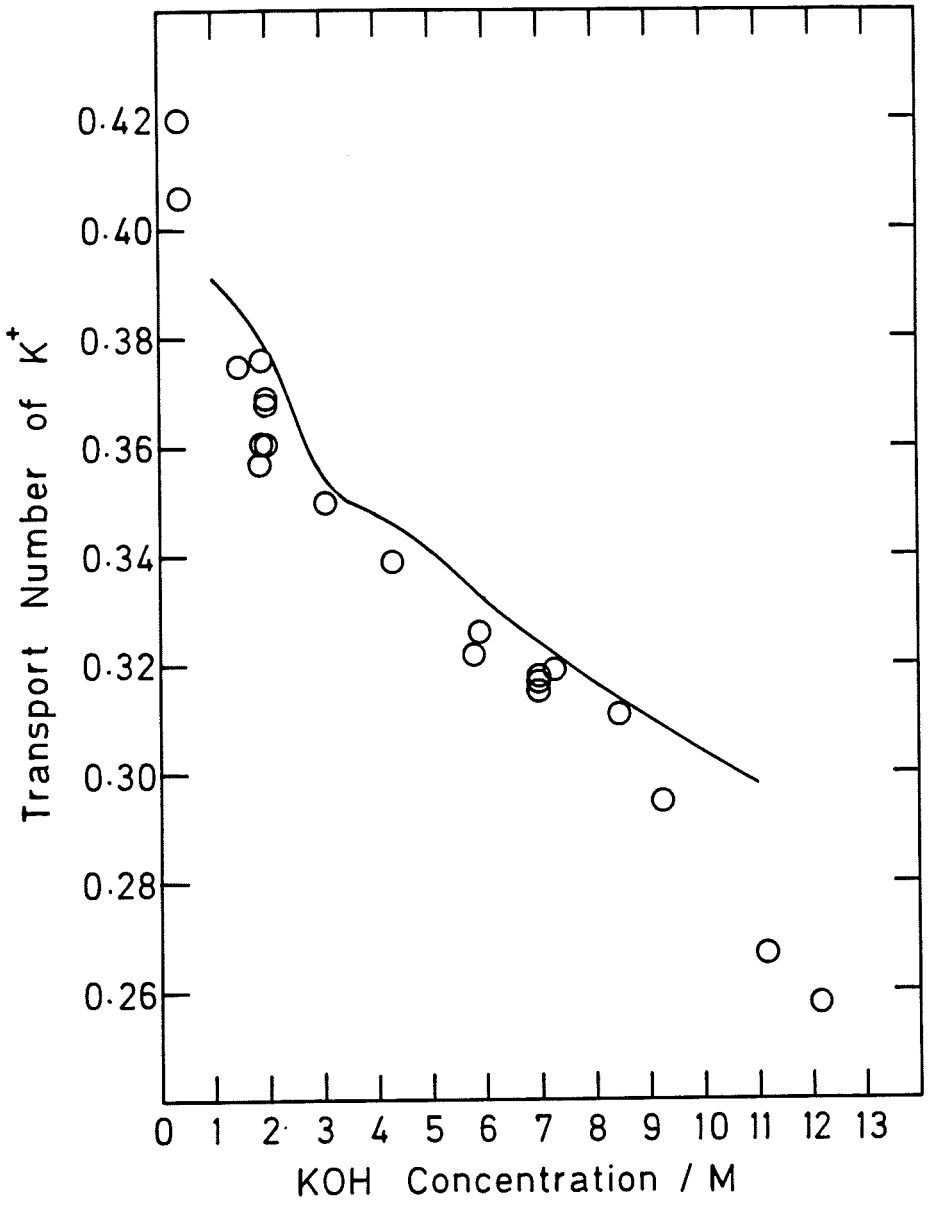


KEY solid line, this study
O Ref. (80)

Figure 3.12 Comparison of water transference numbers through PUDO 193 Cellophane.

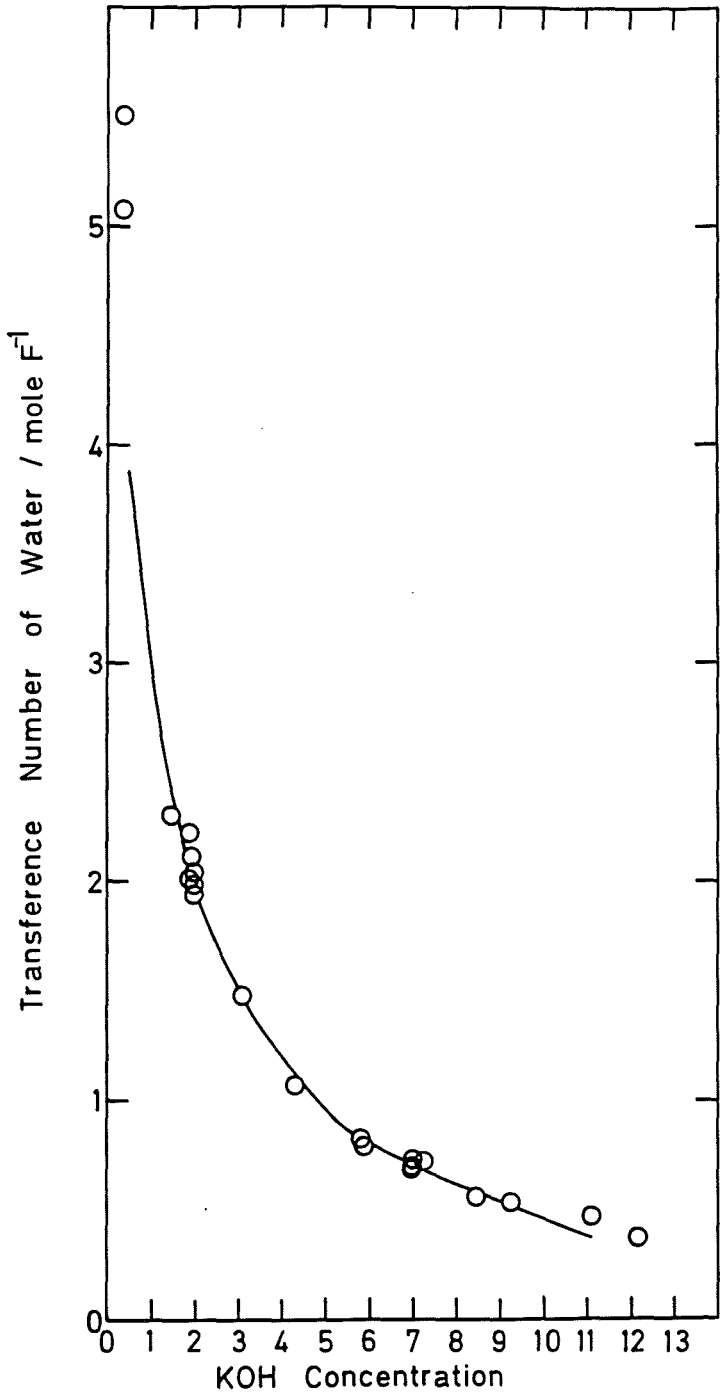

(i) For the transference of water both sets of results follow the same curve with little deviation.

(ii) For the transport of potassium ions, a similar shaped curve is obtained in each case but the results reported by Jenkins et al [80] are slightly lower than the results reported here.

To the knowledge of this author the only previous work on this system was by Shaw and Remanick [90]. They measured transport of $K^+$ and water through PUDO-600 Cellophane and Visking V-7 sausage casing over a wide range of KOH solutions., using the technique of Kressman et al [71], but the precision was poor. Although the effects of diffusion and concentration polarisation were eliminated by determining a range for time and current density in which the transport number of the potassium ion remained constant they were only able to show that the transport number of potassium decreased by 20% with increasing concentration. Their results have been reproduced in figures (3.13) and (3.14) to highlight the precision in the data in the present work.

Shaw and Remanick reported a variation in transport number of 0.06 for several runs at a single external electrolyte concentration. This contrasts with a variation of 0.006 in the worst case reported here, over the same number of runs. Inefficient removal of electrolyte from the cell is a possible cause of the substantial errors occurring in Shaw and Remanick's work.

Lee et al [91] have shown that for a wide range of ion-exchange membranes the water transference data may usually be represented by a straight line plot of $t_{H2O}$ vs. $Wt_K+$. W is the number of moles of water in the membrane per equivalent of counter-ion. Figure (3.15) shows this type of plot for Cellophane in KOH. The best line through all the points is

$$t_{H_2O} = 0.275 W t_{K^+} + 0.120 \qquad (3.31)$$

shown on figure (3.15) as a dotted line. The intercept at $Wt_K+ = 0$ is indicative of the amount of water transported directly with the hydroxyl ion. A small value indicates that very little water is transported and a positive intercept of unity would be compatible

Figure 3.13 Comparison of potassium ion transport numbers through Cellophane.

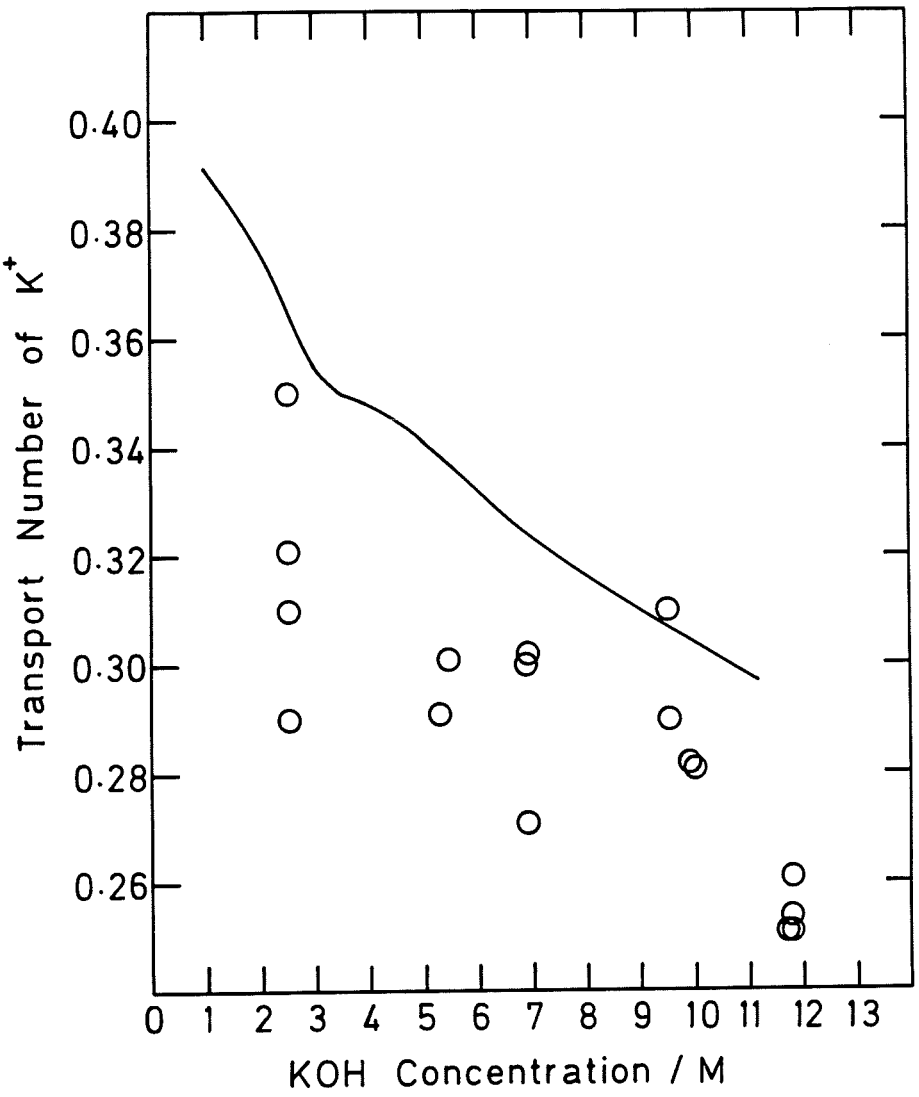

Figure 3.14 Comparison of water transference numbers through Cellophane.

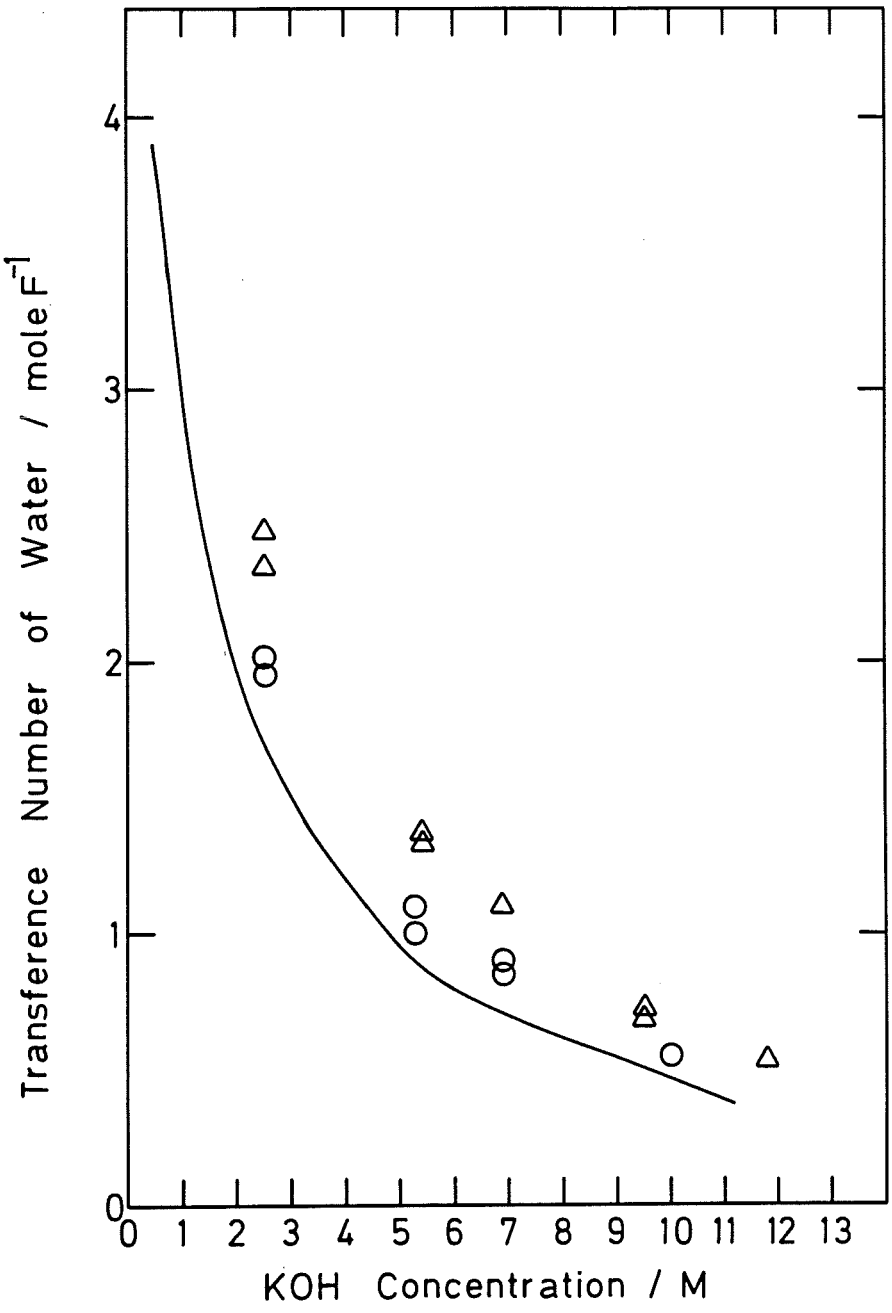


KEY solid line, this study at 25°C
△ Ref.( 90 ) at 30°C
○ Ref.( 90 ) at 0°C

Figure 3.15 $T_{H2O}$ vs. $WT_K$+ for Cellophane.

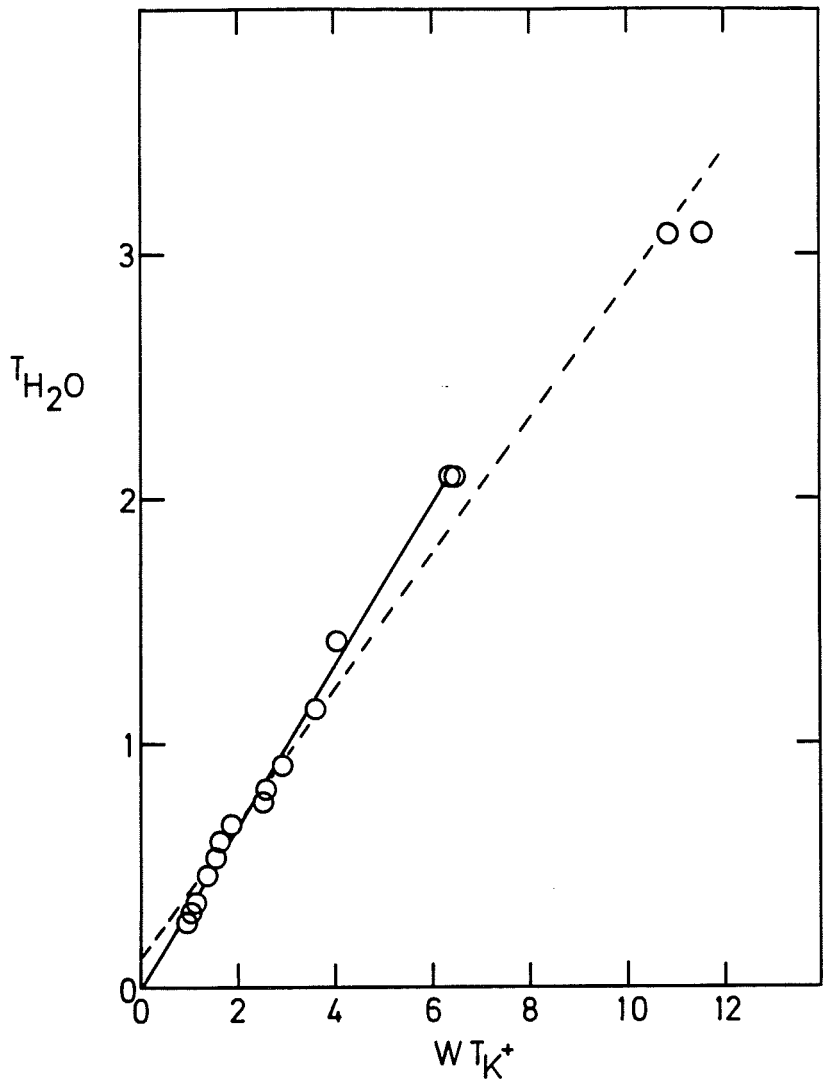

with transport of hydroxyl ions entirely by a Grotthus chain mechanism. The slope of 0.275 indicates that the water in the membrane moves in the same direction as the K+ ions but with an average velocity of 27.5% of the counter ions.

Jenkins et al [92] quote an intercept of 0.040 and a slope of 0.336. However not all the data shown in figure (3.12) was taken into account; the water transference numbers greater than 2.6 were excluded. If the two highest water transference number data sets from figure (3.15) are ignored, so that the data set is now comparable with Jenkins et al [85] the best line through the points is

$$t_{H_2O} = 0.327 W t_{K^+} - 0.003 \qquad (3.32)$$

which is closer to the line reported by Jenkins et al [92] and is shown on figure (3.15) as a solid line.

### 3.3.4 Permion 2291 40/30

Initial results indicated a decrease in transport number with increase in electrolyte concentration, as expected, but the data did not have quite the precision of that obtained with PUDO 193. As already emphasised a feature of the technique is the maintenance of constant and equal concentrations on either side of the membrane. In the work with PUDO 193 no account was taken of the volume changes in the two electrolyte compartments during a run.

With Permion 2291 40/30, at low concentration, the transport number of potassium and water were such that the volume of the catholyte could be twice that of the anolyte at the end of the run. Such differences in volume diminished with increase in external electrolyte concentration and even reversed at the highest electrolyte concentrations so that the final anolyte volume was greater than the final catholyte volume. By adding electrolyte of the same concentration as the initial electrolyte to the deficient compartment during a run it was possible to keep the electrolyte levels similar in the two compartments and as a result the precision of the data was improved.

Transport numbers of potassium and the transference number of water through Permion, within the 3% drift criteria, with correction for spray and recovery and using the modified technique for maintaining similar volumes of electrolyte are shown in figures (3.16) and (3.17), the relevant data are tabulated in table (3.2(g)) and (3.2(h)). Extrapolation of the curve, in figure (3.16), to infinite dilution yields a potassium ion transport number of unity. This behaviour is expected for an ion-exchange membrane such as Permion which is fully ionised and with zero co-ion concentration at infinite dilution.

Similar results were obtained with stacks of 10 or 5 sheets of membrane showing that the effects of diffusion and osmosis had been eliminated. Some further consideration of possible hydraulic flow effects arising from different electrolyte levels in the two compartments is appropriate. Using the data from runs 3.58, 3.60, 3.61, 3.64, 3.65, 3.69, 3.70, 3.73, 3.74, 3.77 and 3.78 which were carried out disregarding electrolyte level differences, the loss or gain of water in each compartment due to transport, electrolysis and additions to maintain concentration constant, were calculated. From the duration of the run the rate of gain of water by the anolyte compared with the rate of gain of water by the catholyte was obtained. This is expressed as a function of external electrolyte concentration in figure (3.18).

By interpolation it can be seen that at an external concentration of 9.0M the rate of gain of water by the catholyte equals the rate of gain of water by the anolyte.

At lower concentrations than 9.0M, hydraulic flow is possible from the catholyte to the anolyte. If significant hydraulic flow occurred then the measured transport numbers would be less than the true values i.e. those obtained with the modified anolyte additions whereby the electrolyte levels in the two compartments were similar. At concentrations greater than 9.0M hydraulic flow would be in the reverse direction i.e. from the anolyte to the catholyte thus enhancing the measured transport numbers as compared with the true values.

Figures (3.19) and (3.20) show data from all the runs in table (3.2). In figure (3.19) all values fall on or below the line through the data shown in figure (3.16) (actual points have been omitted). For concentrations less than 9.0M this is to be expected since

Figure 3.16 Potassium ion transport numbers through Permion 2291 40/30 vs. KOH concentration. Data corrected for spray and recovery and was obtained using the modified technique for maintaining similar volumes of electrolyte on either side of the membrane.

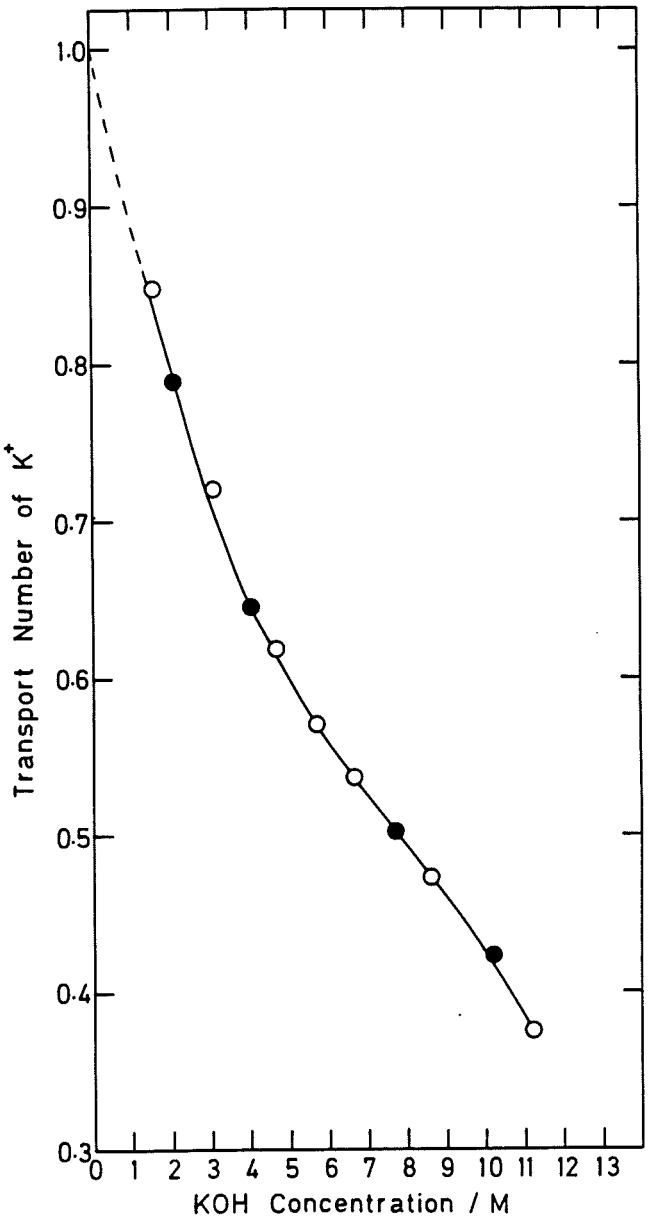


KEY ○ 10 sheets of Permion, ● 5 sheets of Permion

Figure 3.17 Water transference numbers through Permion 2291 40/30 vs. KOH concentration. Data corrected for spray and recovery and was obtained using the modified technique for maintaining similar volumes of electrolyte on either side of the membrane.

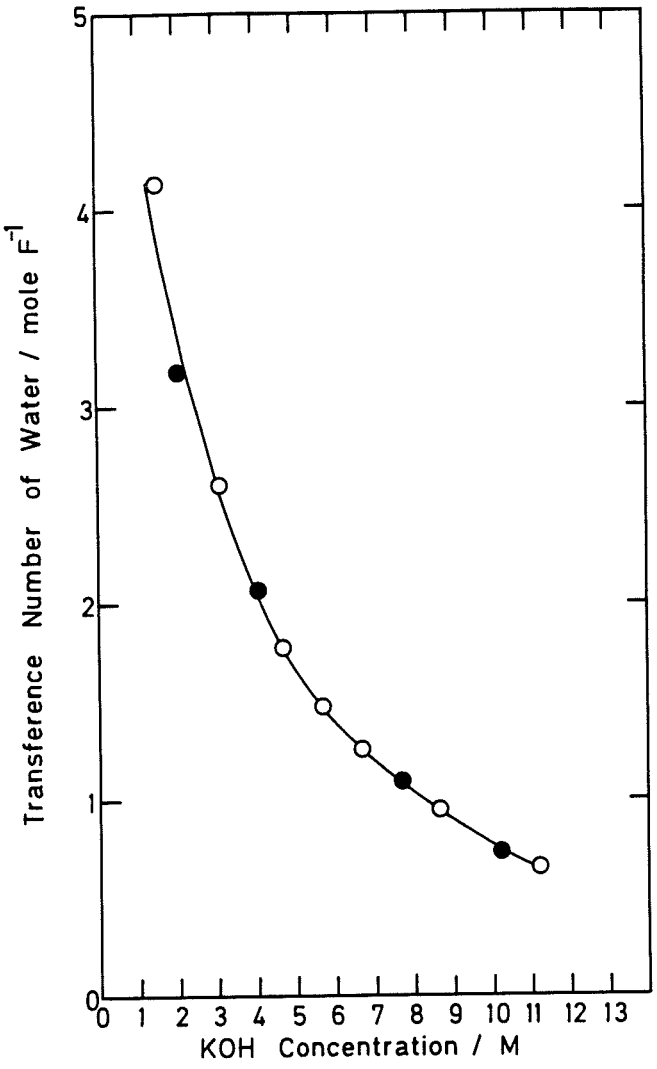


KEY ○ 10 sheets of Permion
● 5 sheets of Permion

Figure 3.18 Rate of gain of water by the catholyte minus rate of gain of water by the anolyte vs. KOH concentration.

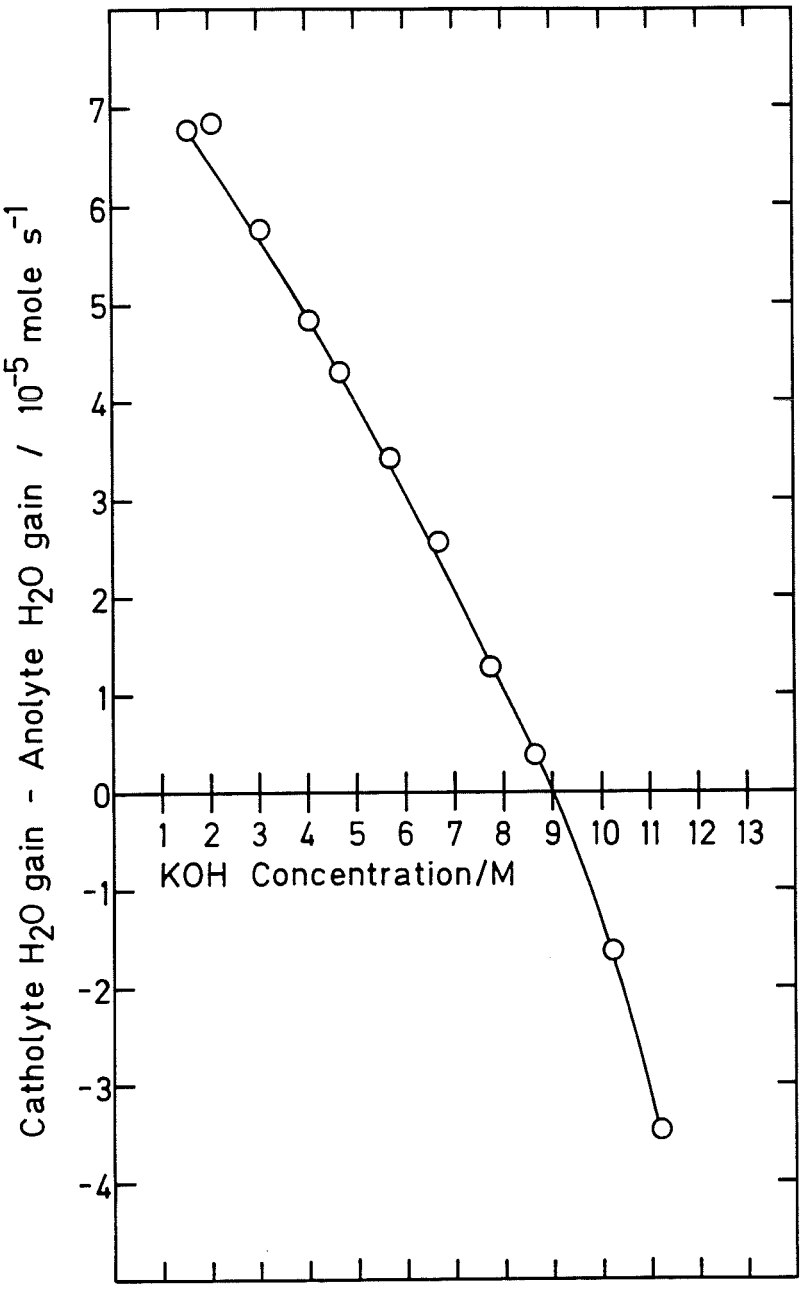

Figure 3.19 Potassium ion transport numbers through Permion 2291 40/30 vs. KOH concentration. All data presented in table (3.2) is shown.

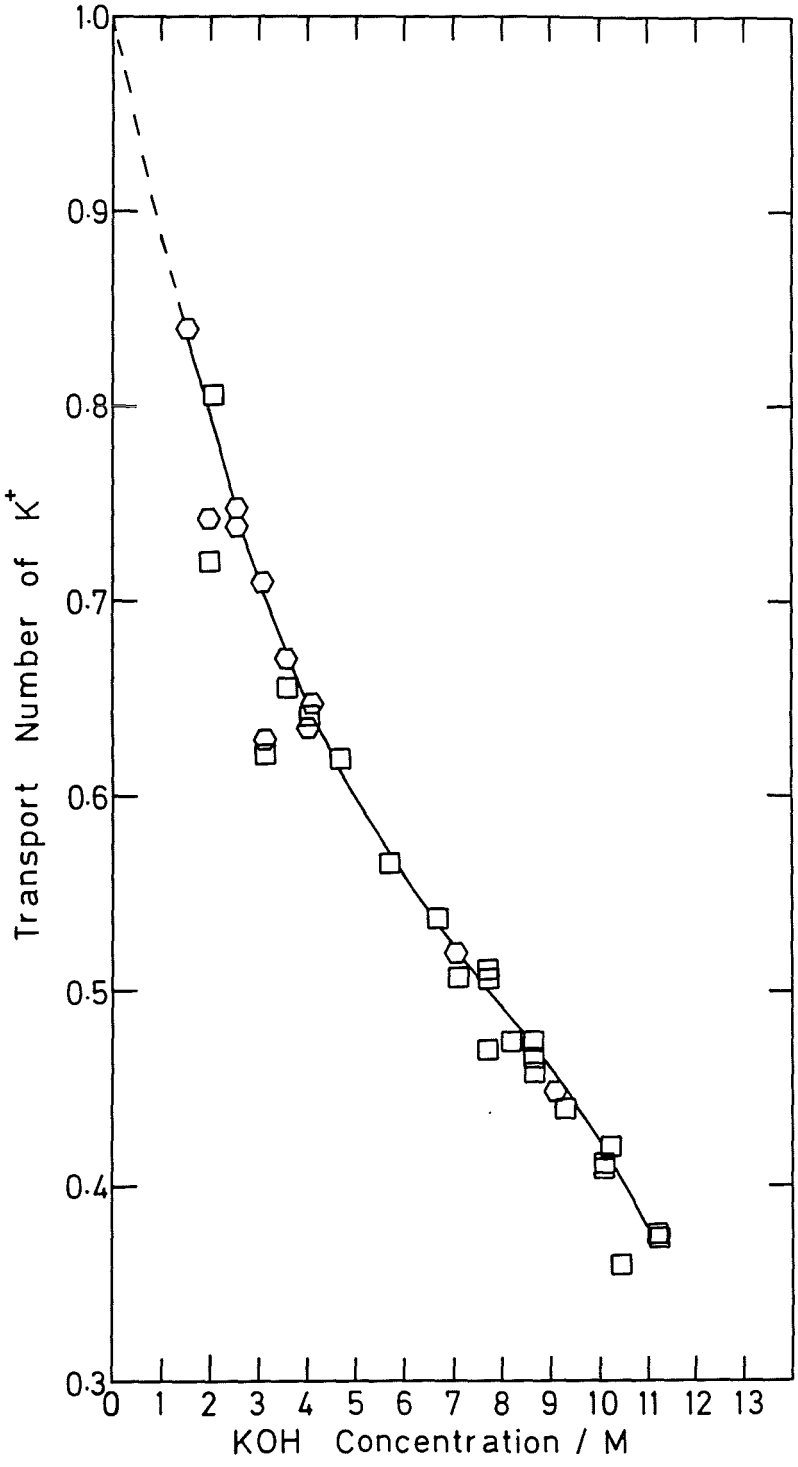

Figure 3.20 Water transference numbers through Permion 2291 40/30 vs. KOH concentration. All data presented in table (3.2) is shown.

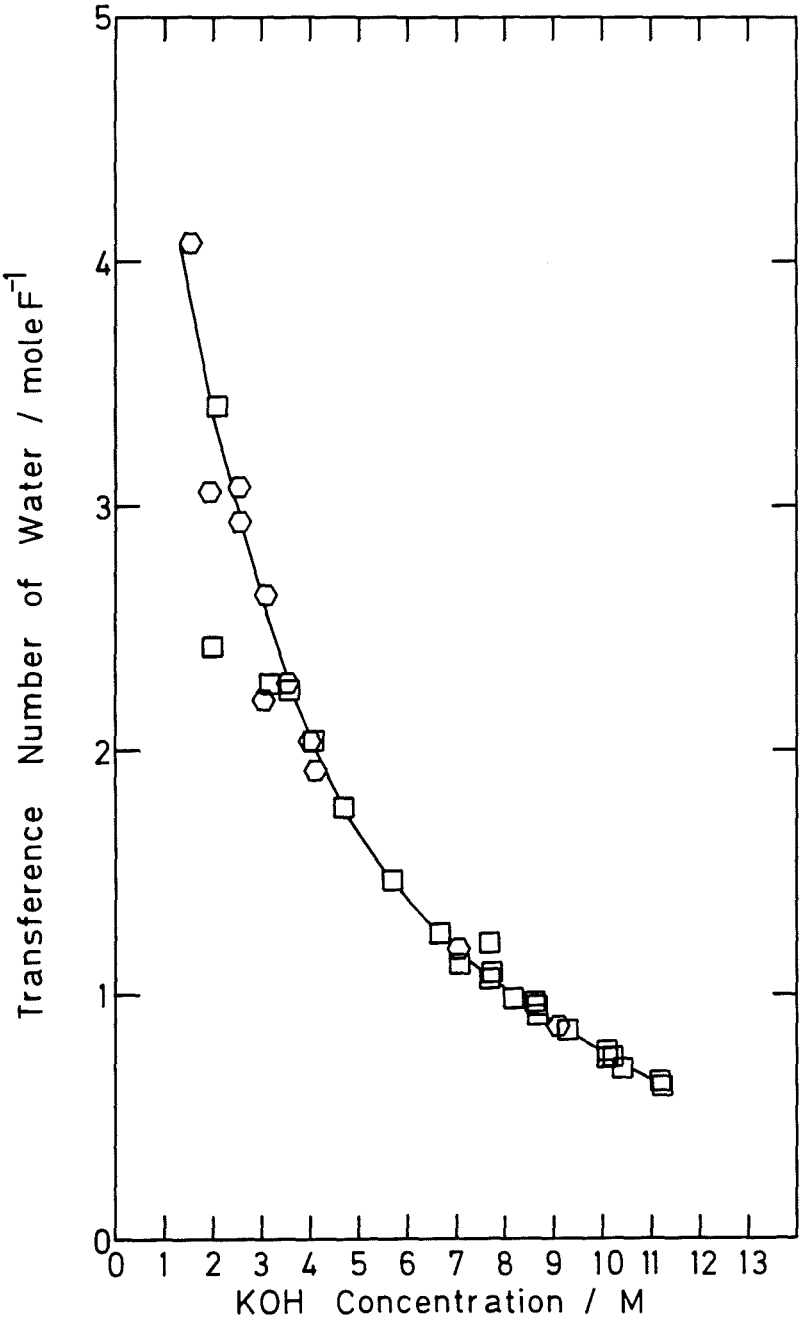

Table 3.2(a) Potassium ion transport numbers through Permion 2291 40/30 (Batch used by previous workers [46]).

| Run | Conc. [M] | No. of Layers | $T_{K^+}$ Anolyte | $T_{K^+}$ Catholyte | $T_{K^+}$ | 3% |
|---|---|---|---|---|---|---|
| 3.26 | 3.080 | 10 | 0.742 | 0.697 | 0.727 | |
| 3.27 | 3.080 | 10 | 0.765 | 0.748 | 0.759 | |
| 3.28 | 1.037 | 10 | 0.917 | 0.912 | 0.915 | |
| 3.29 | 1.037 | 10 | 0.920 | 0.917 | 0.919 | ✓ |
| 3.30 | 4.133 | 10 | 0.699 | 0.708 | 0.702 | |
| 3.31 | 4.133 | 10 | 0.689 | 0.690 | 0.689 | |
| 3.34 | 5.130 | 10 | 0.641 | 0.654 | 0.643 | |
| 3.35 | 5.130 | 10 | 0.637 | 0.636 | 0.636 | ✓ |

Table 3.2(b) Water transference numbers through Permion 2291 40/30 (Batch used by previous workers [46]).

| Run | Conc. [M] | No. of Layers | $T_{H2O}$ Anolyte | $T_{H2O}$ Catholyte | $T_{H2O}$ | 3% |
|---|---|---|---|---|---|---|
| 3.26 | 3.080 | 10 | 3.76 | 2.82 | 3.45 | |
| 3.27 | 3.080 | 10 | 2.91 | 2.56 | 2.80 | |
| 3.28 | 1.037 | 10 | 4.74 | 4.26 | 4.58 | |
| 3.29 | 1.037 | 10 | 4.39 | 4.19 | 4.32 | ✓ |
| 3.30 | 4.133 | 10 | 1.95 | 2.00 | 1.96 | |
| 3.31 | 4.133 | 10 | 1.88 | 1.76 | 1.84 | |
| 3.34 | 5.130 | 10 | 1.55 | 1.58 | 1.56 | |
| 3.35 | 5.130 | 10 | 1.72 | 1.66 | 1.70 | ✓ |

Table 3.2(c) Potassium ion transport numbers through Permion 2291 40/30 corrected for recovery.

| Run | Conc. [M] | No. of Layers | $T_K$+ Anolyte | $T_K$+ Catholyte | $T_K$+ | 3% |
|---|---|---|---|---|---|---|
| 3.36 | 4.132 | 10 | 0.651 | 0.640 | 0.647 | |
| 3.37 | 1.986 | 10 | 0.742 | 0.741 | 0.741 | |
| 3.38 | 1.986 | 10 | 0.722 | 0.716 | 0.720 | ✓ |
| 3.39 | 3.140 | 10 | 0.631 | 0.625 | 0.629 | |
| 3.40 | 3.140 | 10 | 0.627 | 0.611 | 0.621 | ✓ |
| 3.41 | 4.020 | 10 | 0.639 | 0.625 | 0.635 | |
| 3.42 | 2.550 | 10 | 0.745 | 0.725 | 0.738 | |
| 3.43 | 3.572 | 10 | 0.675 | 0.660 | 0.670 | |
| 3.44 | 3.572 | 10 | 0.660 | 0.649 | 0.656 | ✓ |
| 3.45 | 2.550 | 10 | 0.750 | 0.742 | 0.748 | |
| 3.46 | 7.075 | 10 | 0.518 | 0.522 | 0.519 | |
| 3.47 | 9.112 | 10 | 0.451 | 0.444 | 0.869 | |
| 3.48 | 7.075 | 10 | 0.510 | 0.501 | 0.507 | ✓ |
| 3.49 | 9.280 | 10 | 0.440 | 0.440 | 0.440 | ✓ |
| 3.50 | 8.184 | 10 | 0.477 | 0.469 | 0.474 | ✓ |
| 3.51 | 7.704 | 10 | 0.471 | 0.468 | 0.470 | ✓ |
| 3.52 | 8.688 | 10 | 0.469 | 0.460 | 0.466 | ✓ |
| 3.53 | 7.704 | 10 | 0.518 | 0.496 | 0.510 | ✓ |
| 3.54 | 8.688 | 10 | 0.462 | 0.450 | 0.458 | ✓ |
| 3.55 | 10.43 | 10 | 0.355 | 0.369 | 0.360 | ✓ |
| 3.56 | 10.08 | 10 | 0.409 | 0.411 | 0.409 | ✓ |
| 3.57 | 10.08 | 10 | 0.411 | 0.412 | 0.412 | ✓ |

Table 3.2(d) Water transference numbers through Permion 2291 40/30 corrected for recovery.

| Run | Conc. [M] | No. of Layers | $T_{H2O}$ Anolyte | $T_{H2O}$ Catholyte | $T_{H2O}$ | 3% |
|---|---|---|---|---|---|---|
| 3.36 | 4.132 | 10 | 1.96 | 1.83 | 1.92 | |
| 3.37 | 1.986 | 10 | 3.10 | 2.97 | 3.06 | |
| 3.38 | 1.986 | 10 | 2.31 | 2.96 | 2.53 | ✓ |
| 3.39 | 3.140 | 10 | 2.19 | 2.25 | 2.21 | |
| 3.40 | 3.140 | 10 | 2.28 | 2.26 | 2.27 | ✓ |
| 3.41 | 4.020 | 10 | 2.13 | 1.84 | 2.04 | |
| 3.42 | 2.550 | 10 | 3.21 | 2.81 | 3.08 | |
| 3.43 | 3.572 | 10 | 2.35 | 2.14 | 2.28 | |
| 3.44 | 3.572 | 10 | 2.32 | 2.11 | 2.25 | ✓ |
| 3.45 | 2.550 | 10 | 3.00 | 2.81 | 2.94 | |
| 3.46 | 7.075 | 10 | 1.21 | 1.13 | 1.18 | |
| 3.47 | 9.112 | 10 | 0.857 | 0.893 | 0.448 | |
| 3.48 | 7.075 | 10 | 1.15 | 1.10 | 1.13 | ✓ |
| 3.49 | 9.280 | 10 | 0.860 | 0.874 | 0.865 | ✓ |
| 3.50 | 8.184 | 10 | 0.973 | 1.01 | 0.985 | ✓ |
| 3.51 | 7.704 | 10 | 1.07 | 1.06 | 1.07 | ✓ |
| 3.52 | 8.688 | 10 | 0.969 | 0.941 | 0.960 | ✓ |
| 3.53 | 7.704 | 10 | 1.28 | 1.09 | 1.21 | ✓ |
| 3.54 | 8.688 | 10 | 0.902 | 0.946 | 0.917 | ✓ |
| 3.55 | 10.43 | 10 | 0.685 | 0.740 | 0.703 | ✓ |
| 3.56 | 10.08 | 10 | 0.760 | 0.791 | 0.770 | ✓ |
| 3.57 | 10.08 | 10 | 0.737 | 0.755 | 0.743 | ✓ |

Table 3.2(e) Potassium ion transport numbers through Permion 2291 40/30, corrected for recovery. Data used as a precursor for the runs shown in table 3.2(g).

| Run | Conc. [M] | No. of Layers | $T_K$+ Anolyte | $T_K$+ Catholyte | $T_K$+ | 3% |
|---|---|---|---|---|---|---|
| 3.58 | 5.693 | 10 | 0.567 | 0.564 | 0.566 | ✓ |
| 3.60 | 4.683 | 10 | 0.620 | 0.619 | 0.620 | ✓ |
| 3.61 | 6.670 | 10 | 0.538 | 0.536 | 0.538 | ✓ |
| 3.64 | 1.542 | 10 | 0.842 | 0.832 | 0.839 | |
| 3.65 | 3.096 | 10 | 0.715 | 0.697 | 0.709 | |
| 3.68 | 11.19 | 10 | 0.374 | 0.380 | 0.376 | ✓ |
| 3.69 | 8.633 | 10 | 0.474 | 0.474 | 0.474 | ✓ |
| 3.70 | 11.21 | 10 | 0.370 | 0.384 | 0.374 | ✓ |
| 3.73 | 4.050 | 10 | 0.642 | 0.640 | 0.641 | ✓ |
| 3.74 | 7.733 | 10 | 0.504 | 0.509 | 0.506 | ✓ |
| 3.77 | 2.063 | 10 | 0.811 | 0.794 | 0.806 | ✓ |
| 3.78 | 10.23 | 10 | 0.424 | 0.415 | 0.421 | ✓ |

Table 3.2(f) Water transference numbers through Permion 2291 40/30, corrected for recovery. Data used as a precursor for the runs shown in table 3.2(h).

| Run | Conc. [M] | No. of Layers | $T_{H2O}$ Anolyte | $T_{H2O}$ Catholyte | $T_{H2O}$ | 3% |
|---|---|---|---|---|---|---|
| 3.58 | 5.693 | 10 | 1.50 | 1.41 | 1.47 | ✓ |
| 3.60 | 4.683 | 10 | 1.80 | 1.71 | 1.77 | ✓ |
| 3.61 | 6.670 | 10 | 1.25 | 1.25 | 1.25 | ✓ |
| 3.64 | 1.542 | 10 | 4.20 | 3.83 | 4.08 | |
| 3.65 | 3.096 | 10 | 2.70 | 2.51 | 2.63 | |
| 3.68 | 11.19 | 10 | 0.632 | 0.672 | 0.645 | ✓ |
| 3.69 | 8.633 | 10 | 0.974 | 0.980 | 0.976 | ✓ |
| 3.70 | 11.21 | 10 | 0.620 | 0.655 | 0.632 | ✓ |
| 3.73 | 4.050 | 10 | 2.09 | 1.93 | 2.04 | ✓ |
| 3.74 | 7.733 | 10 | 1.10 | 1.08 | 1.09 | ✓ |
| 3.77 | 2.063 | 10 | 3.53 | 3.18 | 3.41 | ✓ |
| 3.78 | 10.23 | 10 | 0.714 | 0.808 | 0.746 | ✓ |

Table 3.2(g) Potassium ion transport numbers through Permion 2291 40/30 corrected for recovery and volume.

| Run | Conc. [M] | No. of Layers | $T_K$+ Anolyte | $T_K$+ Catholyte | $T_K$+ | 3% |
|---|---|---|---|---|---|---|
| 3.59 | 5.693 | 10 | 0.572 | 0.570 | 0.571 | ✓ |
| 3.62 | 4.683 | 10 | 0.622 | 0.616 | 0.620 | ✓ |
| 3.63 | 6.670 | 10 | 0.540 | 0.532 | 0.537 | ✓ |
| 3.66 | 1.542 | 10 | 0.851 | 0.843 | 0.848 | ✓ |
| 3.67 | 3.096 | 10 | 0.726 | 0.711 | 0.721 | ✓ |
| 3.71 | 8.633 | 10 | 0.472 | 0.474 | 0.473 | ✓ |
| 3.72 | 11.21 | 10 | 0.373 | 0.381 | 0.375 | ✓ |
| 3.75 | 4.050 | 5 | 0.646 | 0.645 | 0.646 | ✓ |
| 3.76 | 7.733 | 5 | 0.503 | 0.503 | 0.503 | ✓ |
| 3.79 | 2.063 | 5 | 0.796 | 0.777 | 0.790 | ✓ |
| 3.80 | 10.23 | 5 | 0.422 | 0.427 | 0.424 | ✓ |

Table 3.2(h) Water transference numbers through Permion 2291 40/30 corrected for recovery and volume.

| Run | Conc. [M] | No. of Layers | $T_{H2O}$ Anolyte | $T_{H2O}$ Catholyte | $T_{H2O}$ | 3% |
|---|---|---|---|---|---|---|
| 3.59 | 5.693 | 10 | 1.50 | 1.44 | 1.48 | ✓ |
| 3.62 | 4.683 | 10 | 1.82 | 1.71 | 1.78 | ✓ |
| 3.63 | 6.670 | 10 | 1.27 | 1.24 | 1.26 | ✓ |
| 3.66 | 1.542 | 10 | 4.29 | 3.82 | 4.13 | ✓ |
| 3.67 | 3.096 | 10 | 2.66 | 2.52 | 2.61 | ✓ |
| 3.71 | 8.633 | 10 | 0.953 | 0.949 | 0.952 | ✓ |
| 3.72 | 11.21 | 10 | 0.651 | 0.677 | 0.660 | ✓ |
| 3.75 | 4.050 | 5 | 2.12 | 1.97 | 2.07 | ✓ |
| 3.76 | 7.733 | 5 | 1.12 | 1.06 | 1.10 | ✓ |
| 3.79 | 2.063 | 5 | 3.29 | 2.96 | 3.18 | ✓ |
| 3.80 | 10.23 | 5 | 0.731 | 0.754 | 0.739 | ✓ |

the hydraulic flow is in the reverse direction to the current and therefore the potassium ion and water flux. The data does not deviate uniformly from the line and the greatest deviation is not necessarily found at the lowest concentration where the difference in electrolyte volumes is greatest.

Another point to note is that some values lie on the line even if there was no modification in the technique to take into account difference in height during that run. An explanation for this is the differing permeability of the membrane as suggested by its non-uniform swelling properties (see section (2.3.1)).

It is believed that modifying the technique to allow for the differences in electrolyte volumes is not important in all cases, only if the permeability of a particular sheet is such that substantial hydraulic flow could occur.

Now consider concentrations greater than 9.0M. Figure (3.19) shows that values still fall below the true $t_K+$ values shown on figure (3.16) which is contrary to expectation. A possible explanation for this is that the catholyte contains twice as much gas as the anolyte and this "expands" the catholyte level above the anolyte level even at concentrations greater than 9.0M. The line drawn through the data in figure (3.19) represents the height corrected situation for external electrolyte concentrations less than 9.0M and the best fit through the points below the corrected line for external electrolyte concentrations greater than 9.0M. The majority of the water transference data falls on or below the line in figure (3.20).

Variability between batches of Permion 2291 40/30 film is shown in figures (3.21) and (3.22). The graph shows the line from figure (3.16) together with transport numbers obtained using the same membrane but from a batch manufactured a few years earlier. Slightly different properties give rise to different transport numbers.

As with Cellophane in the previous section, the water transference data may be represented as a straight plot of $t_{H2O}$ vs. $Wt_K+$ as shown in figure (3.23). The best line through all the points is

$$t_{H_2O} = 0.413 Wt_{K^+} - 0.084 \qquad (3.33)$$

Figure 3.21 Potassium ion transport numbers through Permion 2291 40/30 vs. KOH concentration showing the variability between different batches of the membrane.

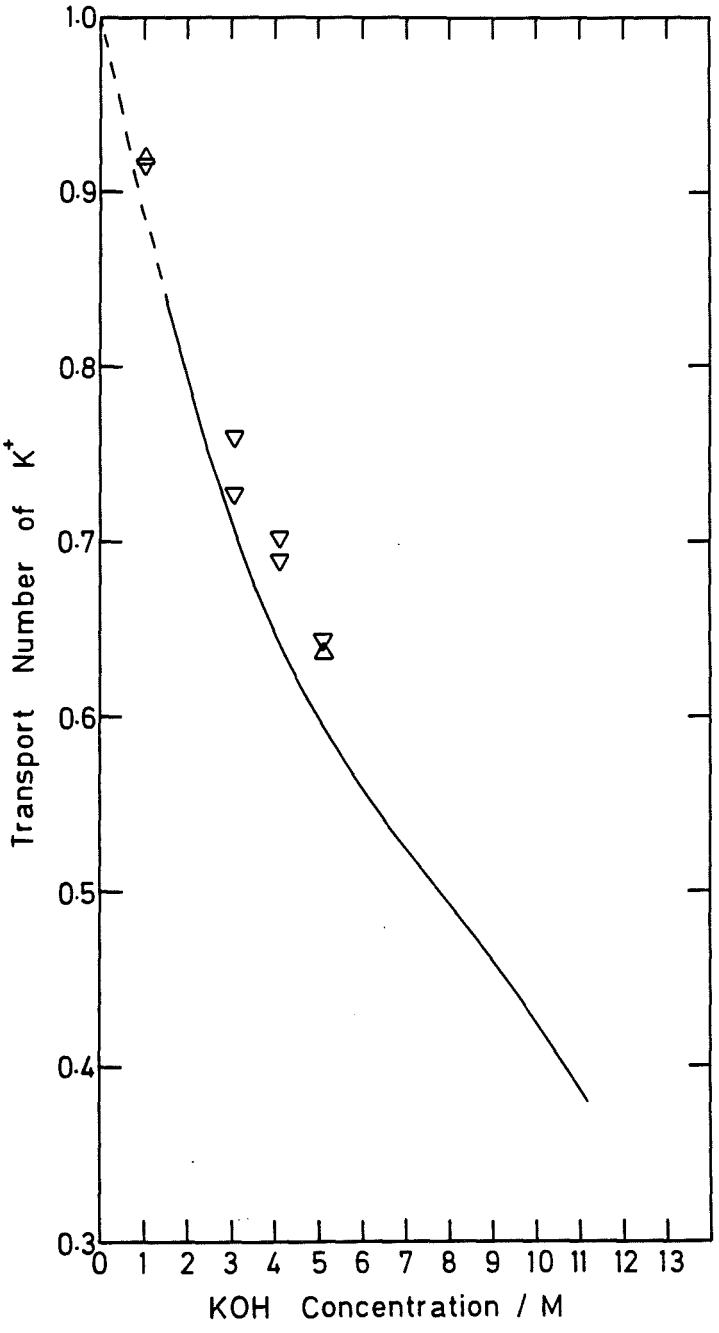


KEY △ within 3%
▽ without 3%
solid line, from figure 3.16

Figure 3.22 Water transference numbers through Permion 2291 40/30 vs. KOH concentration showing the variability between different batches of the membrane.

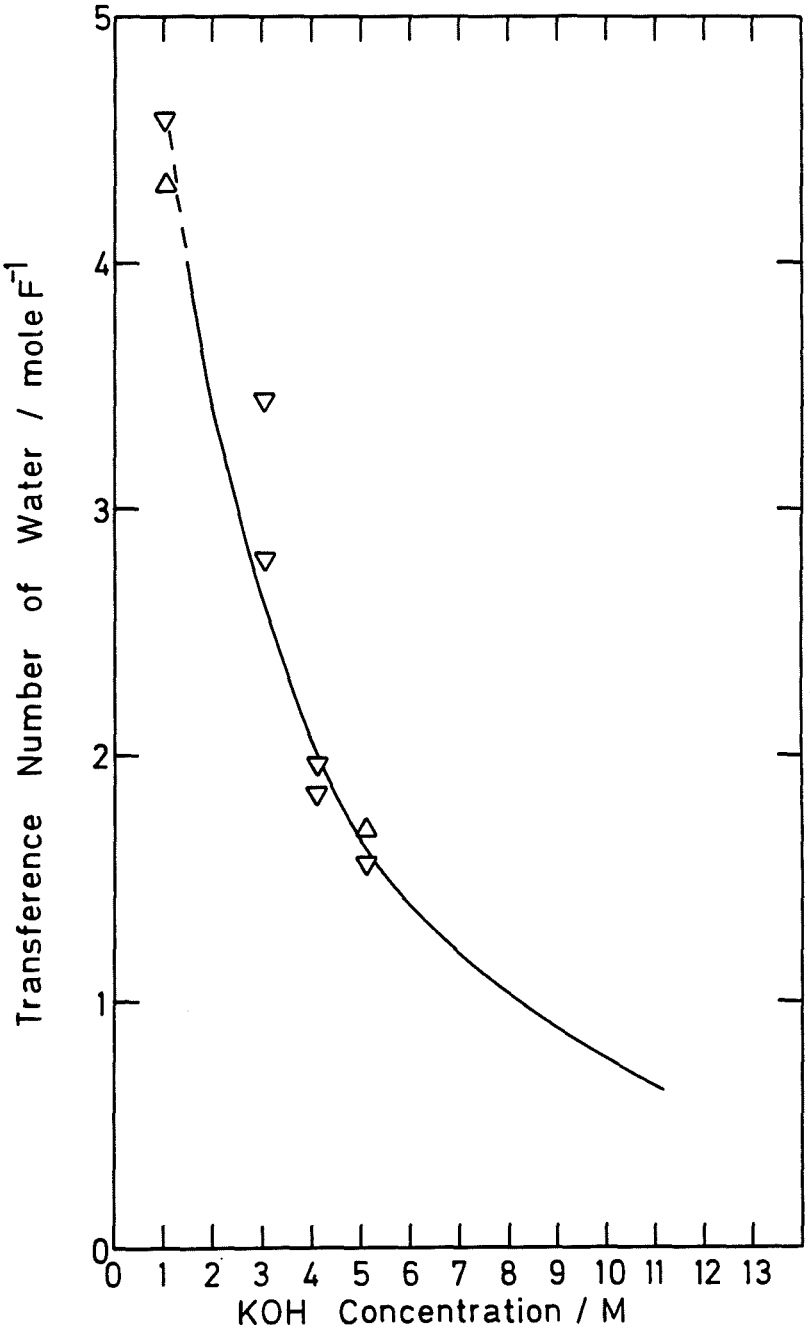


KEY △ within 3%
▽ without 3%
solid line, from figure 3.17

Figure 3.23 $T_{H2O}$ vs. $WT_{K}+$ for Permion 2291 40/30.

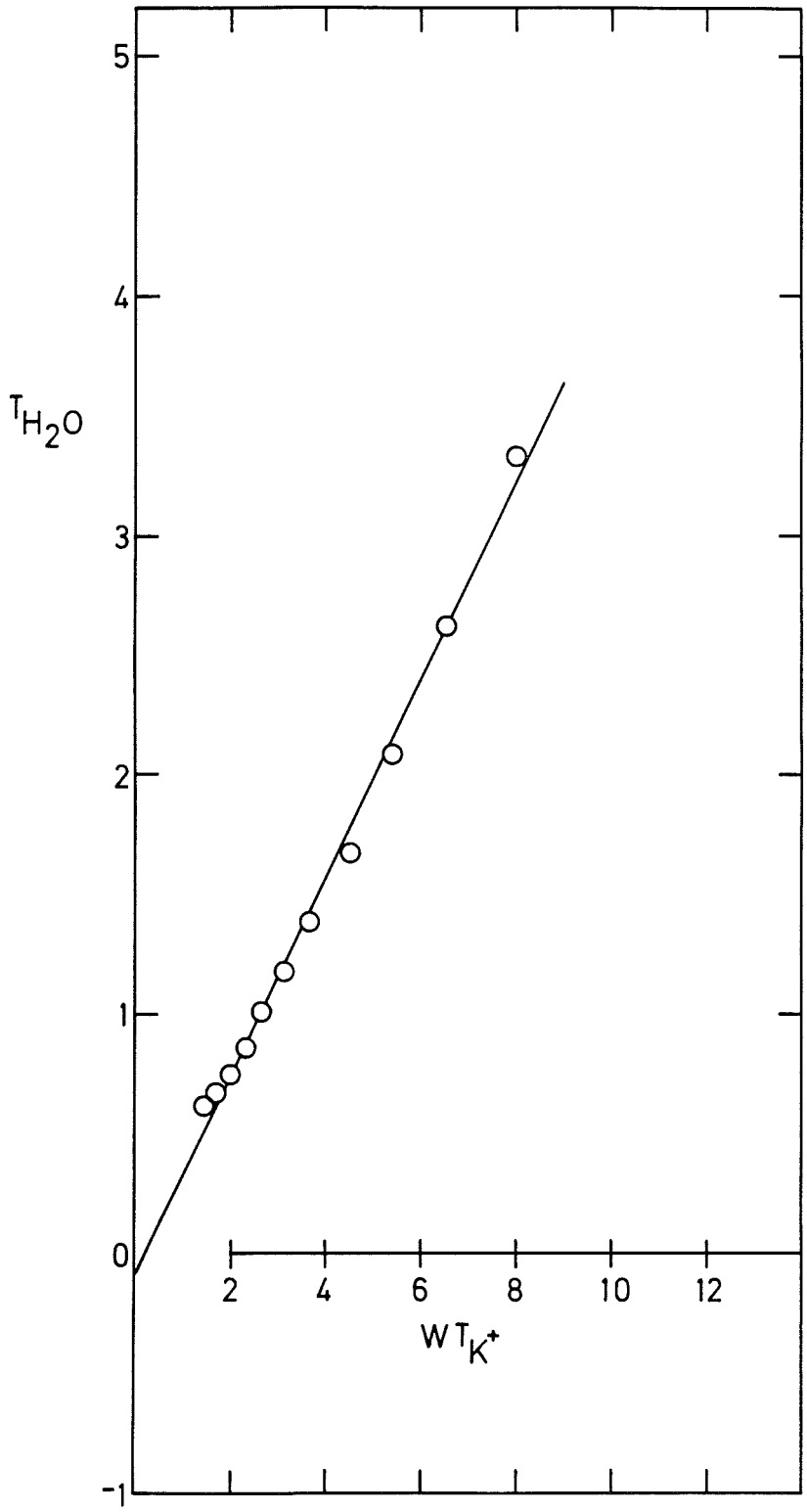

The small value of the intercept again indicates that very little water is transported with the hydroxyl ion. The slope of 0.413 indicates that the water in the membrane moves in the same direction as the $K^+$ ions but with an average velocity of 41.3% of the counter ions. This is higher than the 32.7% found with Cellophane.

A comparison of the transport properties of the grades of Permion 2291 investigated by Atieh and Cheh [70] with Permion 2291 40/30 is shown in figures (3.24 and 3.25). Potassium ion transport numbers for Permion 2291 40/100 are similar to those obtained for Permion 2291 40/30 whereas potassium ion transport numbers for Permion 2291 40/20 are significantly lower. The general trend of a decrease in transport number with an increase in external electrolyte concentration is observed. Water transference numbers for both the 40/100 and the 40/20 grade are both higher than for Permion 2291 40/30. Neither the potassium ion transport numbers nor the water transference numbers show a trend over the three grades which may be due to differences in the experimental technique, since Atieh and Cheh did not maintain concentrations constant on either side of the membrane (as in this work) but kept the catholyte volume large compared to the anolyte. This would lower but not eliminate the effects of diffusion.

### 3.3.5 A Comparison of mass transport through PUDO 193, Cellophane and Permion 2291 40/30.

Comparison of transport and transference numbers for the two types of membrane are shown in figures (3.26 and 3.27). The large difference in transport numbers at a single concentration is ideal for the investigation of transport through combinations of the two membranes. Chapter (5) examines behaviour of assemblies of the two types when either the Cellophane or the Permion is adjacent to the catholyte.

Figure 3.24 Comparison of potassium ion transport numbers obtained using different grades of Permion 2291 vs. KOH concentration.

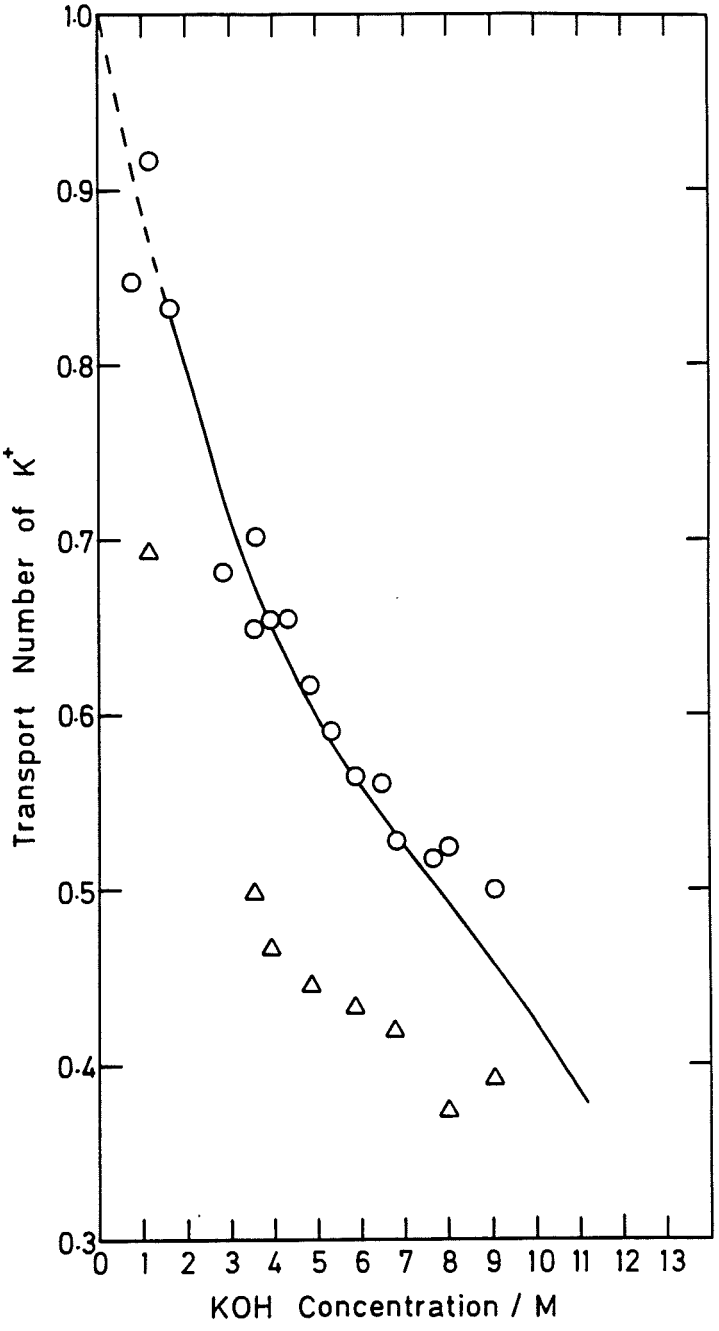

Figure 3.25 Comparison of water transference numbers obtained using different grades of Permion 2291 vs. KOH concentration.

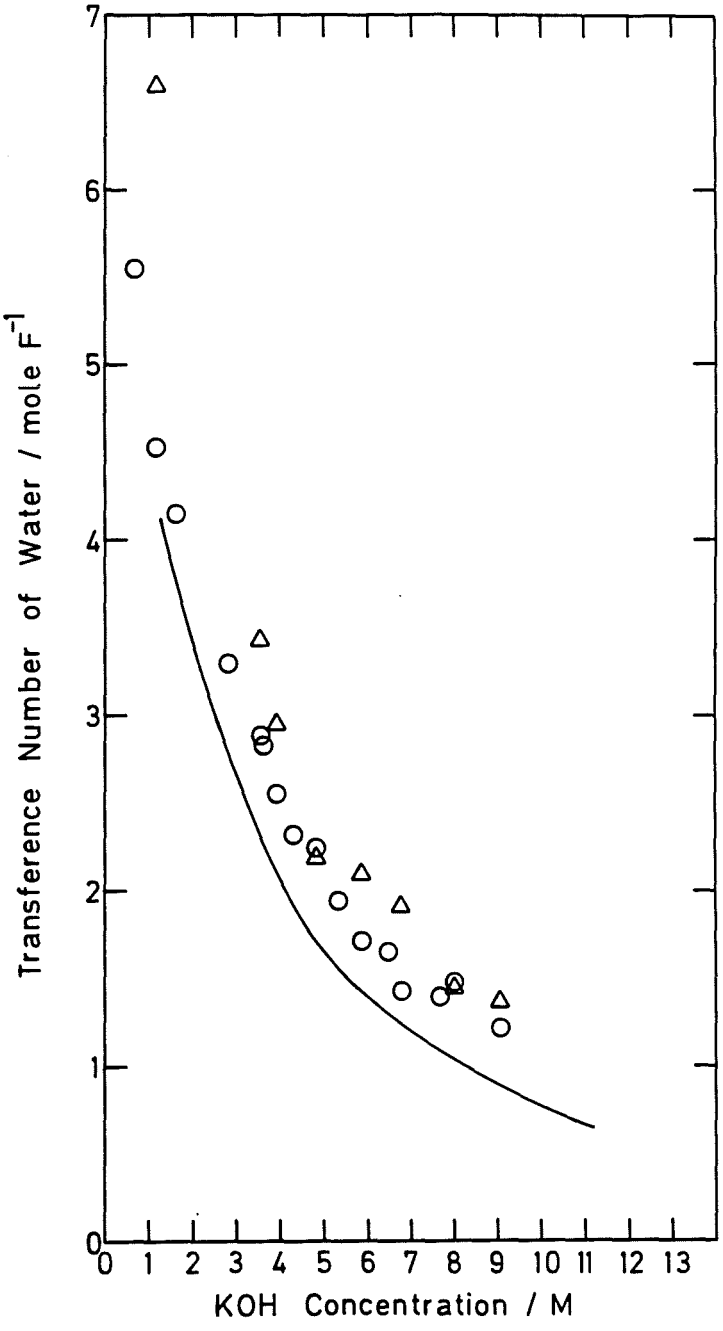


KEY solid line Permion 2291 40/30
○ Permion 2291 40/100 Ref.( 70 )
△ Permion 2291 40/20 Ref.( 70 )

Figure 3.26 Comparison of the transport number of the potassium ion VS. KOH concentration for PUDO 193 Cellophane and Permion 2291 40/30.

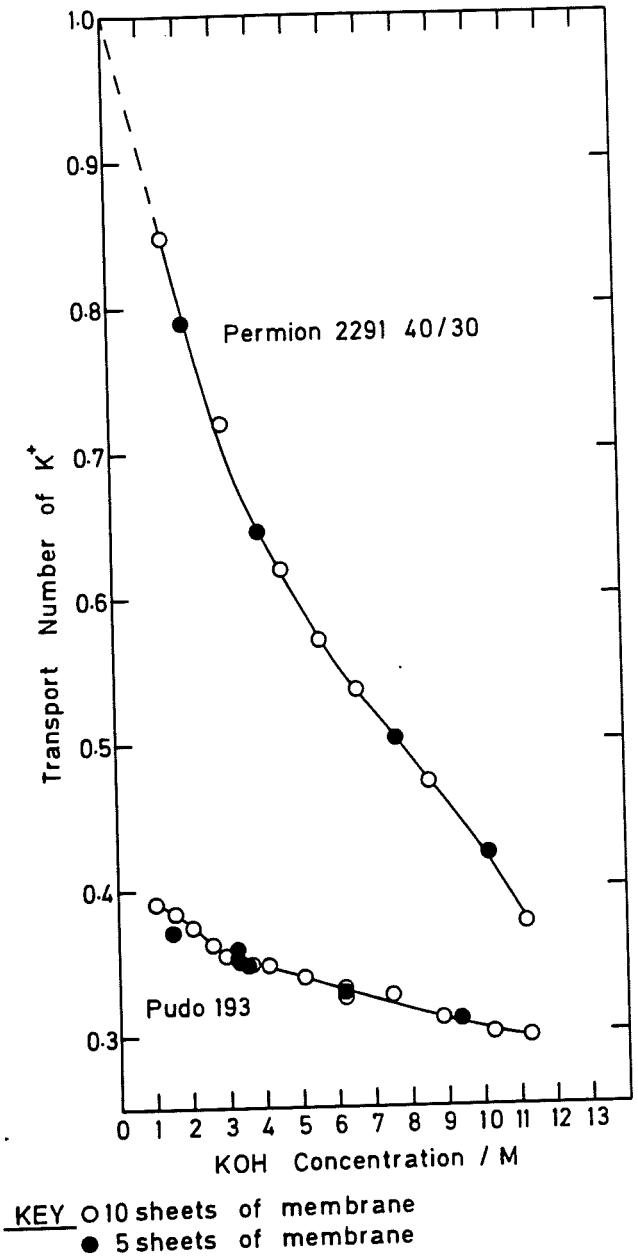

Figure 3.27 Comparison of the transference number of the water VS. KOH concentration for PUDO 193 Cellophane and Permion 2291 40/30.

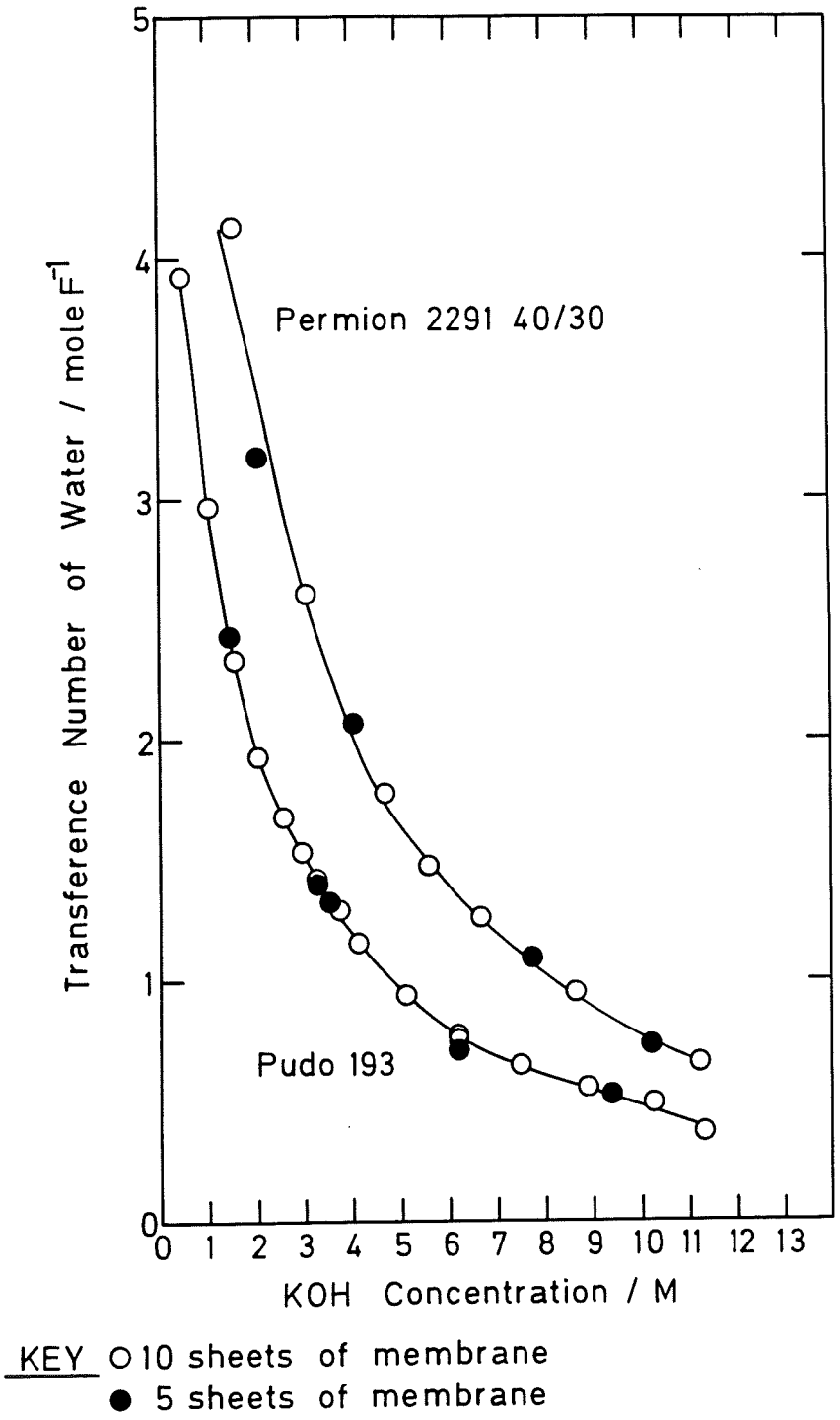

## 3.4 Conclusion

The accurate determination of transport numbers that depend solely on the influence of an electric field and are specific to a given external electrolyte concentration is not easy. The careful approach used in this study, of cell testing and the application of relevant correction factors, has produced a credible set of results.

The confidence gained in the technique used for single membrane types provides a sound basis for measuring and subsequently understanding transport behaviour in the less obvious situation, namely in assemblies of membranes.

# CHAPTER 4

# DETERMINATION OF IONIC CONDUCTIVITY AND THE DERIVATION OF IONIC MOBILITY WITHIN CELLOPHANE AND PERMION

## 4.1 Introduction

### 4.1.1 The mobility of an ion.

An ion in an electrolyte solution between two electrodes is subject to a force, F (newtons) created by an electric field, E ($Vm^{-1}$) where

$$F = zeE \tag{4.1}$$

ze (coulombs) is the charge on the ion where z is positive for cations and negative for anions. The force accelerates the ion, but as it moves through the solution a frictional force retards it. The ion is only accelerated to a limiting "drift" velocity which is dependent on the strength of the applied field and the viscosity of the solvent. The retarding force is expressed by Stokes' formula

$$F = 6\pi a\eta v \tag{4.2}$$

where a (m) is the radius of the ion, $\eta$ (poise) is the viscosity and v ($ms^{-1}$) is the drift velocity. The drift velocity is established when the accelerating force balances the retarding force.

$$6\pi a\eta v = zeE \tag{4.3}$$

Equation (4.3) may be rearranged in terms of the drift velocity

$$v = \frac{zeE}{6\pi a\eta} \tag{4.4}$$

The drift velocity is proportional to the applied field where the constant of proportionality is the mobility, $u_{\pm}$ ($m^2s^{-1}V^{-1}$) of the ion.
Thus,

$$u_{\pm} = \frac{ze}{6\pi\eta a} \tag{4.5}$$

### 4.1.2 Membrane tortuosity

Compared with free solution the polymer framework of a membrane or separator presents an obstacle to the movement of ions. The effect is further complicated in membranes due to their ion-exchange properties. In order to traverse the membrane ions have to travel round the polymer chains which from point to point may obstruct their direct path. The effect of the obstruction is to make the average path travelled by the ion in crossing the membrane greater by a factor $\theta$, than the path travelled by the ions through an equal thickness of solution, in which the mobility of the ion is u. The factor $\theta$, is the tortuosity and is defined as,

$$\theta = \frac{\text{mean path length}}{\text{membrane thickness}} > 1 \qquad (4.6)$$

Figure 4.1 Effect of an increased path length on the mobility of an ion in the membrane.

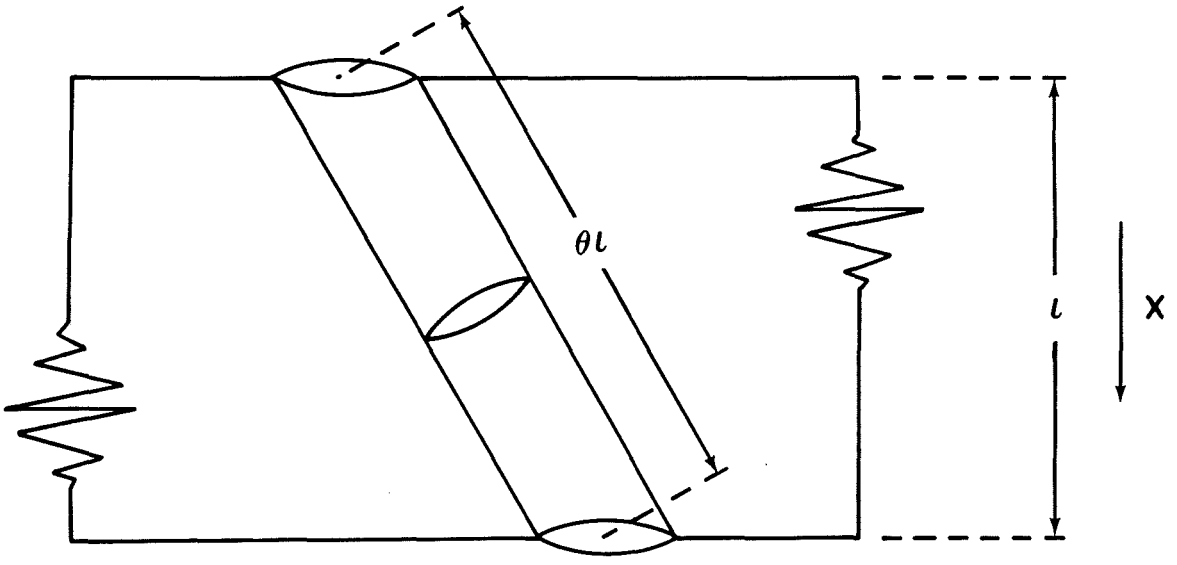

Figure 4.1 shows the effect of the increased path length on the mobility of an ion in the membrane. An ion subject to a force E, travelling in the x direction along the free solution path ι, has a velocity Eu. For an ion constrained to move along the tortuous path in the membrane, θι the force component in this direction is E/θ and the velocity of the ion is Eu/θ. Thus the velocity component of the ion travelling in the x direction in the membrane is $Eu/\theta^2$. Hence the apparent mobility, $\bar{u}'$ of an ion in the membrane is,

$$\bar{u}'_{\pm} = \frac{u}{\theta^2} \tag{4.7}$$

Equation (4.7) shows that the mobility of ions in the membrane is reduced by a tortuosity factor squared compared with the mobility of ions in free solution.

### 4.1.3 Conductivity of a membrane

The conductivity, $\bar{\kappa}$ ($\Omega^{-1}cm^{-1}$), of a swollen membrane is related to ionic mobilities within the membrane by equation (4.8) [93].

$$\bar{\kappa} = F(\bar{c}_+\bar{u}_+ + \bar{c}_-\bar{u}_-)(1 - V_p) \tag{4.8}$$

where $(1-V_p)$ is the porosity of the swollen membrane, $\bar{c}_+(1-V_p)$ and $\bar{c}_-(1-V_p)$, with units mole $cm^{-3}$, are the concentrations of the mobile species related to the total membrane volume, $\bar{u}_+$ and $\bar{u}_-$ are the real ionic mobilities in the pore fluid and F is the Faraday constant. Ionic mobilities are also related to transport numbers t, as shown in equations (4.9 and 4.10).

$$\bar{t}_+ = \frac{\bar{c}_+\bar{u}_+}{(\bar{c}_+\bar{u}_+ + \bar{c}_-\bar{u}_-)} \tag{4.9}$$

$$\bar{t}_- = \frac{\bar{c}_-\bar{u}_-}{(\bar{c}_+\bar{u}_+ + \bar{c}_-\bar{u}_-)} \tag{4.10}$$

Combination of equations (4.8) and (4.9) yields an expression for the mobility of the cation within the membrane,

$$\bar{u}_+ = \frac{\bar{\kappa}\bar{t}_+}{F\bar{c}_+(1-V_p)} \tag{4.11}$$

while combination of equations (4.8) and (4.10) yields an expression for the mobility of the anion within the membrane.

$$\bar{u}_- = \frac{\bar{\kappa}\bar{t}_-}{F\bar{c}_-(1-V_p)} \tag{4.12}$$

The above approach has neglected the effects of tortuosity which, as was shown in section (4.1.2) reduced the mobility of the ions in the membrane by a tortuosity factor squared compared to the mobility of ions in free solution. Using equation (4.7) to correct for the tortuosity of the membrane equations (4.8, 4.11 and 4.12) become.

$$\bar{\kappa} = \frac{F(\bar{c}_+\bar{u}_+ + \bar{c}_-\bar{u}_-)(1-V_p)}{\theta^2} \tag{4.13}$$

$$\bar{u}_+ = \frac{\bar{\kappa}\bar{t}_+\theta^2}{F\bar{c}_+(1-V_p)} \tag{4.14}$$

$$\bar{u}_- = \frac{\bar{\kappa}\bar{t}_-\theta^2}{F\bar{c}_-(1-V_p)} \tag{4.15}$$

Internal ionic concentrations of Cellophane were obtained from figure (2.14), and internal ionic concentrations of Permion were obtained from figures (2.10 and 2.11). The porosity of swollen Cellophane was obtained from figure (2.7) and equation (2.24) was used to calculate the porosity of swollen Permion. Potassium ion transport numbers through Cellophane and Permion were taken from figures (3.9 and 3.16) respectively. The tortuosity of a swollen membrane is discussed in the following section. Measurement of the membrane conductivity at an external electrolyte concentration thus allows the derivation of ionic mobilities at that concentration.

### 4.1.4 Tortuosity models

Mackie and Meares [94] have derived an expression for tortuosity in terms of the volume fraction of the gel framework. Movement of ions was between sites on a cubic lattice of coordination number 6 in such a way that if forward sites were blocked ions move laterally by a distance $\lambda$ to an unoccupied site. Ions could only move forward when they were above an unoccupied site. It was expected that an average fraction of one half of the four nearest neighbour lateral sites would be expected to be blocked off by the same polymer chain and of the remaining lateral sites a fraction $V_p$ would be occupied by other polymer links. Hence the chance of an ion being above an unoccupied site after one lateral jump is $1-(\frac{1}{2}+\frac{1}{2}V_p)$. Thus a fraction $V_p[\frac{1}{2}(1+V_p)]$ of ions required a second lateral jump before being able to move forward. Similarly, $V_p[\frac{1}{2}(1+V_p)]^2$ require a third, etc. For each lateral jump the ion travelled an extra distance $\lambda$. Hence to make $\delta/\lambda$ forward steps the total distance $\delta'$ travelled by an ion was

$$\delta' = \frac{\delta}{\lambda}\lambda\left[1 + V_p\sum_{n=0}^{\infty}(\tfrac{1}{2}(1+V_p))^n\right] \qquad (4.16)$$

In general a geometric series a, ar, $ar^2$, $ar^3$ ... $ar^{n-1}$ may be expressed as follows [95]

$$S_n = \frac{a(1-r^n)}{1-r} \qquad (4.17)$$

Hence equation (4.16) becomes

$$\frac{\delta'}{\delta} = 1 + \left[\frac{V_p(1-r^n)}{1-\frac{1}{2}(1+V_p)}\right] \tag{4.18}$$

Since $\frac{1}{2}(1+V_p) < 1$, r will approach zero as n becomes infinite and as $\delta'/\delta$ is equal to $\theta$ the following expression for tortuosity is obtained.

$$\theta = \frac{(1+V_p)}{(1-V_p)} \tag{4.19}$$

The approach of Lee et al [96] was to assume that the fraction of ions able to take a normal step was $(1 - V_p)$ and the fraction requiring an abnormal step due to blocking was $V_p$. The fraction requiring two, three, etc. abnormal steps before a normal one was $V_p^2$, $V_p^3$ etc. which leads to the following expression

$$\delta' = \frac{\delta}{\lambda}\lambda\left[V_p + 2V_p^2 + 3V_p^3 \ldots nV_p^n\right] \tag{4.20}$$

Since $V_p < 1$ and with reference to equation (4.17), equation (4.20) becomes

$$\theta = \frac{1}{(1-V_p)} \tag{4.21}$$

A recent method by Maskell [97] derived an equation for the tortuosity factor in non-homogeneous membranes such as cellulose. The argument in support of this equation is as follows. The inhomogeneity is a result of non-conducting regions or particles dispersed within an homogeneous conducting medium. A system representing a range of particle sizes is given as follows [98 and 99]

$$\frac{\kappa'}{\bar{\kappa}} = (1-\bar{x}V_p)^{-3/2} \qquad (4.22)$$

where $\kappa'$ ($\Omega^{-1}cm^{-1}$) is the conductivity of the homogeneous component of a heterogeneous membrane, $\bar{\kappa}$ ($\Omega^{-1}cm^{-1}$) is the ionic conductivity of the membrane and $\bar{x}V_p$ is the volume fraction of the membrane occupied by the non-conducting particles.

The blocking matrix is considered to comprise two fractions, $\bar{x}$ (by weight or volume), the non-conducting (heterogeneous) component and $1-\bar{x}$, the conducting (homogeneous) component. The total blocking fraction, $V_p$ is thus split into two fractions $\bar{x}V_p$ (heterogeneous) and $(1-\bar{x})V_p$ (homogeneous) with the imbibed electrolyte making up the remaining fraction $(1-V_p)$ and this is homogeneously mixed with the blocking fraction $(1-\bar{x})V_p$. The resulting conducting volume fraction is $(1-V_p)+(1-\bar{x})V_p$ i.e. $(1-\bar{x}V_p)$. The effective blocking fraction of the homogeneous gel is thus

$$V_{p^2} = \frac{(1-\bar{x})V_p}{(1-\bar{x}V_p)} \qquad (4.23)$$

Modification of equation (4.13) yields the conductivity of the homogeneous component as follows

$$\kappa' = \frac{F(\bar{c}_+\bar{u}_+ + \bar{c}_-\bar{u}_-)(1-V_{p^2})}{\theta_2^2} \qquad (4.24)$$

where $\theta_2$ is the tortuosity factor within the homogeneous component as follows

$$\theta_2 = \frac{(1+V_{p^2})}{(1-V_{p^2})} \qquad (4.25)$$

note that equation (4.25) is equivalent to equation (4.19). Eliminating $\kappa'$ and $\theta_2$ between

equations (4.22, 4.24 and 4.25) reveals

$$\bar{\kappa} = F(\bar{c}_+\bar{u}_+ + \bar{c}_-\bar{u}_-)(1-\bar{x}V_p)^{3/2}(1-V_{p^2})^3(1+V_{p^2})^{-2} \qquad (4.26)$$

where $V_p^2$ is given by equation (4.23). Comparison of equation (4.13) and (4.26) shows that

$$\theta^2 = (1-V_p)(1-\bar{x}V_p)^{-3/2}(1-V_{p^2})^{-3}(1+V_{p^2})^2 \qquad (4.27)$$

## 4.2 Experimental : Measurement of ionic conductivity

### 4.2.1 Apparatus

The perspex conductivity cell was designed to split into two identical sections, each comprising three layers (figures (4.2 and 4.3)) [100]. The outer layer was hollow with inlet tubes to a water jacket. The middle layer was solid apart from a hole drilled from the edge of the cell to the centre, surfacing on one face of the layer. This enabled a wire electrical connection to run from the platinum disc electrode to the outside of the cell.

The inner compartment acted as a water jacket and housed the electrodes. The platinised platinum disc electrode was permanently fixed to a steel bolt, which was located through the centre of the compartment with a rubber sealing washer behind the electrode. It was held firm in its counter-sunk hole with a nut and washer tightening onto the wire electrical connection. Inlet capillaries fed electrolyte into the space between the electrodes.

"O" ring seals in grooves on the layers sealed the cell when all layers of each half were secured with 11/2" long cap head screws.

Calculation of conductivity required knowledge of an area term. In theory this is relative to the membrane but in practice the area of the electrode was used, the platinum electrodes therefore had to be directly opposite each other every time the cell was assembled. This was accomplished by aligning two pegs from one half of the cell with corresponding holes on the other half of the cell. Four bolts which passed through the whole assembly sealed the cell. Measuring marks one on either half of the cell enabled the separation of the electrodes to be determined.

Figure 4.2 Schematic diagram of conductivity cell

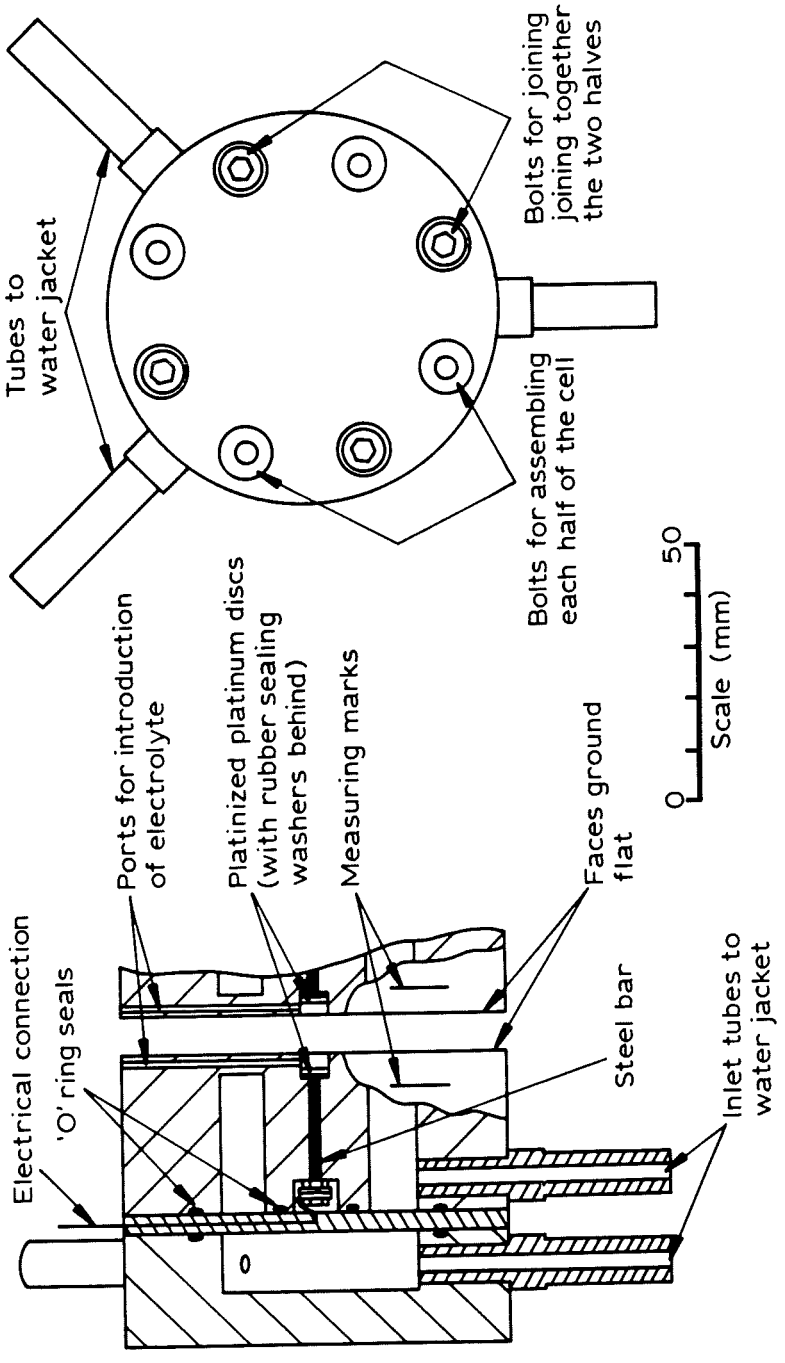

Figure 4.3 Photograph of conductivity cell

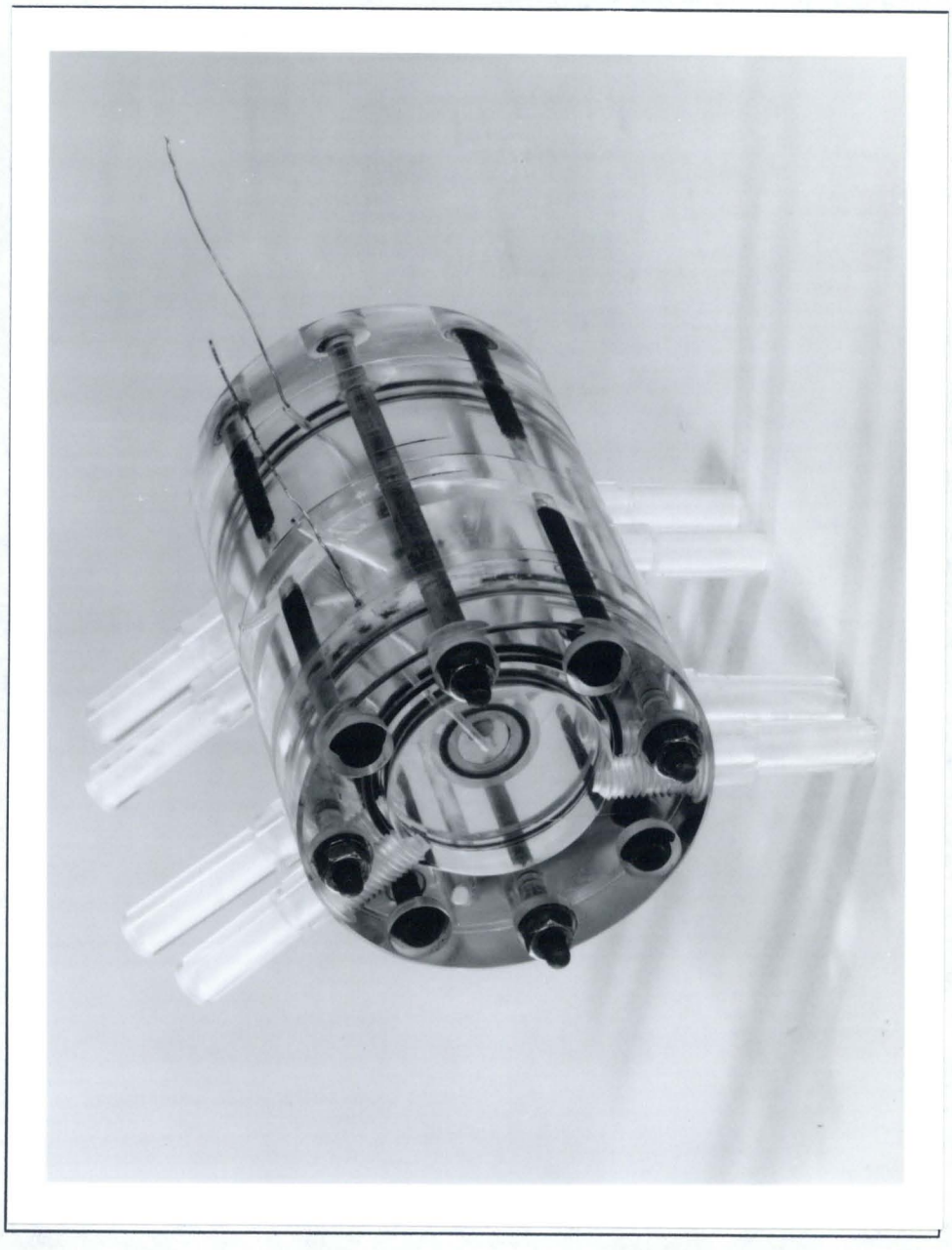

### 4.2.2 Platinisation of the electrodes

Prior to use the electrodes were platinised. They were removed from the cell, cleansed with chromic acid and washed with distilled water. A platinisation solution of 0.072M chloroplatinic acid with 0.00013M lead acetate was used [101] to platinise each electrode. For platinisation the cell was arranged as shown in figure (4.4). A collar of "blue-tac" surrounded the electrode and was filled with the platinisation solution. The other electrode contact consisted of a platinum wire extending from the solution. A current of 30mA/cm$^2$ was applied for 5 minutes so that the Pt ions could coat the cell electrode surface. After platinisation the electrodes were washed and mopped dry with tissue paper. Care was taken not to touch the electrode surface after this stage.

Figure 4.4 Arrangement of cell during the platinisation of the electrodes

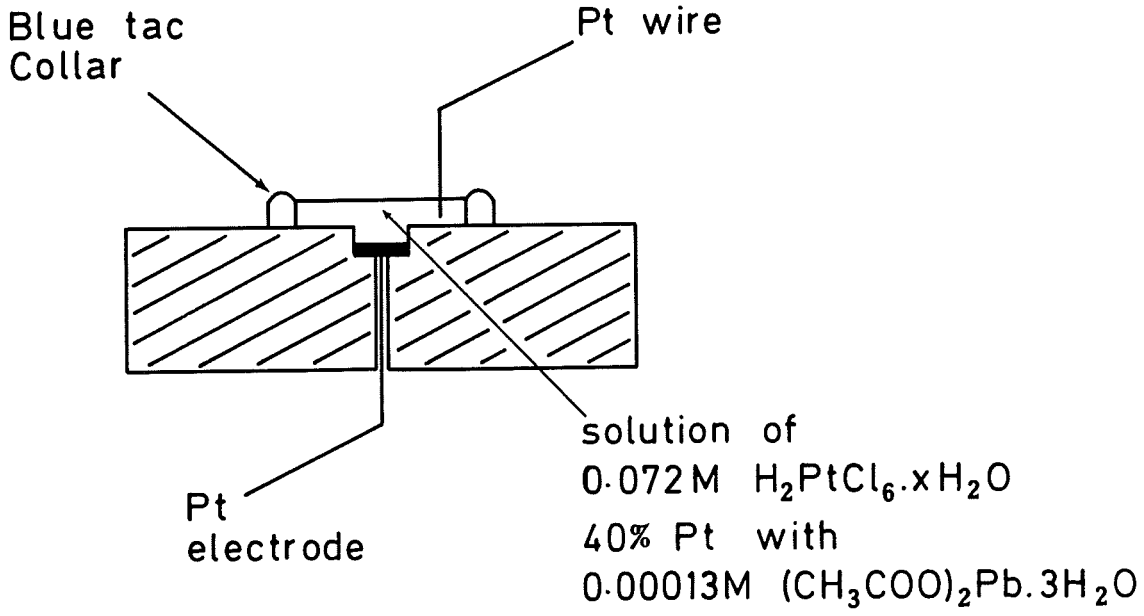

### 4.2.3 Determination of the cell constant

The electrode separation was determined by measuring the recess of each electrode from the inner face of each half of the cell using a sigameasure. This was found to be 1.641mm for one half and 1.465mm for the other. Throughout this work the separation of the electrodes was taken to be 3.106mm. The diameter of the orifice defining the area of membrane exposed to electrolyte ie. the area of the electrode was taken to be 6.15mm. This value was measured using a cathetometer by the previous workers [100]. The cell constant, l/A, was thus 0.1046mm where l (cm) is the separation of the electrodes, A ($cm^2$), is the area of the electrodes.

The accuracy of the cell constant was checked by measuring the conductivity of, 0.01M, 0.1M and 1.0M KCl solutions prepared from Analar grade potassium chloride supplied by BDH. Resistance measurements were made across these solutions with either 0,3,5 or 8 polythene spacers between the two halves of the cell. Conductivity of the KCl solution was determined by the equation

$$K = \frac{l}{R \times A} \qquad (4.28)$$

where K ($\Omega^{-1}cm^{-1}$) is the conductivity and R ($\Omega$), is the resistance determined from the intercept of a linear plot of resistance versus the number of spacers, figure (4.5), after correction for current refraction, (see section (4.3.1)). The lines drawn on figure (4.5) were obtained by linear regression.

The conductivities of the KCl electrolyte solutions are expressed in table (4.1). The values obtained were compared with the literature and confidence gained in the value of the determined cell constant. There is good agreement between results obtained at 1.0M and 0.1M and reasonable agreement at 0.01M.

Figure 4.5 Resistance vs. number of spacers in various KCl solutions before and after correction for current refraction at 25°C.

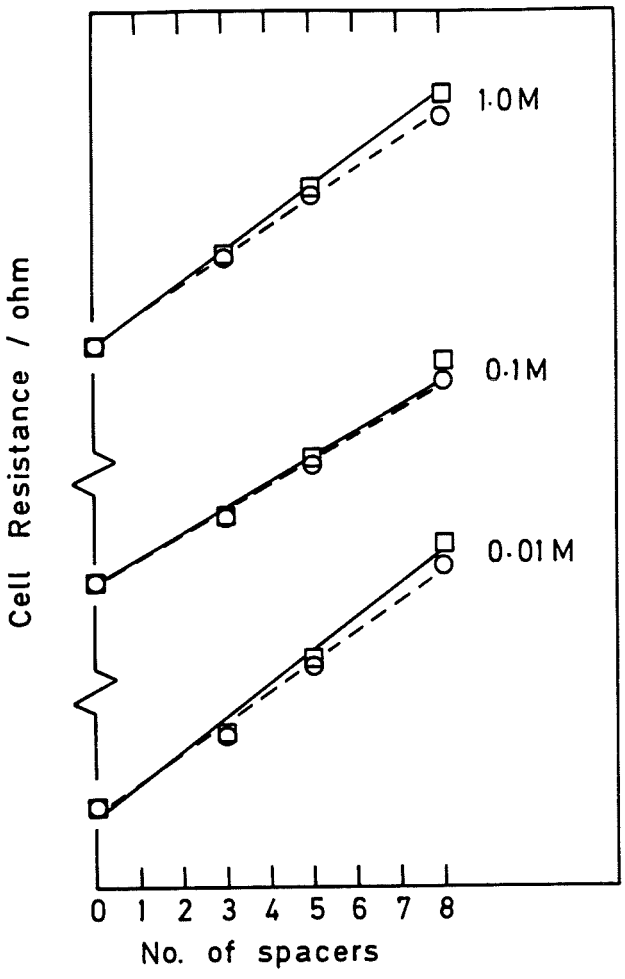


| Solid line | Intercept / Ω |
|---|---|
| 1.0M KCl | 9.690 |
| 0.1M KCl | 79.67 |
| 0.01M KCl | 680.8 |

Table 4.1 Comparison between the conductivity of KCl solutions determined using the cell used in this study with literature values.

| [KCl] / M | Conductivity ($\Omega^{-1}cm^{-1}$) at 25°C | | | |
|---|---|---|---|---|
| | This study | Ref. [102] | Ref. [103] | Ref. [68] |
| 1.0 | 0.1076 | 0.1080 | 0.111733 | |
| 0.1 | 0.01308 | 0.01279 | 0.0128862 | 0.01290 |
| 0.01 | 0.001531 | 0.001424 | 0.00141145 | 0.00141 |

### 4.2.4 Method used for single membrane types

The following method was adopted for all conductivity measurements on single membranes. The apparatus had been used in previous work [100] and therefore before any measurements were made the cell was completely dismantled and thoroughly cleaned.

The cell was cleaned and dried before use. The surface of each electrode was wetted and the inlet capillary flushed with the electrolyte to be studied. The wetting procedure ensured that the complete electrode surface was carrying the current. The two halves of the cell were fixed together using the four through bolts tightened to an even torque of 0.5Nm using a Radio Spares constant torque screwdriver. After the first bolt had been tightened, the second bolt chosen was opposite and not adjacent, to ensure even pressure on the cell.

Electrolyte solution was injected down one of the four capillary tubes via a 1ml syringe fitted with a hypodermic needle. Solution was injected until the compartment and capillaries were full and devoid of air bubbles, which were prone to cling to electrode and membrane surfaces. The electrode solution had been brought to 25°C in a water bath prior to use. This temperature was maintained throughout the cell by passing water at 25°C through the water jacket.

The resistance of the cell was measured using a Wayne-Kerr Automatic Component Bridge, B605 and Component Adaptor, JU4 at a frequency of 1kHz. The

resistance was recorded after a few minutes when the cell and the solution had equilibrated at 25°C, as judged by a constant resistance reading. Resistance measurements were taken across numbers of layers of membrane over a wide range of KOH concentrations. For each experiment the resistance was recorded with say 0, 1, 3, 5, 7 and 10 layers of membrane.

The KOH solutions were prepared and analyzed as in section (2.1.2). Membrane films were soaked in electrolyte for at least 1 day in a sealed container. They were removed individually from the electrolyte and stacked by a roller action lightly pressing each layer. Before mounting the membrane stacks between the two halves of the cell a template was used so that holes could be punched in the stack to allow access for the through bolts and alignment pegs (figure (4.6)). In some experiments the relative separation of the electrodes was recorded by training a travelling microscope on the measuring marks.

The swollen thickness of individual membrane layers was measured using a sigameasure fitted with a 9.54mm flat anvil, taking the average of 10 readings.

### 4.2.5 Method used for assemblies

The procedure described in section (4.2.4) was followed except that resistance was measured across pairs of alternate membranes, ie. a 2 pair assembly was made up of one layer of cellophane, one layer of Permion, one layer of cellophane and one layer of Permion.

Figure 4.6 Template showing the positions of the through bolts and alignment pegs

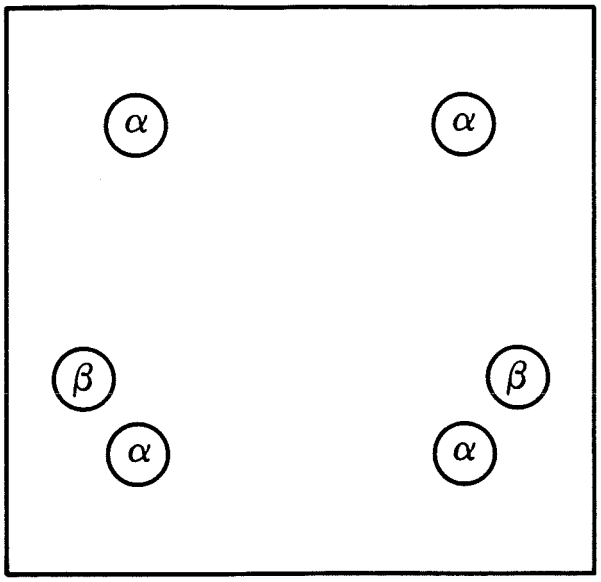


α through-bolt holes

β alignment peg holes

## 4.3 Results and discussion

### 4.3.1 Conductivity data

Primary data of membrane resistance vs. membrane thickness have been obtained for both membranes over a wide range of KOH concentrations. A specimen plot is shown in figure (4.7). Such plots display slight curvature due to current refraction into the membrane in the region where it is clamped between the two halves of the cell. Plots such as figure (4.7) have been used to obtain a value of the true ionic conductivity of the membrane by determining the tangent to the slope at zero membrane thickness [104]. This is difficult to assess and therefore it is more satisfactory to correct for the refraction and obtain a straight line slope. Jenkins et al [100] have used the mathematically exact treatment of Barrer et al [105] to achieve this.

Figure (4.8), shows a cross section of the cell and a schematic representation of current flow into the refraction region. Appendix (D) contains the equations required to calculate a correction factor F which when applied to the primary data corrects for the refraction. The correction factor F is a function of l, the thickness of the membrane, b, the radius of the area into which refraction occurs and a, the radius of the electrode. In the Jenkins, Maskell and Tye paper [100], F was computed for the range $b/a > 4$ and $l/a < 1$. In this region a plot was obtained the equation for which is given below

$$F = 1 - 0.313\left(\frac{l}{a}\right) + 0.017\left(\frac{l}{a}\right)^2 \qquad (4.29)$$

The correction factor F, given by equation (4.29) was used on the resistance data by applying the following equation.

$$R_1' = \frac{(R_1 - R_0)}{F} + R_0 \qquad (4.30)$$

$R_1$ and $R_0$ are the measured cell resistances with and without the membrane respectively and $R_1'$ is the cell resistance corrected for refraction. Figure (4.9) shows the data from

Figure 4.7 Resistance vs. number of layers of Cellophane in a 1.021M solution of KOH at 25°C.

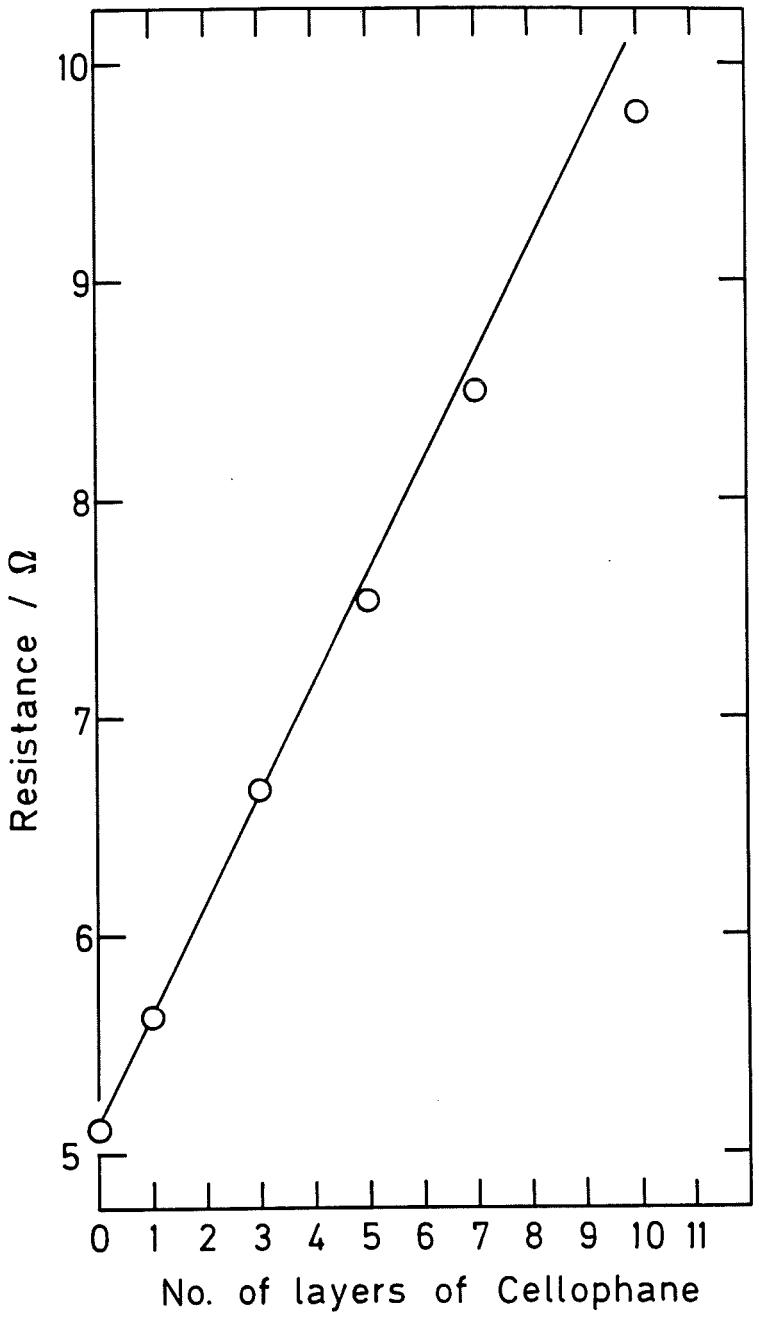


solid line shows the corrected data from figure 4.9 .

Figure 4.8 Cross section of the cell and a schematic representation of current flow into the refraction region

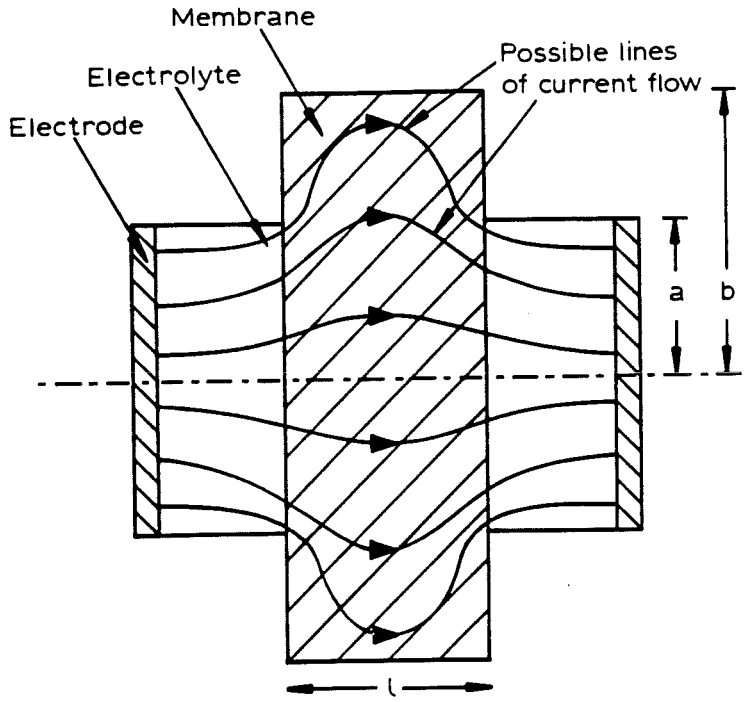

Figure 4.9 Resistance vs. number of layers of Cellophane in a 1.021M solution of KOH before and after correction for current refraction at 25°C.

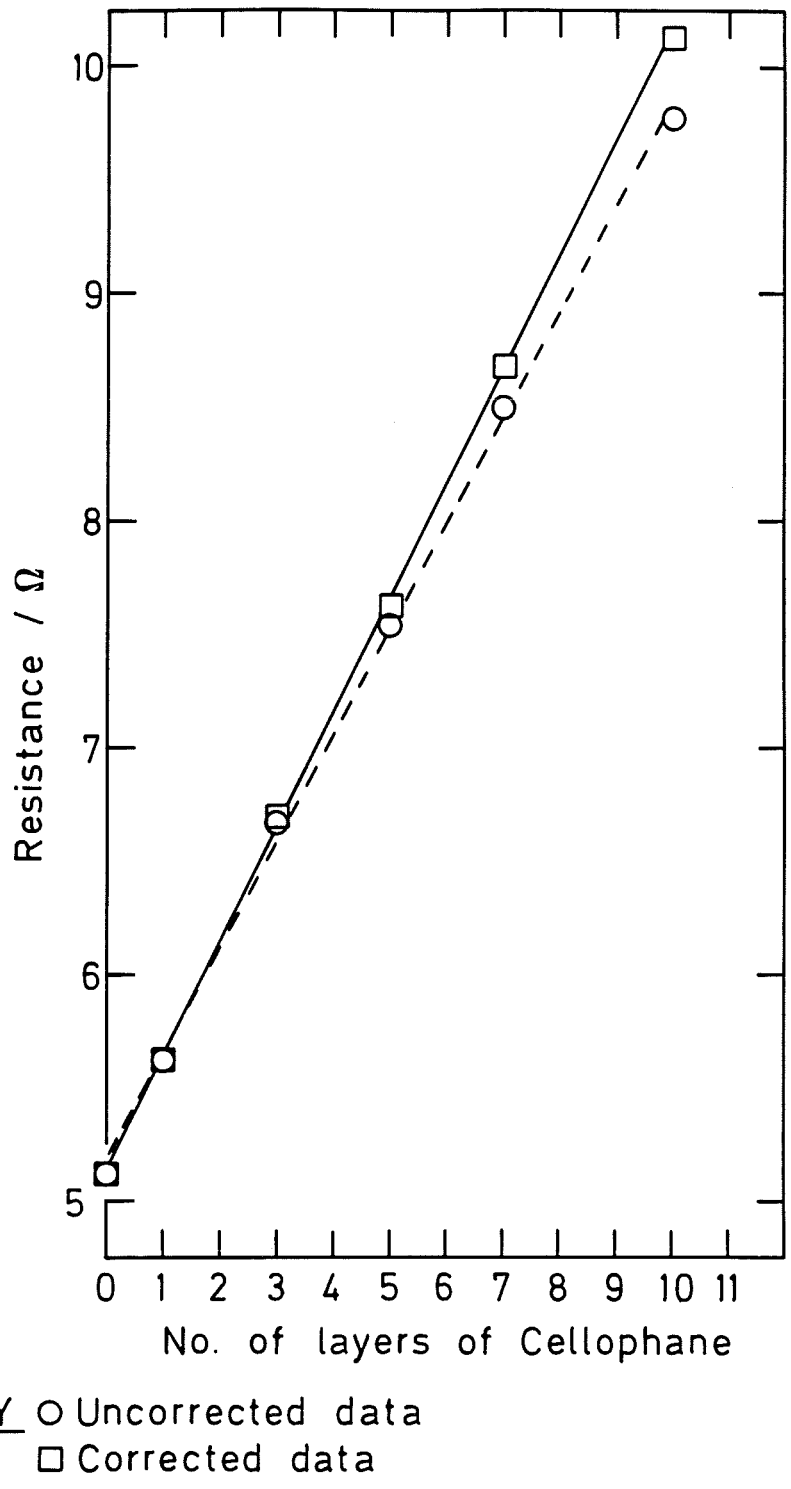

figure (4.7) before and after the application of equations (4.27 and 4.28). A straight line regression analysis was performed on the corrected and uncorrected data which resulted in correlation coefficients of 0.99967 and 0.99860 respectively. A value of 1 is expected when all points fit perfectly on a straight line. Figures (4.10 to 4.14) show corrected and uncorrected data for both membranes over a range of KOH concentrations, the slopes and intercepts of the corrected data are shown in table (4.2).

Although equation (4.27) covers the range of l/a and b/a appropriate to most membrane conductivity work Jenkins et al [100] did not fully investigate how F was affected by extremes of l, a and b. The present author has explored the situation and figure (4.15) shows the relationship between F and l/a over a wide range of b/a. For all reasonable values of b/a, as l the membrane thickness increases then the calculated value of F deviates from the line given by equation (4.27) and tends towards a constant. If the value b is fixed and l is large then any further increase in l will have little change on the refraction pattern and hence the constant value of F.

For a given value of l/a as b increases then F again tends towards a constant since refraction into the membrane approaches a limit. This is sensible since it is not plausible that given a membrane of infinite area that the lines of refraction would have an effect over the whole area. With b approaching a then the area of the membrane has a greater influence on the refraction and hence on F. Correction of actual data must be where b is sufficiently large so as to allow unhindered refraction. A decrease in l/a decreases the influence b has on the correction factor. If the membrane is very thin then there is less opportunity for current refraction.

The method given in Appendix (D) has been used successfully to correct the conductivity data of other authors [68 and 106], which fell outside of the range of applicability of equation (4.27) [100].

From the intercept of each corrected "resistance vs. no. of membrane layers" graph (figures 4.10 to 4.14) and the cell constant the conductivity of the electrolyte was determined. This is shown vs. external electrolyte concentration in figure (4.16) and as expected is independent of the membrane. The conductivity of KOH has been previously reported [102, 107 and 108] and a comparison between the literature and the data obtained by this worker is shown in figure (4.17), for clarity the actual points shown in figure (4.16) have been omitted. The data obtained in this study fit very closely to the

Figure 4.10 Resistance vs. number of layers of Cellophane in various KOH solutions before and after correction for current refraction at 25°C.

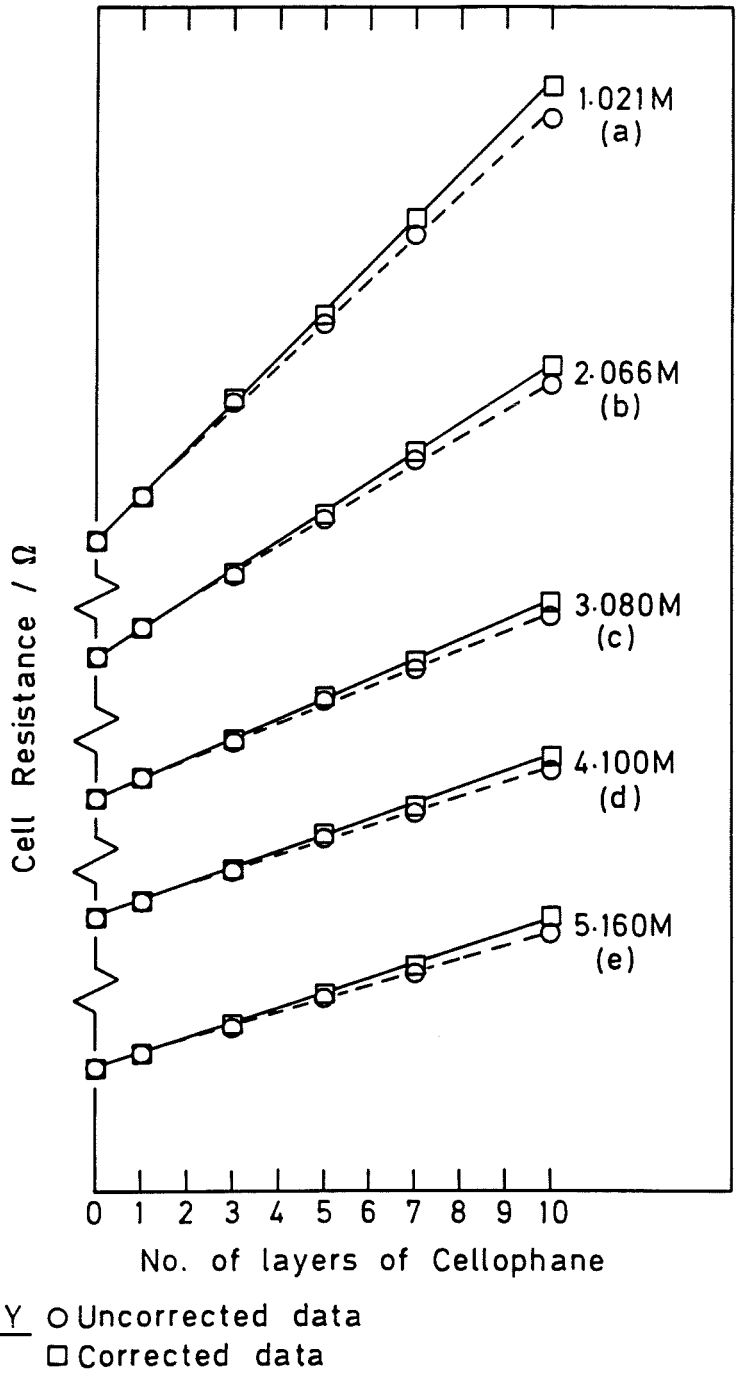

Figure 4.11 Resistance vs. number of layers of Cellophane in various KOH solutions before and after correction for current refraction at 25°C.

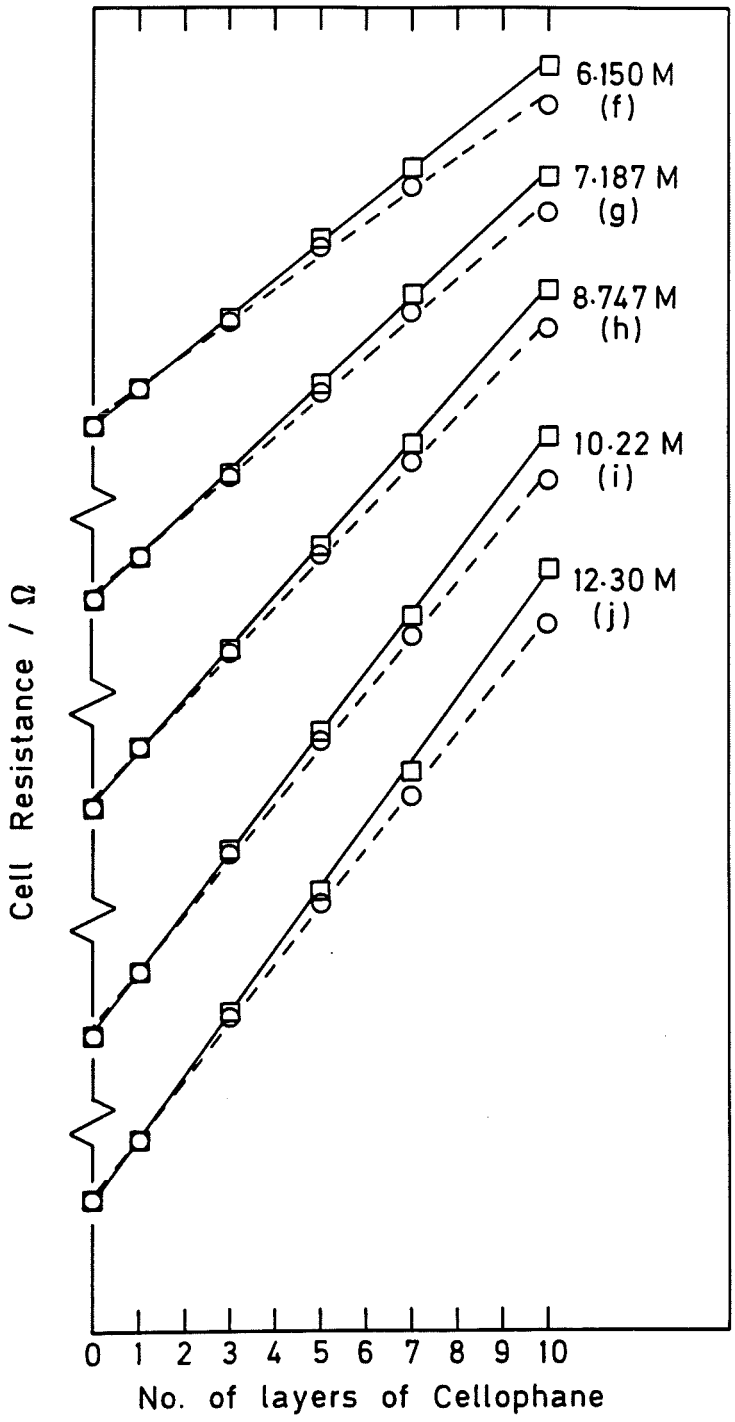

Figure 4.12 Resistance vs. number of layers of Permion in various KOH solutions before and after correction for current refraction at 25°C.

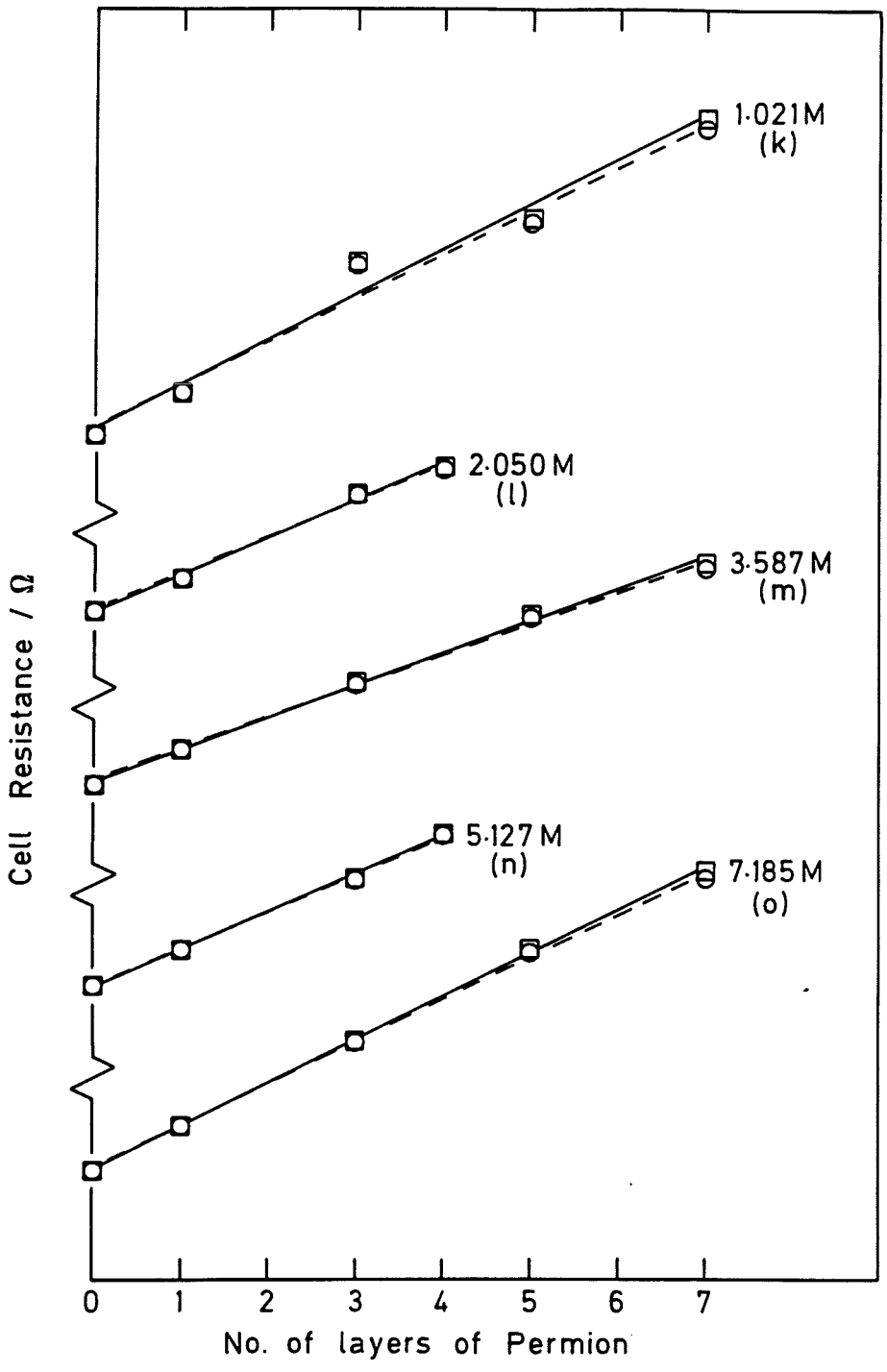

Figure 4.13 Resistance vs. number of layers of Membrane in various KOH solutions before and after correction for current refraction at 25°C.

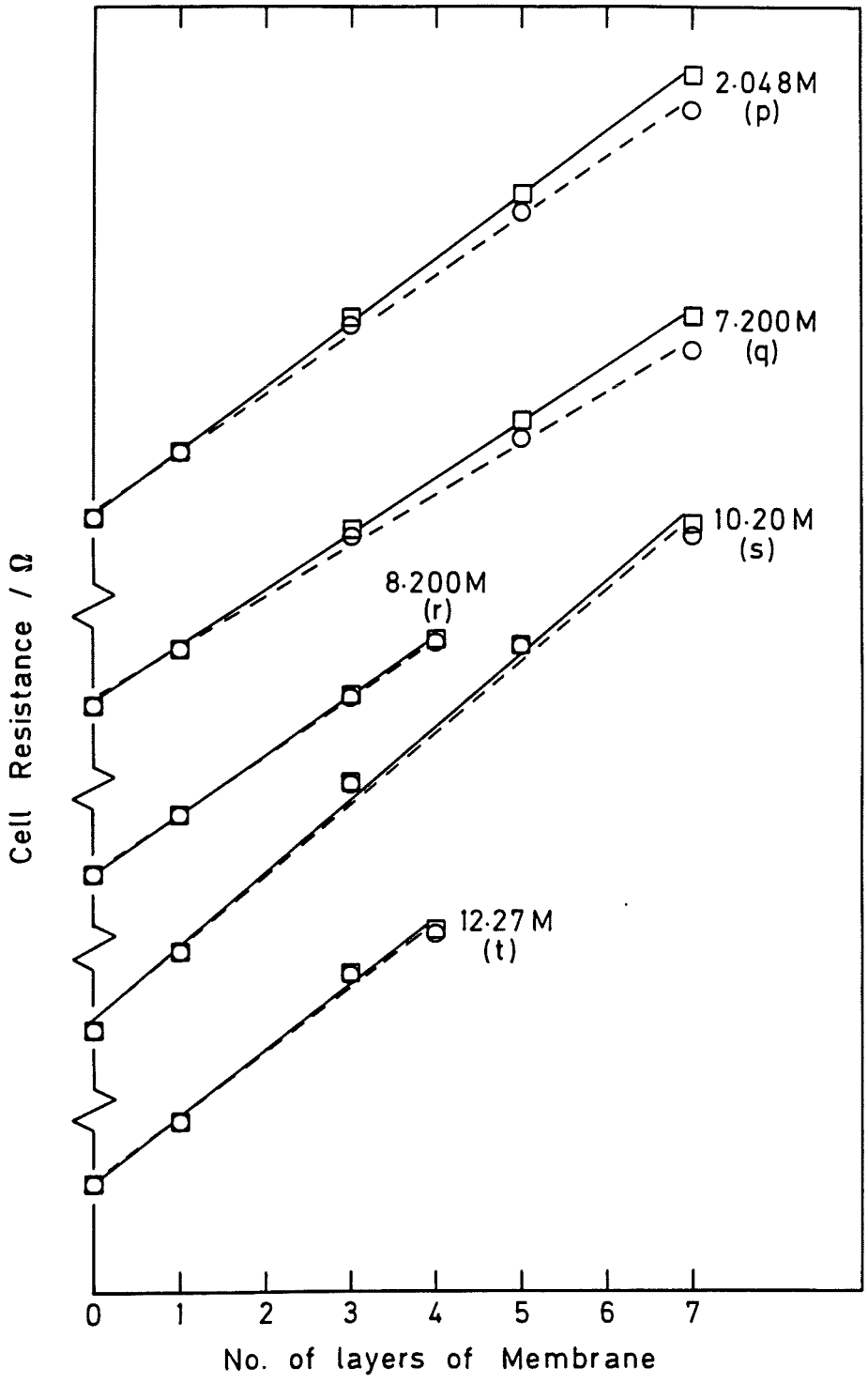

Figure 4.14 Resistance vs. number of layers of Membrane in various KOH solutions before and after correction for current refraction at 25°C.

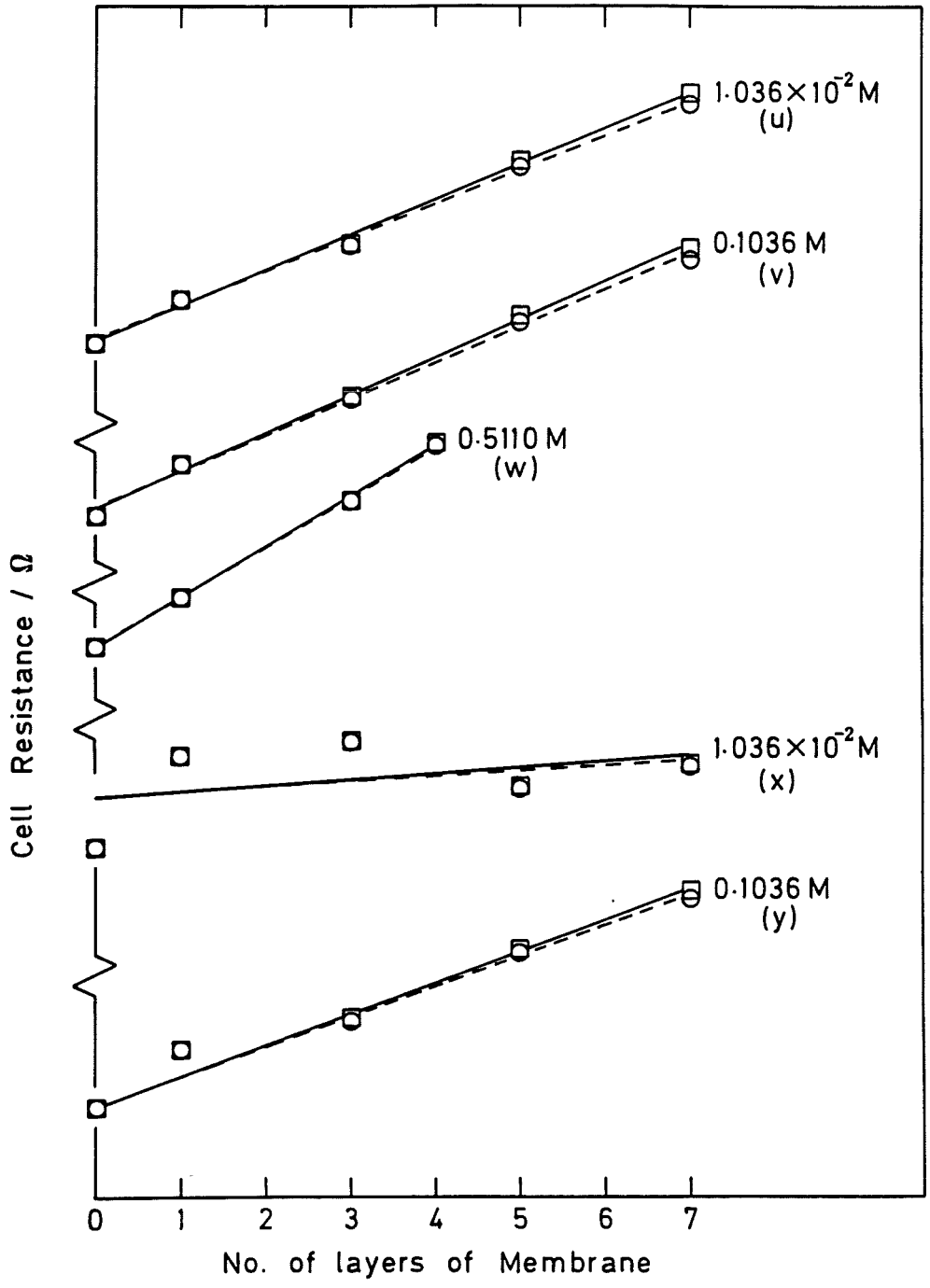

Table 4.2 Slopes and intercepts of the membrane resistance data shown in figures (4.9 to 4.13)

| Graph | Membrane | [KOH] M | Slope Ω per layer | Intercept Ω |
|---|---|---|---|---|
| (a) | Cellophane | 1.021 | 0.5011 | 5.146 |
| (b) | Cellophane | 2.066 | 0.3218 | 2.854 |
| (c) | Cellophane | 3.080 | 0.2178 | 2.314 |
| (d) | Cellophane | 4.100 | 0.1774 | 2.010 |
| (e) | Cellophane | 5.160 | 0.1649 | 1.851 |
| (f) | Cellophane | 6.150 | 0.1590 | 1.776 |
| (g) | Cellophane | 7.187 | 0.1875 | 1.811 |
| (h) | Cellophane | 8.747 | 0.2256 | 1.916 |
| (i) | Cellophane | 10.22 | 0.2618 | 2.112 |
| (j) | Cellophane | 12.30 | 0.2755 | 2.563 |
| (k) | Permion | 1.021 | 0.5092 | 5.223 |
| (l) | Permion | 2.050 | 0.4307 | 3.116 |
| (m) | Permion | 3.587 | 0.3675 | 2.187 |
| (n) | Permion | 5.127 | 0.4300 | 1.844 |
| (o) | Permion | 7.185 | 0.4911 | 1.771 |
| (p) | Assembly | 2.048 | 0.7417 | 3.078 |
| (q) | Assembly | 7.200 | 0.6512 | 1.884 |
| (r) | Permion | 8.200 | 0.6917 | 1.874 |
| (s) | Permion | 10.20 | 0.8543 | 2.170 |
| (t) | Permion | 12.27 | 1.543 | 2.534 |
| (u) | Cellophane | 0.01036 | 41.53 | 357.5 |
| (v) | Cellophane | 0.1036 | 4.440 | 41.02 |
| (w) | Permion | 0.5110 | 0.5966 | 9.462 |
| (x) | Permion | 0.01036 | 2.932 | 378.0 |
| (y) | Permion | 0.1036 | 1.473 | 40.23 |

Figure 4.15 Computed F values vs. l/a over a range of b/a

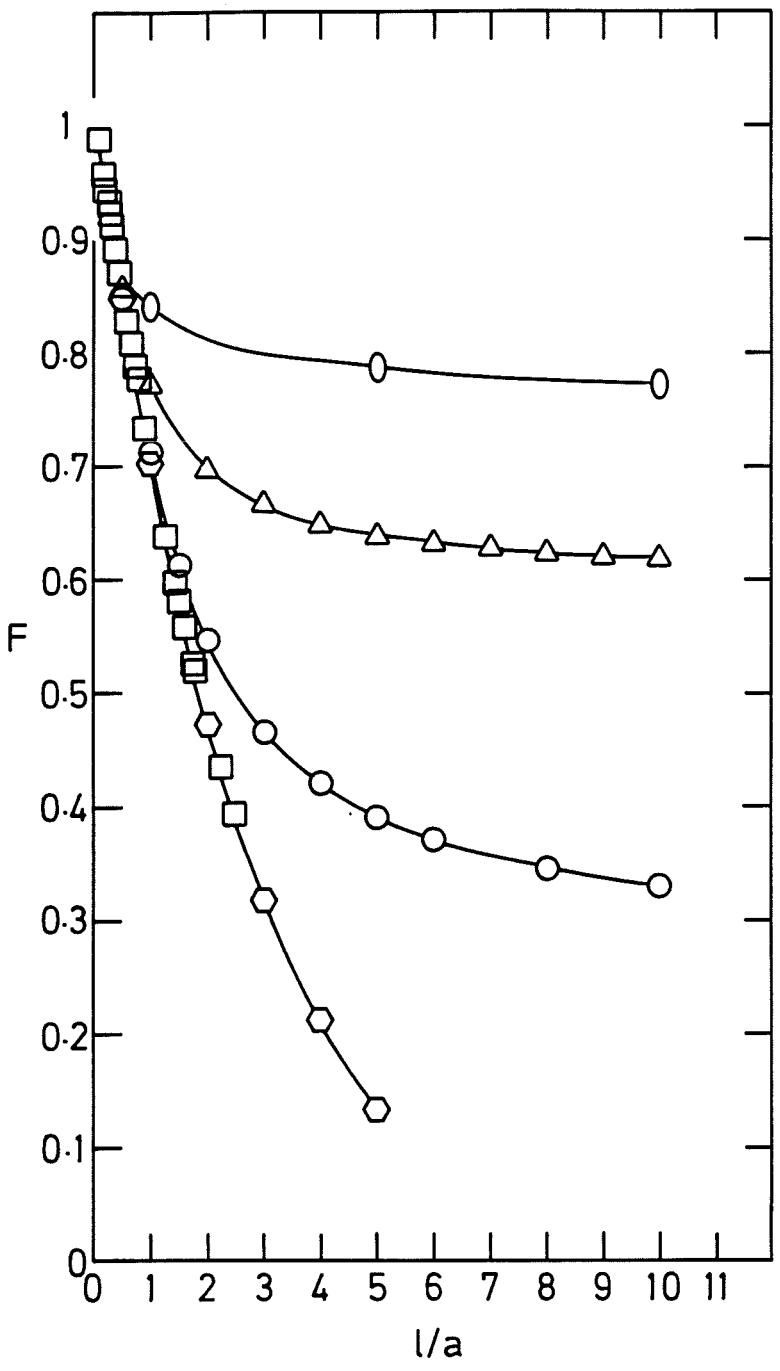


KEY ○ b/a = 1·1 , △ b/a = 1·2 , ○ b/a = 1·5
□ b/a = 4 , ⬡ b/a = 10

Figure 4.16 KOH conductivity as a function of concentration at 25°C.

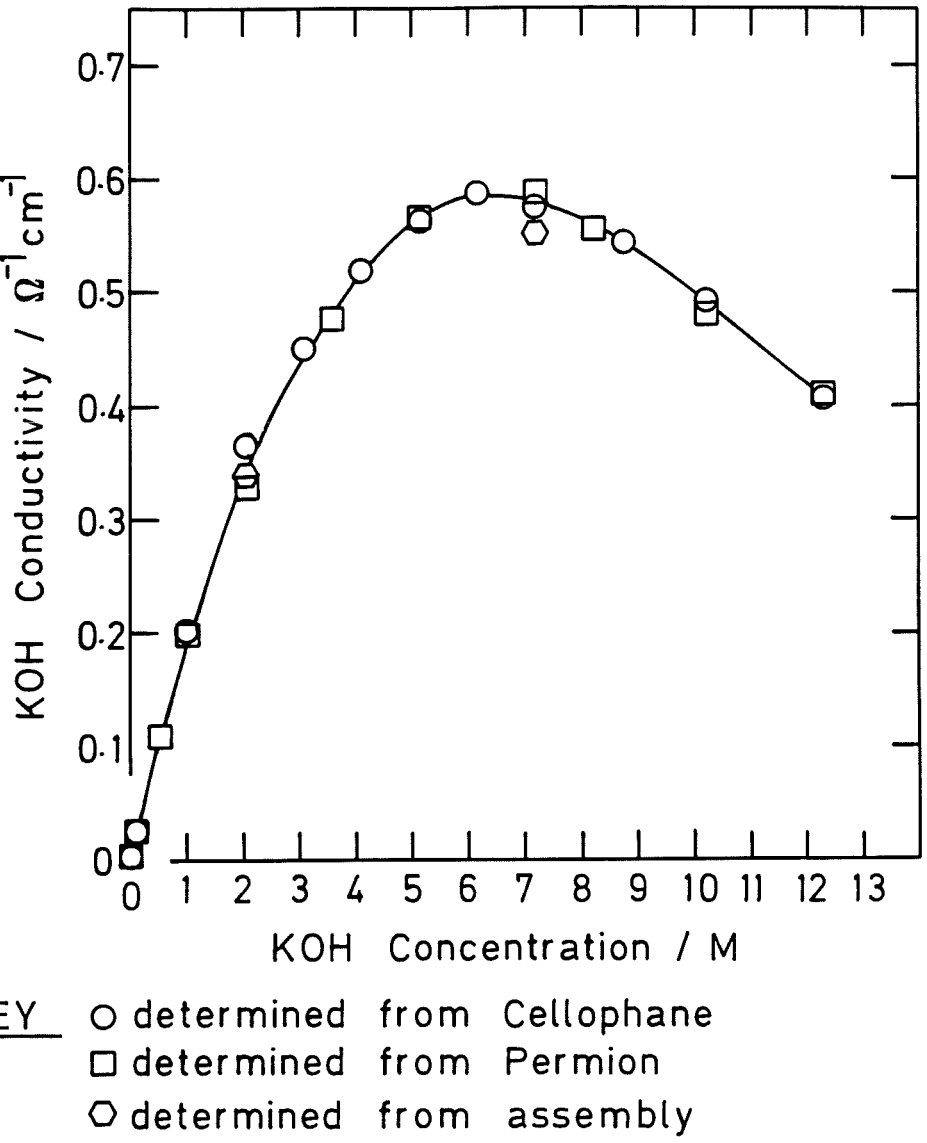

Figure 4.17 Electrical conductivities of KOH solutions as a function of concentration at 25°C.

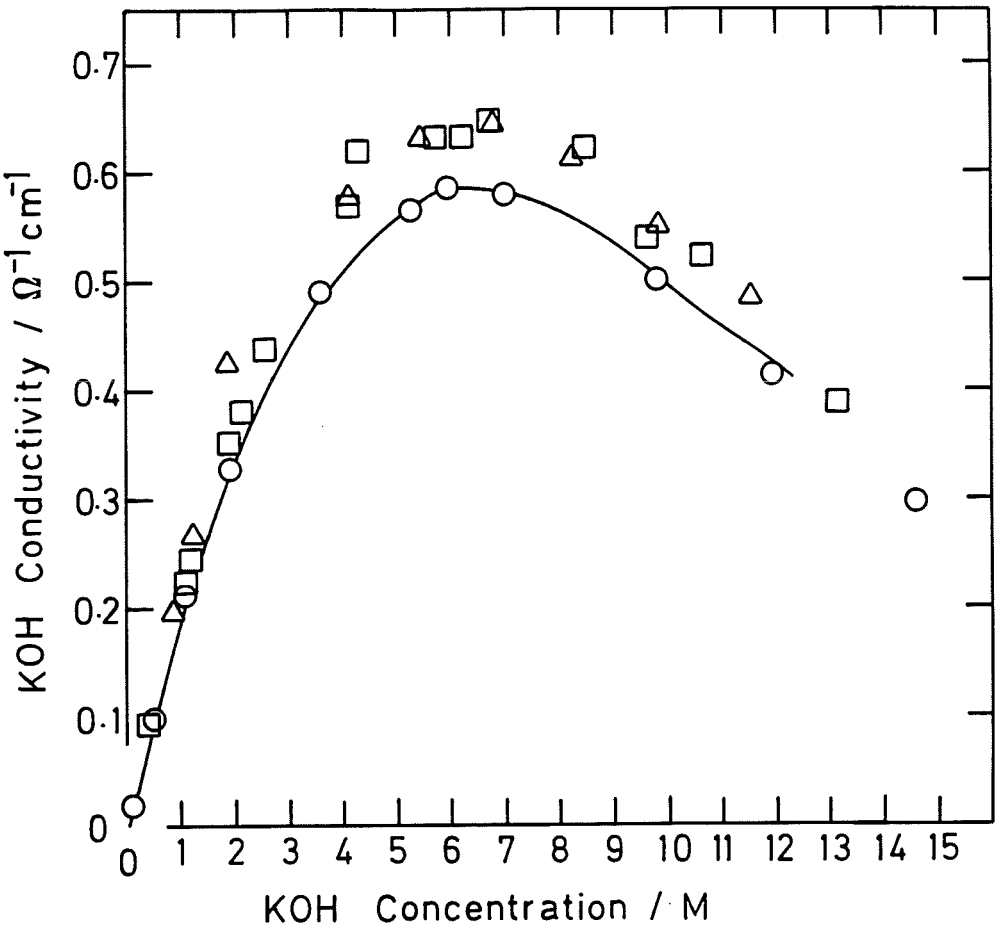


KEY solid line , this study
○ , Ref.(102) ; □ , Ref.(103) ; △ , Ref. ( 68 ).

data obtained by Jenkins et al [102]. Conductivity is dependent on concentration and mobility as shown in equation (4.31).

$$\kappa = FC(u_+ + u_-) \tag{4.31}$$

Mobility is also concentration dependent and decreases as concentration increases. Figure (4.16) shows that up to around 6M the influence of concentration is dominant and an increase in conductivity is observed with an increase in concentration. After 6M the decrease in mobility with concentration outweighs the further increase in concentration and the conductivity falls.

From the slope of the corrected resistance plots, (table (4.2)), and the area of the cell orifice the conductance of each membrane was determined and is shown in figure (4.18). Incorporation of the swollen thickness data reported in chapter (2) enabled the conductivities to be calculated and the results are shown in figure (4.19).

Membrane resistances were determined from single membranes and from assemblies of Cellophane and Permion. Table (4.3) shows that the combined resistance of Cellophane and Permion is equivalent to the resistance of an assembly of the two membranes at a given external electrolyte concentration. This is to be expected since the effective resistance of two resistors in series (i.e. the assembly) is the sum of the individual resistors (i.e. the resistances of Cellophane and Permion).

Figure 4.18 Variation of membrane conductance with electrolyte concentration at 25°C.

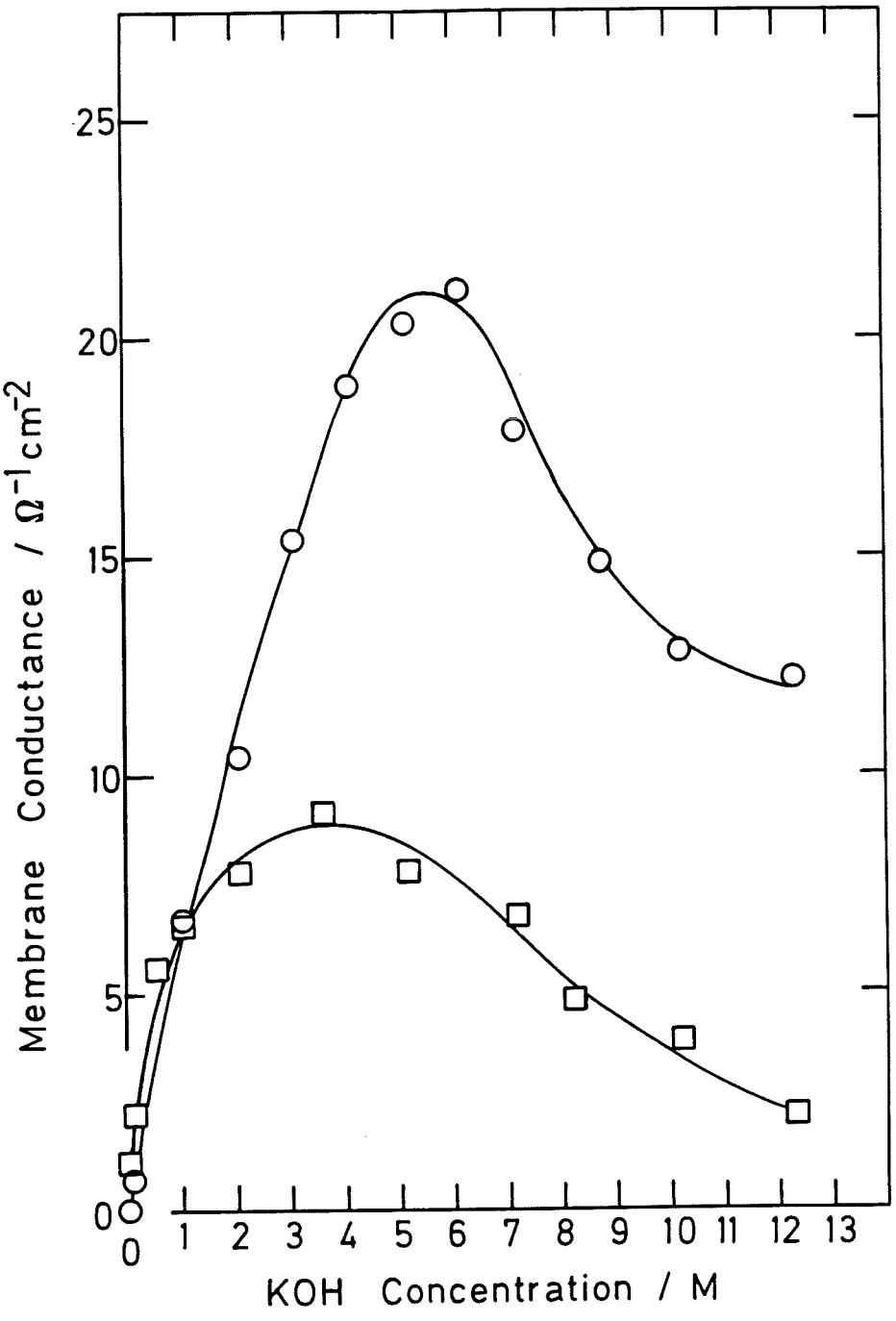

Figure 4.19 Variation of membrane conductivity with electrolyte concentration at 25°C.

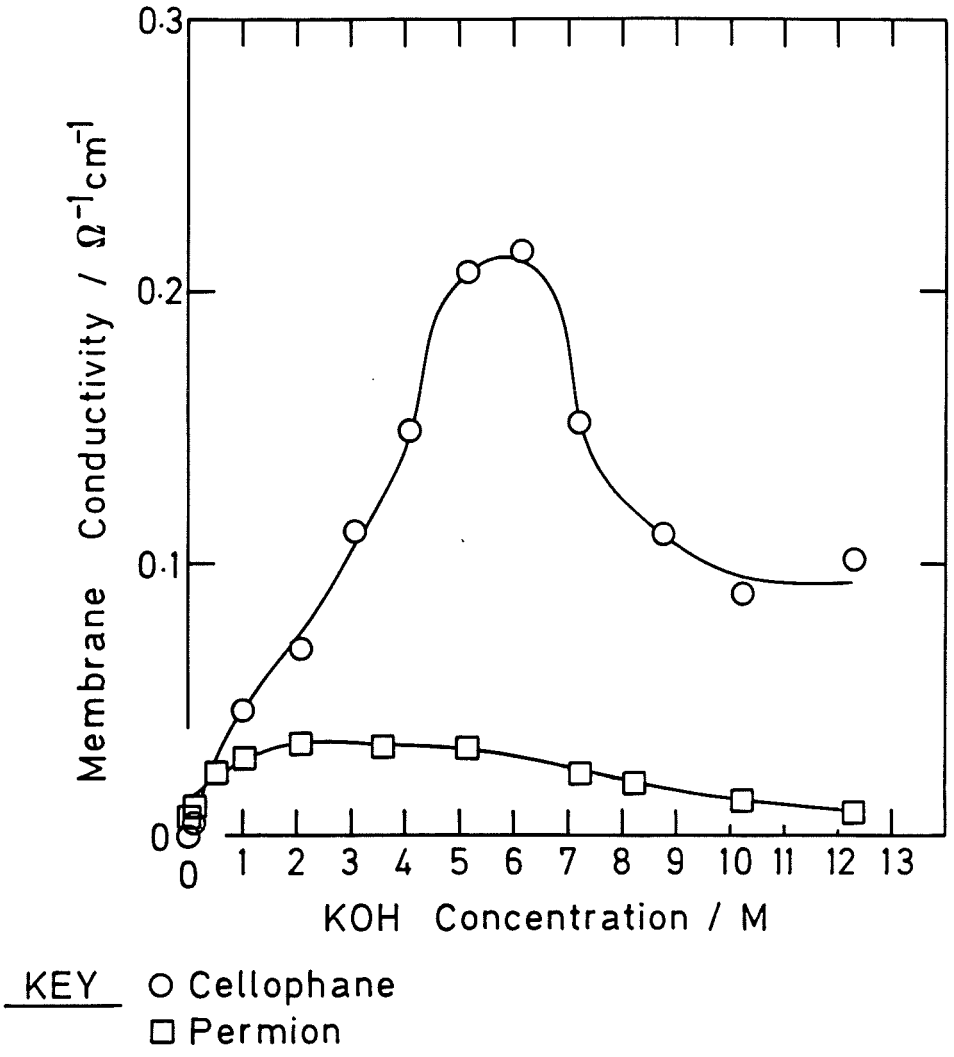

Table 4.3 A comparison of the addition of single membrane resistances with the resistance of an assembly of the two membranes at 25°C.

| Membrane | KOH Concentration M | Resistance $\Omega cm^2$ |
|---|---|---|
| Cellophane | 2.066 | 0.096 |
| Permion | 2.050 | 0.128 |
| Cellophane + Permion | | 0.224 |
| Assembly | 2.048 | 0.221 |
| Cellophane | 7.187 | 0.056 |
| Permion | 7.185 | 0.146 |
| Cellophane + Permion | | 0.202 |
| Assembly | 7.200 | 0.194 |

### 4.3.2 Derivation of ionic mobilities

Using the electrolyte conductivity data presented in figure (4.17), mobilities of the potassium and hydroxyl ions in free solution were calculated. As reported earlier in the chapter electrolyte conductivity is related to anion and cation mobility by equation (4.31).

$$\kappa = FC(u_+ + u_-) \tag{4.31}$$

The transport number of the $K^+$ ion in free solution is given by equation (4.32). Values for the transport number of the hydroxyl ion in free KOH solution were taken from the literature [109].

$$t_+ = \frac{u_+}{u_+ + u_-} \tag{4.32}$$

Rearrangement of equation (4.32) followed by substitution into equation (4.31) results in an expression for cation mobility in free solution as shown in equation (4.33).

$$u_+ = \frac{t_+ \kappa}{FC} \tag{4.33}$$

Equation (4.34) shows anion mobility in free solution and is derived from equation (4.32).

$$u_- = \frac{u_+ (1 - t_+)}{t_+} \tag{4.34}$$

Figure (4.20) shows the mobilities of $K^+$ and $OH^-$ in free solution vs. KOH concentration. This figure forms the basis for a comparison between mobilities in free solution and the membrane phase. Both cation and anion mobilities decrease with an increase in external electrolyte concentration due to the increasing viscosity of the electrolyte. In addition to this viscous effect two electrical effects must be considered. The electrophoretic effect arises in the following way. When an ion moves through a viscous medium it tends to drag along with it the solution in its vicinity. The central ion experiences a viscous drag as it moves through the solution and this determines its drift velocity and hence its conductivity. Ions surrounding the central ion therefore have to move not through a stationary medium but with or against the stream depending on whether they are moving in the same direction as the central ion or in the opposite direction. The effect is concentration dependent falling to zero at infinite dilution.

Ions in solution are surrounded by an ionic atmosphere of opposite charge. The influence of an electric field changes the position of the central ion. The ionic atmosphere, however has a certain inertia and cannot instantaneously readjust itself to the new position of the central ion. Thus around a moving ion the ionic atmosphere becomes asymmetric. Behind the ion there is a net accumulation of opposite charge which exerts an electrostatic drag, decreasing the ionic velocity in the field direction. The effect which will obviously be greater at higher ionic concentration is called the asymmetric or relaxation effect because the formation and decay of the atmosphere is a kind of relaxation into an equilibrium distribution of the ions.

The mobilities of the potassium and hydroxyl ions within Cellophane and Permion have been determined without correction for tortuosity using equations (4.11 and 4.12) and are given in tables (4.4 and 4.5). With Cellophane a comparison of table (4.4) with figure (4.20) shows, if there is no correction for tortuosity at all concentrations both cation and anion mobilities are less than the free solution situation. Comparison of table (4.5) with figure (4.20) shows that the same is true for Permion except for the mobility of the anion at low external electrolyte concentrations where the internal anion concentration is low and consequently difficult to assess accurately. The conclusion must be that correction for tortuosity is required.

Figure 4.20 Variation of ionic mobilities in free solution with KOH concentration at 25°C.

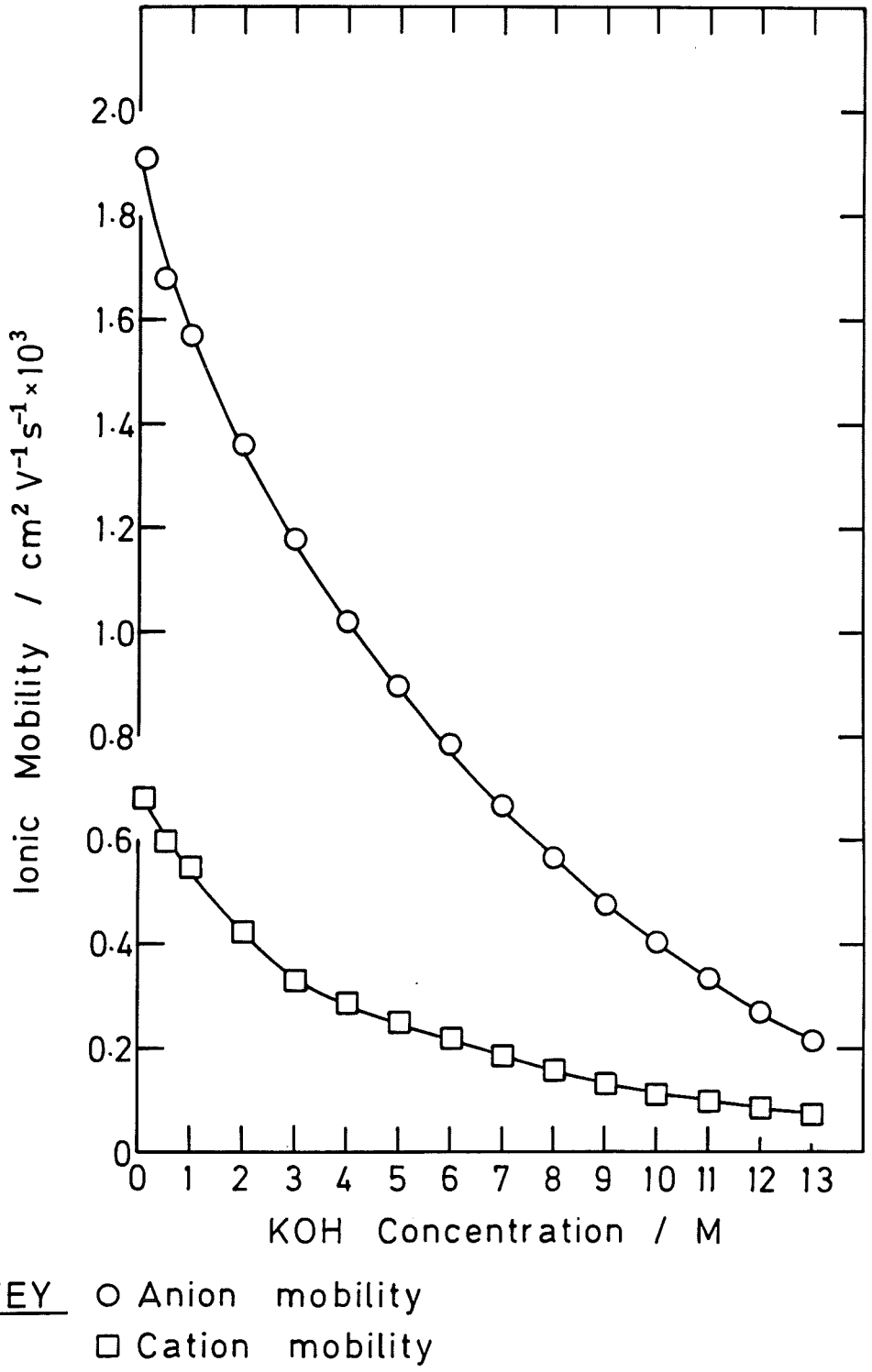

Table 4.4 Ionic mobilities in Cellophane at 25°C without correction for tortuosity.

| External [KOH] M | Cation mobility $cm^2V^{-1}s^{-1} \times 10^3$ | Anion mobility $cm^2V^{-1}s^{-1} \times 10^3$ |
|---|---|---|
| 1.021 | 0.181 | 0.722 |
| 2.066 | 0.138 | 0.483 |
| 3.080 | 0.156 | 0.484 |
| 4.100 | 0.156 | 0.423 |
| 5.160 | 0.168 | 0.411 |
| 6.150 | 0.151 | 0.366 |
| 7.187 | 0.0941 | 0.258 |
| 8.747 | 0.0583 | 0.171 |
| 10.22 | 0.0401 | 0.118 |
| 12.30 | 0.0365 | 0.104 |

Table 4.5 Ionic mobilities in Permion at 25°C without correction for tortuosity.

| External [KOH] M | Cation mobility $cm^2V^{-1}s^{-1} \times 10^3$ | Anion mobility $cm^2V^{-1}s^{-1} \times 10^3$ |
|---|---|---|
| 0.01036 | 0.0554 | |
| 0.1036 | 0.0832 | |
| 0.5110 | 0.166 | 2.75 |
| 1.021 | 0.186 | 1.59 |
| 2.050 | 0.191 | 0.999 |
| 3.587 | 0.144 | 0.353 |
| 5.127 | 0.111 | 0.220 |
| 7.185 | 0.0633 | 0.122 |
| 8.200 | 0.0525 | 0.102 |
| 10.20 | 0.0328 | 0.0765 |
| 12.27 | 0.0194 | 0.0668 |

One method of comparing cation and anion mobilities with values obtained in free solution is to look at the ratio of the cation with respect to the anion as a function of concentration as shown in figure (4.21). An advantage of this method is its independence upon the expressions for tortuosity. In free solution the ratio $u_+/u_-$ is independent of concentration in between 3 and 10M KOH.

For both Cellophane and Permion the $u_+/u_-$ ratio at low external electrolyte concentrations is lower than in free solution. This could be due to a lower than expected value for $u_+$, a higher than expected value for $u_-$ or both. Low $u_+/u_-$ ratios have been reported in the literature. Schlögl [110] measured the self-diffusion coefficients of $Na^+$ and $Br^-$ in a phenol-sulphonic acid-formaldehyde membrane. The $u_+/u_-$ ratio was very small at low external concentrations of NaBr but increased with increasing electrolyte concentration. Meares [111] measured self-diffusion coefficients of $Na^+$ and $Cl^-$ in a phenol-sulphonic acid cation-exchange membrane. The coefficient of the co-ion was close to free solution values (after correction for tortuosity effects), whilst this was not so for the counter-ion. The self-diffusion coefficient of the $Na^+$ was very low in 0.01M NaCl and increased at higher external electrolyte concentrations. Jakubovic et al [112 and 113] proposed that in highly swollen gels there is little overlap of potential fields derived from fixed charges. A potential barrier is created which impedes the movement of counter-ions from one region of fixed charge to another, hence low values of $u_+$ are obtained. Schlögl [110] reports that the presence of co-ions will tend to eliminate the effect by concentrating in regions remote from the fixed charges, hence reducing the potential barrier. Helfferich [114] attributed the increase to an increase in the number of mobile counter ions in the membrane. Jenkins et al [92] considered the counter-ions to be of two types with a dynamic interchange between them : these were exchange counter-ions which balanced the charge on the fixed anions and non-exchange counter-ions balancing the mobile anions. Exchange counter-ions were considered to be strongly attracted by, and therefore tended to be localised in the vicinity of the fixed charge groups [115 and 116]. This coulombic attraction retarded the counter-ions reducing their mobility. Obviously co-ions were not impeded. Jenkins et al [95] suggested the low $u_+/u_-$ ratio at low external concentrations was due to retardation of exchange $K^+$ due to coulombic interaction with the fixed charges.

Figure 4.21 Ratio of ionic mobilities in free solution, Cellophane and Permion vs. KOH concentration at 25°C.

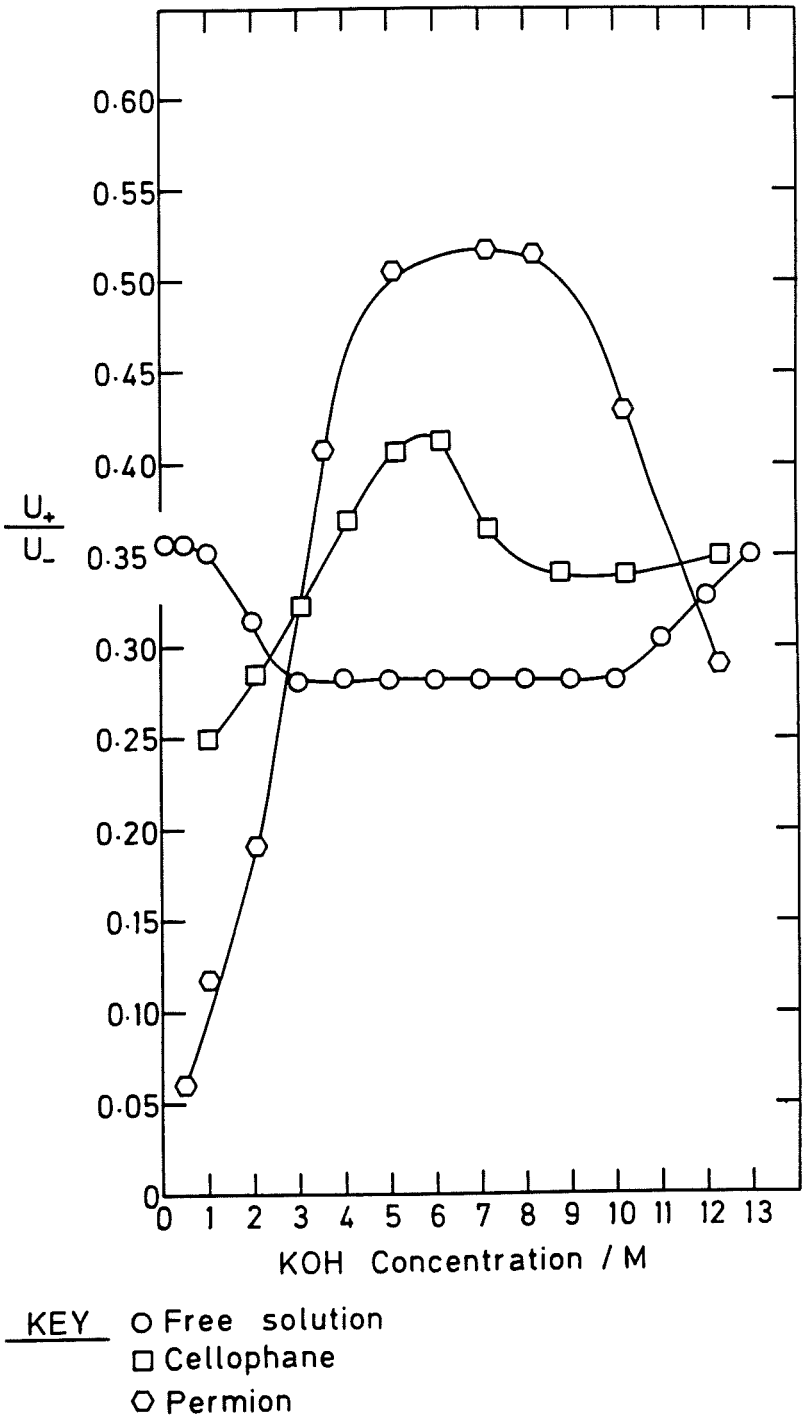

At around 3M KOH in figure (4.21) the $u_+/u_-$ ratio for both membranes rises above the free solution value. Under a potential gradient the greater number of counter-ions transfer more momentum than co-ions to interstitial water. This process as discussed in chapter 3 is electroconvection. Electroconvection results in an increased mobility of counter-ions and a decreased mobility of co-ions relative to mobilities observed in its absence i.e. in free solution; hence the increase in the $u_+/u_-$ ratio that was found above 3M KOH. Ferguson et al [117] reported an approximate 100% increase for $Na^+$ counter-ions with the polyethylene/polystyrene sulphonate graft membranes AMF C60N and C60E. An enhanced mobility ratio was also reported by Jenkins et al [92] for the Cellophane/KOH system. A ratio of 10-20% of the free solution value was found at infinite dilution, this rose to 20-30% above the free solution value up until 8M KOH.

At 8.5M the $u_+/u_-$ ratio for Permion started to fall. Values for Cellophane also peaked and showed a decrease at higher concentrations. Yeager et al [118] and Mauritz et al [119] suggested that a decrease observed in their systems was due to enhanced anion mobility in an environment of decreasing water content i.e. in the stronger electrolyte solution.

Atieh and Chen [70] wrongly made the assumption that the mobility ratio is independent of concentration in their Permion/KOH system. They quote a mobility ratio of 0.59 for the membrane Permion 2291 40/100 and 0.40 for Permion 2291 40/20 in 10M KOH. This may be compared with the value of 0.43 at a concentration of 10.2M KOH reported here for Permion 2291 40/30. Hence the order of the three ratios is consistent with the resistances of the three grades of Permion 2291.

The mobilities of the potassium and hydroxyl ions within Cellophane and Permion have been determined from equations (4.14 and 4.15) using the expressions for tortuosity given in equations (4.19 and 4.21) and are shown in tables (4.6 and 4.7).

The variation of cation mobility vs. ionic strength of the internal electrolyte solution for Cellophane is presented in figure (4.22). Ionic strength, I ($molekg^{-1}$) was chosen for the abscissa to take into account only the mobile ion concentration within the membrane and was calculated using equation (4.35)

$$I = \tfrac{1}{2} \sum m_i z_i^2 \qquad (4.35)$$

Table 4.6 Ionic mobilities in Cellophane at 25°C with correction for tortuosity.

| External [KOH] M | Tortuosity Factor | | | |
|---|---|---|---|---|
| | $\frac{1}{(1 - V_p)}$ | | $\frac{(1 + V_p)}{(1 - V_p)}$ | |
| | Cation mobility $cm^2V^{-1}s^{-1} \times 10^3$ | Anion mobility $cm^2V^{-1}s^{-1} \times 10^3$ | Cation mobility $cm^2V^{-1}s^{-1} \times 10^3$ | Anion mobility $cm^2V^{-1}s^{-1} \times 10^3$ |
| 1.021 | 0.588 | 2.35 | 1.23 | 4.92 |
| 2.066 | 0.404 | 1.41 | 0.808 | 2.83 |
| 3.080 | 0.409 | 1.27 | 0.780 | 2.42 |
| 4.100 | 0.339 | 0.918 | 0.592 | 1.60 |
| 5.160 | 0.300 | 0.737 | 0.471 | 1.16 |
| 6.150 | 0.270 | 0.654 | 0.423 | 1.02 |
| 7.187 | 0.195 | 0.535 | 0.333 | 0.912 |
| 8.747 | 0.135 | 0.397 | 0.245 | 0.717 |
| 10.22 | 0.0924 | 0.272 | 0.166 | 0.488 |
| 12.30 | 0.0782 | 0.224 | 0.136 | 0.388 |

Table 4.7 Ionic mobilities in Permion at 25°C with correction for tortuosity.

| External [KOH] M | Tortuosity Factor | | | |
|---|---|---|---|---|
| | $\frac{1}{(1 - V_p)}$ | | $\frac{(1 + V_p)}{(1 - V_p)}$ | |
| | Cation mobility $cm^2V^{-1}s^{-1} \times 10^3$ | Anion mobility $cm^2V^{-1}s^{-1} \times 10^3$ | Cation mobility $cm^2V^{-1}s^{-1} \times 10^3$ | Anion mobility $cm^2V^{-1}s^{-1} \times 10^3$ |
| 0.01036 | 0.503 | | 1.40 | |
| 0.1036 | 0.764 | | 2.13 | |
| 0.5110 | 1.58 | 26.2 | 4.43 | 73.7 |
| 1.021 | 1.86 | 15.9 | 5.28 | 45.0 |
| 2.050 | 2.12 | 11.1 | 6.13 | 32.1 |
| 3.587 | 1.89 | 4.64 | 5.61 | 13.8 |
| 5.127 | 1.75 | 3.46 | 5.36 | 10.6 |
| 7.185 | 1.31 | 2.53 | 4.15 | 8.01 |
| 8.200 | 1.26 | 2.45 | 4.07 | 7.90 |
| 10.20 | 1.11 | 2.56 | 3.71 | 8.64 |
| 12.27 | 0.990 | 3.41 | 3.43 | 11.8 |

Figure 4.22 Cation mobility through Cellophane vs. ionic strength of the internal electrolyte at 25°C.

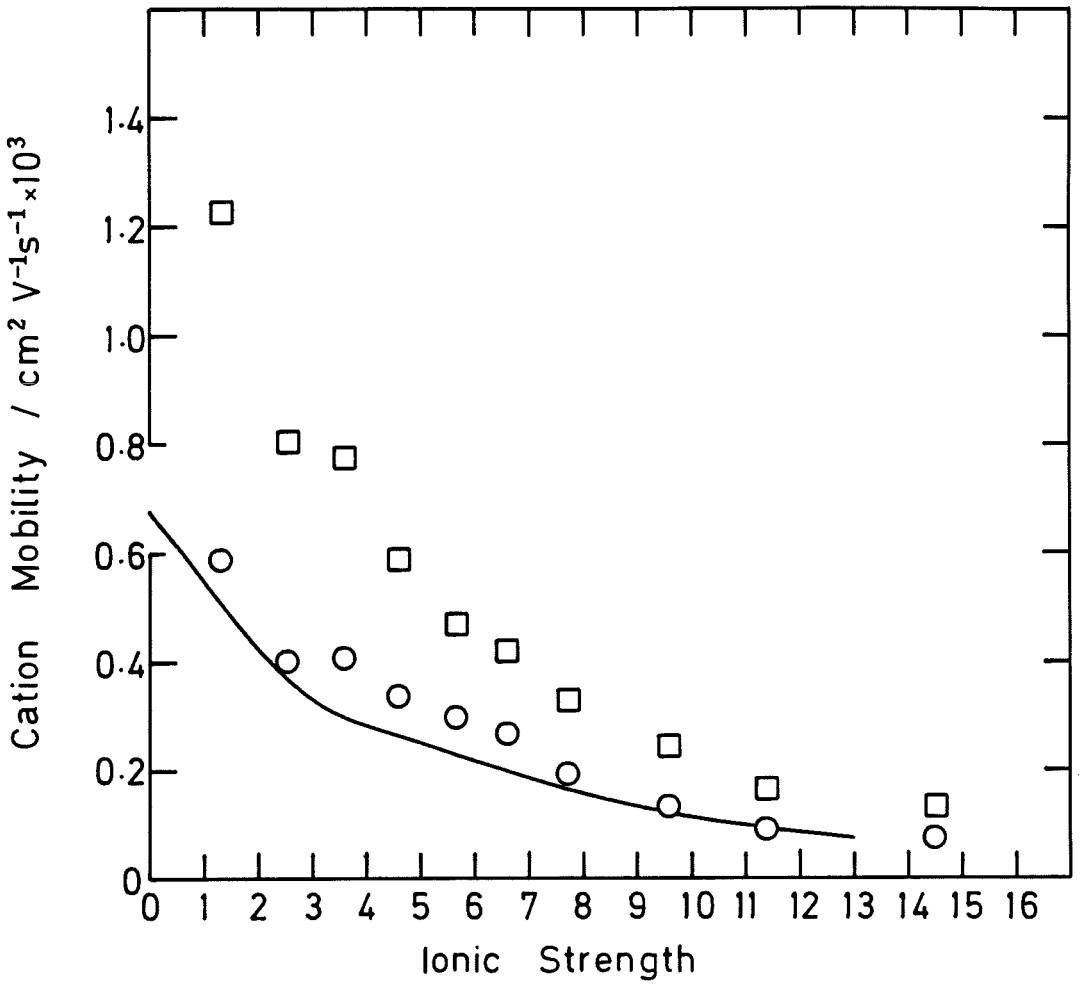


KEY solid line, free solution

○ mobility calculated using $\theta = \frac{1}{(1-V_p)}$

□ mobility calculated using $\theta = \frac{(1+V_p)}{(1-V_p)}$

where m ($molekg^{-1}$) was the molality and z was the charge of species i. The graph displays three set of data, cation mobilities in free solution and two sets of cation mobilities in the membrane taking into account the expressions for tortuosity given in equations (4.19 and 4.21). An analogous treatment for anion mobilities through Cellophane is shown in figure (4.23). Both cation and anion mobilities in Cellophane decrease with increasing ionic strength due to an increase in the viscosity of the electrolyte [120].

Figure (4.22) shows that cation mobilities determined using the expression for tortuosity given in equation (4.21) [96] are in reasonable agreement with cation mobilities in free solution. The Mackie and Meares [94] expression appears to over-estimate the tortuosity. With the cellulose membrane it has previously been shown (chapter 2) that swelling was greatest at an external electrolyte concentration of around 5.7M. In figure (4.22) cation mobilities in the cellulose membrane deviate a little from the model in this region. As mentioned earlier, electroconvection may enhance cation mobilities within a membrane and the effect would be expected to be greatest in this region where swelling is at a maximum.

Anion mobilities for Cellophane, figure (4.23), fall below free solution values when calculated using the Lee et al [96] expression for tortuosity presumably due to electroconvection. Anion mobilities calculated using the Mackie and Meares [94] expression fall above the model suggesting that equation (4.19) over-estimates the tortuosity of Cellophane.

The expression for tortuosity derived by Maskell [97] given in equation (4.27) was not used to calculate ionic mobilities through Cellophane since figures (4.22 and 4.23) show that equation (4.21) adequately described the tortuosity of swollen cellulose.

Table (4.7) shows cation mobilities in Permion calculated from equations (4.14 and 4.15) using the expressions for tortuosity given in equations (4.19 and 4.21). When equation (4.19) was used the cation mobilities were large compared with free solution and the equation clearly over-estimates the tortuosity. Equation (4.21) also over-estimated the tortuosity but to a lesser extent. Figure (4.24) shows cation mobility vs. ionic strength of the internal electrolyte solution for Permion. The graph shows three sets of data, cation mobilities in free solution, cation mobilities calculated using equation (4.21) and cation mobilities calculated using a tortuosity of one, as shown in table (4.5).

Figure 4.23 Anion mobility through Cellophane vs. ionic strength of the internal electrolyte at 25°C.

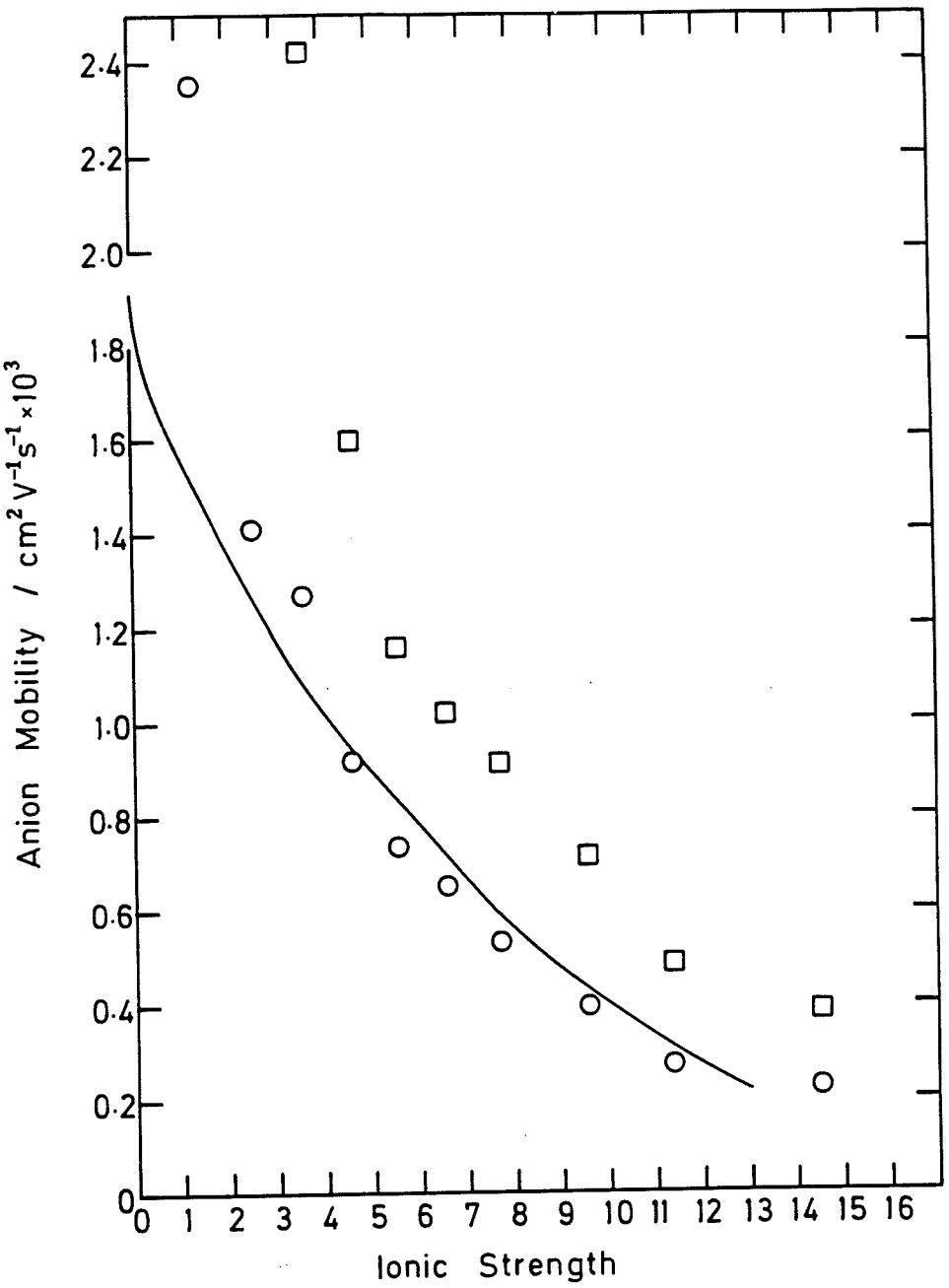


KEY solid line, free solution

○ mobility calculated using $\theta = \frac{1}{(1-V_p)}$

□ mobility calculated using $\theta = \frac{(1+V_p)}{(1-V_p)}$

Figure 4.24 Cation mobility through Permion vs. ionic strength of the internal electrolyte at 25°C.

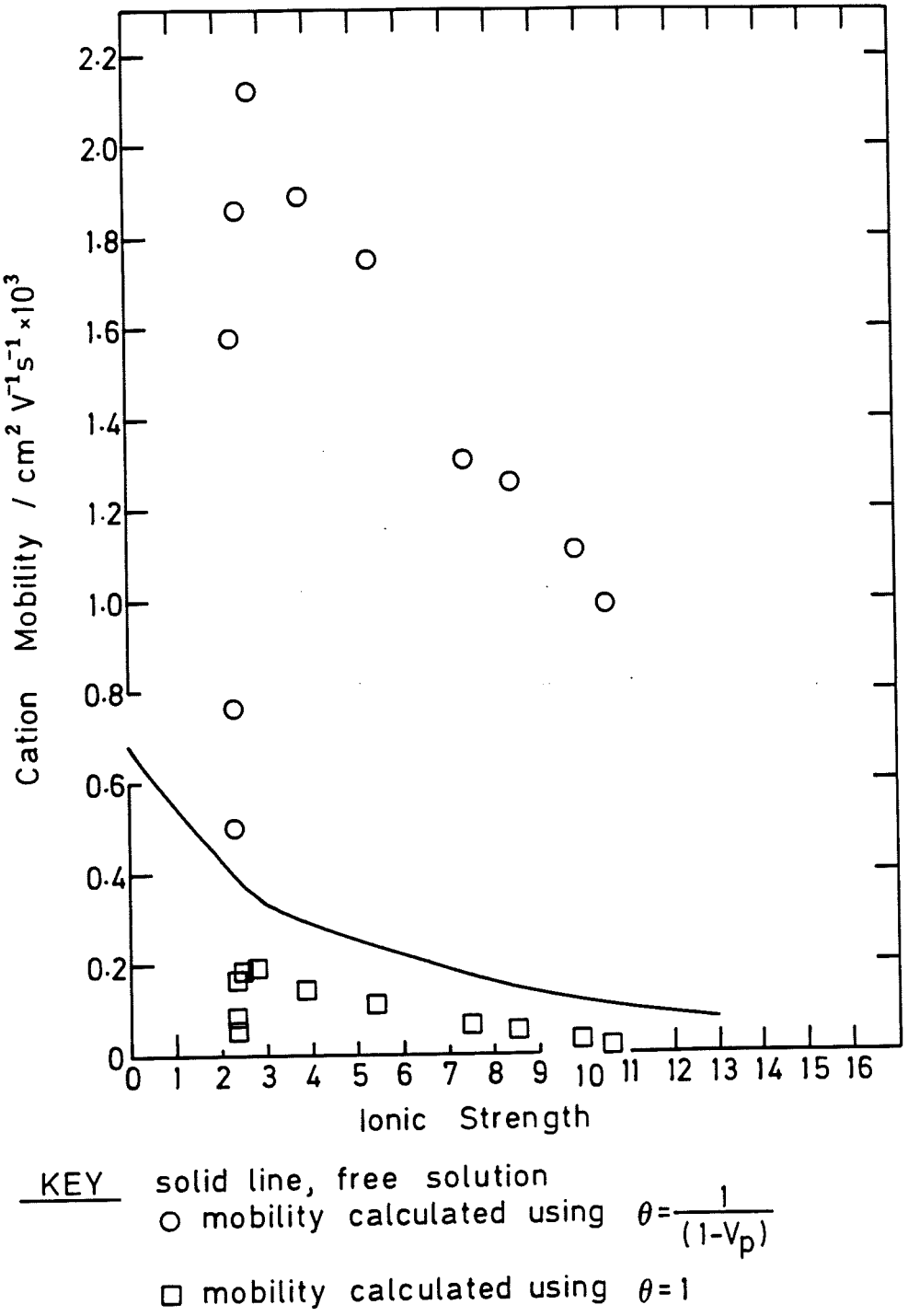

A tortuosity of unity means that the pores run straight through the membrane perpendicular to the plane of the membrane film. Figure (4.24) shows that neither the tortuosity given in equation (4.21) nor a tortuosity of one give cation mobilities close to free solution values. The correct expression for tortuosity must be somewhere in between. Nevertheless the results are still very interesting. Figure (2.7), the ionic content of Permion vs. external electrolyte concentration, shows that the co-ion concentrations were very low until the external concentration exceeded 1M KOH. This in turn, figure (4.24), kept the cation mobility low until there were sufficient hydroxyl ions in the membrane. For Permion, a low value of $u_+/u_-$ at low external electrolyte concentrations is observed as shown in figure (4.21). Both estimates of tortuosity show that over a small range of ionic strength the mobility increased rapidly. At higher values of ionic strength when the co-ion concentration becomes significant cation mobilities decrease due to an increase in the viscosity of the electrolyte.

The anion mobilities in Permion given in table (4.7) also show that equations (4.19 and 4.21) over-estimate the tortuosity. Figure (4.25) shows the anion mobility in free solution together with the anion mobility calculated using a tortuosity of unity and confirms that the tortuosity in Permion is inbetween the expression given in equation (4.21) and a tortuosity of one. It must again be noted that for Permion at low ionic strength anion mobilities are inaccurate, rising above free solution values in figure (4.25), due to the difficulty of measuring the anion concentration.

Figure 4.25 Anion mobility through Permion vs. ionic strength of the internal electrolyte at 25°C.

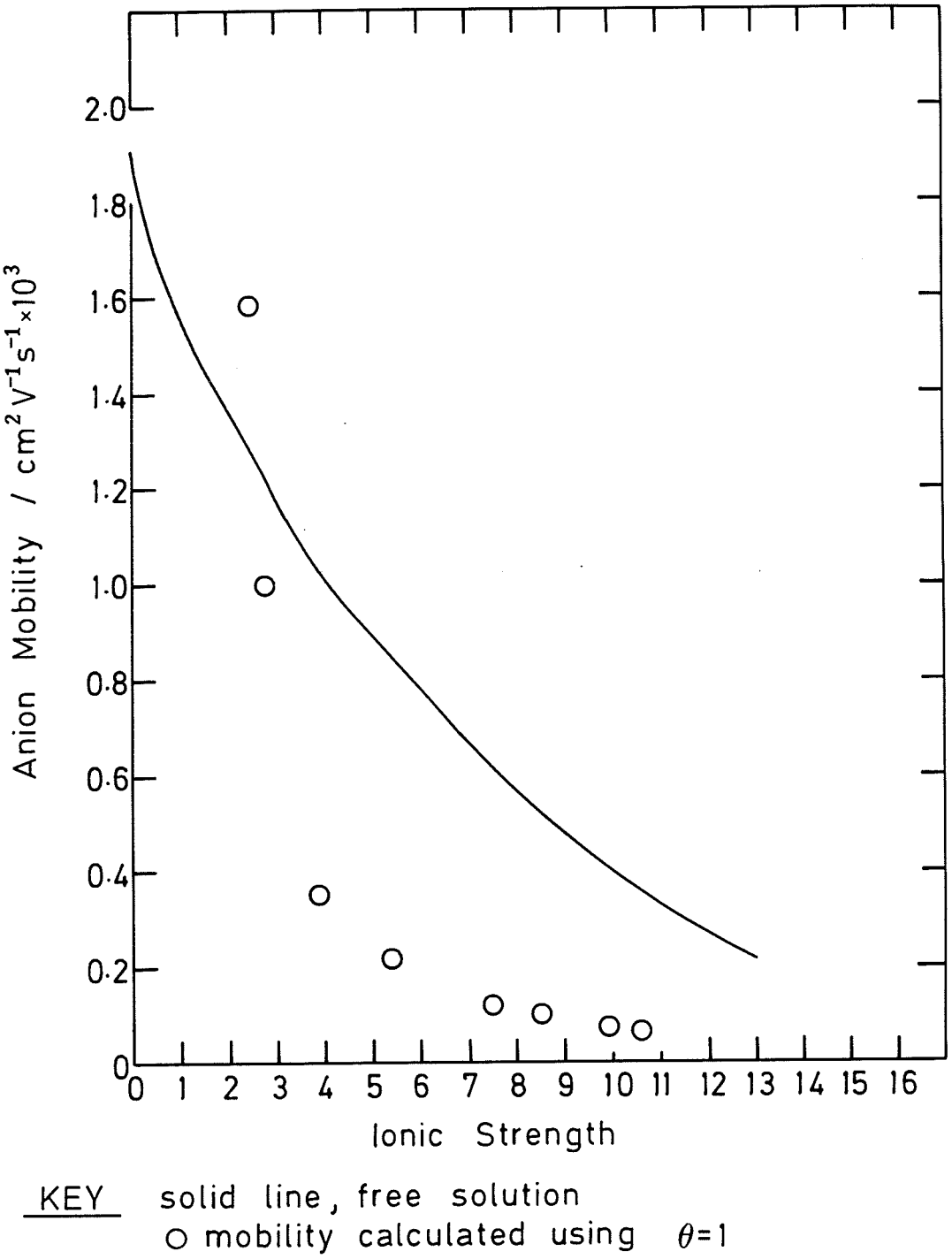

## 4.4 Conclusion

The dependence of KOH conductivity on concentration and mobility was confirmed. From figure (4.16) up to around 6M the influence of concentration was dominant and an increase in conductivity was observed with an increase in concentration. After 6M the decrease in mobility with concentration outweighed the further increase in concentration and the conductivity fell.

For Cellophane and Permion the ratio $u_+/u_-$ at low external electrolyte concentrations was lower than in free solution because of a lower than expected value for $u^+$ due to retardation of exchange $K^+$ due to coulombic interaction with the fixed charges. With Permion the low value of the ratio $u_+/u_-$ was also due to a higher than expected value for $u_-$ arising from the difficulty in assessing accurately the internal anion content of Permion. Above around 3M KOH the $u_+/u_-$ ratio for both membranes rose above free solution values due to electroconvection which increased the mobility of the counter-ions and decreased the mobility of the co-ions. Above around 8.5M KOH the $u_+/u_-$ ratio for both membranes decreased due to enhanced anion mobility in an environment of decreasing water content.

A comparison between the mobilities of $K^+$ and $OH^-$ in free solution with the mobilities within Cellophane and Permion without correction for tortuosity showed that a correction for tortuosity was required. Of the two models investigated, the model for tortuosity given in equation (4.21) yielded ionic mobilities within Cellophane which were closest to mobilities in free solution. This model for tortuosity therefore accurately described the blocking effects of Cellophane. Although for Permion a model for tortuosity which accurately described the blocking effects was not obtained, it was apparent that the correct tortuosity factor was between a tortuosity of one (i.e. for a membrane with straight through pores perpendicular to the plane of the membrane) and the tortuosity given in equation (4.21).

# CHAPTER 5

# MASS TRANSPORT THROUGH ASSEMBLIES OF CELLOPHANE AND PERMION

## 5.1 Introduction

### 5.1.1 General

A schematic diagram of an assembly of two membrane types and their relation to the electrodes and the electrolyte is shown in figure (5.1).

Figure 5.1 An assembly of two membrane types

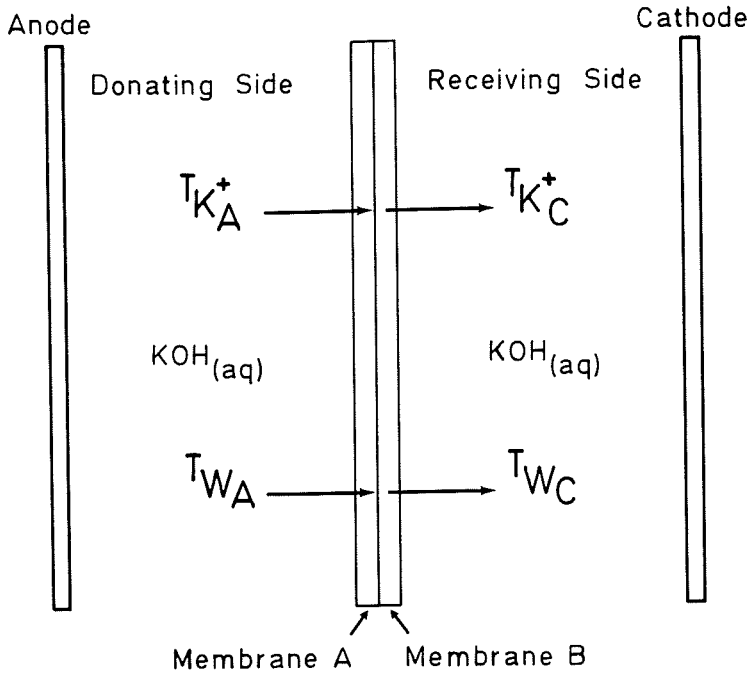


If membranes A and B are Cellophane and Permion the question then arises as to how the transport properties are affected by whether Cellophane or Permion is on the receiving side ?

### 5.1.2 The advantages of laminating Permion 2291 to Cellophane

Laminates of Permion and Cellophane were developed to extend the shelf and cycle life of primary and secondary batteries. The Permion 2000 series was developed to meet a wide range of drain and temperature requirements for AgO/Zn, $Ag_2O$/Zn, HgO/Zn, Ag/Zn, Hg/Zn, Ni/Zn, and vented Ni/Cd cells.

Laminates benefit from a synergistic effect to produce a product superior than either of the membranes alone. Permion is stable to chemical oxidation and retards the degradation of Cellophane on the anode side [50]. The life of the Cellophane is therefore extended. Cellophane acts as a sacrificial barrier to silver and mercury ion diffusion and the laminate is therefore able to retard larger quantities of these ions than the single membranes [50]. A further advantage of lamination is improved handling properties. The membranes are die cut for production line use, Permion on its own has a tendency to curl around the die and lamination with Cellophane reduces this [121].

Duracell Batteries, partial sponsors of this work mainly use Permion 2192 40/30, a triple laminate with one layer of Permion 2291 40/30 sandwiched between two layers of Cellophane as shown in figure (5.2).

Figure 5.2 The triple laminate, Permion 2192

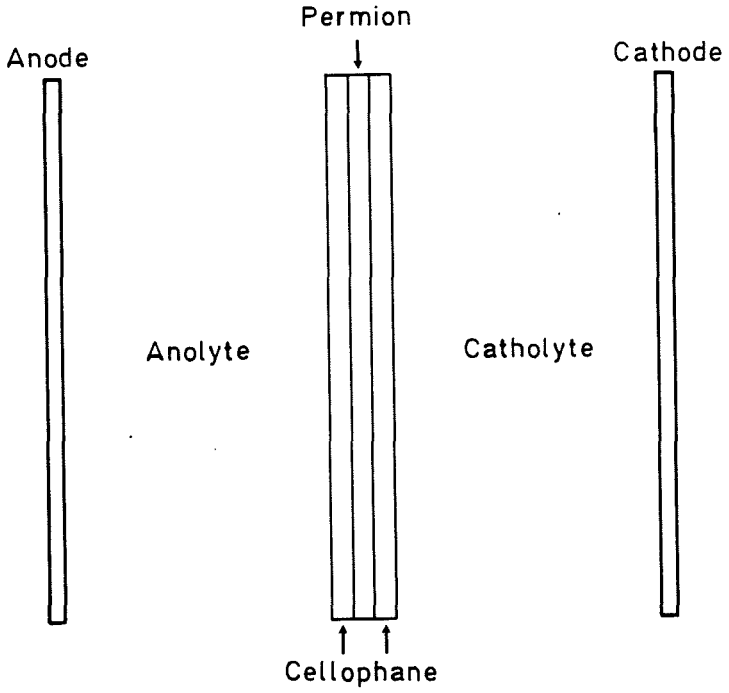


This type of lamination has a Cellophane/Permion interface and a Permion/Cellophane interface in the one assembly as described in section (1.5). The transport properties of each interface is discussed in section (5.3).

## 5.2 Experimental

### 5.2.1 Procedure for combinations

The experimental technique described in section (3.2), on the measurement of transport numbers through single membrane types was used. All the work on combinations of membranes was carried out at a concentration of 7.2 ± 0.01M KOH, a concentration chosen because of its battery interest. Stacks of individual membrane types were combined and positioned in the cell with either Cellophane on the receiving side, i.e. adjacent to the cathode, or with Permion on the receiving side.

### 5.2.2 Cellophane on the receiving side

Preliminary experiments used additions, made to maintain concentrations constant and equal on either side of the combination, based on transport numbers obtained for Cellophane at this concentration. It became necessary to refine the approximations and to use additional solution of the concentration being studied to maintain an equal volume of solution on either side of the membrane.

In all cases 7,200 Coulombs of charge were passed, with the majority of runs lasting for two hours at a current of 1 Amp. A few experiments were carried out for one hour at a current of 2 Amps.

The following combinations were studied :- 2, 5 and 10 layers of each membrane, 8 layers of Permion with 2 layers of Cellophane, 2 layers of Permion with 8 layers of Cellophane and 1 layer of Permion with 9 layers of Cellophane.

In some experiments the electrolyte solution found at the Permion/Cellophane interface at the end of a run was analysed. The electrolyte solution from each compartment was removed as normal and the cell turned on its side as if to be opened for the mopping procedure. Having removed the uppermost steel plate and water jacket, the anode and anolyte compartment were lifted clear of the cell revealing the horizontal membrane combination.

A hypodermic needle fit into a syringe was slipped between the different membranes, and the interface solution removed. This was then weighed, analysed for KOH and expressed as a molality.

Due to the delicacy of the procedure, emphasis had to be on either accurately removing the interface solution or alternatively ensuring correct mopping of the compartment and more importantly the membrane surface. Obviously, it was important that the external electrolyte did not contaminate the interface solution and vice-versa.

As the membranes were bowed and thus in an extended condition at the finish of runs, a series of experiments was conducted to ascertain whether the distortion affected the transport properties. Transport numbers were obtained through two layers of Cellophane at 7.2M KOH. The same two layers were then incorporated into a membrane assembly, with two layers of Permion and transport numbers determined. Finally the Cellophane was used for a third time in an identical experiment to the first. A parallel trio of experiments investigated any effect with respect to the Permion membrane.

### 5.2.3 Permion on the receiving side

Preliminary experiments on these combinations used additions based on transport numbers obtained for Permion at this concentration. Transport numbers from these early results were then used to calculate the necessary additions. The height correction procedure described in section (3.2.5) to ensure equal volumes of electrolyte on either side of the assembly was also used.

For transport number determinations the amount of charge passed varied from 1,800 to 14,400 Coulombs. For these the addition solutions calculated for 7,200 Coulomb runs were scaled up or down accordingly.

Additions were made at times given by equation (5.1) [80]

$$\left[\frac{(2r - 1)Z}{2n}\right]^n \qquad (5.1)$$

where n is the number of additions, Z is the length of the run in minutes and r = $r^{th}$ addition. For example, six additions during a one hour run would be made after 5, 15, 25, 35, 45 and 55 minutes. Similar combinations as described in section (5.2.2) were studied, but positioned in the cell with Permion on the receiving side.

The effect of altering the current density whilst keeping the charge passed constant was investigated by running the experiment for 1 hour at 2A, 2 hours at 1A and 4 hours at 0.5A with either 2 or 5 layers of each membrane.

In some runs the potential across the cell, and hence the resistance, was monitored with time. A Linises chart recorder was connected across the cell and switched on at the same time as the current was supplied through the circuit. The time was noted when the resistance of the cell increased rapidly. Runs were made for 2, 5 and 10 layers of each membrane over a range of currents from 3 to 10 Amps.

In order to assess whether concentration gradients existed in the membrane assembly the potassium content of each membrane layer was determined at the end of some transport number runs. Differences in concentration would tend to equilibrate as soon as the current was switched off, to minimise this it was important to isolate the individual layers as quickly as possible. A concertina arrangement of the membrane was developed.

Strips of membrane, 8cm. by 40cm., were cut from along each roll and soaked overnight in the electrolyte. Each strip was folded like a concertina until five layers thick and cut to a similar shape as the cell, ensuring minimal membrane at the folds. The concertina was pressed slightly by a small roller to remove excess electrolyte and air bubbles. A minimal length of membrane at the fold was desirable since electrolyte had a tendency to collect in this region.

The two concertinas were placed one on top of the other and pressed together by the roller. The cell was assembled and the experiment was conducted as normal. At the end of the run the electrolyte was removed as quickly as possible but with care to ensure maximum recovery. The concertina was mopped on either face and then separated at the Permion/Cellophane interface. With each concertina individual layers were peeled apart, either starting with the layer which had been adjacent to the electrolyte solution or alternatively with the layer which had been adjacent to the Permion/Cellophane interface.

The potassium was extracted from the membrane and analysed by Atomic Absorption techniques using the method described in section (2.2.4). A more relevant determination of the $K^+$ content was made by cutting out the area of membrane in direct contact with the electrolyte solution, and analysing this, instead of analyzing the whole

membrane layer.

The water content, which when combined with the $K^+$ content yielded the KOH concentration in each layer was obtained by weighing each cut out area of membrane before and after the analysis. The membrane was dried after determining the $K^+$ and water contents so that values could be quoted per gram of dry membrane.

## 5.3 Results and discussion

### 5.3.1 General

Table (5.1) compares transport numbers as measured by analysis of the anolyte or the catholyte when only one type of membrane was used.

Table 5.1 Comparison of anolyte and catholyte transport numbers for assemblies of one type of membrane

| Membrane Type | [KOH] M | $T_K(A)$ | $T_K(C)$ | $T_W(A)$ | $T_W(C)$ |
|---|---|---|---|---|---|
| Cellophane | 5.10 | 0.34 | 0.34 | 0.98 | 0.91 |
| Cellophane | 6.21 | 0.34 | 0.32 | 0.74 | 0.66 |
| Cellophane | 7.20 | 0.32 | 0.32 | 0.69 | 0.66 |
| Cellophane | 8.88 | 0.32 | 0.30 | 0.55 | 0.58 |
| Permion | 5.69 | 0.57 | 0.57 | 1.50 | 1.44 |
| Permion | 6.67 | 0.54 | 0.53 | 1.27 | 1.24 |
| Permion | 7.20 | 0.51 | 0.51 | 1.22 | 1.18 |
| Permion | 8.63 | 0.47 | 0.47 | 0.95 | 0.95 |

There is good agreement between each pair of $K^+$ transport numbers and each pair of water transference numbers. From this it can be concluded that there is no significant change in the content of ions and water in the membrane assembly. In other words identical amounts of ions both enter and leave the assembly and similarly for the water.

Table (5.2) shows that this agreement was not obtained when assemblies of two different types of membrane were used. The notation used in the first column, e.g. 10P:10C signifies that 10 layers of each membrane were used in the assembly and that Cellophane was adjacent to the catholyte. Conversely, 10C:10P indicates that Permion was adjacent to the catholyte.

Table 5.2 Comparison of anolyte and catholyte transport numbers for assemblies of Cellophane and Permion in 7.2 molar KOH

| Assembly | TK(A) | TK(C) | TW(A) | TW(C) |
|---|---|---|---|---|
| 10P:10C | 0.50 | 0.37 | 1.37 | 0.49 |
| 10P:10C | 0.49 | 0.38 | 1.30 | 0.49 |
| 5P:5C | 0.49 | 0.36 | 1.32 | 0.42 |
| 5P:5C | 0.48 | 0.37 | 1.28 | 0.47 |
| 10C:10P | 0.38 | 0.45 | 0.75 | 1.23 |
| 5C:5P | 0.45 | 0.49 | 1.06 | 1.26 |
| 5C:5P | 0.42 | 0.46 | 0.97 | 1.21 |

Two points are clear from these results :-

(i) for membrane combinations, $t_A \neq t_C$ in contrast with the single membrane situation.

(ii) in general the transport numbers differ from the single membrane situation, at the chosen external electrolyte concentration of 7.2M KOH.

Tables (5.1 and 5.2) are abridged versions of tables (3.1 and 3.2) for single membranes and tables (5.3 and 5.5) for membrane combinations respectively.

Table (5.2) shows when Cellophane was the membrane type closest to the cathode, the transport numbers for both $K^+$ and water were smaller from the membrane assembly to the catholyte than from the anolyte to the membrane assembly. This can only mean that KOH and water were collecting in the membrane assembly. Reference to table (5.1) shows that this behaviour is predictable from the transport numbers of assemblies containing only one type of membrane.

Table (5.2) also shows that when Permion was the membrane type closest to the cathode, the transport numbers for both $K^+$ and water were larger from the membrane assembly to the catholyte than from the anolyte to the membrane assembly. This must mean that KOH and water were being withdrawn from the membrane assembly during the transference experiments. Again this is in accordance with expectations derived from the data given in table (5.1) for single membrane assemblies.

### 5.3.2 Permion on the receiving side.

The results from all experiments with Permion on the receiving side are presented in table (5.3). From the work of Kressman et al [65] a prediction of the behaviour of the assembly would be that transport numbers through the assembly would depend on the receiving side situation. This means transport numbers would be similar to those observed for Permion at this concentration, Permion would thus modify transport through Cellophane to that expected for Permion. Table (5.2) shows this was not the case. The work on transport numbers through single membranes, reported in Table (5.1), showed that $T_{K^+Permion} > T_{K^+Cellophane}$ and $T_{W\ Permion} > T_{W\ Cellophane}$ for a given external electrolyte concentration. In other words the mass transport of potassium hydroxide solutions was greater through Permion than through Cellophane. Application of Kressman's theory [65] would suggest that the transport through Cellophane would rise to values equivalent to Permion on its own. The following sections investigate the behaviour of the membrane assembly where Permion is on the receiving side.

Table 5.3(a) Potassium ion transport numbers with Permion on the receiving side.

| Run | Duration (Hours) | Current (Amps) | Assembly | $T_K(A)$ | $T_K(C)$ |
|---|---|---|---|---|---|
| 5.1 | 2 | 1 | 5C:5P | 0.453 | 0.489 |
| 5.3 | 2 | 1 | 5C:5P | 0.440 | 0.486 |
| 5.5 | 2 | 1 | 8C:2P | 0.386 | 0.422 |
| 5.7 | 2 | 1 | 8C:2P | 0.378 | 0.422 |
| 5.9 | 2 | 1 | 9C:1P | 0.334 | 0.358 |
| 5.11 | 2 | 1 | 2C:8P | 0.465 | 0.481 |
| 5.13 | 3 | 1 | 5C:5P | 0.462 | 0.469 |
| 5.14 | 1 | 1 | 5C:5P | 0.426 | 0.479 |
| 5.15 | 2 | 1 | 2C:2P | 0.471 | 0.458 |
| 5.16 | 1 | 1 | 2C:2P | 0.460 | 0.468 |
| 5.17 | 2 | 1 | 2C:2P | 0.451 | 0.460 |
| 5.18 | 2 | 1 | 5C:5P | 0.424 | 0.460 |
| 5.19 | 2.5 | 1 | 5C:5P | 0.422 | 0.449 |
| 5.20 | 0.5 | 1 | 5C:5P | 0.415 | 0.479 |
| 5.21 | 0.5 | 1 | 2C:2P | 0.430 | 0.475 |
| 5.22 | 1.5 | 1 | 5C:5P | 0.420 | 0.467 |
| 5.23 | 2 | 1 | 10C:10P | 0.378 | 0.451 |
| 5.24 | 1 | 1 | 10C:10P | 0.355 | 0.466 |
| 5.25 | 1.5 | 1 | 2C:2P | 0.444 | 0.455 |
| 5.26 | 4 | 1 | 5C:5P | 0.434 | 0.456 |
| 5.27 | 3 | 1 | 10C:10P | 0.383 | 0.450 |
| 5.28 | 1.25 | 1 | 2C:2P | 0.439 | 0.452 |
| 5.29 | 1 | 2 | 5C:5P | 0.444 | 0.480 |
| 5.30 | 4 | 0.5 | 5C:5P | 0.453 | 0.482 |
| 5.31 | 1 | 2 | 2C:2P | 0.444 | 0.446 |
| 5.32 | 4 | 0.5 | 2C:2P | 0.457 | 0.457 |
| 5.34 | 0.8 | 2.5 | 5C:5P | 0.432 | 0.432 |
| 5.35 | 0.833 | 2.4 | 5C:5P | 0.435 | 0.482 |
| 5.38 | 1 | 1 | 5C:5P | 0.430 | 0.481 |
| 5.45 | 1 | 2 | 5C:5P | 0.441 | 0.481 |
| 5.48 | 1 | 2 | 5C:5P | 0.435 | 0.482 |
| 5.49 | 1 | 2 | 5C:5P | 0.436 | 0.475 |

Table 5.3(b) Water transference numbers with Permion on the receiving side.

| Run | Duration (Hours) | Current (Amps) | Assembly | $T_w(A)$ | $T_w(C)$ |
|---|---|---|---|---|---|
| 5.1 | 2 | 1 | 5C:5P | 1.06 | 1.26 |
| 5.3 | 2 | 1 | 5C:5P | 1.03 | 1.26 |
| 5.5 | 2 | 1 | 8C:2P | 0.855 | 1.11 |
| 5.7 | 2 | 1 | 8C:2P | 0.899 | 1.11 |
| 5.9 | 2 | 1 | 9C:1P | 0.762 | 0.890 |
| 5.11 | 2 | 1 | 2C:8P | 1.06 | 1.19 |
| 5.13 | 3 | 1 | 5C:5P | 1.10 | 1.20 |
| 5.14 | 1 | 1 | 5C:5P | 0.908 | 1.30 |
| 5.15 | 2 | 1 | 2C:2P | 1.09 | 1.14 |
| 5.16 | 1 | 1 | 2C:2P | 1.07 | 1.19 |
| 5.17 | 2 | 1 | 2C:2P | 1.07 | 1.08 |
| 5.18 | 2 | 1 | 5C:5P | 0.971 | 1.21 |
| 5.19 | 2.5 | 1 | 5C:5P | 1.01 | 1.22 |
| 5.20 | 0.5 | 1 | 5C:5P | 0.959 | 1.25 |
| 5.21 | 0.5 | 1 | 2C:2P | 1.06 | 1.22 |
| 5.22 | 1.5 | 1 | 5C:5P | 0.970 | 1.27 |
| 5.23 | 2 | 1 | 10C:10P | 0.752 | 1.23 |
| 5.24 | 1 | 1 | 10C:10P | 0.546 | 1.31 |
| 5.25 | 1.5 | 1 | 2C:2P | 1.07 | 1.13 |
| 5.26 | 4 | 1 | 5C:5P | 1.03 | 1.18 |
| 5.27 | 3 | 1 | 10C:10P | 0.846 | 1.27 |
| 5.28 | 1.25 | 1 | 2C:2P | 1.08 | 1.17 |
| 5.29 | 1 | 2 | 5C:5P | 1.09 | 1.28 |
| 5.30 | 4 | 0.5 | 5C:5P | 1.00 | 1.27 |
| 5.31 | 1 | 2 | 2C:2P | 1.03 | 1.01 |
| 5.32 | 4 | 0.5 | 2C:2P | 1.05 | 1.04 |
| 5.34 | 0.8 | 2.5 | 5C:5P | 0.987 | 0.962 |
| 5.35 | 0.833 | 2.4 | 5C:5P | 1.05 | 1.33 |
| 5.38 | 1 | 1 | 5C:5P | 0.967 | 1.18 |
| 5.45 | 1 | 2 | 5C:5P | 1.12 | 1.24 |
| 5.48 | 1 | 2 | 5C:5P | 1.06 | 1.29 |
| 5.49 | 1 | 2 | 5C:5P | 1.11 | 1.28 |

### 5.3.3 Analysis of the $K^+$ and water contents of the individual membrane layers at the end of a transference experiment

An estimation of the practical concentration profile through a membrane stack after a run where concentrations at the interface deplete may be made by measuring the potassium content of each layer after a run. A plot of $K^+$ content versus membrane layer is shown in figure (5.3) and represents data for experiments (5.48, 5.49 and 5.50) where only the area of membrane adjacent to the electrolyte was analysed. In experiments (5.48 and 5.50) the outermost layer was the first to be separated from the assembly, whereas in experiment (5.49) the innermost layer was the first. The straight line drawn through the points places greater emphasis on the first layers to be separated because the final layers to be separated will be the ones most likely affected by diffusion. There is a decrease in $K^+$ as the interface is approached.

In experiment (5.50), by direct measurement of the amount of solution sorbed by each membrane it was possible to calculate the water content of the membrane assembly. The data which are presented in figures (5.4 and 5.5), show clearly the set-up of diffusion gradients and that the depletion occurred mainly in the Cellophane and to a greater extent in the layers closest to the interface with the Permion. Using the data from figures (5.4 and 5.5) the potassium content was obtained as a molality.

As distinct from the loss of $K^+$ and $H_2O$, the change in electrolyte concentration in the membrane assembly may be obtained by considering the change in the ratio of $K^+$:$H_2O$ in the membrane. This is achieved from the knowledge of the final and initial contents of each compartment and additions made during the run, with corrections for transport, electrolysis and spray.

Calculations were made on the data from experiment numbers (5.1, 5.3, 5.5, 5.7, 5.9, 5.11, 5.13, 5.14, 5.16 to 5.32, 5.34 and 5.36). In all but two of the 27 cases the ratio of $K^+$ : $H_2O$ gained by the electrolyte was less than the equilibrium ratio of $K^+$ : $H_2O$ in each membrane obtained from swelling and ion-exchange data. The inference is that the concentration in the membrane is rising, a fact compatible with water being sucked from the membrane.

Figure 5.3 The potassium content of the membrane assembly at the finish of experiments (5.48, 5.49 and 5.50).

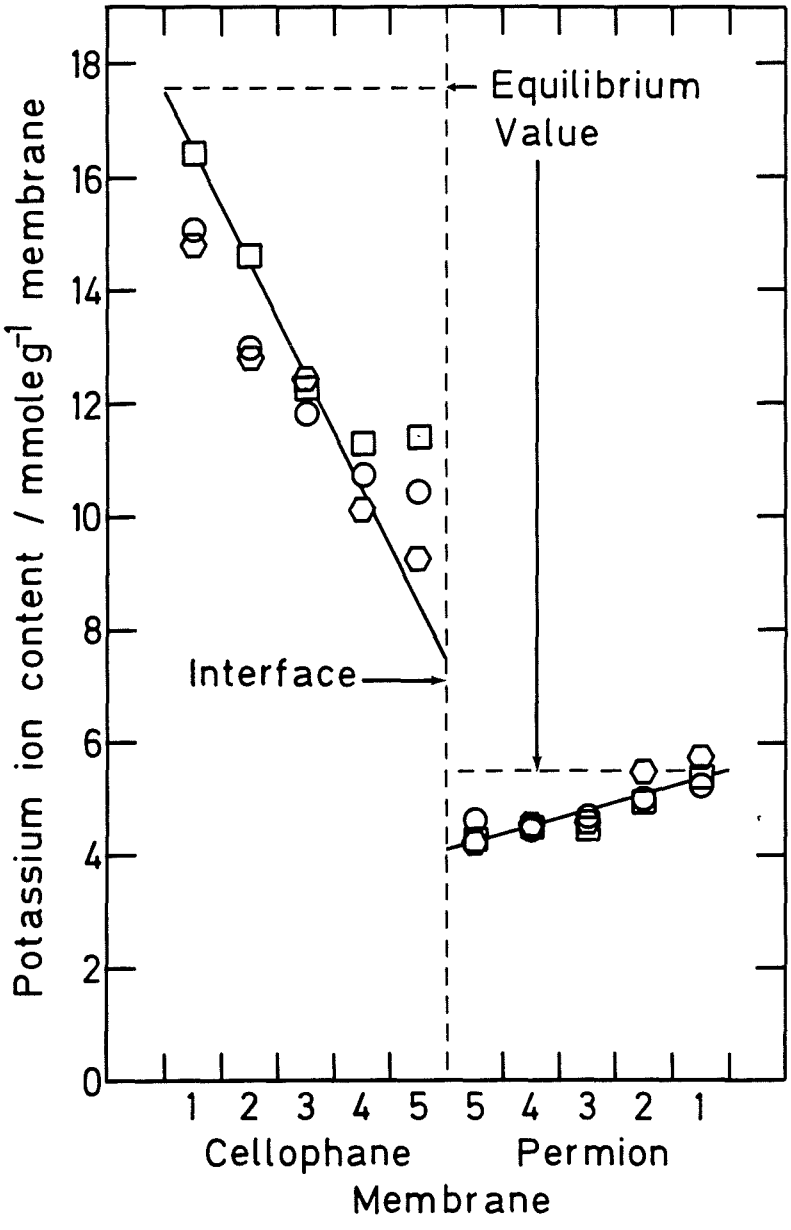


KEY ○, Run 48, ⬡, Run 49, and □, Run 50

Figure 5.4 The potassium content of the membrane assembly at the finish of experiment (5.50).

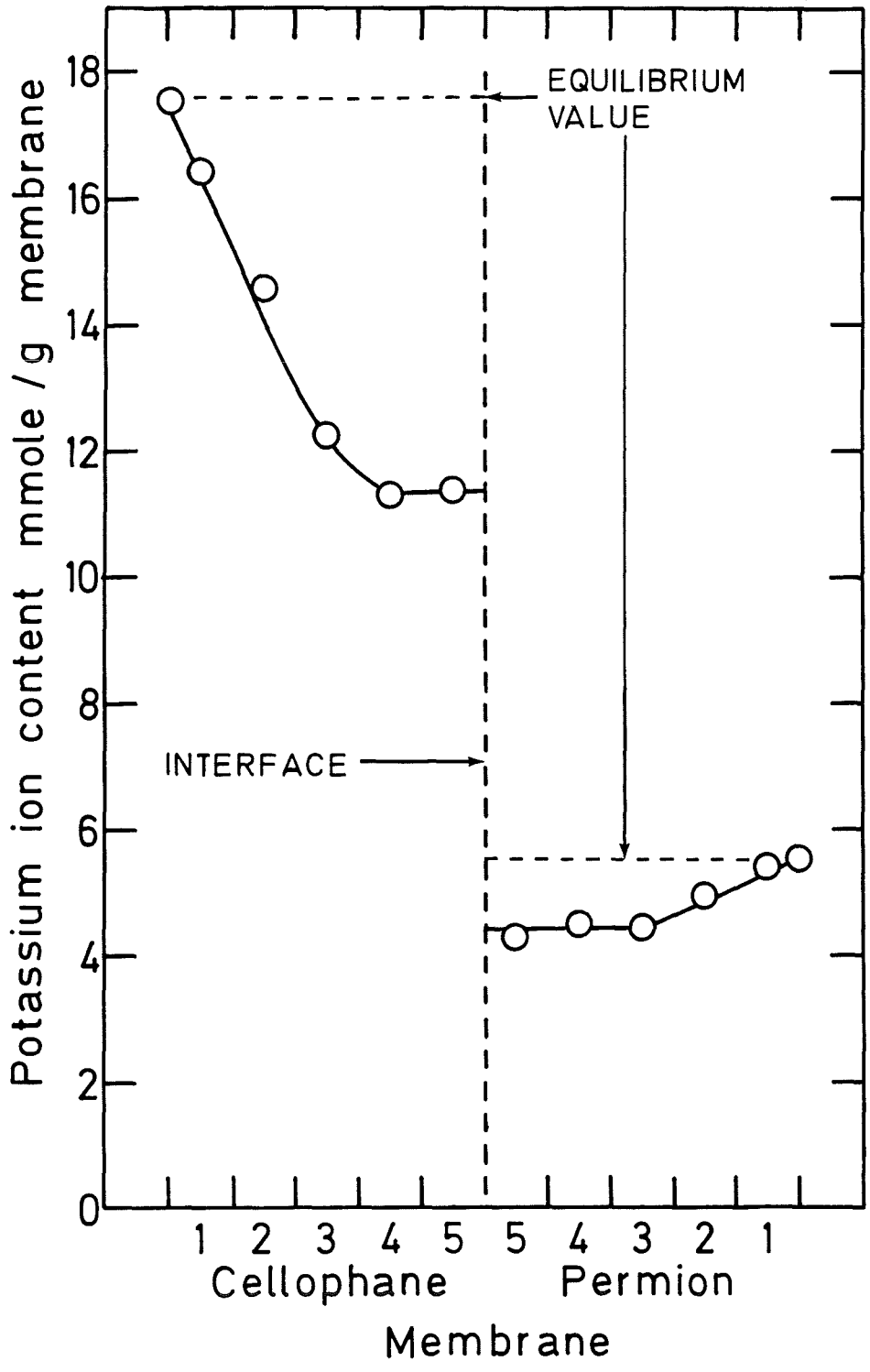

Figure 5.5 The water content of the membrane assembly at the finish of experiment (5.50).

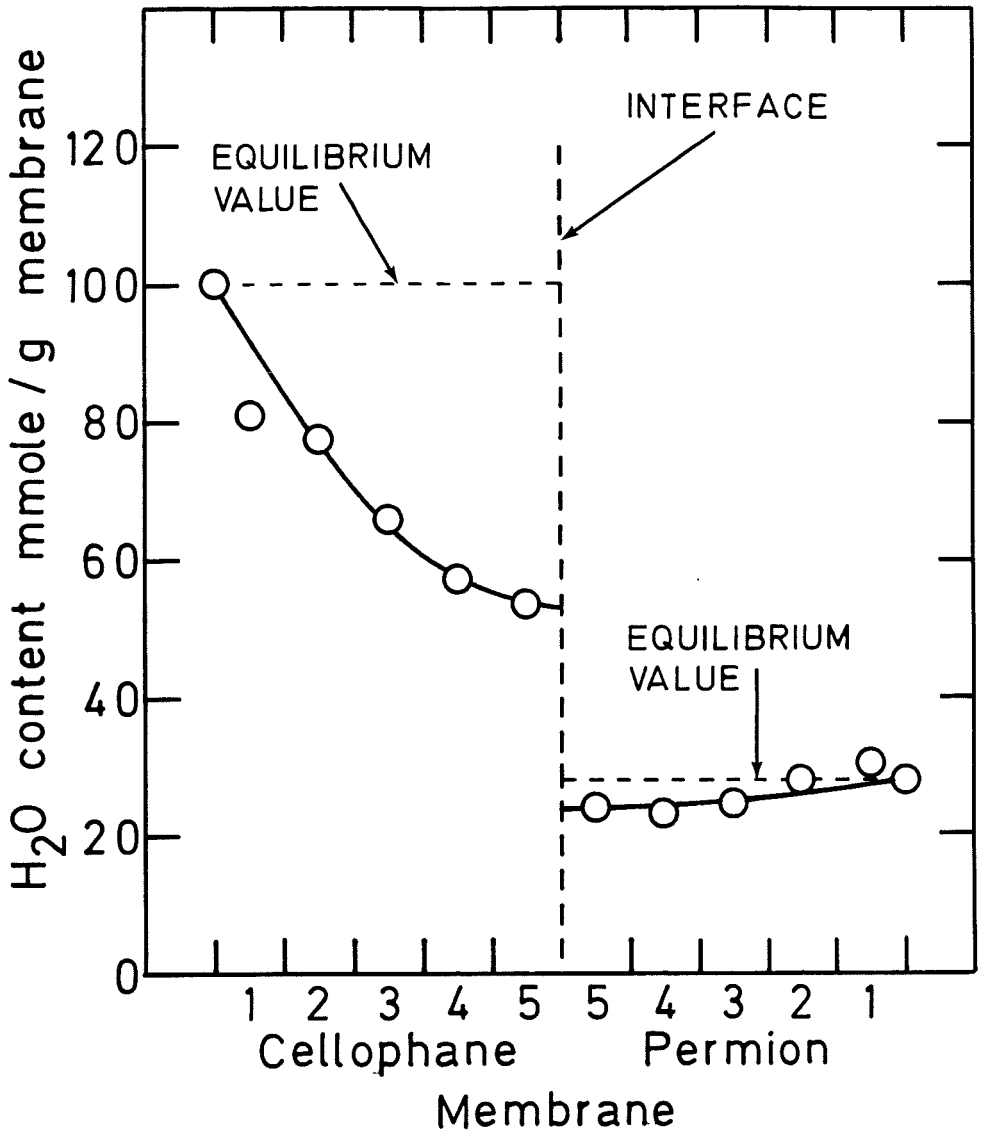

### 5.3.4 Steady state transport numbers

The process of electrolyte depletion, caused by the differences in the transport numbers of Cellophane and Permion, introduces the effects of diffusion. It is conceivable that once the diffusion gradients across the membranes have been set up the amount of depletion might reach a constant state. So far all transport numbers have been calculated from the amount of mass transport that has occurred since the start of a run. It is of course possible to use the data to calculate transport numbers for other time periods e.g. during the second hour of a run. The transport number in the second hour of a two hour run and the second and third hours of a three hour run are clearly more likely to approach steady state transport numbers, especially if the steady state has been reached by the end of the first hour. This possibility is investigated in table (5.4) which shows transport of $K^+$ and transference of water through assemblies comprising of sub-assemblies of 2, 5, and 10 sheets of each membrane for time periods at the start of, during and at the end of selected runs. For each sub-assembly and for the transport of both potassium and water, the transport numbers into and out of the assembly become closer together during time periods towards the end of a run compared to the start of the run. The inference being the approach of a steady state.

Another method of estimating the approach of a steady state is to calculate the amounts of KOH and water removed from an assembly as a function of the number of coulombs passed [122]. Figures (5.6 and 5.7) show for an assembly of 5 sheets of Cellophane and 5 sheets of Permion that the amounts of KOH and water removed from the assembly increased steadily with the number of coulombs passed. There are however indications that a steady state was being approached after the passage of 14,000 coulombs. At a steady state condition, transference of KOH and water from the anolyte to the membrane assembly would equal the amounts transferred from the assembly to the catholyte. Clearly the number of coulombs, which must be passed before a steady state is reached, depends upon the amounts of KOH and water which have to be withdrawn from the membrane assembly. This would be less for an assembly of 2 layers of Cellophane and 2 layers of Permion than for an assembly which contained 10 layers of each type of membrane. This conclusion is supported indirectly by figures (5.8 and 5.9) which show that the differences between the transport numbers out of and into the

Table 5.4 Steady State Transport Numbers

| Run | Assembly | Duration Hours | TK(A) | TK(C) | TW(A) | TW(C) |
|---|---|---|---|---|---|---|
| 5.21 | 2C:2P | 0.5 | 0.430 | 0.475 | 1.06 | 1.22 |
| 5.16 | 2C:2P | 1 | 0.460 | 0.468 | 1.07 | 1.19 |
| 5.17 | 2C:2P | 2 | 0.451 | 0.460 | 1.07 | 1.08 |
| | | 0-0.5 | 0.430 | 0.475 | 1.06 | 1.22 |
| | | 0.5-1 | 0.489 | 0.461 | 1.08 | 1.15 |
| | | 1-2 | 0.443 | 0.452 | 1.07 | 0.979 |
| 5.14 | 5C:5P | 1 | 0.426 | 0.479 | 0.908 | 1.30 |
| 5.18 | 5C:5P | 2 | 0.424 | 0.460 | 0.971 | 1.21 |
| 5.26 | 5C:5P | 4 | 0.434 | 0.456 | 1.03 | 1.18 |
| | | 0-1 | 0.426 | 0.479 | 0.908 | 1.30 |
| | | 1-2 | 0.423 | 0.440 | 1.03 | 1.13 |
| | | 2-4 | 0.443 | 0.451 | 1.10 | 1.14 |
| 5.24 | 10C:10P | 1 | 0.355 | 0.466 | 0.546 | 1.31 |
| 5.23 | 10C:10P | 2 | 0.378 | 0.451 | 0.752 | 1.23 |
| 5.27 | 10C:10P | 3 | 0.383 | 0.450 | 0.846 | 1.27 |
| | | 0-1 | 0.355 | 0.466 | 0.546 | 1.31 |
| | | 1-2 | 0.401 | 0.436 | 0.956 | 1.14 |
| | | 2-3 | 0.396 | 0.447 | 1.03 | 1.34 |

Figure 5.6 The amount of KOH removed from an assembly of 5 layers of each membrane type as a function of the number of coulombs passed.

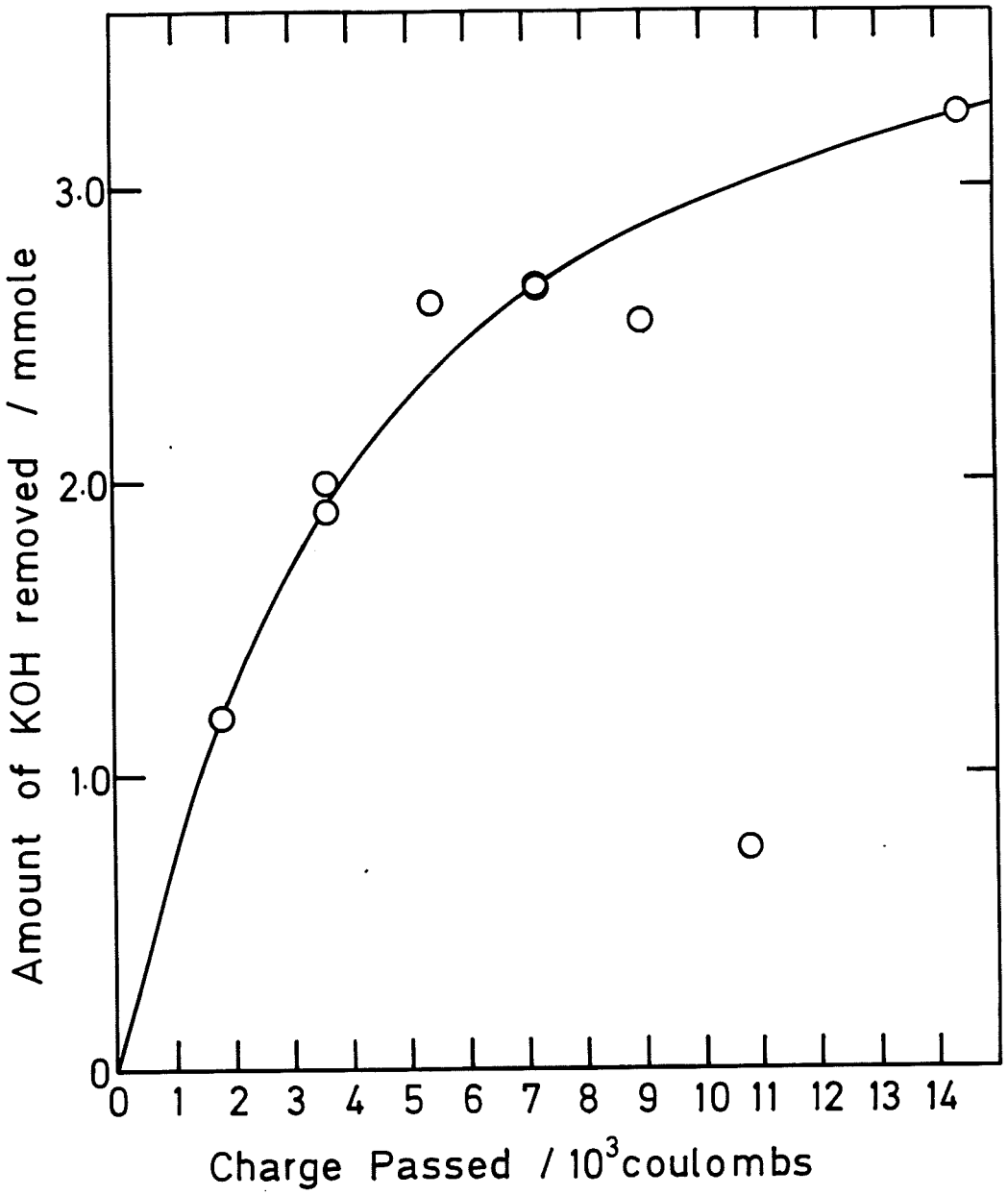

Figure 5.7 The amount of water removed from an assembly of 5 layers of each membrane type as a function of the number of coulombs passed.

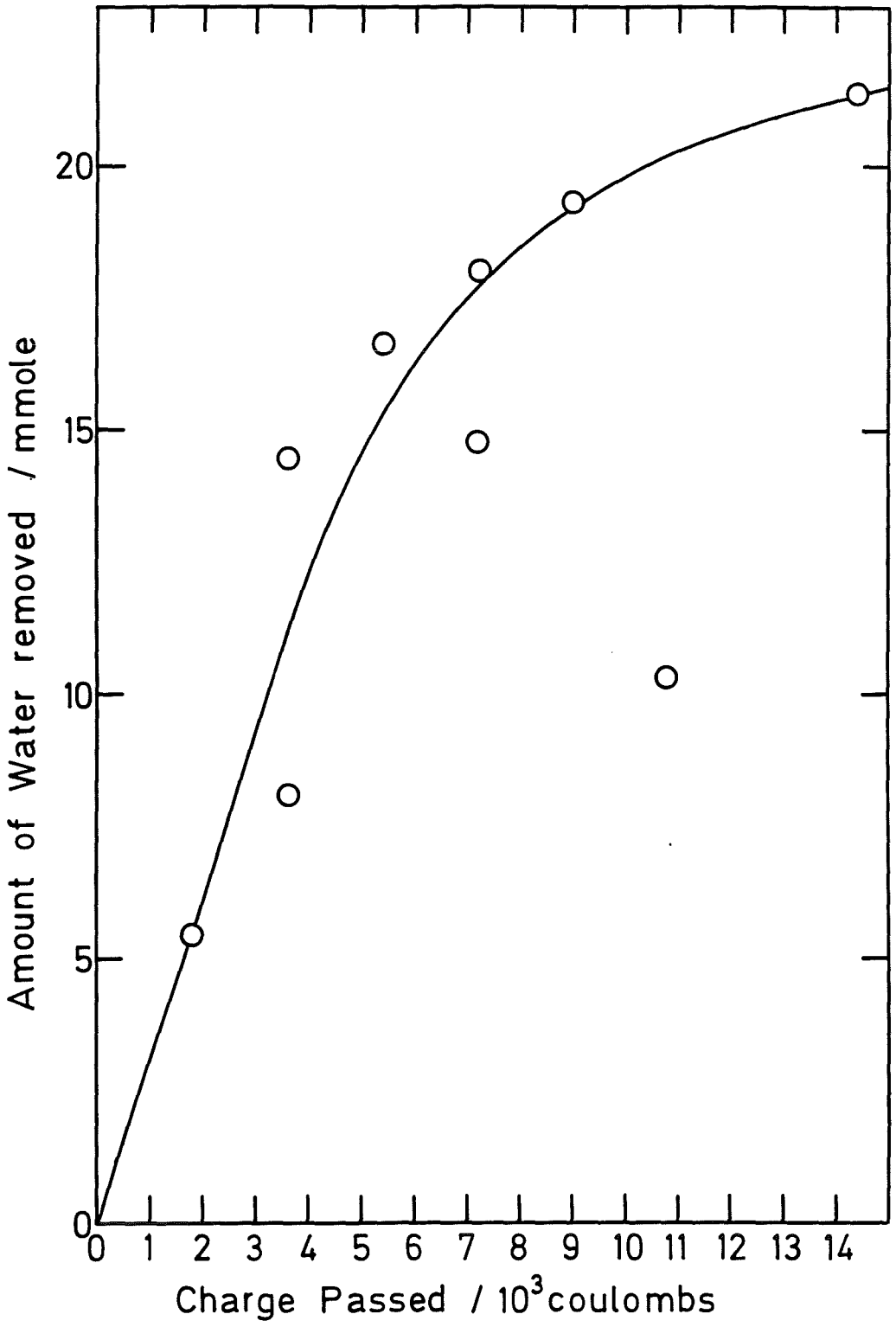

Figure 5.8 The difference between the $K^+$ transport numbers out of and into the membrane assembly as a function of the number of layers of each type of membrane, for runs of a 2 hour duration.

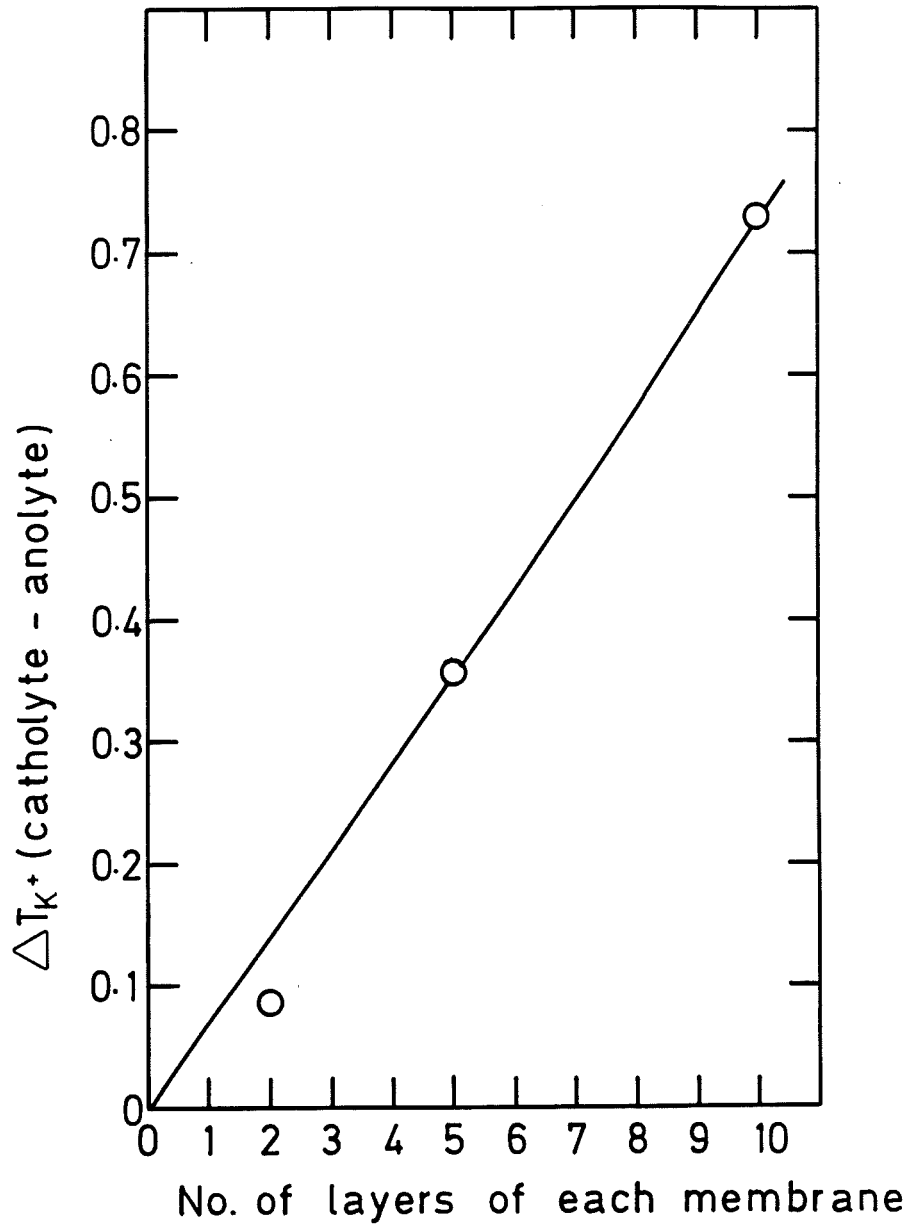

Figure 5.9 The difference between the Water transport numbers out of and into the membrane assembly as a function of the number of layers of each type of membrane, for runs of a 2 hour duration.

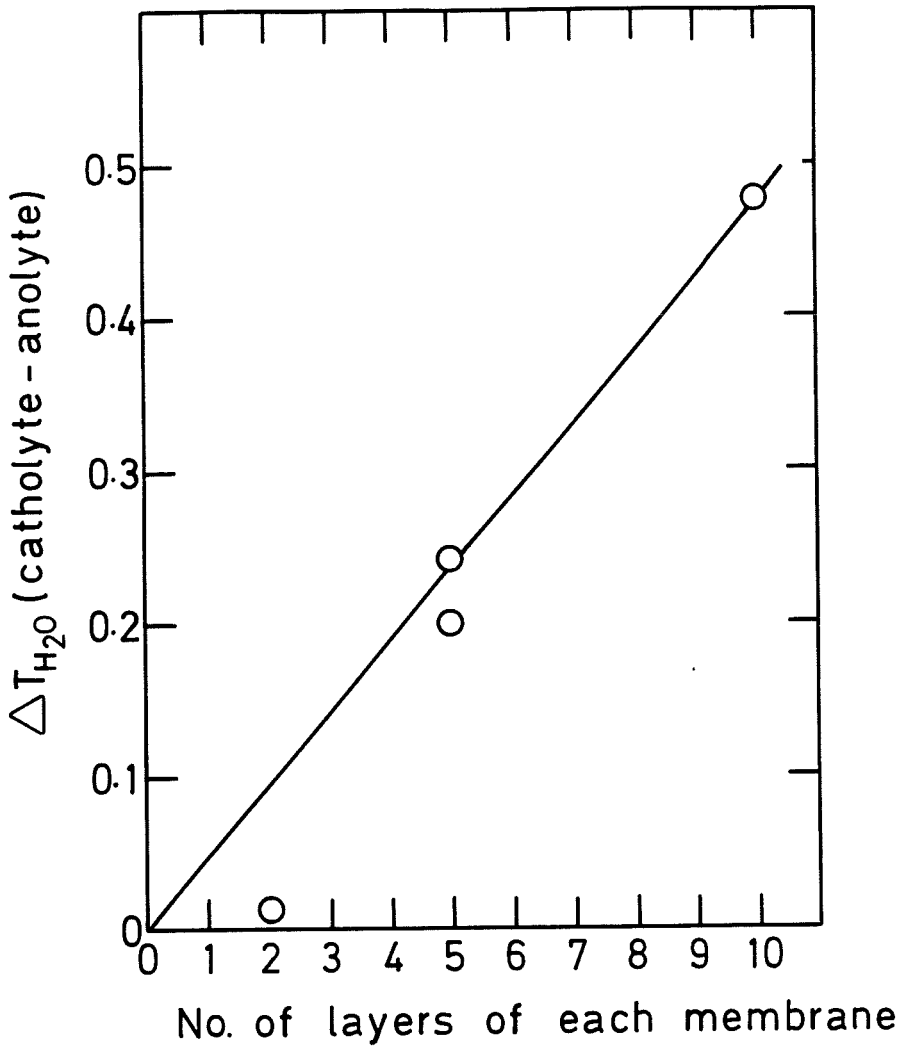

membrane assembly decreased with the number of layers for both $K^+$ and water. The differences were close to zero for an assembly of 2 layers of Cellophane and 2 layers of Permion demonstrating that a steady state existed for most of this transference experiment.

Figures (5.10, 5.11 and 5.12) show the results obtained from a series of experiments using assemblies containing 2, 5 and 10 layers of each membrane type. Transport numbers into the assembly, as calculated from analysis of the anolyte compartment and transport numbers from the assembly, as calculated from analysis of the catholyte compartment are shown as a function of the duration of the run.

With reference to figures (5.10, 5.11 and 5.12) all $T_K$+ data sets fall in between values expected for single membranes at this concentration and exhibit a decrease in the difference between the transport as measured from either compartment as the no. of coulombs passed is increased. Hence as a function of time the transport number measured by analysis of the anolyte approximated to the transport number measured by analysis of the catholyte. The conclusion must be that the measured transport numbers have been modified by diffusion. A steady state condition being reached when transport and diffusion into the assembly equals transport and diffusion out of the assembly.

Figures (5.10, 5.11 and 5.12) show increasing divergence of the water transference number as the number of layers of each membrane is increased. In figures (5.11 and 5.12) water transport to the catholyte in each case is similar to that for Permion alone, whereas water transport from the anolyte rises above that expected for Cellophane. With 5 and 10 sheets of membrane it becomes increasingly more difficult for Permion to suck water through the Cellophane from the anolyte and the difference in $T_{H2O}^{A}$ and $T_{H2O}^{C}$ must result in water being sucked out of the assembly. For the 2:2 combination, figure (5.10), the hydraulic resistance of 2 layers of Cellophane is low and in consequence Permion sucks water through the Cellophane and water transference numbers from both compartments converge, resulting in the approach of a steady state. As discussed earlier in the section a steady state will be reached sooner for the 2:2 combination than with 5 and 10 sheets of each membrane because there is less water to be removed. With the 2:2 combination although the observed transport number is closer to that of Permion than to that of Cellophane it is clearly below the Permion value. This is unexpected and possibly due to two reasons. Firstly water is not a current carrying

Figure 5.10 The transport numbers of $K^+$ and water through assemblies of 2 sheets of each membrane type as a function of the duration of the run.

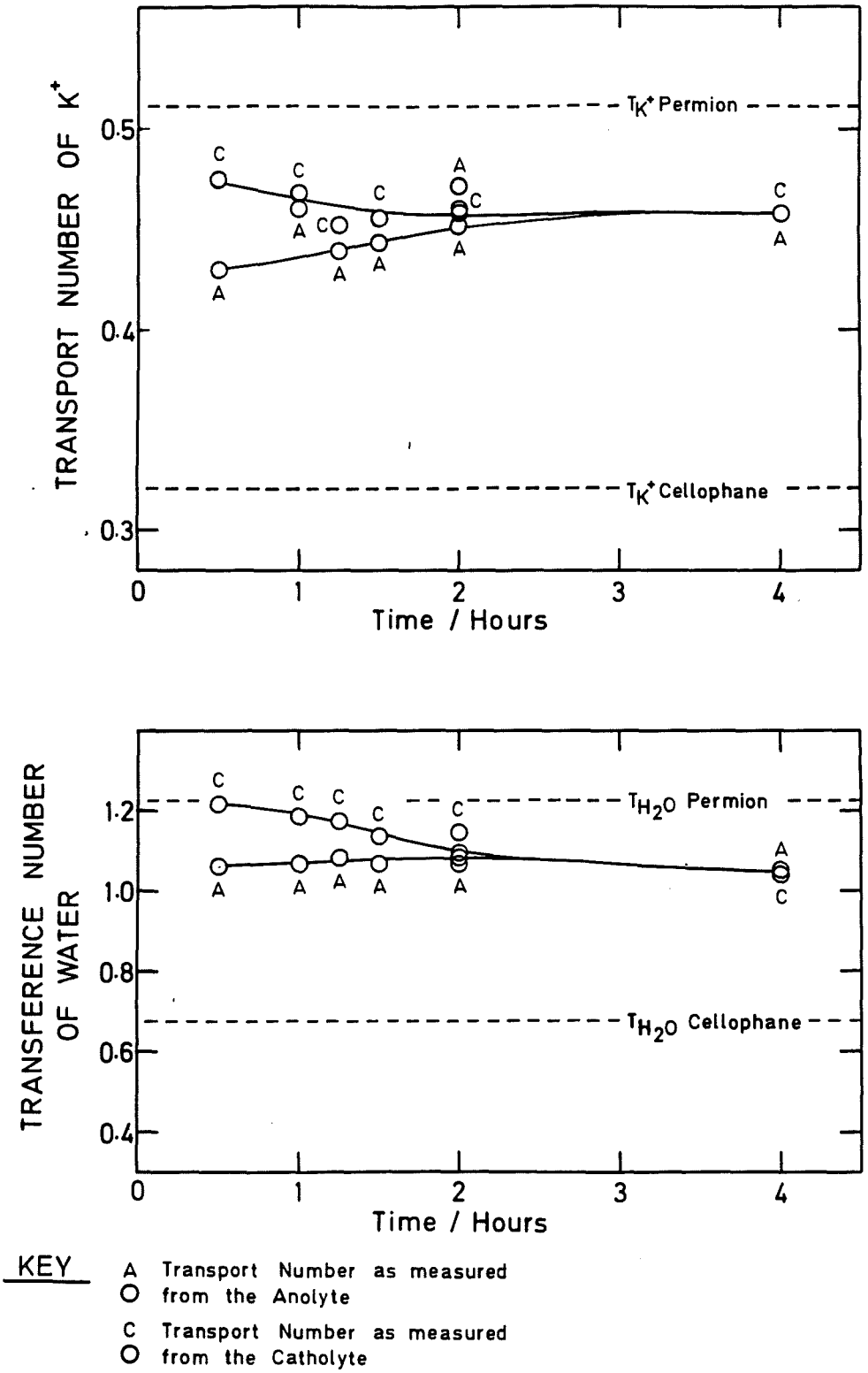

Figure 5.11 The transport numbers of $K^+$ and water through assemblies of 5 sheets of each membrane type as a function of the duration of the run.

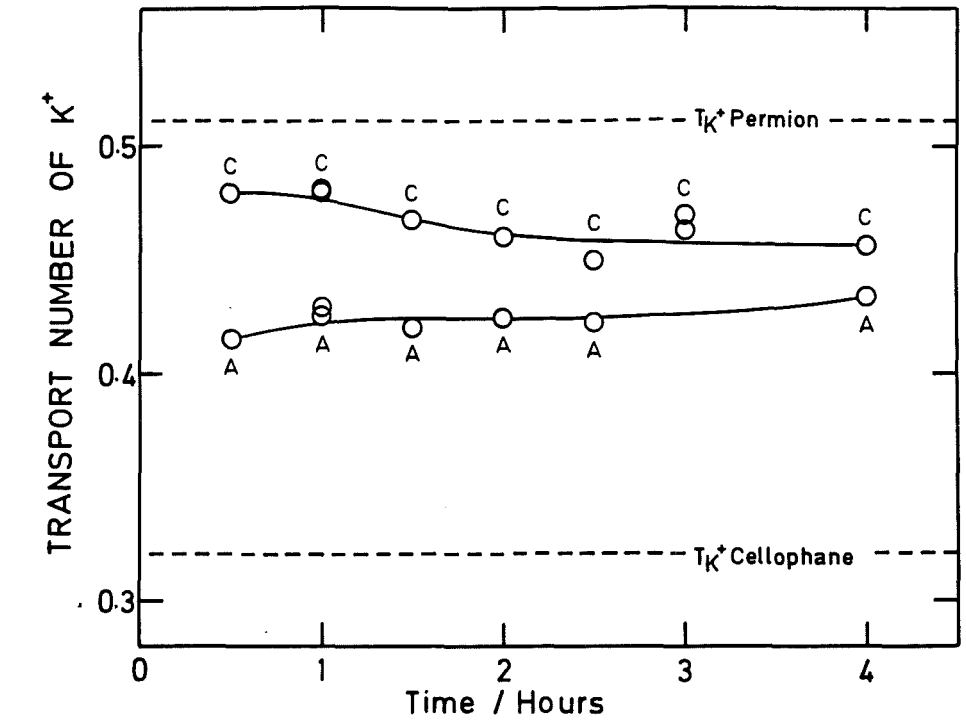


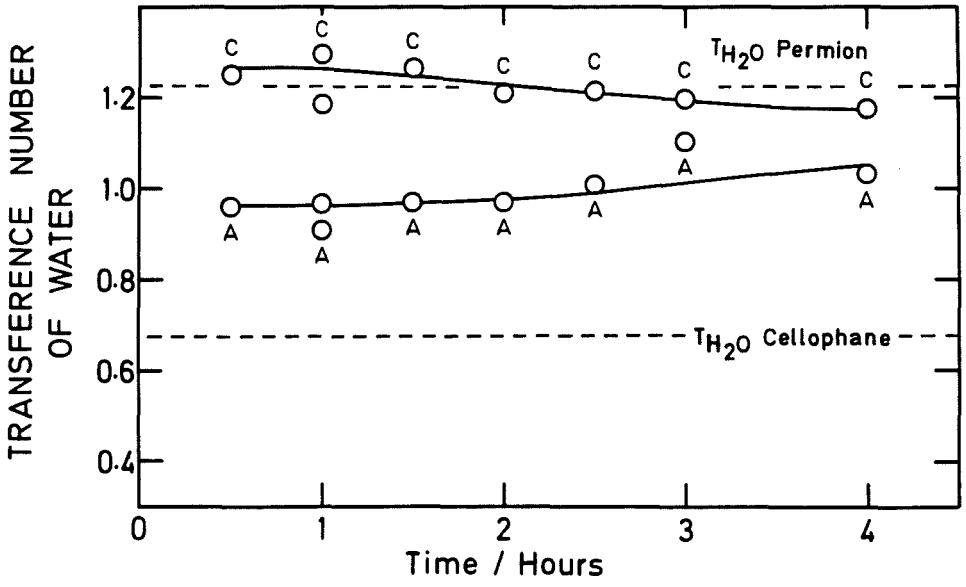


KEY

A Transport Number as measured
O from the Anolyte

C Transport Number as measured
O from the Catholyte

Figure 5.12 The transport numbers of $K^+$ and water through assemblies of 10 sheets of each membrane type as a function of the duration of the run.

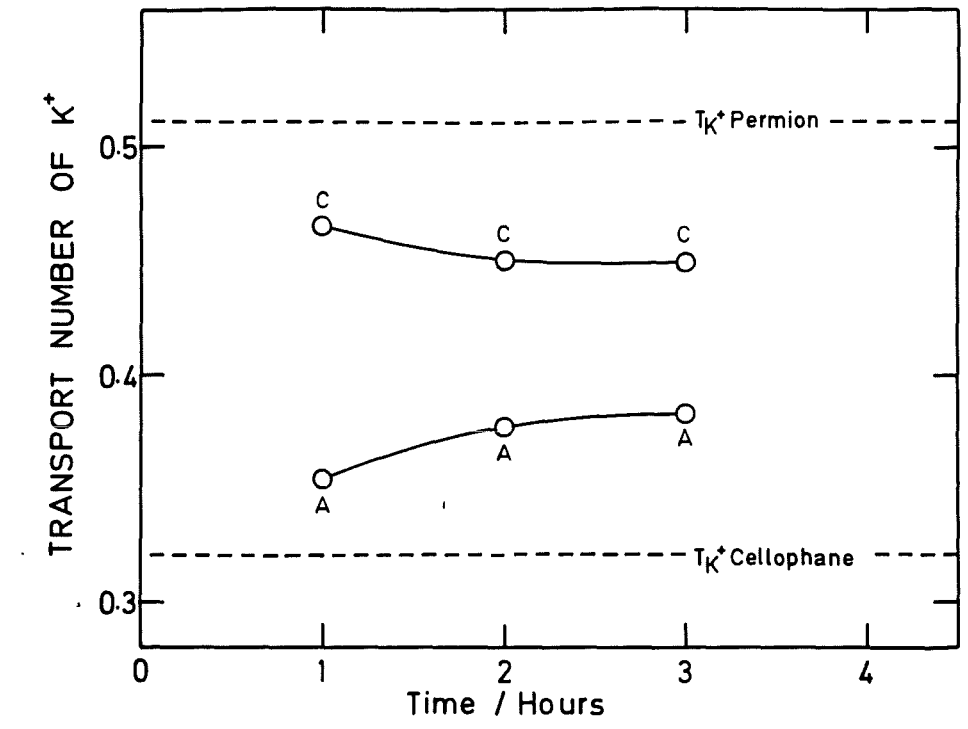


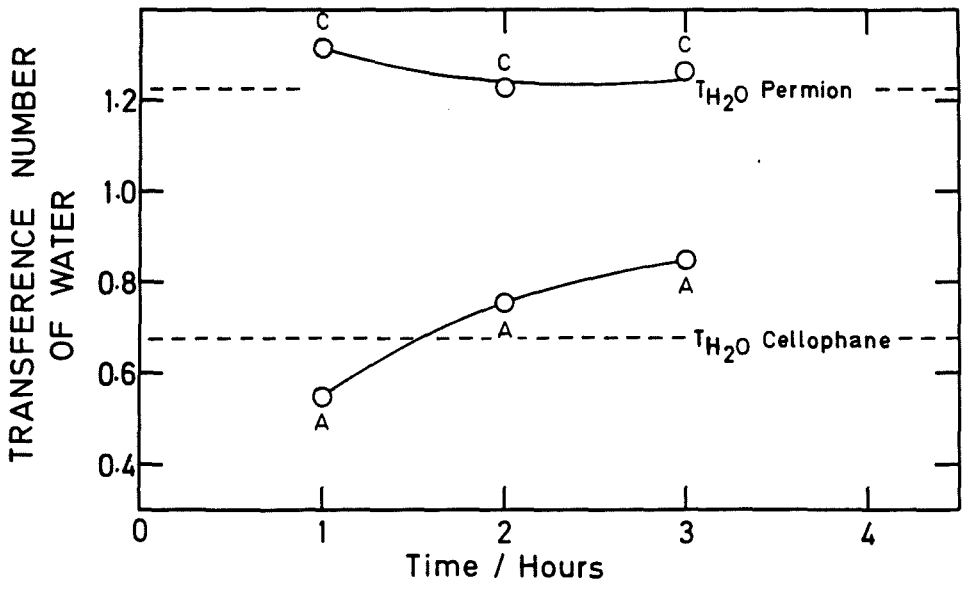


KEY

A O Transport Number as measured from the Anolyte

C O Transport Number as measured from the Catholyte

species and as a consequence water transference numbers are dependent on potassium ion transport numbers, which as also shown in figure (5.10) converge below a value for Permion alone. Secondly the hydraulic strength of 2 layers of Permion is compared with 5 and 10 layers hence the ability of the Permion suck water through the Cellophane is reduced.

Evidence that the electrolyte contents of the Cellophane layers have changed is shown in figure (5.13), a plot of water content versus potassium ion content of Cellophane after equilibration in a range of KOH solutions. Superimposed on this plot are data for potassium and water contents of the Cellophane used in experiment (5.50). The sheet nearest the interface shows the greatest deviation from equilibrium values which shows that more electrolyte is removed from the layers of Cellophane closest to the Cellophane/Permion interface.

An alternative way of presenting the results of figures (5.10, 5.11 and 5.12) may be gained in a plot of the difference in measured transport numbers versus time, figure (5.14). All results tend towards the x-axis with time. Experimentally a steady state may be reached but since calculation of transport numbers includes a period of non-steady state operation then $t_C$ can only equal $t_A$ at infinite time. The period of non-steady state occurs at the start of any run where there is always a finite time whilst the diffusion gradients are set-up. Of course, as the duration of the run increases the significance of this amount decreases. Better estimates of steady state transport numbers may be obtained by subtraction of the initial mass transport from the final measured values.

Some investigations were carried out varying the number of layers of membrane with respect to each other. The results are shown in figure (5.15). Ten sheets of membranes were used in each assembly, so for example in experiment (5.7) the assembly comprised of 8 sheets of Cellophane with 2 sheets of Permion. With an increase in the number of sheets of Cellophane from 0 to 10, (with a corrisponding decrease in the number of sheets of Permion), potassium ion transport numbers and water transference numbers proceed from values close to Permion alone to values close to Cellophane alone. The trend is not progressive, Permion is clearly the dominant partner, with transport numbers only approaching values for Cellophane when the number of sheets of Cellophane is large compared to the number of sheets of Permion.

Data approaches values for Cellophane with increasing number of Cellophane

Figure 5.13 A plot of water content v.s. $K^+$ content of Cellophane equilibrated in a range of KOH solutions. Filled circles refer to the electrolyte content of the Cellophane layers used in experiment (5.50).

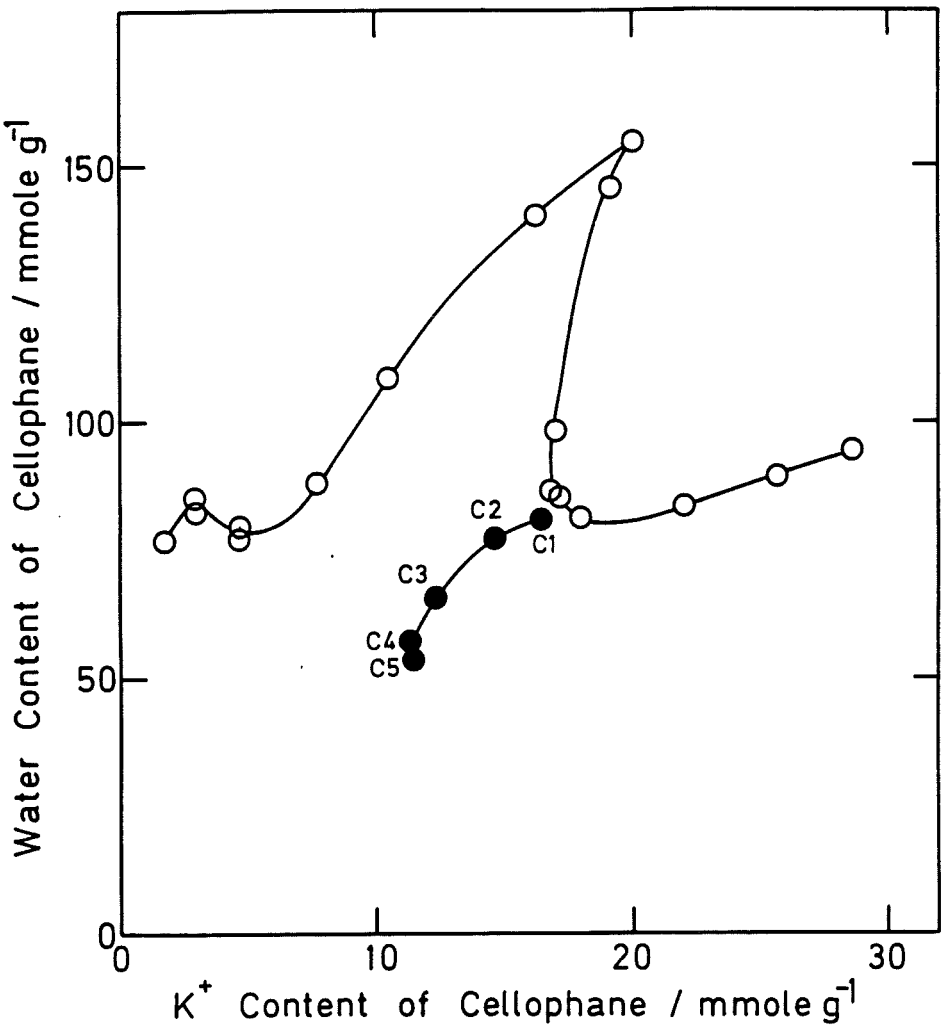

Figure 5.14 The difference between transport numbers of $K^+$ and water measured by the analysis of the anolyte and catholyte for 2, 5, and 10 layers of each membrane type as a function of the duration of the experiment.

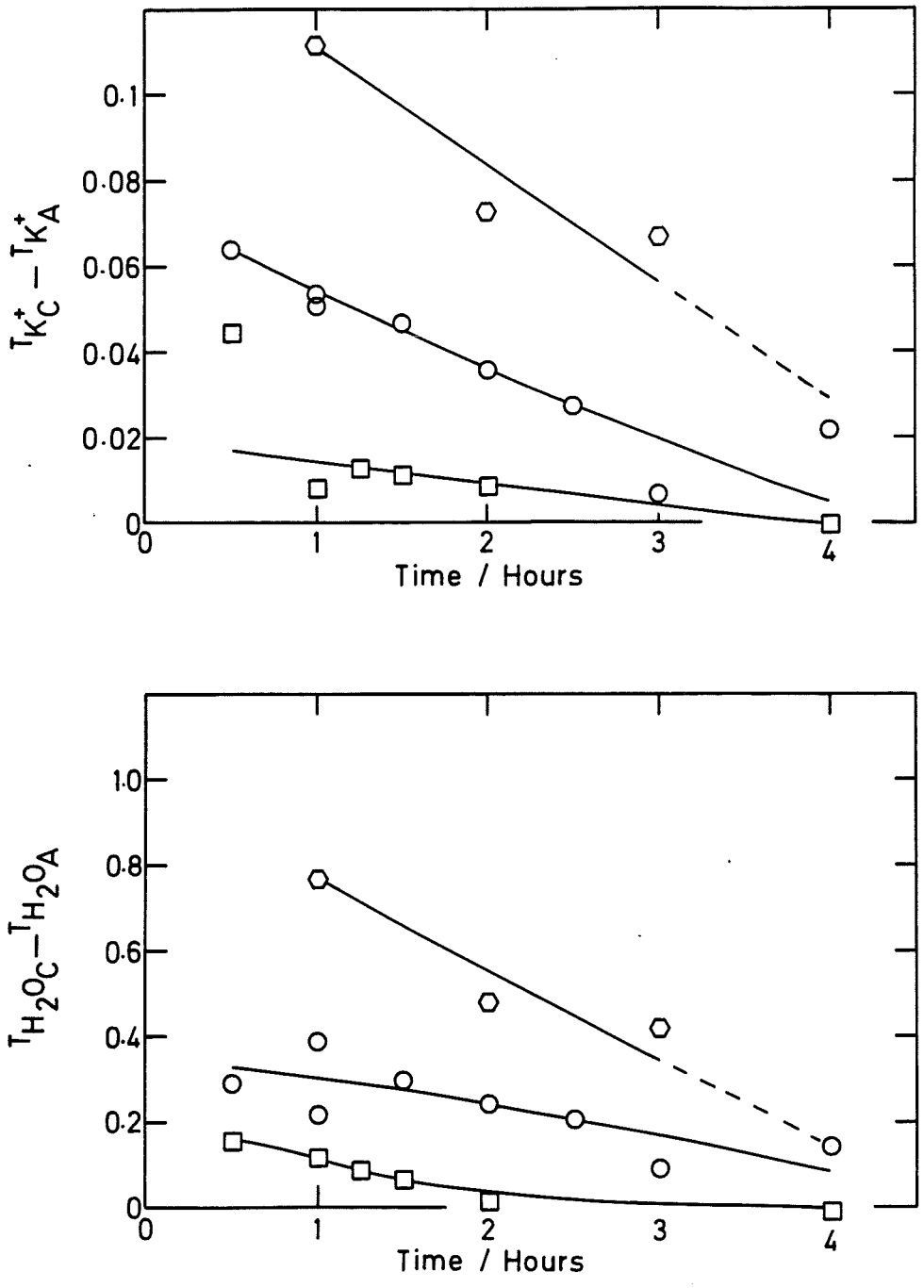

Figure 5.15 Transport numbers as measured by analysis of the anolyte and catholyte for experiments where unequal numbers of each membrane type were used as a function of the membrane assembly with Permion on the receiving side.

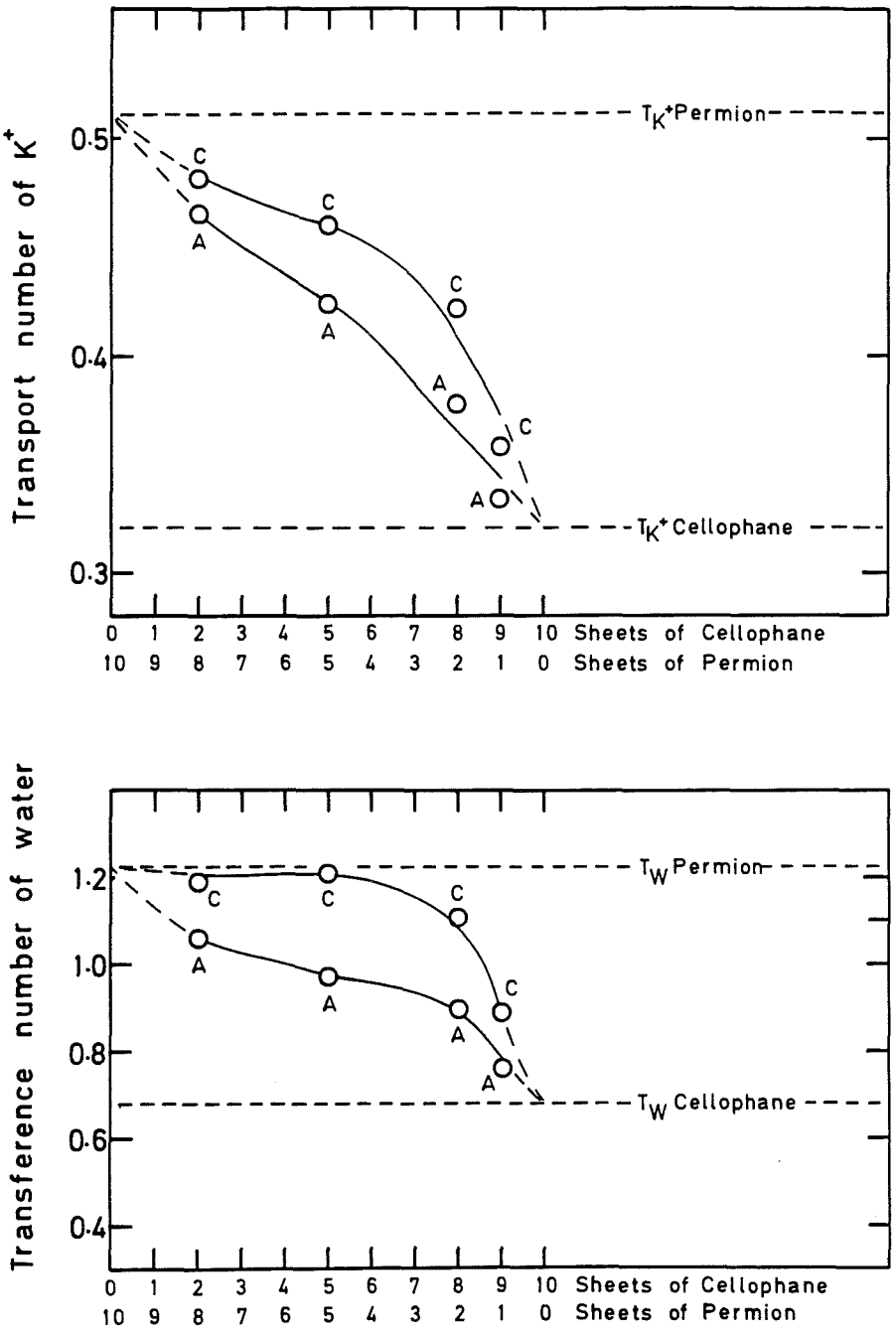


KEY

A Transport Number as measured
O from the Anolyte

C Transport Number as measured
O from the Catholyte

layers since a thicker Cellophane barrier reduces diffusion and a thinner Permion barrier allows diffusion. This has the effect that Cellophane cannot replace the transported potassium at a sufficient rate to allow for the level of transport normally sustained by the Permion and so the potassium concentration falls more extensively at the interface, which causes greater compensating diffusion through the "thin" Permion, thus lowering its mass transport. When the number of sheets of Cellophane were increased with respect to the number of sheets of Permion the value of $T_{H2O}^{C}$ fell below the value for Permion alone. The reason for this may be illustrated by the situation, 9C:1P, the hydraulic force exerted by 1 sheet of Permion is not sufficient to suck the amount of water required to maintain $T_{H2O}^{C}$ through 9 sheets of Cellophane.

The work presented so far in this section was conducted at one current density, 200 $mAcm^{-2}$ at the start of a run. The following discussion examines the effect of altering the current density on the approach to the steady state.

In the first instance the total charge passed was kept constant at 7,200 coulombs and the time and current adjusted accordingly. The results are shown in figure (5.16). It was thought an increase in the current density would achieve the steady state sooner with the observation of similar anolyte and catholyte transport numbers. The approximately equidistant separations in the anolyte and catholyte transport numbers show this is not the case and indicate current density is not the controlling factor in the approach of the steady state. Presumably higher current densities result in steeper concentration profiles within the membrane with the effect that more electrolyte needs to be removed to reach a steady state.

Section (5.3.3) reported results at a relatively high current density where depletion of electrolyte at the Cellophane/Permion interface is rapid leading to the decomposition of the membrane. The steady state condition is not reached, again because of steeper concentration profiles at higher current densities, and decomposition occurs because Permion sucks all the solution out of the Cellophane.

Figure 5.16 The effect of altering the current density on transport numbers as a function of the duration of the experiment. 5 sheets of each membrane were used. The error bar represents the standard deviation ($\delta n$) of 4 or 3 runs after a duration of 1 or 2 hours respectively.

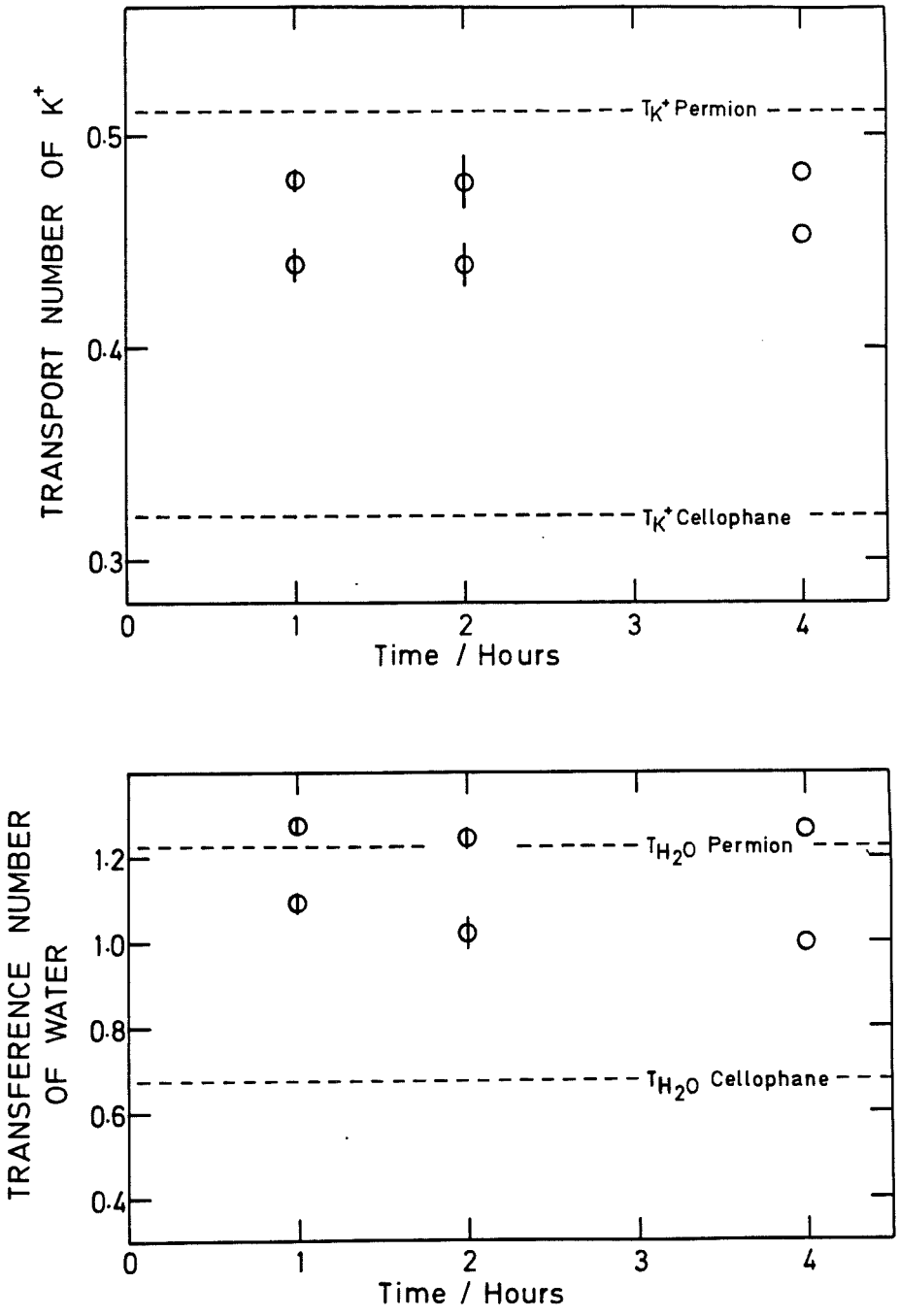


KEY

A Transport Number as measured
O from the Anolyte

C Transport Number as measured
O from the Catholyte

### 5.3.5 Additional evidence of electrolyte depletion

In experiment (5.31), a run with two sheets of each membrane, at an initial current density of 400 $mAcm^{-2}$ and duration 1 hour, when the cell was dismantled it was noticed that the Cellophane was slightly discoloured in the region where the membranes had been clamped by the cell. It is proposed that because of the electrolyte depletion the resistance of the Cellophane increases and the discolouration/decomposition arises from the consequent heating effect. Further, the process maybe aided by the removal of water due to suction as described in section (5.3.3).

An increase in the current density to 800 $mAcm^{-2}$ in experiment (5.33) had the effect of decomposing the Cellophane around the annular ring before the requisite amount of charge had been passed. It is interesting to note that the decomposition occurs in an annular ring adjacent to the cell wall. Section (4.3.1) and work by Jenkins et al [100], on the measurement of the ionic conductance of regenerated cellulose suggests current refraction into the region of the membrane clamped between the two faces of the cell. They go further by saying that the current density is higher close to the cell wall. This could be an explanation as to why the Cellophane decomposes at the annular ring.

A transition time, T, was defined as the time period of power supply in which current flows before the concentration of the mobile species in the membrane falls to zero. This results in the decomposition of the Cellophane. Lee et al [123] showed that T is proportional to $1/i^2$, where i is the current and the constant of proportionality is dependent on the separator. Figure (5.17) shows plots of T versus $1/i^2$ for 2, 5 and 10 layers of each membrane.

With 2 layers of each membrane the points fall on a straight line. For 5 and 10 layers a best line fit has been drawn through the data obtained when working at the highest current densities. The non-linearity at low current densities with both 5 and 10 layers is probably due to deficiencies in the experimental technique.

In retrospect the experimental technique used to acquire this data could be improved. Approximate volumes of initial electrolyte were added and determined accurately by weight. Since current density contains an area term it would have been more appropriate to admit the electrolyte volumetrically. In the preparation of membrane assembly electrolyte between the membrane layers is removed by rolling. It might have

been advisable to mop the surface of each membrane film to minimise the membrane/membrane interface electrolyte since excess electrolyte in this region would prolong the time to burn-through.

A further problem is the need to maintain concentrations constant on either side of the assembly throughout the run. Additions of electrolyte and water increase the volume in the compartment and decrease the effective current density, thus increasing the burn through time.

For the highest current density runs burn through is so rapid that additions are not required and the initial current densities are maintained. But for the lowest current densities there is a cumulative effect of longer runs requiring more additions, and more additions mean an increase in electrolyte volume and hence a decreased current density and a falsely increased burn through time. It would have been possible to minimise the effect by removing a volume of electrolyte from each compartment equivalent to the addition after each addition.

Figure 5.17 The time taken in minutes for Cellophane to decompose v.s. the reciprocal of the applied current squared ($Amps^{-2}$)

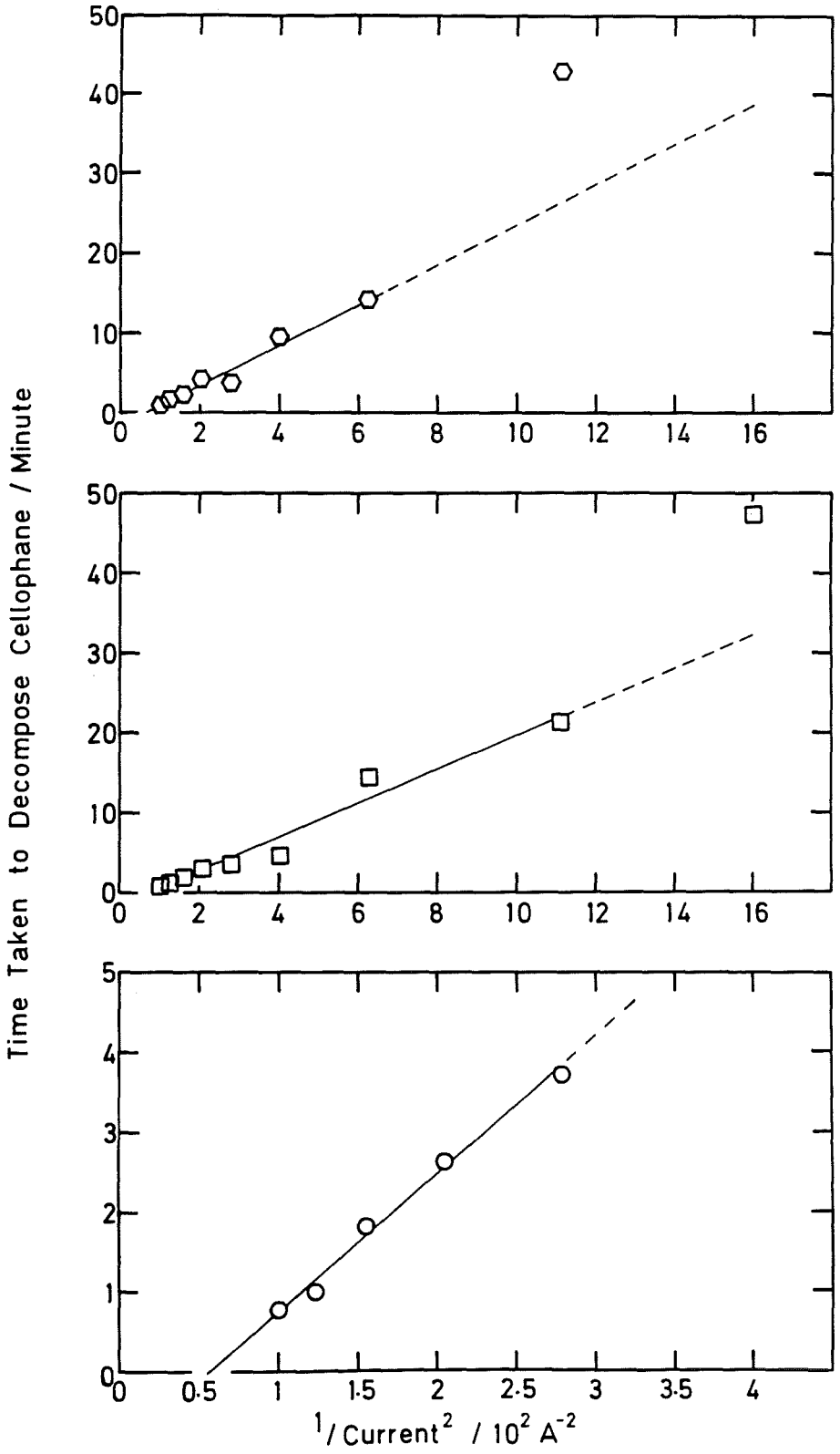


KEY ○2, □5, and ○10 sheets of each membrane

### 5.3.6 Cellophane on the receiving side

The results from transport experiments where Cellophane was on the side receiving the cation are shown in table (5.5).

Table 5.5(a) Potassium ion transport data from all experiments where Cellophane was on the receiving side.

| Run | Duration Hours | Current Amps | Assembly | $T_K$(A) | $T_K$(C) |
|---|---|---|---|---|---|
| 5.2 | 2 | 1 | 5P:5C | 0.452 | |
| 5.4 | 2 | 1 | 5P:5C | 0.471 | 0.434 |
| 5.6 | 2 | 1 | 2P:8C | 0.441 | 0.351 |
| 5.8 | 2 | 1 | 2P:8C | 0.400 | 0.336 |
| 5.10 | 2 | 1 | 1P:9C | 0.405 | 0.318 |
| 5.12 | 2 | 1 | 8P:2C | 0.472 | 0.370 |
| 5.36 | 2 | 1 | 5P:5C | 0.494 | 0.362 |
| 5.37 | 2 | 1 | 10P:10C | 0.494 | 0.379 |
| 5.39 | 1 | 2 | 2C | 0.320 | 0.321 |
| 5.40 | 1 | 2 | 2P:2C | 0.480 | 0.385 |
| 5.41 | 1 | 2 | 2C | 0.318 | 0.321 |
| 5.42 | 1 | 2 | 2P | 0.510 | 0.515 |
| 5.43 | 1 | 2 | 2P:2C | 0.476 | 0.366 |
| 5.44 | 1 | 2 | 2P | 0.506 | 0.511 |
| 5.46 | 2 | 1 | 5P:5C | 0.484 | 0.368 |
| 5.47 | 2 | 1 | 10P:10C | 0.500 | 0.370 |

Table 5.5(b) Water transference data from all experiments where Cellophane was on the receiving side.

| Run | Duration Hours | Current Amps | Assembly | $T_w(A)$ | $T_w(C)$ |
|---|---|---|---|---|---|
| 5.2 | 2 | 1 | 5P:5C | 1.14 | |
| 5.4 | 2 | 1 | 5P:5C | 1.22 | 0.928 |
| 5.6 | 2 | 1 | 2P:8C | 1.16 | 0.530 |
| 5.8 | 2 | 1 | 2P:8C | 1.09 | 0.643 |
| 5.10 | 2 | 1 | 1P:9C | 1.16 | 0.607 |
| 5.12 | 2 | 1 | 8P:2C | 1.13 | 0.442 |
| 5.36 | 2 | 1 | 5P:5C | 1.32 | 0.415 |
| 5.37 | 2 | 1 | 10P:10C | 1.30 | 0.489 |
| 5.39 | 1 | 2 | 2C | 0.698 | 0.640 |
| 5.40 | 1 | 2 | 2P:2C | 1.27 | 0.559 |
| 5.41 | 1 | 2 | 2C | 0.689 | 0.656 |
| 5.42 | 1 | 2 | 2P | 1.25 | 1.19 |
| 5.43 | 1 | 2 | 2P:2C | 1.30 | 0.461 |
| 5.44 | 1 | 2 | 2P | 1.22 | 1.18 |
| 5.46 | 2 | 1 | 5P:5C | 1.28 | 0.467 |
| 5.47 | 2 | 1 | 10P:10C | 1.37 | 0.493 |

Before discussing table (5.5) in detail it is important to consider an experimental observation. The membrane did not stay as a packed assembly. The membranes separated at the Permion/Cellophane interface due to the accumulation of solution which

arose since $t_{H2O}$(Permion) > $t_{H2O}$(Cellophane). This resultant bowing of the assembly is schematically represented in figure (5.18).

Figure 5.18 Membrane assembly showing the effect of bowing.

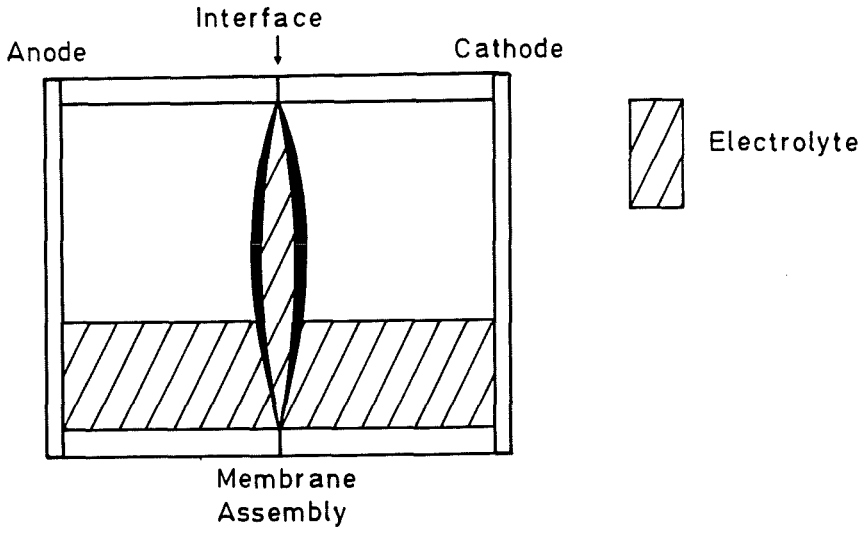


### 5.3.7 Analysis of the interface solution

Due to the bowing effect, apart from the region where the membranes are clamped together in the cell, the membranes can no longer be considered as an assembly. Setting aside any clamping effects for a moment the situation is shown in figure (5.19). The anolyte is on the donating side of the Permion and the interface solution is on the receiving side of the Permion, similarly the interface solution is on the donating side of the Cellophane and the catholyte is on the receiving side of the Cellophane. Application of the theory of Kressman et al [65] suggests that the transport of ions and water through the Permion can be expected to depend on the concentration of the membrane/membrane interface solution and the transport through Cellophane can be expected to depend on the concentration of the catholyte.

Figure 5.19 Schematic diagram showing when Cellophane is on the receiving side that the membranes can no longer be considered as an assembly.

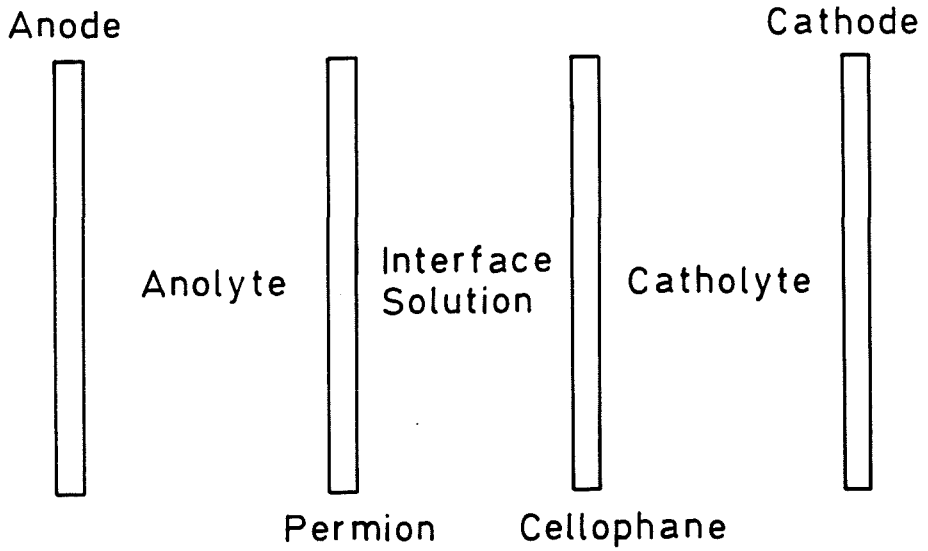


The interface solution is receiving the cation through the Permion and the catholyte is receiving the cation through the Cellophane. Using transport numbers obtained through single membranes at the appropriate concentration it is possible to calculate how much solution is transported into the membrane/membrane interface through the Permion and how much is transported out through the Cellophane, if there were no diffusion, hydraulic flow or osmosis. From the difference it is possible to calculate the molality of the interface solution. This was found to be 22.70m. After careful removal of the interface solution from experiments (36 and 37) analysis showed it to be of molality 8.273m and 8.487m respectively. This corresponds to an average molarity of 7.5M, the external electrolyte solution of 7.2M has a molality of 8.074m. Thus the interface solution is of slightly higher concentration than the anolyte and catholyte but much less than the calculated molality which is of a concentration where precipitation would have occurred. The large difference between the measured molality and the calculated molality must mean that the effects of diffusion, osmosis and/or hydraulic flow are present.

Using the observed i.e. experimental "diffusion modified" transport numbers the molality of the membrane/membrane interface solution was recalculated. A second method of predicting the molality of the membrane/membrane interface solution was to determine what proportion of the initial solution was lost compared to the final solution. Anolyte and catholyte were dealt with together and changes due to spray and the electrolysis of water were taken into account. A comparison of the two calculated molalities with the measured molality of the interface solution is shown in table (5.6). The weights of solution involved is also shown.

Table 5.6 Comparison of experimentally obtained and calculated molalities together with the weights of solution involved.

| Run | 5.36 | 5.37 |
|---|---|---|
| Experimental molality (m) | 8.273 | 8.487 |
| Weight of solution (g) | 0.9964 | 0.7088 |
| Calculated (1) molality (m) | 8.176 | 7.823 |
| Weight of solution (g) | 1.687 | 1.495 |
| Calculated (2) molality (m) | 8.150 | 7.880 |
| Weight of solution (g) | 1.835 | 1.647 |

The calculated molalities are similar to the measured molalities albeit slightly smaller. The good agreement between the calculated molalities is not unexpected since apart from differences due to spray they are calculated from the same primary data. The similarity between calculated molality and the molality of the initial external electrolyte solution is also not unexpected since concentrations are maintained in both compartments during the run. What is surprising is the difference in weight of solution used in the calculations and the weight of solution actually retrieved, 0.94g in the best case.

It is conceivable that a part of the discrepancy is due to inefficient removal of the interface solution, but it seems unlikely that the whole of the discrepancy can be explained in this way. Previously it has been stated that this arrangement can only be considered as a combination where the membranes are clamped i.e. around the edges of the cell. In section (5.3.5) where the Permion is on the receiving side it was suggested that due to refraction current density was highest in the region where the membranes were clamped and conditions were such that solution was sucked out of the Cellophane at this point.

If solution can be sucked out of a membrane, it seems feasible that under certain conditions the membrane could be expected to swell beyond its equilibrium capacity. Data on swelling behaviour, chapter (2) figure (2.2), has shown that at 7.2M the cellophane is not at its maximum swelling capacity. It is interesting to speculate, if these experiments had been conducted at concentrations which induce maximum swelling, would a rupture of the membrane be seen due to the extra swelling? Jenkins et al [30] report the disintegration of swollen cellophane films in 3M LiOH and 2-4M NaOH.

The measured molality in table (5.6) is higher than the calculated molality which is compatible with water swelling the membrane further. The effect that the bowing may have had on transport numbers was investigated in the series of experiments, (5.39-5.44). Transport numbers were determined through both single membrane types, before and after their use in an assembly. Since similar values were obtained the conclusion was that individual transport numbers appear to be unaffected by any swelling changes.

In conclusion, the apparent rise in concentration of the interface solution must introduce diffusion and osmosis which must severely affecting the experimentally determined transport numbers when Cellophane is on the receiving side.

### 5.3.8 The effects of diffusion and osmosis on measured transport numbers

The discussion of the results of the previous section introduced the presence of diffusion and osmosis between the interface solution and the anolyte and catholyte. The meticulous experimental technique described in chapter (3) was specifically designed to minimise the effects of diffusion and osmosis on experimentally determined transport numbers. Diffusion and osmosis are an inherent problem when determining transport

numbers through a membrane assembly where Cellophane is on the receiving side since the transport numbers through the individual membranes are different. Although the assembly may be in equilibrium with the anolyte and catholyte before the start of the experiment as soon as any charge is passed solution starts to accumulate at the membrane/membrane interface followed by inevitable diffusion gradients.

To understand the behaviour of a membrane assembly with Cellophane on the receiving side requires assessment of the amount of diffusion and osmosis. Figure (5.20) illustrates the magnitudes of these effects for 7.2M KOH with the length of each arrow being proportional to the amount of transference. The length of the $T_K+$ and $T_{H2O}$ arrows are representative of the transport numbers through Cellophane and Permion as single membrane types as determined from experiments (5.41 and 5.44) respectively. The length and direction of the arrows representing diffusion and osmosis were obtained from the difference between transport numbers from experiments (5.41 and 5.44) and anolyte and catholyte transport numbers from experiment (5.36), where an assembly of 5 sheets of each membrane type was used and Cellophane was on the receiving side. For example, in experiment (5.36) the potassium transport number associated with the anolyte compartment was 0.4943. This is 0.0131 less than the transport number of potassium through Permion as a single membrane type, (experiment (5.44)), and is equivalent to the amount of diffusion from the interface solution to the anolyte compartment, i.e. in the opposite direction to $T_K+$.

The experimentally determined transport numbers were the net result of the two processes shown in figure (5.20). Clearly diffusion and osmosis had a much greater effect on the Cellophane sub-assembly than on the Permion sub-assembly.

The consequence of figure (5.20) on the value of experimentally determined transport numbers compared with transport numbers from single membranes is as follows :-

(i) $t_K+$ donating would be expected to be lower since potassium has diffused back through the membrane.

(ii) $t_K+$ receiving would be expected to be higher since the experimentally determined transport number is the sum of the single membrane transport number plus an amount due to diffusion.

Figure 5.20 Magnitude of transference processes

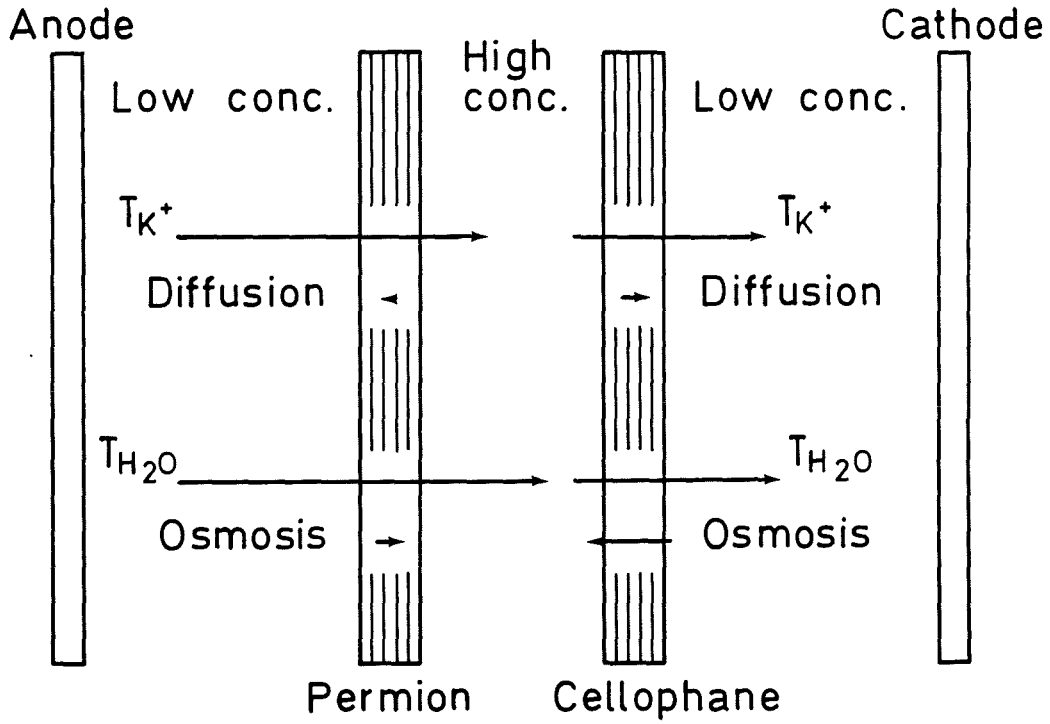

(iii) $t_{H2O}$ donating would be expected to be higher since if potassium is diffusing in the opposite direction to $t_{H2O}$ donating then osmosis will occur in the direction of water transport thus increasing the net flux of water.

(iv) $t_{H2O}$ receiving would be expected to be lower since with potassium diffusing in the same direction as $t_{H2O}$ receiving then osmosis will occur in the opposite direction to water transport hence decreasing the net flux of water.

Apart from the value obtained for $t_{H2O}$ receiving from experiment (5.4), reference to table (5.5) shows that all results substantiate the suggested trends when an equal number of Permion and Cellophane layers were used.

Figure (5.21) shows how transport numbers are influenced when unequal numbers of membrane layers are used. As the size of the membrane assembly increases relative to the number of layers of Permion so the potassium ion transport numbers tend towards the values for just Cellophane. The result is similar to figure (5.15) where Permion is on the receiving side, and emphasises an increase in diffusion due to the smaller proportion of one membrane type in a given membrane assembly. Transference numbers for water however tend towards values found for single membranes suggesting that osmosis is not a dominant factor and that Permion is relatively resistant to hydraulic flow.

Figure 5.21 Transport numbers as measured by analysis of the anolyte and catholyte for experiments where unequal numbers of each membrane type were used as a function of the membrane assembly with Cellophane on the receiving side.

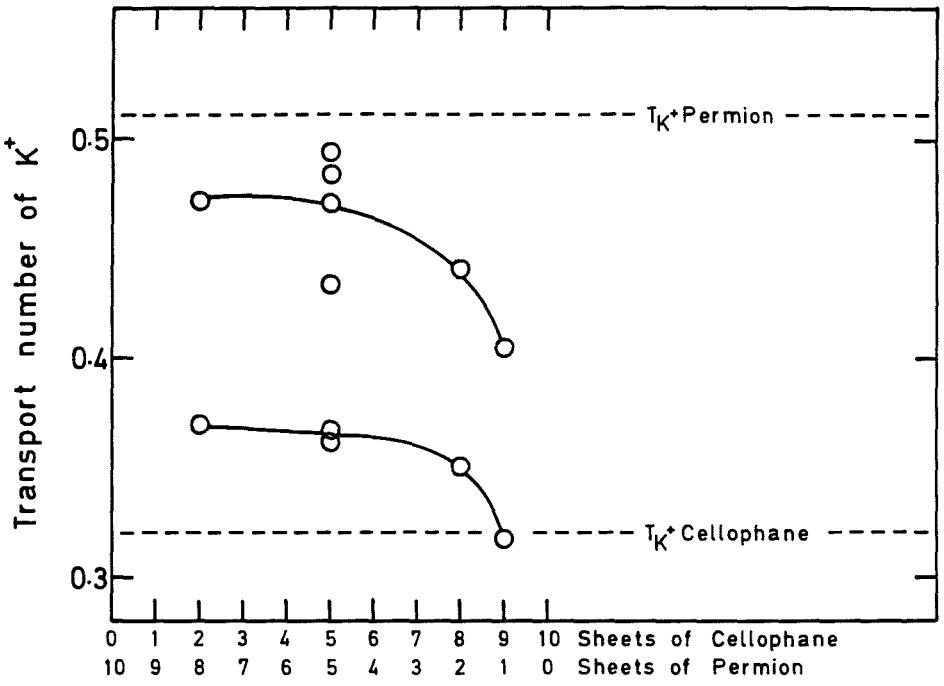


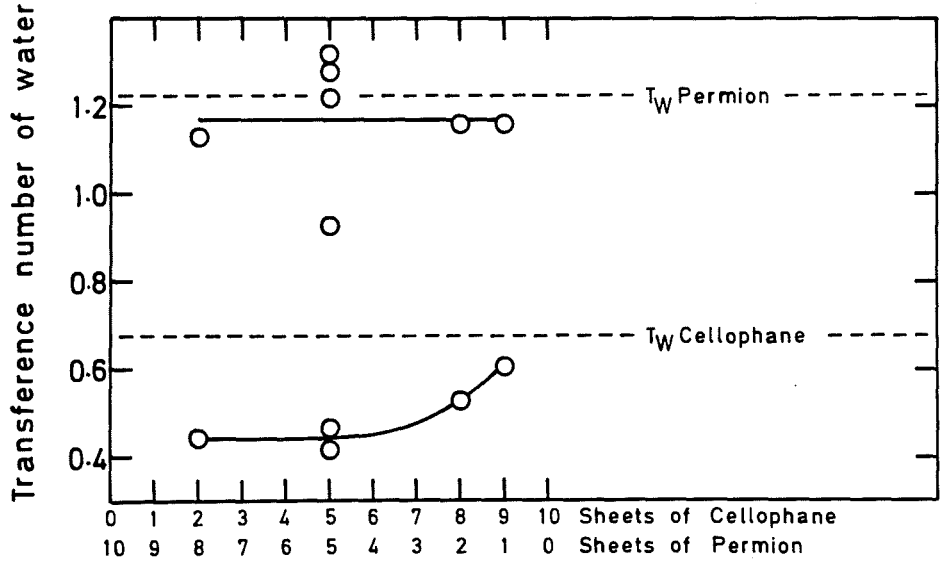


KEY

A ○ Transport Number as measured from the Anolyte

C ○ Transport Number as measured from the Catholyte

5.3.9 Calculation of a diffusion coefficient

The explanation of the experimental results in this section has largely been based on the influence of diffusion. Calculation of a diffusion coefficient to substantiate the theories is therefore desirable.

Diffusion coefficients for experiments (5.36 and 5.37) have been calculated from equation (5.2)

$$J = \bar{D} A \frac{dc}{dx} \qquad (5.2)$$

where J (moles) is the amount of KOH transported by diffusion as a function of time and is calculated from the difference between measured and "diffusion free" transport numbers. $\bar{D}$ ($cm^2s^{-1}$) is the diffusion coefficient through the membrane, A ($cm^2$) is the area through which diffusion occurs and dc/dx the difference in concentration between the interface solution and the anolyte or catholyte as a function of the thickness of the membrane stack.

In separators diffusion coefficients may be determined using equation (5.3),

$$\frac{K}{\bar{K}} = \frac{D}{\bar{D}} \qquad (5.3)$$

where K ($\Omega^{-1}cm^{-1}$) is the conductivity of the electrolyte in free solution and $\bar{K}$ is the conductivity of the separator. D ($cm^2s^{-1}$) is the diffusion coefficient in free solution, and for a 1:1 electrolyte such as KOH may be calculated from equation (5.4) [124]

$$D = \frac{2D_C D_A}{D_C + D_A} \qquad (5.4)$$

where $D_C$ and $D_A$ are the diffusion coefficients of the cation and anion respectively [125]. Equation (5.3) has been applied to Cellophane and Permion, this though a

reasonable approach at high electrolyte concentrations would not be applicable to dilute solutions since here the Donnan exclusion of co-ions significantly reduces diffusion of electrolyte in membranes. The results are tabulated below.

Table 5.7 Comparison of diffusion coefficients

| Run | Permion $\bar{D}/cm^2s^{-1}$ | Cellophane $\bar{D}/cm^2s^{-1}$ |
|---|---|---|
| 5.36 | $3.6 \times 10^{-6}$ | $1.2 \times 10^{-5}$ |
| 5.37 | $4.6 \times 10^{-6}$ | $2.3 \times 10^{-5}$ |
| From Equation 5.3 | $1.2 \times 10^{-6}$ | $8.4 \times 10^{-6}$ |

The diffusion of KOH in free solution was calculated as $2.86 \times 10^{-5}$ $cm^2s^{-1}$. The practical diffusion coefficients in table (5.7) are of a similar order suggesting that reasonable coefficients have been obtained.

A concentration profile for the membrane assembly where Cellophane is on the receiving side is proposed in figure (5.23). The lines connecting internal concentrations on either side of each membrane are a schematic representation of possible concentration profiles.

Figure 5.22 Proposed concentration profile with Cellophane on the receiving side

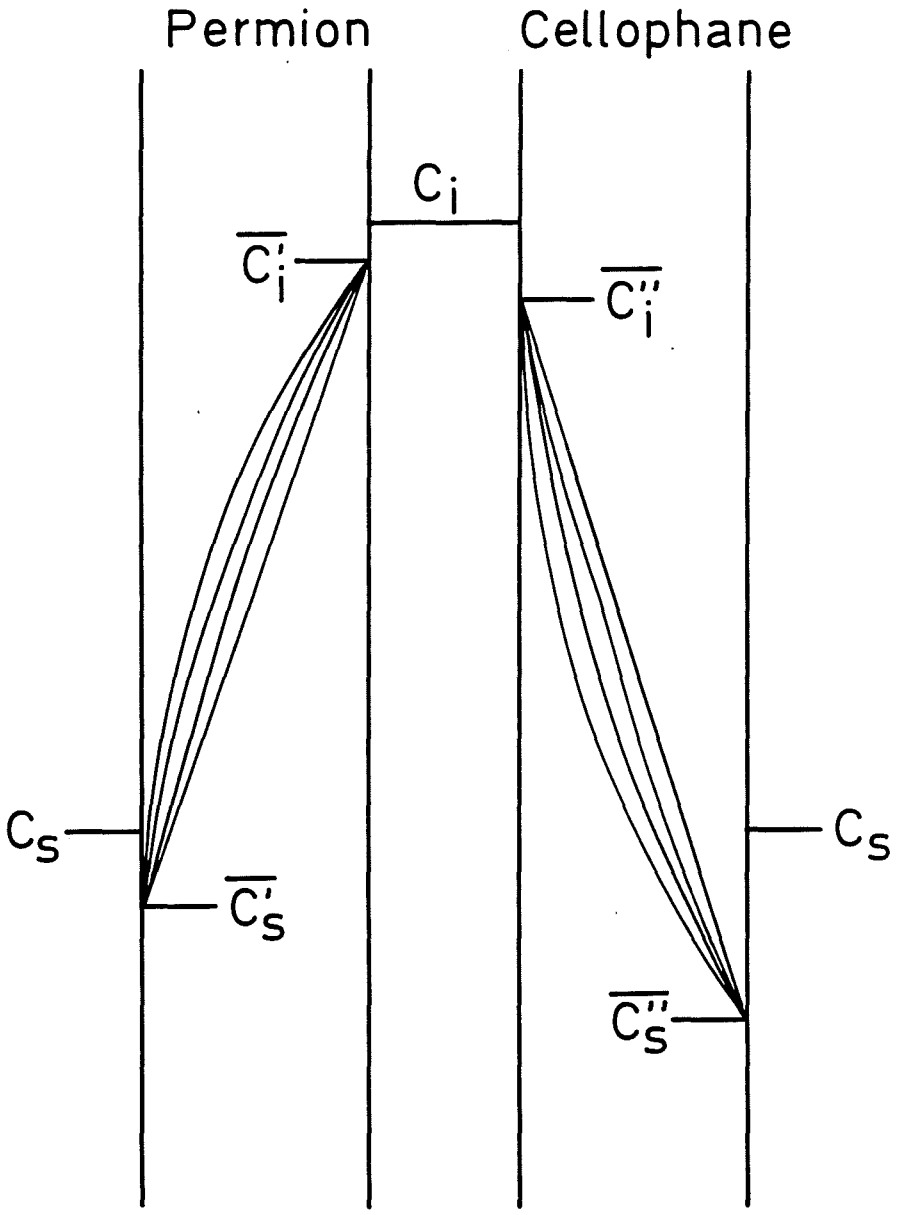

## 5.4 Conclusion

The transport behaviour of assemblies of Cellophane and Permion in the two possible orientations is understandable from the transport properties of the individual membranes.

With Permion on the receiving side and at low current densities a steady state was reached and depletion of electrolyte at the interface was replaced by diffusion mainly in the Cellophane. At high current densities depletion of electrolyte at the interface was rapid causing the decomposition of the Cellophane.

With Cellophane on the receiving side accumulation of electrolyte occurred at the interface. The difference between measured and predicted transport numbers was accounted for by the effects diffusion and osmosis again mainly in the Cellophane.

# CHAPTER 6

# CONCLUSIONS AND FURTHER WORK

## 6.1 Conclusions

The observed swelling behaviour of Cellophane and Permion when equilibrated in solutions of KOH is a consequence of their structure. The complex swelling and ion-exchange behaviour of Cellophane, noted by Jenkins et al [30], has been confirmed. At external electrolyte concentrations below 3M swelling was limited and caused by the penetration of the electrolyte into amorphous regions. Intramolecular hydrogen bonds were broken and new intermolecular hydrogen bonds were formed between water molecules and the primary alcohol groups of the Cellophane. Above 3M and up to 5.7M swelling increased sharply due to exchange of $H^+$ by $K^+$ on primary alcohol groups in crystalline regions. At even higher concentrations there was a dramatic reduction in swelling due to association between the fixed charge groups and the cation to form a complex. At the highest external electrolyte concentrations swelling increased further due to the exchange of protons on secondary alcohol groups.

Compared with Cellophane the thickness swelling of Permion was significantly less due to cross-linking, whereas increases in width and length were marginally higher. A tri-laminate of Cellophane and Permion is used in batteries. Setting aside the effects of mass transport the significant differences in width and length swelling of the two membranes might cause the laminate to separate. Differences in thickness swelling would have no undesirable effect. It is likely that in a battery the pressure caused by the casing on the components would prevent the laminate from separating.

Permion was fully exchanged at low external electrolyte concentrations and since the membrane is mono-functional the ion-exchange capacity determined using the Topp and Pepper method [45], did not change over the concentration range used in this study. The ion-exchange capacity of Permion was also obtained by an indirect method using a $Cl^-$ tracer. Similar results were obtained validating the indirect technique for use with Cellophane whose ion-exchange capacity could not be obtained using the pH titration method.

Accurate measurement of ionic transport numbers require a meticulous technique. Transport numbers are dependent on concentration and since transport numbers are usually measured by allowing a change in concentration to develop, the problem arises as to which concentration applies to the measured transport number. The change in

concentration also causes diffusion gradients to be set-up through the membrane, resulting in measured transport numbers being affected by diffusion transport. The technique of Jenkins et al [80] developed further in this study produced transport numbers at a specific electrolyte concentration and with minimal influence of diffusion. The dedicated approach of initial cell testing combined with the use of relevant correction factors produced a consistent set of results of greater precision than was obtained in the comparable studies by Shaw and Remanick [90] on cellulose and by Atieh and Cheh [70] on Permion.

With both Cellophane and Permion potassium and water transport numbers decreased with increasing external electrolyte concentration. This behaviour, typical of ion-exchange membranes, was due to the decreasing effectiveness of co-ion exclusion with increasing bulk solution concentration. Similar transport numbers were obtained through 10, 5 or 2 sheets of each membrane; the implication was that diffusion of $K^+$ and osmosis of $H_2O$ in the reverse direction had been eliminated. The flux was solely due to the passage of current. Plots of $t_{H2O}$ vs. $Wt_K+$, where W is the number of moles of water in the membrane per equivalent of counter-ion, indicated that very little water was transported with the hydroxyl ion.

The confidence gained in the technique used for single membrane types provided a firm basis for measuring and understanding transport behaviour in less obvious situations, namely in assemblies of membranes.

The use of a non-empirical correction factor improved the accuracy of membrane conductivity data by correction for current refraction into the region where the membrane was clamped between the two halves of the conductivity cell. Combination of the conductivity data with the swelling, ion-exchange and mass transport data allowed the derivation of ionic mobilities in the pore liquid corrected for tortuosity on the basis of various models. An overall understanding of the behaviour of each membrane whilst swollen in solutions of KOH provides a firm basis for understanding the behaviour of assemblies.

The model for tortuosity proposed by Lee et al [96] accurately described the blocking effects of Cellophane. The blocking effects of Permion was less and although an accurate model was not found the pores in Permion were less tortuous than in Cellophane. This correlates with the water velocity in Permion having a value closer to

that of potassium which indicates that compared to Cellophane the Permion structure exerted less drag.

The behaviour of an assembly of Cellophane and Permion was directly related to the orientation of the assembly. If Permion was on the side of the assembly receiving the cation predictions from single membrane transport numbers were confirmed and depletion of electrolyte occurred at the Cellophane/Permion interface. If Cellophane was on the receiving side accumulation of electrolyte occurred at the interface, again confirming predictions from single membrane transport numbers. In the Cellophane/Permion/Cellophane tri-laminate used in button cells these effects will occur simultaneously.

Permion was the dominant partner in assemblies with the apparent transport numbers through Cellophane rising to values closer to those for Permion alone than to those for Cellophane alone. At high current densities and with Permion on the receiving side the decomposition of Cellophane at the interface with Permion confirmed the depletion of electrolyte. Although measured transport numbers through Cellophane were enhanced by diffusion, if depletion of electrolyte was rapid then diffusion rates to replace the lost electrolyte were insufficient and decomposition of the Cellophane occurred. Calculation of transport numbers over periods towards the end of transport runs confirmed that depletion reached a constant state at the lower current densities.

With Cellophane on the receiving side the difference between measured and predicted transport numbers was accounted for by the effects of diffusion and osmosis.

At low current densities the Cellophane/Permion/Cellophane tri-laminate may behave as follows. Initially solution will accumulate at the Permion/Cellophane interface and deplete at the Cellophane/Permion interface. A steady state will be reached and the effects will be less than reported for both orientations on their own since although Permion is the dominant partner it will be restricted by the Cellophane adjacent to the anolyte with a knock on effect reducing the accumulation of electrolyte at the Permion/Cellophane interface. At high current densities decomposition of the Cellophane adjacent to the anolyte will be rapid leaving a Permion/Cellophane assembly which will behave as described in section (5.3.8).

## 6.2 Further work

The swelling behaviour of Cellophane was found to be complex. Experimentally the data was obtained by equilibration of the dry membrane in a series of solutions of various concentrations. In other words membranes immersed at the high concentrations had never been in contact with KOH solutions of lower concentration. Further work is necessary to elucidate behaviour on progression of a single piece of membrane through a series of concentrations. Under these conditions the decrease in swelling and ion-exchange at concentrations above 5.7M seems unlikely.

Although a satisfactory expression for the tortuosity of Cellophane was found, a good estimate of the tortuosity of Permion was not obtained. It was difficult to asses accurately the thickness swelling and hence the porosity of the Permion due to the irregular thickness of the film. If the porosity of Permion could be measured accurately, perhaps by an Archimedes type density measurement method, using a fluid which Permion did not sorb then greater confidence could be gained when applying the porosity data to tortuosity models.

In this study transport measurements were made through assemblies of two membranes, and theories provided to explain the experimental data. The work should be extended to tri-laminates of Cellophane/Permion/Cellophane and Permion/Cellophane/Permion. Predictions could be made based on this study and compared with experimental results.

# References


[1] Ruetschi, P. (Leclanché S.A., Switzerland) ISE Meeting, Venice 1980.

[2] Ruetschi, P., Alkaline Electrolyte-Lithium Minature Primary Batteries, J. Power Sources, 7, (1981/82), p165-180.

[3] Tye, F.L., Primary Batteries For Civilian Use, Electrochemical Power Sources, Ed. M. Barak., Pub. Peter Peregrinus Ltd. on behalf of The Institution of Electrical Engineers, London (1980), p75.

[4] Vincent, C.A. with Bonino, F., Lazzari, M. and Scrosati, B. Modern Batteries, An Introduction to Electrochemical Power Sources. Pub. E. Arnold (1986) p85 and 87.

[5] Ref. [3], p76.

[6] Ruben, S., "Balanced alkaline dry cells", Trans. Electrochem. Soc., 92, (1947), pp.183-193.

[7] Hull, M.N., and James, H.I.: "Why alkaline cells leak", J. Electrochem. Soc., 124, (1977), pp.332-339.

[8] Lee, J.A., Maskell, W.C., and Tye, F.L., "Separators and membranes in electrochemical power sources" in Meares, P. (Ed.) Membrane separation processes (Elsevier, 1976), p.404.

[9] André, H., "L'accumulator agent-zinc", Bull. Soc. Fr. Electr., (1941), 1, pp.132-146.

[10] Dirske, T.P., and De Haan, F., "Corrosion of the zinc electrode in the silver-zinc-alkali cell", J. Electrochem. Soc., (1958), 105, pp.311-315.

[11] Mendzheritskii, E.A., and Bagotski, V.S., "Cathodic reduction of the mercuric oxide electrode", Elektrokhimiya, (1966), 2, pp.1312-1316.

[12] Ruetschi, P., "The electrochemical reactions in the mercuric oxide-zinc cell" in Collins, D.H. (Ed.) Power Sources 4 (Oriel Press, 1972), pp.381-400.

[13] Antikainen, P.J., Hietanen, S., and Sillen, L.G., "Studies on the hydrolysis of metal ions. 27. Potentiometric study of the argentate (I) complex in alkaline solution", Acta Chem. Scand. Ser. A., 14, (1960), pp.95-101.

[14] Payen, A., Troisieme Memoire sur les Developpements des Vegetaux, Extrait des Memoires de l'Academie Royale des Sciences; Tome III des savants etrangers, Imprimerie Royale, Paris (1842).

[15] Straudinger, H., Die hochmolekularen organischen Vertindungen Kautschuk und Cellulose, Springer Verlag, Berlin-Göttingen-Heidelberg, (1932, reprinten 1960).

[16] Honeyman, J. and Parsons, M.A., "Recent Advances in the Chemistry of Cellulose and Starch", (Honeyman, J. ed.), Heywood, London, (1959), pp.49-74.

[17] Haworth, W.N., Helv. Chim. Acta 11, (1928), p.534.

[18] Haworth, W.N., Ber. Dtsch. Chem. Ges. (A) 65, (1932), p.43.

[19] Freudenberg, K., Friedrich, K., and Bumann, I., Liebigs Ann., 494, (1932), p.41.

[20] Freudenberg, K., and Blomqvist, C., Ber. Dtsch. Chem. Ges., 68(B), (1935), p.2070.

[21] Krässig, H., Cellulose and its derivatives, Kennedy, J.F. et al (eds.). Chichester: Ellis Horwood, (1985), pp.3-25.

[22] Woods, H.J., "Recent Advances in the Chemistry of Cellulose and Starch", (Honeyman, J. ed.), Heywood, London, (1959), pp.134-146.

[23] Post, R.E., "Zinc-Silver Oxide Batteries", (Fleischer, A. and Lander, J.J., eds.), Wiley, New York, (1971), pp.263-269.

[24] Kirk-Othmer Encyclopedia of Chemical Technology, Vol. 9, (1966), Wiley, New York, p.153.

[25] Nicoll, W.D., Cox, N.L., and Conaway, R.F., "Cellulose and Cellulose Derivatives", Part 2, (Ott, E. et al, eds.), (1954), Interscience, New York, pp.825-881.

[26] Meyer, K.H., and Misch, L., Ber. 70 B, (1937), p.266.

[27] Meyer, K.H., and Misch, L., Helv. Chim. Acta, 20, (1937), p.232.

[28] Meyer, K.H., and Mark, H.F., Z. Phys. Chem., B2, (1929), p.115.

[29] Andress, K.R., Z. Phys. Chem., 34, (1929), p.190.

[30] Jenkins, A.A., Maskell, W.C., and Tye, F.L., Power Sources 8, Thompson, J. ed., Academic Press, London, (1981), pp.163-182.

[31] Phillips, G.O., Chemistry in Britain, Vol. 25, No. 10, (1989), p.1006-1009.

[32] Kamide, K., Okajima, K., Kowsaka, K., and Matsui, T., Polymer Journal, Vol. 17, No. 5, (1985), pp.701-706.

[33] Blackwell, J., and Marchessault, R.H., "Cellulose and Cellulose Derivatives", part 4., eds. Bikales, N.M., and Segal, L., Wiley, New York, (1971), pp.1-37.

[34] Hermans, P.H., de Booys, J., and Maan, C., Kolloid-Z, 102, (1943), p.169.

[35] Hermans, P.H., "Physics and Chemistry of Cellulose Fibres", Elsevier, New York, (1949).

[36] Mann, J., and Marrinan, H.J., Trans. Faraday Soc., 52, (1956), p.177.

[37] Mann, J., and Marrinan, H.J., J. Polymer Sci., 32, (1958), p.125.

[38] Marchessault, R.H., and Liang, C.Y., J. Polymer Sci., 43, (1960), p.71.

[39] D'Agostino, V., and Lee, J., "Manufacturing Methods for High Performance Grafted Polyethylene Battery Separators", AFML-TR-72-13, (1972).

[40] D'Agostino, V., Lee, J., and Orban, G., "Zinc-Silver Oxide Batteries", (Fleischer, A. and Lander, J.J., eds.), Wiley, New York, (1971), pp.271-281.

[41] Strathmann, H., 4th European Summer School in Membrane Science, Chester, (1987).

[42] Pintauro, P.N., Mass Transport of Electrolytes in Membranes, Ph.D. dissertation, U.C.L.A., (1980).

[43] Ref. [8], p.421.

[44] Yeo, R.S., "Intrinsic Conductivity of Perfluorosulfonic Acid Membranes and its Implication to the Solid Polymer Electrolyte Technology", in Transport Processes in Electrochemical Systems, Yeo, R.S. et al (eds.), The Electrochemical Society Symposium, (1982).

[45] Topp, N.E., and Pepper, K.W., J. Chem. Soc., (1949), p.3299.

[46] Jenkins, A.A., Maskell, W.C., and Tye, F.L., Proceedings of the Symposium on Ion Exchange, Transport and Interfacial Properties, Eds. Yeo, R.S., and Buck, R.P., Electrochem. Soc., Vol. 81-82, pp.307-310.

[47] Urquart, A.R., "Recent Advances in the Chemistry of Cellulose and Starch", (Honeyman, J. ed.), Heywood, London, (1959), pp.240-264.

[48] Mann, J., "Cellulose and Cellulose Derivatives", part 4., eds. Bikales, N.M., and Segal, L., Wiley, New York, (1971), pp.89-116.

[49] Neale, S.M., J. Textile Inst. Trans., 20, (1929), T373.

[50] RAI, Research Corporation, Permion Battery Separators Brochure.

[51] Helfferich, F., "Ion-Exchange", McGraw-Hill, New York, (1962), p.102.

[52] Warwicker, J.O., "Cellulose and Cellulose Derivatives", part 4., eds. Bikales, N.M., and Segal, L., Wiley, New York, (1971), pp.325-379.

[53] Maskell, W.C., unpublished data.

[54] Ref. [51], p.145.

[55] Tye, F.L., J. Chem. Soc., (1961), p.4787.

[56] Robinson, R.A., and Stokes, R.H., "Electrolyte Solutions", Butterworths, London, (1955), pp.479,489.

[57] King, E.J., "Acid-Base Equilibria", Permagon, Oxford, (1965), pp. 12, 293.

[58] Atkins, P.W., Physical Chemistry, (1978), Oxford University Press, 1st edition, p.829.

[59] Moore, W.J., Physical Chemistry, (1972), Longman Group Limited, 5th edition, p.431.

[60] Ref. [59], p.427.

[61] Ref. [51], p.326.

[62] Lengyel, S., Giber, J., Beke, Gy., and Vértes, A., Acta. Chim. Acad. Sci. Hung., 39 (3), (1963), pp.357-364.

[63] Ref. [8], p.451.

[64] Ref. [56], p.99.

[65] Kressman, T.R.E., and Tye, F.L., Trans. Faraday Soc., No. 440, Vol. 55, Part 8, (1959), p.1441.

[66] Oda, Y. and Yawataya, T., Bull. Chem. Soc. Jap., 29, (1956), p.673.

[67] Gregor, H.P., and Wetstone, D.M., Discuss. Faraday Soc., 21, (1956), p.162.

[68] Lorimer, J.W., Boterenbrood, E.I., and Hermans, J.J., Discuss. Faraday Soc., 21, (1956), p.141.

[69] Rosenberg, N.W., George, J.H.B., and Potter, W.D., J. Electrochem. Soc., 104, (1957), p.111.

[70] Atieh, S., and Cheh, H.Y., J. Mem. Sci., 42, (1989), pp.243-257.

[71] Kressman, T.R.E., Stanbridge, P.A., and Tye, F.L., Trans. Faraday Soc., 59, (1963), p.2129.

[72] Staverman, G., Trans. Faraday Soc., 48, (1952), p.176.

[73] Scatchard, G., J. Am. Chem. Soc., 75, (1955), p.2883.

[74] Winger, A.G., Ferguson, R., and Kunin, R., J. Phys. Chem., 60, (1956), P.556.

[75] Hale, D.K., and McCauley, D.J., Trans. Faraday Soc., 57, (1961), p.135.

[76] Dewhurst, D.J., Trans. Faraday Soc., 56, (1960), P.599-605.

[77] Kressman, T.R.E., and Tye, F.L., Faraday Soc. Discuss, 21, (1956), p.185.

[78] Zelman, A., Kwak, J.C.T., Leibovitz, J., and Spiegler, K.S., Experientia. Suppl., 18, (1971), p.679.

[79] Brun, T.S., Berg, A., and Spiegler, K.S., Proceedings of the Symposium on Ion Exchange, Transport and Interfacial Properties, Eds. Yeo, R.S., and Buck, R.P., Electrochem. Soc., Vol. 81-82, p.303.

[80] Jenkins, A.A., Maskell, W.C., and Tye, F.L., J. Mem. Sci., 11, (1982), pp.231-242.

[81] Dotson, R.L., Lynch, R.W., and Hilliard, G.E. Proceedings of the Symposium on Ion Exchange, Transport and Interfacial Properties, Eds. Yeo, R.S., and Buck, R.P., Electrochem. Soc., Vol. 81-82, pp.268-289.

[82] Ibanez, J.A., and Tejerina, A.F., Lett. Nuovo. Cimento. Soc. Ital. Fis., Vol 38, part 5, (1983), pp.145-150.

[83] Benavente, J., J. Non-Equilb. Thermodynamics, Vol 9, (1984), pp.217-224.

[84] D'Alessandro, S., J. Mem. Sci., 17, (1984), pp.63-69.

[85] Fabiani, C., Scibona, G., Scuppa, B., Annali di Chimica, 75, (1985), bo società Chimica Italiana, p.515.

[86] Kontturi, K., Ekman, A., and Forsell, P., Acta Chemica Scandinavica, A 39, (1985), p.273-277.

[87] Førland, E., Acta Chemmica Scandinavica, A 30, (1976), p.825-828.

[88] Forsell, P., Kontturi, K., and Ekman, A., Acta Chemica Scandinavica, A 39, (1985), p.279-286.

[89] Handbook of Chemistry and Physics, Chemical Rubber Co., 62nd edn., (1981-82), PD224.

[90] Shaw, M., and Remanick, A.H., Zinc-Silver Oxide Batteries (Fleischer, A., and Lander, J.J., eds.), Wiley, New York, (1971), pp.233-261.

[91] Ref. [8], p.452.

[92] Jenkins, A.A., Maskell, W.C., and Tye, F.L., Power Sources 9, Thompson, J., ed., Academic Press, London, (1983), pp.349-363.

[93] Ref. [8], p.424.

[94] Mackie, J.S., and Meares, P., Proc. Roy. Soc. (London) Ser. A., 232, (1955), pp.498-509.

[95] Hirst, D.M., "Mathematics for Chemists", The Macmillan Press Ltd, (1976), p.140.

[96] Ref. [8], p.425.

[97] Maskell, W.C., unpublished work.

[98] Ref. [8], p.418.

[99] Meredith, R.E., and Tobias, C.W., Advances in Electrochemistry and Electrochemical Engineering, Vol.2, Wiley, New York, (1962), pp.15-47.

[100] Jenkins, A.A., Maskell, W.C., and Tye, F.L., J. Appl. Electrochem., 21, (1991), pp.327-330.

[101] Feltham, A.M., and Spiro, M., Chemical Reviews, Vol 71, No. 2., (1971), pp.177-193.

[102] Jenkins, A.A., Maskell, W.C., and Tye, F.L., unpublished data.

[103] Parsons, R., "Handbook of Electrochemical Constants", Butterworths Scientific Pub., London, 82, (1959).

[104] Tye, F.L., Disc. Faraday Soc., 21, (1956), p.200.

[105] Barrer, R.M., Barrie, J.A., and Roger, M.G., Trans. Faraday Soc., 58, (1962), p.2473.

[106] Tye, F.L., unpublished data.

[107] "Characteristics of Separators for Alkaline Silver Oxide Zinc Secondary Batteries: Screening Methods", Cooper, J.E., and Fleischer, A., (eds.), U.S. Govt. Pub. AD447301, (1964), p.149.

[108] Krutilova, L.E., Maksimova, I.N., Razuvaev, V.E., and Shcherba, M.W., Ukr. Khim. Zh., 42 (9), (1976), p.925.

[109] Ref. [107], p.154.

[110] Schlögl, R. Z. Electrochem., 57, (1953), p.195.

[111] Meares, P., J. Chim Phys., 55, (1958), p.273.

[112] Jakubovic, A.O., Hills, G.J., and Kitchener, J.A., Trans. Faraday Soc., 55, (1959), p.1570.

[113] Jakubovic, A.O., Hills, G.J., and Kitchener, J.A., J. Chim. Phys. Physicochem. Biol., 55, (1958), p.263.

[114] Ref. [51], p.308.

[115] Kitchener, J.A., "Modern Aspects of Electrochemistry, No. 2", Butterworths, London, (1959), pp. 87-159.

[116] Ref. [51] p.162.

[117] Ferguson, H., Gardner, C.R., and Paterson, R., J. Chem Soc., Faraday Trans. 1, (1972), p.2021.

[118] Yeager, H.L., O'Dell, B. and Twardowski, Z., J. Electrochem. Soc., 129, (1982), p.85.

[119] Mauritz, K.A., Branchick, K.J., Gray, C.L. and Lowry, S.R. Polym. Prep. Am. Chem. Soc., Div. Polym. Chem., 20, (1980), p.122.

[120] Despic, A.R., and Hills, G.J., Trans. Faraday Soc., 53 (1957), p.1262.

[121] Stock, M., private communication.

[122] Carter, M. A., Malpas, D.G., and Tye, F.L., "Progress in Batteries and Solar Cells", Vol.9, (1990), pp.96-102.

[123] Ref. [8] p.461.

[124] Ref. [59] p.438.

[125] Atkins, P.W., Physical Chemistry, (1983), Oxford University Press, 2nd edn., p.905.

[126] Abramowitz, M. and Stegun, I.A., Handbook of Mathematical Functions, (1964), Dover Publications, Inc., New York, p.378.

# List of main symbols used

Throughout the text barred species refer to the membrane phase.

| | |
|---|---|
| A | area of the electrode |
| $a_i$ | activity of species i |
| b | radius of the area into which refraction occurs |
| $c_i$ | concentration of species i |
| c | volume of membrane polymer per g of dry membrane |
| D | diffusion coefficient |
| E | electrical potential |
| $E_P$ | modulus of the polymer |
| F | Faraday coefficient |
| I | current |
| J | flux |
| $pK_a$ | dissociation constant of acid |
| $K_b$ | basicity constant |
| $K_w$ | autoprotolysis constant of water |
| k | conductivity |
| l | separation of the electrodes |
| $M_A$ | molecular weight of KOH |
| $M_C$ | molecular weight between cross-links |
| $M_W$ | molecular weight of water |
| $m_\gamma$ | molality of the anion |
| $m_R$ | molality of the fixed charge groups |

List of main symbols used - (continued)

| | |
|---|---|
| $N$ | normality |
| $n$ | number of r additions |
| $P_W$ | partial vapour pressure of water |
| $Q$ | quantity of actual exchanged protons, per unit membrane weight |
| $q_o$ | cross-link density per unit dose |
| $R$ | gas constant |
| $r$ | radiation dose |
| $R_1'$ | cell resistance corrected for refraction |
| $R_1$ | measured cell resistance with membrane |
| $R_0$ | measured cell resistance without membrane |
| $S_n$ | sum of a geometric series |
| $T$ | temperature |
| $t$ | time |
| $T_{K^+}$ | transport number of the potassium ion |
| $T_{OH^-}$ | transport number of the hydroxyl ion |
| $T_{H2O}$ | transference number of water |
| $T_W$ | transference number of water |
| $t_+$ | transport number of the cation |
| $t_-$ | transport number of the anion |
| $t_A$ | transport number calculated from the anolyte |
| $t_C$ | transport number calculated from the catholyte |
| $u_+$ | mobility of the cation |

List of main symbols used - (continued)

$u_-$ mobility of the anion

V volume

$V_P$ gel fraction of the membrane or the volume fraction occupied by the solid in the swollen membrane

$(1-V_P)$ porosity of the swollen membrane

$V_W$ partial molar volume of the solvent in solution

$V_2$ volume of swollen membrane per g of dry membrane

W number of moles of water in the membrane per equivalent of counter-ion

$W_G$ dry weight of film after extraction with xylene

$W_O$ weight of as received film

w molecular weight of the repeating unit in the polymer

X concentration of fixed charge groups

X% initial concentration of KOH in the cell

x total weight of water to be added to the catholyte

Y% concentration of KOH to be added to the anolyte

y total weight of Y% KOH to be added to the anolyte

Z quantity of available protons per unit membrane weight

$z_i$ magnitude of the charge of species i

Greek symbols

| | |
|---|---|
| $\alpha$ | degree of ionisation |
| $\gamma_i$ | activity coefficient of species i |
| $\delta$ | distance between two parallel planes |
| $\eta$ | viscosity |
| $\theta$ | tortuosity factor |
| $\Lambda_o$ | molar ionic conductivity at infinite dilution |
| $\lambda$ | distance between sites on a plane |
| $\mu_i$ | chemical potential of species i |
| $\mu_i^\circ$ | standard chemical potential of species i |
| $\mu_w$ | chemical potential of water |
| $\nu$ | drift velocity |
| $\nu_\pm$ | number of ions required to form one molecule of the salt |
| $\Pi$ | osmotic pressure |
| $\rho$ | density of the polymer |
| $\phi$ | electrical potential |

# APPENDICES

Appendix A

Table A Percentage recovery from the transport cell together with pertinent experimental details

| Test No. | Volume of KOH (ml) | % Recovery | | Time (min) | Experimental Conditions |
|---|---|---|---|---|---|
| | | Anolyte | Catholyte | | |
| 1 | 6 | 98.32 | 100.25 | | The transport cell was emptied immediately after filling. The anolyte compartment was the first to be emptied and mopped. No water jacket. |
| 2 | 6 | 100.73 | 100.03 | | |
| 3 | 10 | 99.91 | 99.99 | | |
| 4 | 10 | 95.44 | 104.12 | | |
| 5 | 10 | 98.60 | 99.69 | | |
| 6 | 10 | 99.18 | 99.78 | | |
| 7 | 10 | 98.58 | 99.56 | | |
| 8 | 10 | 99.09 | 99.69 | | |
| 9 | 10 | 99.97 | 100.00 | | |
| 10 | 10 | 99.69 | 99.55 | | |
| 11 | 20 | 100.03 | 99.76 | | |
| 12 | 20 | 99.75 | 99.17 | | |
| 13 | 20 | 97.01 | 96.15 | | |
| 14 | 6 | 99.10 | 99.15 | | The cell was turned on its side to be emptied, anolyte compartment first. |
| 15 | 6 | 99.94 | 99.98 | | The cell was emptied immediately after filling, anolyte compartment first. The cell was turned on its side when mopped out. Membrane was cut to the shape of the cell. (i) Dropped membrane. |
| 16 | 6 | 99.92 | 99.85 | | |
| 17 | 10 | 99.89 | 99.99 | | |
| 18 | 10 | 99.92 | 99.76 | | |
| 19 | 10 | 99.93 (i) | 99.57 (i) | | |
| 20 | 10 | 99.84 | 99.76 | | |
| 21 | 10 | 99.94 | 99.85 | | |

Table A continued Percentage recovery from the transport cell together with pertinent experimental details

| Test No. | Volume of KOH (ml) | % Recovery | | Time (min) | Experimental Conditions |
|---|---|---|---|---|---|
| | | Anolyte | Catholyte | | |
| 22 | 10 | 99.64 (ii) | 100.00 (ii) | 60 | Conditions as 15-21, the cell was left for a while with no stirring.<br>(ii) Lost one drop.<br>(iii) Pierced membrane. |
| 23 | 10 | 99.96 (iii) | 99.96 (iii) | 205 | |
| 24 | 10 | 99.97 | 99.65 | 120 | Experimental conditions were the same as tests 22-23, with the addition of a water jacket operating at 25°C.<br>(iv) Flask knocked over. |
| 25 | 10 | 99.91 | 99.65 | 90 | |
| 26 | 10 | 99.97 | 99.81 | 85 | |
| 27 | 10 | 100.04 (iv) | 99.67 (iv) | 200 | |
| 28 | 10 | 99.97 | 99.51 | 65 | |
| 29 | 10 | 99.95 | 99.83 | 65 | Experimental conditions were as 24-28. The catholyte compartment was plugged whilst the anolyte compartment was emptied. |
| 30 | 10 | 99.96 | 99.67 | 225 | |
| 31 | 10 | 99.92 | 99.75 | 70 | |
| 32 | 10 | 100.07 | 99.79 | 120 | Catholyte compartment was emptied first , anolyte compartment kept plugged. |
| 33 | 10 | 100.07 | 99.69 | 100 | Catholyte compartment was emptied first. The position of the catholyte stirrer and the access hole was reversed. |
| 34 | 10 | 99.89 | 99.84 | 120 | |
| 35 | 10 | 99.82 | 99.78 | 100 | |
| 36 | 10 | 99.89 | 99.58 | 94 | |
| 37 | 10 | 99.98 | 99.70 | 37 | |
| 38 | 10 | 99.78 | 99.46 | 90 | Platinum anode was exchanged with the nickel cathode. Anolyte compartment was emptied first. |
| 39 | 10 | 100.14 | 99.98 | 216 | |

Table A continued Percentage recovery from the transport cell together with pertinent experimental details

| Test No. | Volume of KOH (ml) | % Recovery | | Time (min) | Experimental Conditions |
|---|---|---|---|---|---|
| | | Anolyte | Catholyte | | |
| 40 | 10 | 96.86 (v) | 102.15 (v) | 53 | Experimental conditions as 38-39 except that the catholyte compartment was emptied first. (v) Pierced membrane. |
| 41 | 10 | 100.05 | 99.91 | 150 | |
| 42 | 10 | 99.93 | 99.89 | 70 | |
| 43 | 10 | 99.54 | 99.00 | 228 | |
| 44 | 10 | 100.00 | 99.63 | 46 | |
| 45 | 10 | 100.13 | 99.17 | 60 | |
| 46 | 10 | 99.25 | 99.51 | 60 | |
| 47 | 10 | 99.65 | 99.72 | 206 | |
| 48 | 10 | 100.06 | 98.26 | 60 | Experimental conditions as 40-47 except the nickel was cut to the same shape as the platinum. |
| 49 | 10 | 100.27 | 99.50 | 206 | Experimental conditions as 48 except the anolyte compartment was emptied first. |
| 50 | 10 | 99.75 | 99.72 | 60 | New piece of nickel was used as the cathode, in original position adjacent to the catholyte compartment. Anolyte compartment was emptied first. |
| 51 | 10 | 100.08 | 99.68 | 140 | |
| 52 | 10 | 99.89 | 99.60 | 70 | |
| 53 | 10 | 99.80 | 99.84 | 100 | |
| 54 | 10 | 100.09 | 99.71 | 120 | Experimental conditions as 50-53 except that the catholyte compartment was mopped first. |
| 55 | 10 | 100.09 | 99.72 | 60 | |

Table A continued Percentage recovery from the transport cell together with pertinent experimental details

| Test No. | Volume of KOH (ml) | % Recovery | | Time (min) | Experimental Conditions |
|---|---|---|---|---|---|
| | | Anolyte | Catholyte | | |
| 56 | 10 | 99.89 | 99.89 | 60 | Moppings were analysed volumetrically. Anolyte compartment was emptied first. |
| 57 | 10 | | | 100 | |
| 58 | 10 | 99.84 | 99.70 | 40 | |
| 59 | 10 | 99.75 | 99.77 | 83 | |
| 60 | 10 | 99.94 | 99.84 | 100 | |
| 61 | 10 | 99.78 | 99.74 | 70 | |
| 62 | 10 | 99.56 | 99.89 | 70 | Experimental conditions as 56-61 except that the electrolyte compartments were exchanged. |

In table (A) column (2), "Volume of KOH (ml)", refers to the initial volume of electrolyte delivered to each compartment. Columns (3) and (4) give the percentage recovery of this electrolyte from each compartment and column (5), "Time (min)", gives the length of time the electrolyte was left in the cell before it was recovered.

Appendix B

Loss from the transport cell by spray and evaporation

This section describes the calculations required to obtain a correction for the loss of electrolyte from the cell by spray and evaporation. From the primary data obtained for calculation of the ionic transport and solvent transference numbers, the loss of KOH during electrolysis (p mole) and the loss of water by evaporation (q mole) may be calculated.

p and q must take into account expected cell recoveries, 99.926% from the anolyte and 99.671% from the catholyte, and the electrolysis of water which generates $0.5 mole F^{-1}$ at the anode and consumes $1.0 mole F^{-1}$ at the cathode.

Hence

$$p = C_{0A} - \left[ (C_{1A} + C_{2A}) \frac{100}{99.926} \right] + C_{0C} - \left[ (C_{1C} + C_{2C}) \frac{100}{99.671} \right] \quad (B.1)$$

and

$$q = W_{0A} - \left[ (W_{1A} + W_{2A}) \frac{100}{99.926} \right] + (0.5Q) + W_{0C} - \left[ (W_{1C} + W_{2C}) \frac{100}{99.671} \right] - Q \quad (B.2)$$

where $C_0$ is the initial moles of KOH and $W_0$ is the moles of $H_2O$ associated with it, $C_1$ is the final moles of KOH and $C_2$ is the moles of KOH in the moppings. $W_1$ and $W_2$ are the moles of water associated with $C_1$ and $C_2$ respectively and the subscripts A and C refer to anolyte and catholyte respectively. Q is the charge passed.

If p moles of KOH are lost as spray this represents a loss of solution of

$$\frac{56.1\, p\, 100}{X \rho_X} \text{ ml} \quad (B.3)$$

This spray contains,

$$\frac{56.1\,p\left(\frac{100}{X} - 1\right)}{18} - 1 \quad \text{moles of water} \tag{B.4}$$

Hence the loss of water by evapouration may be calculated as (q - 1) moles. $\rho_X$ is the density of the solution in $gcm^{-3}$ and X is the concentration expressed as % by weight. Data from these calculations is shown in table (B.1). Individual values for KOH loss, $F^{-1}$ and water loss, $F^{-1}$, i.e. (56.1 p 100 / X $\rho^X$ Q) and ((q - 1) / Q) show extremely large variation and so there is little value in averaging them.

A method, which weights determinations according to the charge passed, results from summing the (56.1 p 100 / X $\rho^X$) and (q -1) values and dividing by the sum of all the charges passed. This method leads to the results in table (B.2) for runs inside the 3% rejection criteria. These indicate average losses by spray and evapouration of $1.54ml F^{-1}$ (solution) and -0.062 mole ($H_2O$) $F^{-1}$ respectively.

Table B.1

| Run | p (mmole) | q (mmole) | loss of KOH by spray (μl) | loss of $H_2O$ by spray (mmole) | loss of $H_2O$ by evap. q-l (mmole) | Q (mF) |
|---|---|---|---|---|---|---|
| 3.2 | 0.1674 | 1.2731 | 81.254 | 4.4054 | -3.1323 | 23.06 |
| 3.4 | -0.2366 | 2.2675 | -57.537 | -3.0254 | 5.2929 | 46.04 |
| 3.5 | -0.2727 | 3.8671 | -53.465 | -2.7635 | 6.6306 | 57.09 |
| 3.6 | -0.1060 | 4.3229 | -36.006 | -1.9261 | 6.2510 | 32.96 |
| 3.7 | 0.1851 | 1.731 | 178.33 | 9.7973 | -8.0663 | 11.70 |
| 3.8 | 0.8493 | -0.541 | 113.38 | 5.5810 | -6.1220 | 74.62 |
| 3.9 | 0.1383 | 0.7465 | 53.606 | 2.8855 | -2.1390 | 28.88 |
| 3.10 | 1.2166 | -1.9407 | 137.049 | 6.3873 | -8.3280 | 74.62 |
| 3.11 | 0.3445 | 1.6391 | 218.665 | 11.931 | -10.292 | 17.64 |
| 3.12 | 0.2711 | 3.2163 | 74.320 | 3.937 | -0.72114 | 40.84 |
| 3.15 | 0.4723 | 3.4611 | 76.153 | 3.8533 | -0.3922 | 69.40 |
| 3.16 | 0.3531 | 1.3733 | 56.852 | 2.8764 | -1.5031 | 69.51 |
| 3.17 | 1.2378 | 5.043 | 199.31 | 10.084 | -5.0412 | 69.53 |
| 3.18 | -0.6653 | -3.8369 | -64.848 | -2.9739 | -0.86299 | 74.63 |
| 3.19 | 1.1327 | -0.7008 | 318.94 | 16.923 | -17.624 | 39.74 |
| 3.20 | 0.3135 | 1.9747 | 95.902 | 5.1106 | -3.1359 | 36.58 |
| 3.21 | 2.4368 | -11.038 | 216.00 | 9.6072 | -20.645 | 74.62 |
| 3.22 | -0.5238 | 3.1118 | -350.77 | -19.158 | 22.270 | 16.71 |
| 3.23 | 1.2677 | 1.1699 | 134.93 | 6.3379 | -5.1680 | 74.62 |
| 3.24 | 0.1600 | -0.5732 | 48.754 | 2.6748 | -3.2480 | 36.72 |
| 3.25 | 0.2295 | 0.7449 | 69.951 | 3.8378 | -3.0929 | 36.71 |
| 3.26 | 0.3149 | -0.7405 | 95.971 | 5.2653 | -6.0058 | 36.71 |
| Total | | | 1606.74 | | -65.0749 | 1042.93 |

Table B.2

All data is within 3% rejection criteria.

| | | |
|---|---|---|
| $\Sigma Q$ (mF) | 1042.927 | sum of all charges passed |
| $\Sigma\left[\frac{56.1\ p\ 100}{X\ \rho_X}\right]$ ($\mu$l) | 1606.744 | sum of loss of KOH by spray |
| $\Sigma$ (q-l) (mmole) | -65.0749 | sum of loss of $H_2O$ by evapouration |
| $\frac{\Sigma\left[\frac{56.1\ p\ 100}{X\ \rho_X}\right]}{\Sigma\ Q}$ (ml | 1.5406102 | |
| $\frac{\Sigma\ (q-l)}{\Sigma\ Q}$ (mole$F^{-1}$) | -0.0623964 | |

Appendix C

Method used to calculate anolyte and catholyte transport numbers from the experimental data

Calculation of potassium ion transport and water transference numbers from the anolyte required the following equations [80].

$$t'_{K_A^+} = \frac{(C_0 - C_1' - C_2')}{Y} \qquad (C.1)$$

and

$$t'_{W_A} = \left(\frac{W_0 - W_1 - W_2}{Y}\right) + 0.5 \qquad (C.2)$$

where $C_0$ is the number of moles of KOH in the original solution plus the number of moles of KOH in the addition solution and $W_0$ is the number of moles of water associated with $C_0$. $C_1'$ is the number of moles of KOH in the main bulk of solution recovered from the anolyte compartment after electrolysis. This value is obtained directly from the volumetric analysis and is expressed as the number of moles of KOH in 1 litre of solution. $W_1$ is the number of moles of water associated with $C_1'$. $C_2'$ is the number of moles of KOH associated with the anolyte moppings and is equal to the number of moles of HCl that was required to neutralise the anolyte solution obtained from the filter paper. $W_2$ is the number of moles of water associated with the anolyte moppings and is given by the equation (C.3) which assumes the anolyte compartment is the same concentration as the moppings.

$$\frac{W_1 C_2'}{C_1'} \qquad (C.3)$$

Y is the number of faradays passed for the duration of the run as shown in equation (C.4).

$$Y = \frac{It}{F} \qquad (C.4)$$

where I is the current passed, t is time and F is the Faraday constant. In equation (C.2) the term 0.5 arises from the anodic production of water.

To calculate the potassium ion transport and water transference numbers from the catholyte compartment equations (C.1) and (C.2) need some rearrangement, which results in equations (C.5) and (C.6).

$$t'_{K_c^+} = \frac{-(C_0 - C_1' - C_2')}{Y} \qquad (C.5)$$

and

$$t'_{W_c} = -\left[\left(\frac{W_0 - W_1 - W_2}{Y}\right) - 1\right] \qquad (C.6)$$

where $C_0$ is the number of moles of KOH in the original solution and $W_0$ is the number of moles of water associated with $C_0$ plus the number of moles of water added during the run. $C_1'$, $C_2'$, $W_1$ and $W_2$ are calculated in the same manner as for the anolyte compartment. In equation (C.6) the term 1 arises from the cathodic consumption of water.

Appendix D

Equations required to calculate current refraction correction factor

The theoretical treatment for refraction into the space outside that defined by the orifice has been defined by Barrer et al [105]. The appropriate equations are.

$$R = \frac{\left(\frac{1 - 16S_n}{\Pi^2}\right) l}{a^2 \Pi \kappa} \qquad (D.1)$$

$$S_n = \sum_{q=1}^{\infty} \frac{1}{q^2} \frac{I_1(q\alpha)}{I_1(q\beta)} [I_1(q\beta) K_1(q\alpha) - K_1(\alpha\beta) I_1(q\alpha)] \qquad (D.2)$$

where R is the resulting electrical resistance, l is the separator thickness, a is the radius of the orifice, $\kappa$ is the specific conductivity of the separator, $\beta = \Pi b/l$, $\alpha = \Pi a/l$ and b is the space into which refraction can occur : $I_1$ and $K_1$ are modified Bessel functions. The theory assumes isotropic conductivity of the separator. The term in the summation, equation (D.2), was calculated using polynomial approximations [126] for the Bessel functions as follows.

For $x \leq 3.75$

$$\begin{aligned} x^{-1} I_1(x) \quad &= 0.5 \\ &+ 0.87890\,594\,(x/3.75)^2 \\ &+ 0.51498\,869\,(x/3.75)^4 \\ &+ 0.15084\,934\,(x/3.75)^6 \\ &+ 0.02658\,733\,(x/3.75)^8 \\ &+ 0.00301\,532\,(x/3.75)^{10} \\ &+ 0.00032\,411\,(x/3.75)^{12} \end{aligned} \qquad (D.3)$$

For $3.75 \leq x < \infty$

$$x^{1/2} e^{-x} I_1(x) = 0.39894\,228 - 0.03988\,024\,(3.75/x) - 0.00362\,018\,(3.75/x)^2 + 0.00163\,801\,(3.75/x)^3 - 0.01031\,555\,(3.75/x)^4 + 0.02282\,967\,(3.75/x)^5 - 0.02895\,312\,(3.75/x)^6 + 0.01787\,654\,(3.75/x)^7 - 0.00420\,059\,(3.75/x)^8 \quad \text{(D.4)}$$

For $x \leq 2$

$$x K_1(x) = x I_1(x) \ln(x/2) + 1 + 0.15443\,144\,(x/2)^2 - 0.67278\,579\,(x/2)^4 - 0.18156\,897\,(x/2)^6 - 0.01919\,402\,(x/2)^8 - 0.00110\,404\,(x/2)^{10} - 0.00004\,686\,(x/2)^{12} \quad \text{(D.5)}$$

For $2 \leq x < \infty$

$$x^{1/2} e^{x} K_1(x) = 1.25331\,414 + 0.23498\,619\,(2/x) - 0.03655\,620\,(2/x)^2 + 0.01504\,268\,(2/x)^3 - 0.00780\,353\,(2/x)^4 + 0.00325\,614\,(2/x)^5 - 0.00068\,245\,(2/x)^6 \quad \text{(D.6)}$$